AGARD-LS-204

AGARD

ADVISORY GROUP FOR AEROSPACE RESEARCH & DEVELOPMENT
7 RUE ANCELLE, 92200 NEUILLY-SUR-SEINE, FRANCE

AGARD LECTURE SERIES 204

Advanced Polymeric & Metallic Composite Materials for Space and Aerospace Vehicle Structures & Strength Optimization of Composite Structures and their Certification

(Les matériaux composites polymèriques et métalliques avancés pour les structures des véhicules spatiaux et aérospatiaux, et l'optimisation de la résistance des structures composites et leur homologation)

The material in this publication was assembled to support a Lecture Series, endorsed by the Structures and Materials Panel of AGARD, implemented by the Technical Cooperation Programme and presented on 11-12 December 1995 at DLR in Stuttgart, Germany, 14-15 December 1995 at ONERA in Châtillon, France, and 18-19 December 1995 in the University of Dayton in Ohio, USA.

NORTH ATLANTIC TREATY ORGANIZATION

Published December 1995

Distribution and Availability on Back Cover

AGARD-LS-204

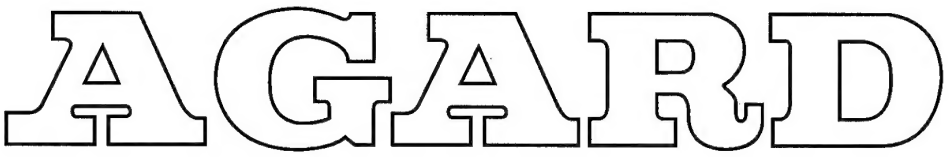

ADVISORY GROUP FOR AEROSPACE RESEARCH & DEVELOPMENT
7 RUE ANCELLE, 92200 NEUILLY-SUR-SEINE, FRANCE

AGARD LECTURE SERIES 204

Advanced Polymeric & Metallic Composite Materials for Space and Aerospace Vehicle Structures & Strength Optimization of Composite Structures and their Certification

(Les matériaux composites polymèriques et métalliques avancés pour les structures des véhicules spatiaux et aérospatiaux, et l'optimisation de la résistance des structures composites et leur homologation)

The material in this publication was assembled to support a Lecture Series, endorsed by the Structures and Materials Panel of AGARD, implemented by the Technical Cooperation Programme and presented on 11-12 December 1995 at DLR in Stuttgart, Germany, 14-15 December 1995 at ONERA in Châtillon, France, and 18-19 December 1995 in the University of Dayton in Ohio, USA.

North Atlantic Treaty Organization
Organisation du Traité de l'Atlantique Nord

The Mission of AGARD

According to its Charter, the mission of AGARD is to bring together the leading personalities of the NATO nations in the fields of science and technology relating to aerospace for the following purposes:

- Recommending effective ways for the member nations to use their research and development capabilities for the common benefit of the NATO community;
- Providing scientific and technical advice and assistance to the Military Committee in the field of aerospace research and development (with particular regard to its military application);
- Continuously stimulating advances in the aerospace sciences relevant to strengthening the common defence posture;
- Improving the co-operation among member nations in aerospace research and development;
- Exchange of scientific and technical information;
- Providing assistance to member nations for the purpose of increasing their scientific and technical potential;
- Rendering scientific and technical assistance, as requested, to other NATO bodies and to member nations in connection with research and development problems in the aerospace field.

The highest authority within AGARD is the National Delegates Board consisting of officially appointed senior representatives from each member nation. The mission of AGARD is carried out through the Panels which are composed of experts appointed by the National Delegates, the Consultant and Exchange Programme and the Aerospace Applications Studies Programme. The results of AGARD work are reported to the member nations and the NATO Authorities through the AGARD series of publications of which this is one.

Participation in AGARD activities is by invitation only and is normally limited to citizens of the NATO nations.

Published December 1995

ISBN 92-836-1027-X

Printed by Canada Communication Group
45 Sacré-Cœur Blvd., Hull (Québec), Canada K1A 0S7

Contents

Abstract

This Lecture Series will present and discuss the scientific problem of advanced polymer and metallic composite materials for aerospace structures, strength optimization of composite structures and their certification. Some challenges of using composite structures, including airframe concept definition are studied. Also fibre orientation optimization principles for composite panels and shells are outlined. Procedures for certification of assemblies made out of composites are dealt with.

Certification requirements, including requirements to estimate static and fatigue strengths are formulated.

Design conditions for composite structures are analyzed, including development.

This Lecture Series, endorsed by the Structures and Materials Panel of AGARD has been implemented by the Technical Cooperation programme.

Abrégé

Ce cycle de conférences est consacré à la présentation et à l'examen du problème scientifique des matériaux composites polymériques et métalliques avancés destinés aux structures aérospatiales, ainsi qu'à l'optimisation des structures composites et à leur certification. Un certain nombre de problèmes posés par l'emploi des structures composites, y compris la définition conceptuelle de la cellule, sont examinés. La question des principes d'optimisation de l'orientation des fibres pour les panneaux et les coques est abordée. Les procédures de certification des ensembles composés de matériaux composites sont traitées.

Les spécifications de certification, y compris les spécifications concernant la résistance statique et la résistance en fatigue, sont formulées.

Les conditions régissant la conception des structures composites sont analysées, y compris le développement.

Ce cycle de conférences est présenté dans le cadre du programme de coopération technique, sous l'égide du Panel AGARD des Structures et Matériaux.

List of Authors/Speakers

Lecture Series Director: Dr. V.I. BIRYUK
Central Aero-Hydrodynamic Institute
TsAGI
Zhukovsky 140160
Moscow Region
RUSSIA

Dr. T.G. SORINA
17 Radio Street
VIAM
Moscow
RUSSIA

Dr. S.E. SALIBEKOV
17 Radio Street
VIAM
Moscow
RUSSIA

Dr. A. Eu USHAKOV
Central Aero-Hydrodynamic Institute
TsAGI
Zhukovsky 140160
Moscow Region
RUSSIA

Dr. V. Ya SENIK
Central Aero-Hydrodynamic Institute
TsAGI
Zhukovsky 140160
Moscow Region
RUSSIA

Dr. Yu P. TRUNIN
Central Aero-Hydrodynamic Institute
TsAGI
Zhukovsky 140160
Moscow Region
RUSSIA

INTRODUCTION AND OVERVIEW

by
V.I. Biryuk
TsAGI, Zhukovsky 140160
Moscow Region, Russia

1. SURVEYING THE USE OF COMPOSITES IN AIRFRAMES

Composite materials are regarded as very promissing from the viewpoints of both extending aircraft capabilities and improving economy figures. Therefore aircraft companies conduct comprehensive projects for utilizing composites.

The international and Russian data available, see Fig. 1, clearly demonstrates permanent growth in aviation composite materials utilization. According to the forecast in the technical literature, the amount of composites in passenger-carrying airplane airframes will by year 2000 be as large as 15 - 20% (referred to the weight of all materials used), and in military airplanes, 35%.

As to the aircraft industry of the Commonwealth of Independent States, all major design offices have mastered these materials. Let us address practical examples of the use of composite materials in domestic airplanes.

In TU-204 passenger-carrying airplane (Fig. 2) the amount of composites is 9% of the weight of all materials used; the plan is to increase this parameter to 15% by introducing composites in structures of vertical and horizontal stabilizers.

In AN-70 transport (Fig. 3) the weight of composites is 25% amongst all materials used. Large-size structures of vertical and horizontal stabilizers are completely manufactured out of composite; sandwich panels are with tubular cores.

A mass-produced MIG-29 fighter (Fig. 4) has 7% fraction of composites (by weight); in future fighters the weight fraction of composites in lifting surfaces, wing high lift devices, and body components will be as high as 30%.

Composite materials were also used in the Buran orbiter: payload bay doors were manufactured out of a carbon/carbon material (Fig. 5).

2. LAYUP AND CHARACTERISTICS

Widespread aviation composite materials are the polymer matrix composites; used as a filler in them are glass, organic and/or graphite fibers. Figure 6 demonstrates usual combinations of components for the fibrous composites utilized in aviation.

Levels of specific strengths and stiffnesses of composites are mainly defined by properties of the fibers. The diagram compares specific strengths and stiffnesses of unidirectional composites with epoxy matrices and various reinforcing fibers.

Glass-reinforced plastics have high allowable strength and low stiffness. Organoplastics can carry high tensile stresses but have a relatively low Young's modulus and low compressive strength. Carbon fiber reinforced plastics are now the main structural materials for load-bearing components of structures. Various fillers can be combined in a material system, forming a hybrid material.

Mechanical properties of a matrix are decisive for shear load capability, buckling behavior, and maximum use temperatures; fatigue and impact resistance depend also on the matrix.

Currently, efforts are undertaken to develop composites based on thermoplastics. The latter yield at elevated temperatures and harden at room temperature. As compared with thermoset composites, the thermoplastic-based systems have a number of advantages:

- ease of use,
- simpler repair, the potential for reuse,
- almost no limitations on prepreg storage duration,
- insignificant sensitivity to moisture,
- high fracture toughness, damage tolerance,

see Fig. 6.

Generally aircraft companies manufacture composite structures from prefabricated prepregs, i.e., unidirectional layers impregnated with a matrix material. The prepregs are built-up in compliance with a prescribed pattern, thereafter united in a final material by polymerizing the stack (Fig. 7). The resulting material has certain average stiffnesses and strengths, which can be controlled by varying the composition parameters such as the total number, layup angles/sequence, and thicknesses of the layers.

The average properties of composites are predicted by analysis based on anisotropic multilayered plate theories. Used as initial data are characteristics of a unidirectional orthotropic ply that are listed in a table in Fig. 7. The ply characteristics are evaluated experimentally.

3. ASPECTS OF FEATURES MEETING THE STATIC AND FATIGUE STRENGTH REQUIREMENTS FOR COMPOSITE STRUCTURES

When designing composite structures, account should be taken of additional factors that weaken the structure. The main factors are as follows (Fig. 8):

- scatter in mechanical properties, more notable than that of metals,
- brittleness and the related sensitivity to stress concentration and impacts,

Paper presented at the AGARD SMP Lecture Series on "Advanced Polymeric & Metallic Composite Materials for Space and Aerospace Vehicle Structures. . .", held in Stuttgart, Germany from 11-12 December 1995; Châtillon, France from 14-15 December 1995 and Ohio, USA from 18-19 December 1995 and published in LS-204.

- sensitivity of structural characteristics to environmental attack and length of service.

The influence of these factors should be allowed for at the design stage, together with the conventional system of measures for meeting the static and fatigue strength requirements developed for metallic structures.

3.1. Notable scatter of mechanical properties

The more significant scatter in strengths of structures made out of composites is taken into account by introducing an additional factor to multiply the ultimate load (Fig. 8).

For each value of failure probability there exists a direct relation of the strength variance to the additional factor (Fig. 8). The variance is determined by experiment; corrections for the sampling amount are introduced.

3.2. The influence of environmental conditions

The presence of moisture results in notable moisture absorption -- and degradation of breaking stresses of a material. Figure 9 demonstrates the results of testing carbon fiber reinforced plastics after attaining a moisture content level 1%; allowable stresses drop by 10 - 15%, and the characteristics become unstable.

Elevated temperatures and long-term influence of moist air cause a further degradation.

The simultaneous action of environment and cyclic loads can produce a more severe reduction of strength characteristics. A plot in Fig. 9 represents the results of a static test of spoilers on a transport airplane. Residual strength of the component after simultaneous application of adverse environment and cyclic loads is 87%, whereas the environmental factors reduce down to 92%.

Designers should allow for environmental attack by introducing a degradation coefficient K_en to be applied to the allowables; this coefficient is to be defined based on

1) operational experience survey and
2) special tests.

3.3. Brittle fracture

Figure 10 compares in-service behavior of metal and composite elements. As to metal structures, a damage (such as scratch, indentation) detectable by eye does not almost degrade the load-bearing capability, while provoking initiation of fatigue cracks. After a crack reaches a critical length, the structure fails.

Damage in a composite structure appears mainly due to accidental mechanical impact that can occur at any time during operational use. In this case the strength characteristics fall suddenly. As a rule, usual variable in-service loads develop damage extremely slowly.

A composite-structure failure mode depends on an impact energy level (Fig. 10). High and medium energy impacts damage a surface; such areas can be detected visually and repaired. The greatest danger is associated with low-energy impacts; indications are difficult to reveal visually, and nondestructive inspection methods should be employed.

Investigations show (see Fig. 10) that a low-energy impact can drastically degrade component strength, and compression load carrying capability reduces more notably than tensile load limit.

The sensitivity to impacts addresses a number of extra requirements on designers:

- the composite structure should be designed as a fail-safe concept, i.e., it must maintain a desired strength after a standardized damage occurs;
- the influence of the standardized damages must be allowed for when specifying the allowable stresses -- by introducing a coefficient K_des;
- operators should establish a systematic pre-flight visual inspection and periodic nondestructive inspections;
- new typical processes for repairing the damaged structures in field conditions should be developed.

4.METAL MATRIX COMPOSITES

In comparison with polymer matrix composites (the Carbon Fibre Reinforced Plastics and Glass Fibre Reinforced Plastics) the metal matrix materials (MMC) have a number of advantages, including:

- a higher working temperature 350° C for composites with Al matrix and over 1200° C for intermetallic composites.
- higher static (shear and compressive) and fatigue strength,
- weldability (certain types of welding),
- higher electric and heat conductivity, no indications of radiation destruction.

However, manufacturing processes are much more sophisticated, higher pressures/temperatures are required, and the process must be monitored very carefully. This is caused by chemical activity of components in most MMCs. Their interaction products degrade properties and restrict the material service life.

Efforts of specialists in the field of MMCs have to be directed to the following major problems:

1. Thorough study of physical and chemical processes at component interfaces. The data, thus obtained, make it possible to derive a proper manufacturing process and to use the fiber strength to a maximum possible extent.
2. The development of transformation processes, including cutting,bending, welding,etc. - on the usual process equipment, as a rule.

3. Manufacture and evaluation of typical structural MMC parts. This offers a certain experience, renders designers confident, and helps establish the fields of the maximum efficiency for the materials.

5.POLYMER MATRIX COMPOSITES OF THE FUTURE GENERATION

Developers of polymer-matrix composites have a number of common problems for the near future:

- improvement of service characteristics (including extension of use temperature ranges),
- development of new, environmentally friendly manufacturing processes which reduce energy/labour requirements at stages of PMC manufacture and transformation into structures,
- improving components (fillers and matrices), making them cheaper, with due employment of new sources of raw materials,
- improving mathematical methods for optimization of PMCs and structures, taking into account features (and "smartness") of these materials.

Currently, we study options for raising the strength and the use temperature of composites by means of the nano-level microstructures and manufacturing processes.

Nano-composites are materials that contain components in the form of particles, fibers, and layers whose cross-sections measure 3-30 nanometers and are arranged in the corresponding matrices. A dimension of such element differs from that of a traditional fiber (glass, graphite, boron) by a factor of 50 to 3,000.

The positive scale-effect is seen in that the probability of surface/internal defects gets less if an element size is smaller.

In comparison with traditional microcomposites the nano-composites are anticipated to show higher mechanical characteristics (the static and fatigue strength, cracking resistance). The nano-composites are stronger due to the following factors:

- the nano-particles suppress growth of globules in a matrix,
- high surface energy and large total interface length affect the microstructure,
- a failure mode changes,
- the nano-reinforcing elements arrest the cracks.

The next direction of development consist in "the smart" materials.

The technology development process shows a turn from the "structural material" concept to the "functional material" concept. The driving force for creating the smart materials is the ever growing demand of modern civil and military technologies for self-adapting devices and structures.

A theoretical foundation of smart materials includes preparation of a comprehensive multifunction system with

- materials components,
-signal-providing and information-processing elements, and
- active components;

these are expected to ensure both improved mechanical properties and the structure condition information (the direct coupling in the system).

The major applications and the fundamental problems dealt with through the use of smart materials may be grouped as follows:

- monitoring of polymer matrix cure when fabricating a composite material,
- structural condition monitoring, estimation of amount of damage during service of flight vehicles,
- structural oscillation dampers for airplanes and engineering technologies,
- skins that change the aerodynamic surface shapes.

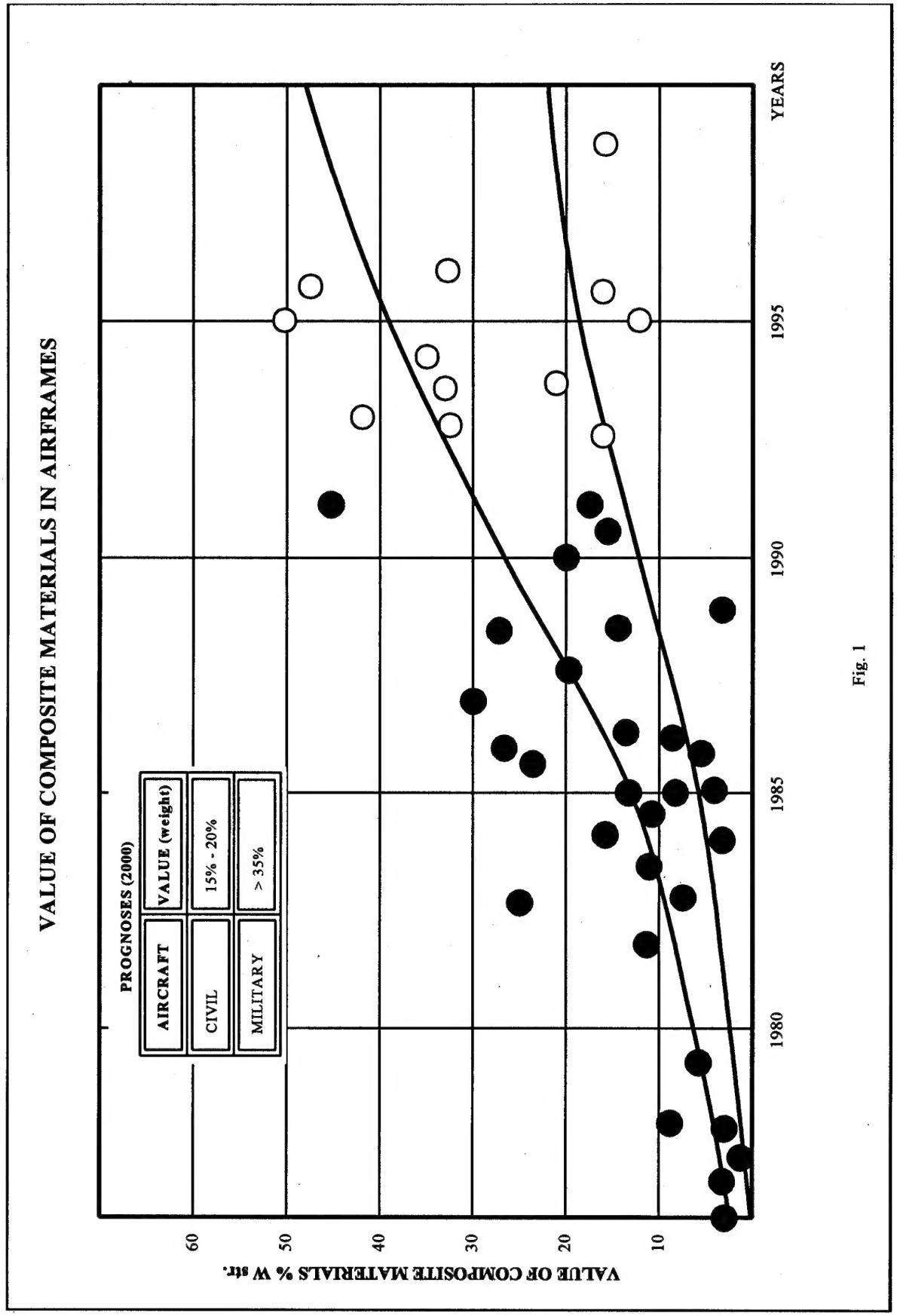
VALUE OF COMPOSITE MATERIALS IN AIRFRAMES
PROGNOSES (2000)
AIRCRAFT
VALUE (weight)
CIVIL
15% - 20%
MILITARY
> 35%
VALUE OF COMPOSITE MATERIALS % W str.
60
50
40
30
20
10
1980
1985
1990
1995
YEARS

Fig. 1

COMPOSITES IN TRANSPORT AIRCRAFT TU-204

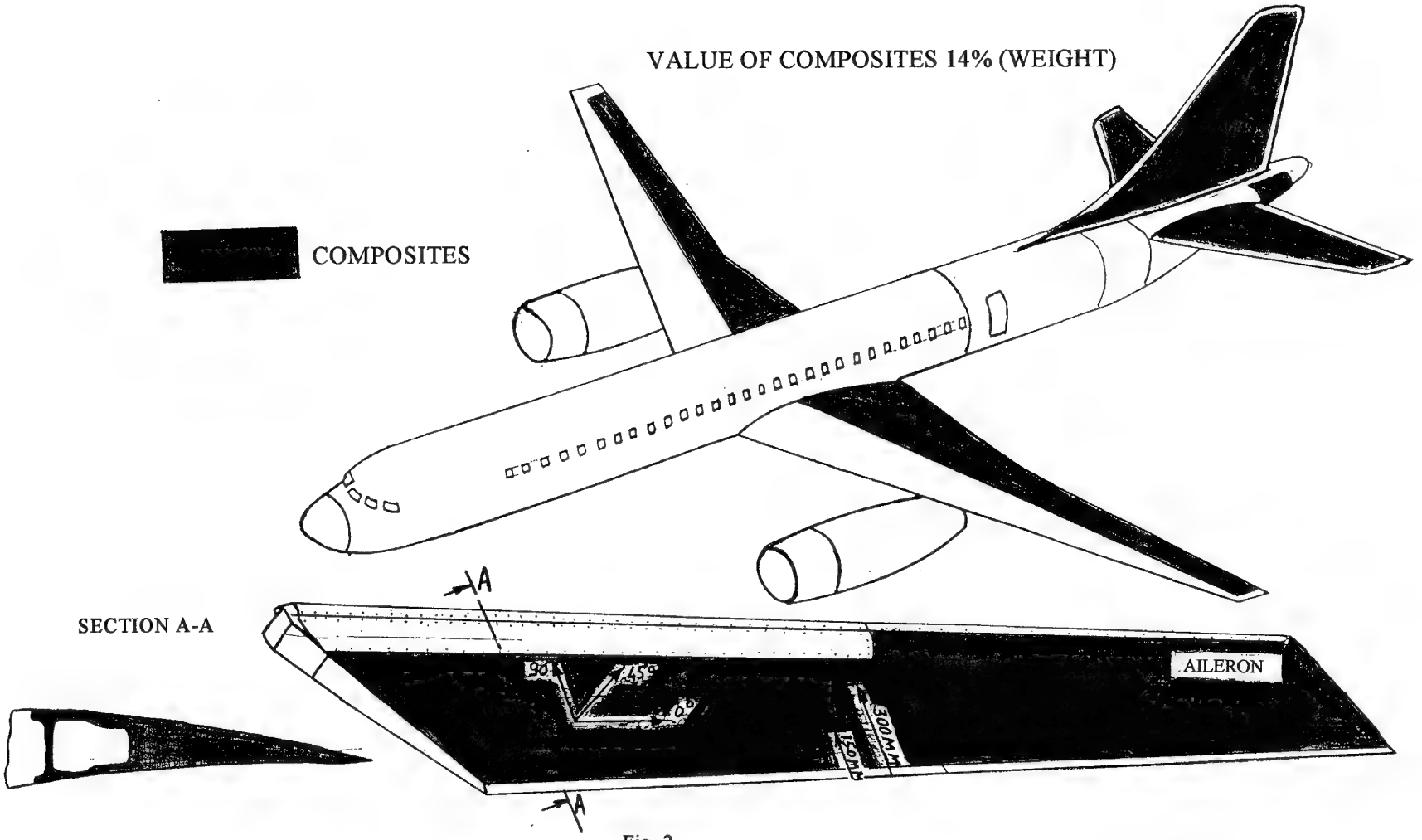

Fig. 2

COMPOSITES IN TRANSPORT AIRCRAFT AN - 70

VALUE OF COMPOSITES 25% (WEIGHT)

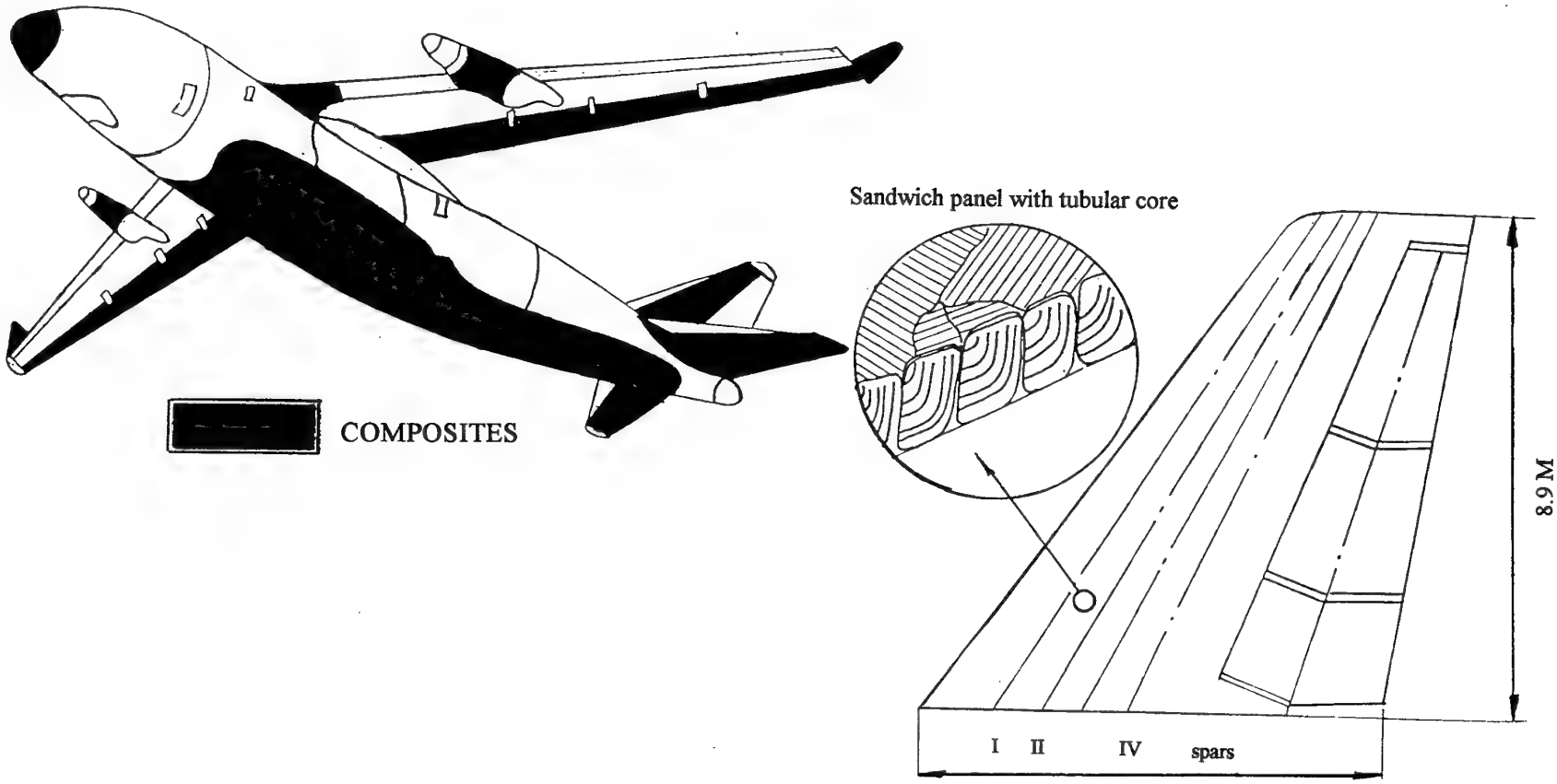

Fig. 3

COMPOSITES IN MIG - 29 FIGHTER

VALUE OF COMPOSITES 14% (WEIGHT)

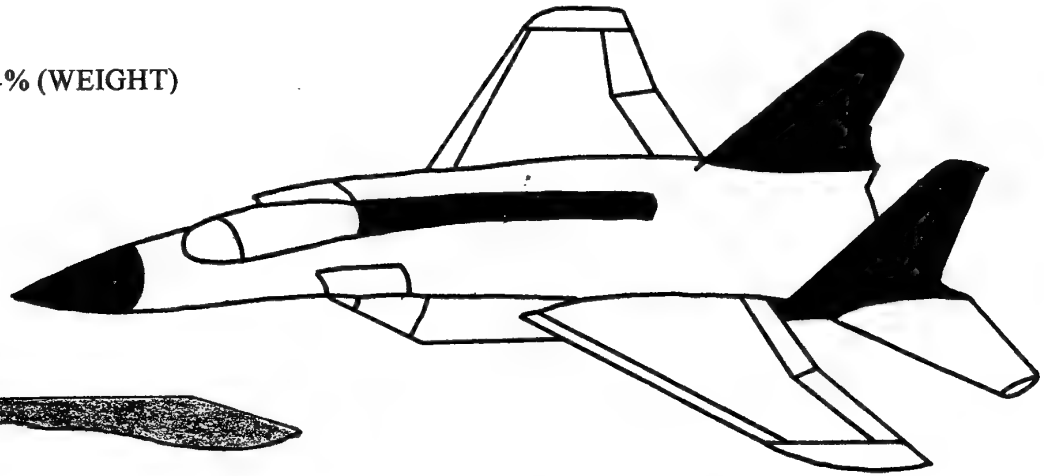

COMPOSITE FOREWING OF LONG-RANGE FIGHTER

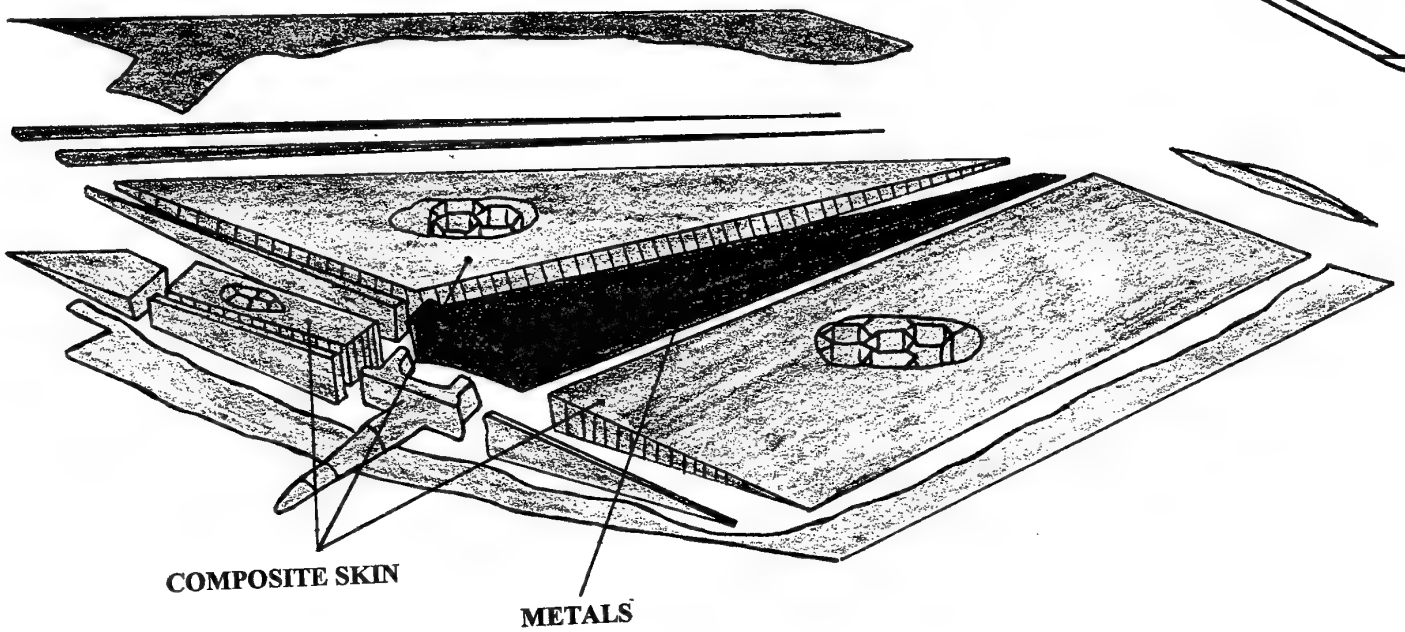

Fig. 4

COMPOSITES IN VEHICLE "BURAN"

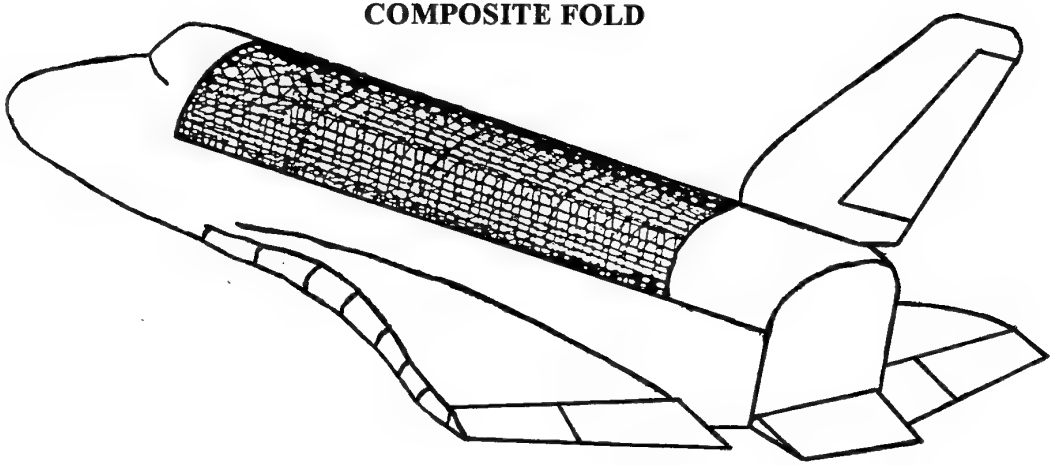

Fig. 5

FIBER COMPOSITES WITH RESIN MATRICE

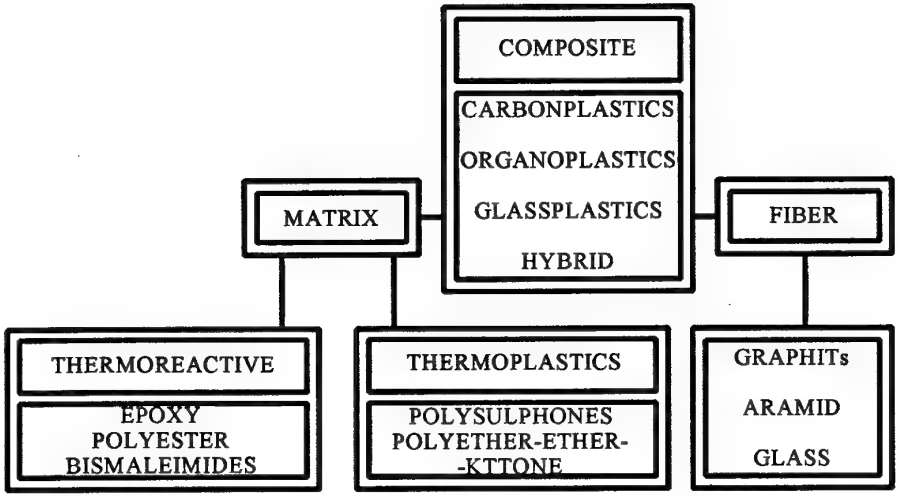

ADVANTAGES OF THERMOPLASTICS MATRIX COMPOSITES

1. MORE TECHNOLOGICAL.
2. MAY BE REPAIRED, MAY BE USED FOR REPATED MANUFACTURING.
3. THERE IS FRACTICALLY UNLIMITED PERIOD OF CEEPING PREPREGS.
4. MORE RESISTANT TO HUMIDITY ACTION.
5. CHARACTERISTICS OF VISCOCITY OF DESTRUCTION AND DAMAGE TOLERANCE ARE BETTER.

UNIT CHARACTERISTICS COMPARISON

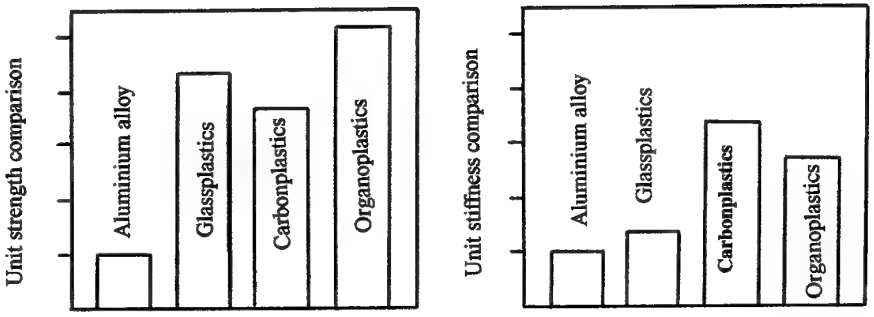

RELATIONSHIP BETWEEN RESIDUAL STRENGTH OF COMPRESSED CARBONPLASTICS WITH VARIOUS MATRICES AND UNIT ENERGY OF IMPACT

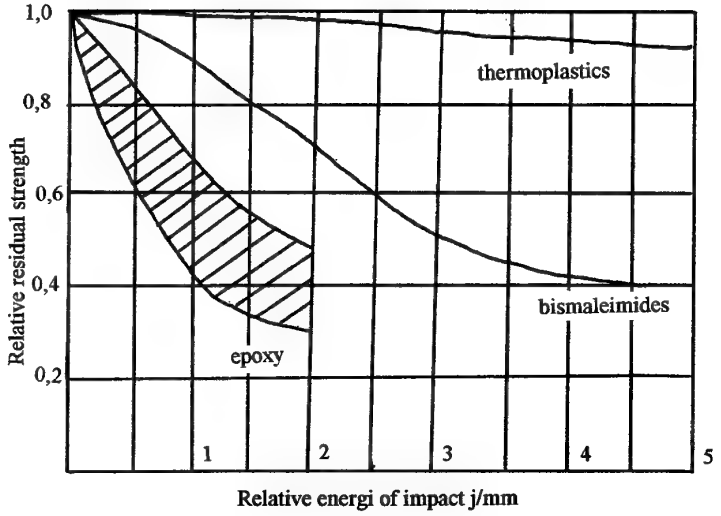

Fig. 6

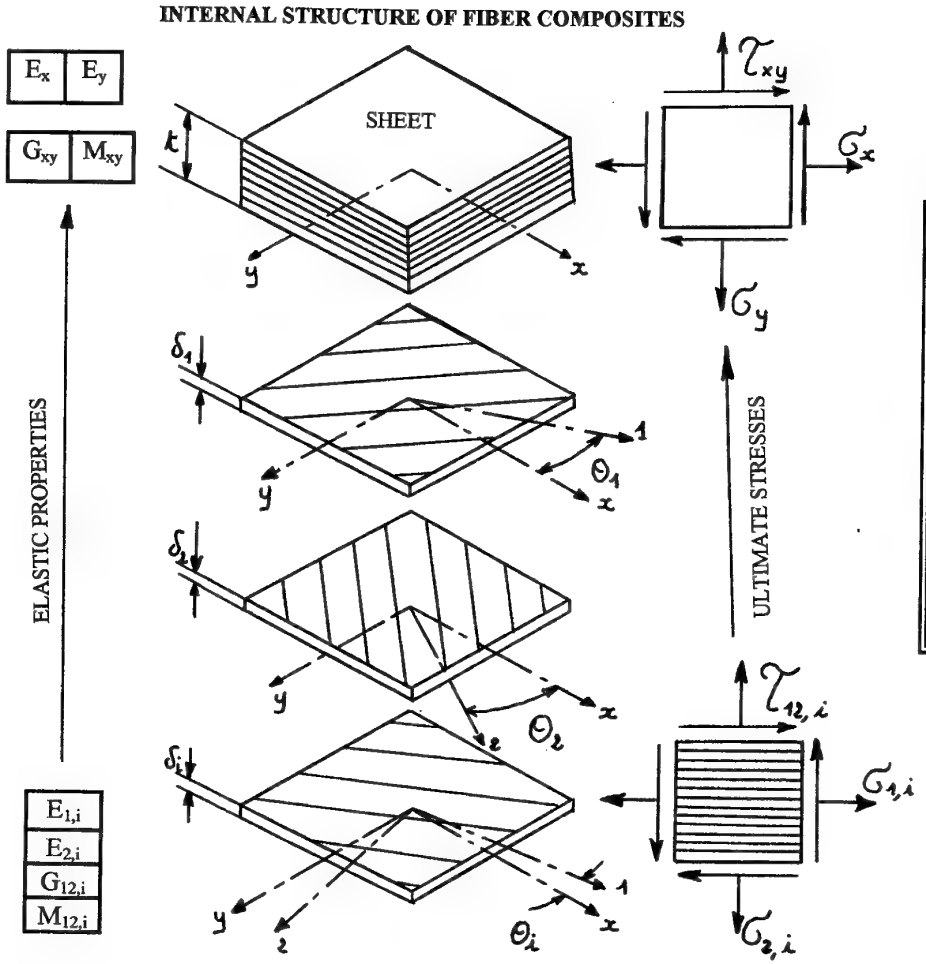

TYPICAL PROPERTIES OF UNIDIRECTIONAL COMPOSITES.

NN	PROPERTIES		MATERIAL DESIGNATION	CARBONPLASTICS EPOXY V=60%	ORGANOPLASTICS EPOXY V=60%	GLASSPLASTICS EPOXY V=45%
1	YOUNG'S MODULUS	ALONG	E_1 kg/mm^2	13000	8000	4000
2		ACROSS	E_2 kg/mm^2	700	600	300
3	SHEARMODULE		G_{12} kg/mm^2	600	200	400
4	POISSONRATIO			0.28	0.34	0.26
5	ULTIMATE STRESS (TENSION)	ALONG	kg/mm^2	110	140	110
6		ACROSS	kg/mm^2	2	1	3
7	ULTIMATE STRESS (COMPRESSION)	ALONG	kg/mm^2	70	20	60
8		ACROSS	kg/mm^2	13	5	12
9	ULTIMATESTRESS (SHEAR)		kg/mm^2	6	3	7

- UNIDIRECTIONAL LAYER PROPERTIES ARE DETERMINED EXPERIMENTALLY
- AVERAGED PROPERTIES OF A LAMINATE ARE DETERMINED NUMERICALLY BY TECHNIQUES BASED ON THEORY OF LAYERED PLATES.

Fig. 7

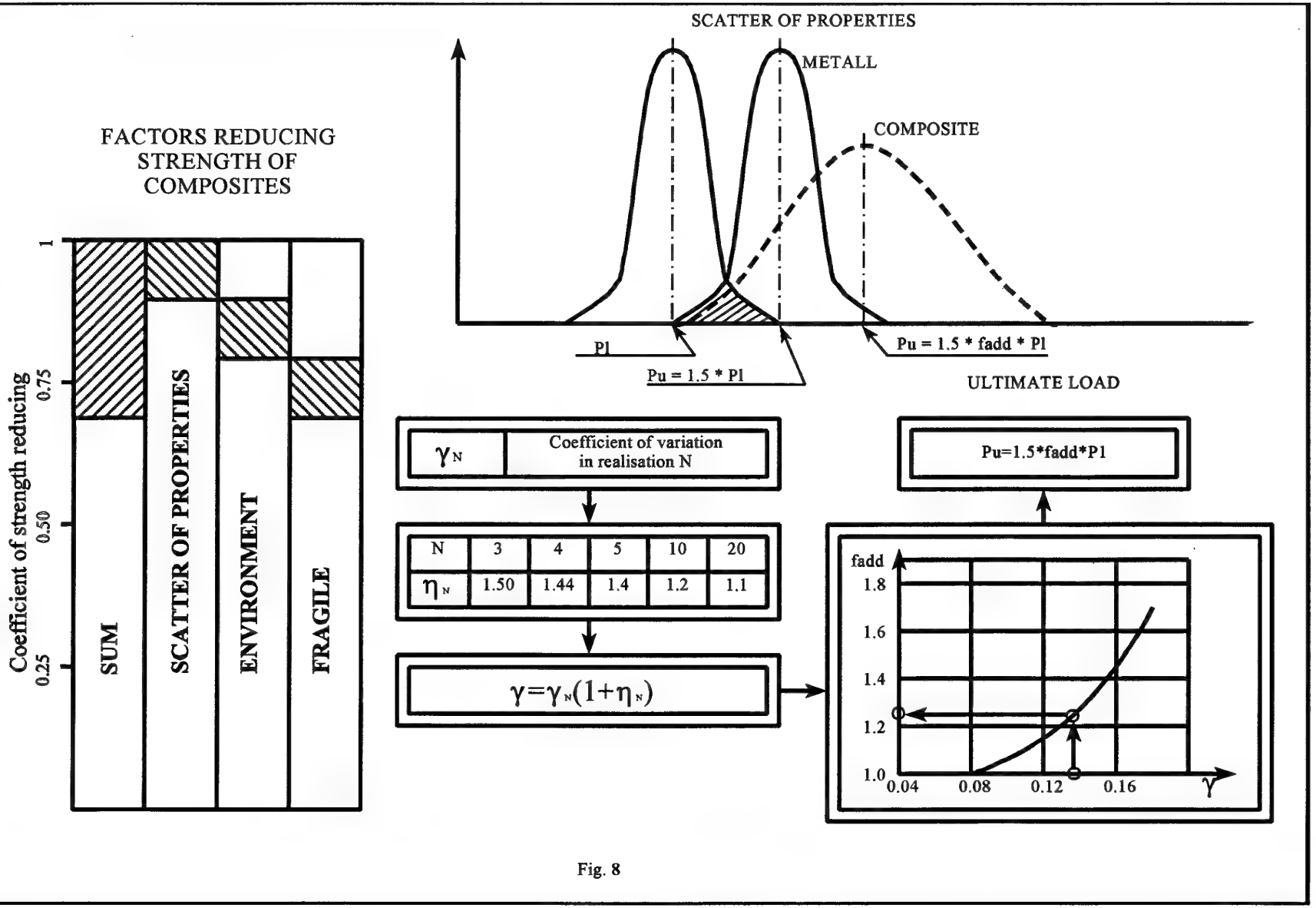
FACTORS REDUCING STRENGTH OF COMPOSITES
Coefficient of strength reducing
1
0.75
0.50
0.25
SUM
SCATTER OF PROPERTIES
ENVIRONMENT
FRAGILE
SCATTER OF PROPERTIES
METALL
COMPOSITE
Pl
Pu = 1.5 * Pl
Pu = 1.5 * fadd * Pl
ULTIMATE LOAD
γN
Coefficient of variation in realisation N
N 3 4 5 10 20
ηN 1.50 1.44 1.4 1.2 1.1
γ=γN(1+ηN)
Pu=1.5*fadd*P1
fadd
1.8
1.6
1.4
1.2
1.0
0.04
0.08
0.12
0.16
γ

Fig. 8

ENVIRONMENT INFLUENCE ON CARBONPLASTIC STRENGTH

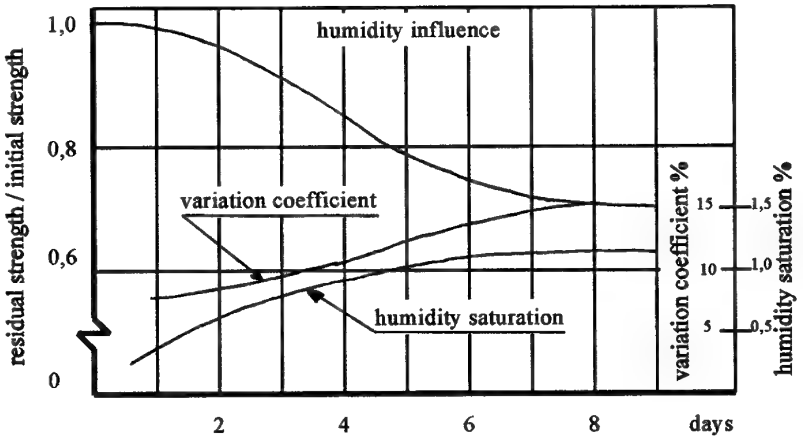

TEMPERATURE AND EXPOSURE INFLUENCE (COMPRESSION)

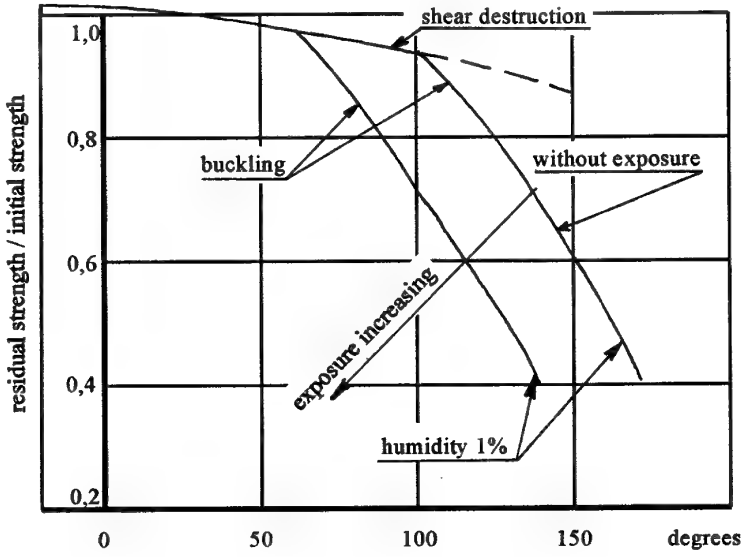

AIR-BRAKE
COMBINED ACTION OF ENVIRONMENT AND LOADS

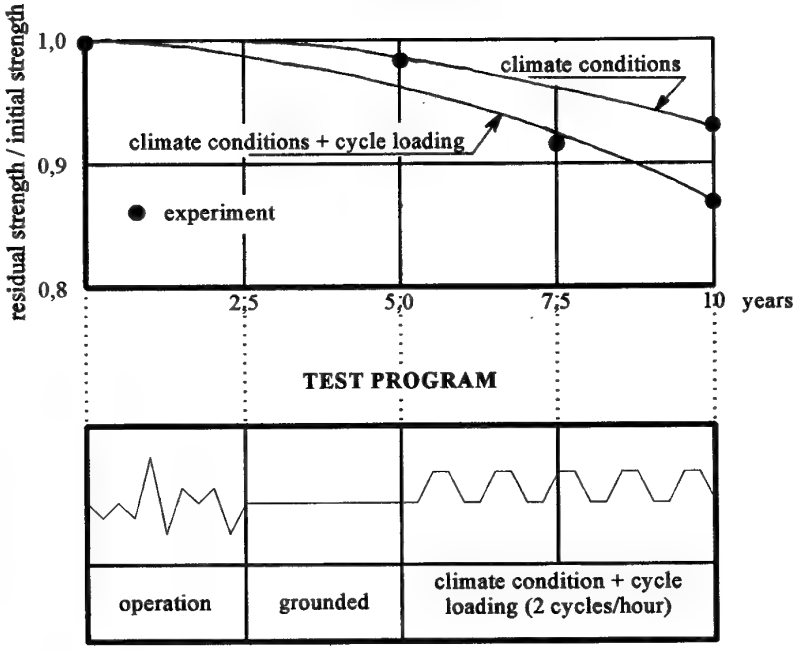

Ken < 1 - correction because of environment influence on design stress choice

Established on a basis of:
- analysis of operating experience.
- experiments

Fig. 9

FRAGILE DESTROYING

BEHAVIOR OPERATION MODEL OF METAL AND COMPOSITE

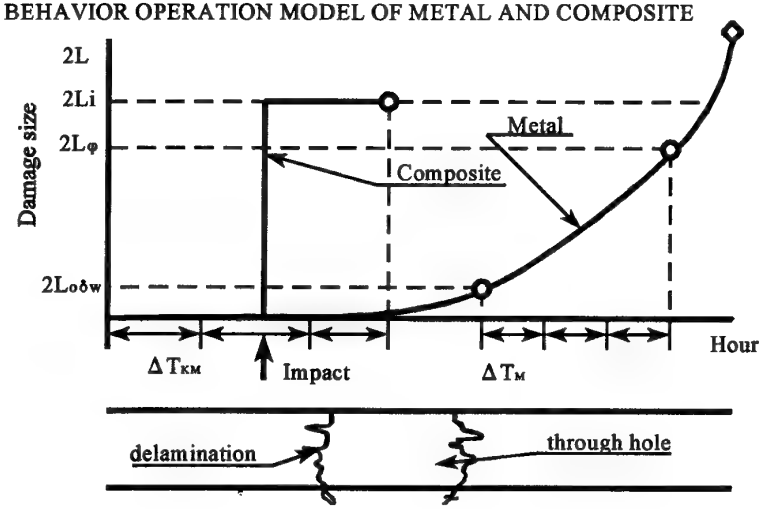

a) HIGH - ENERGY IMPACT

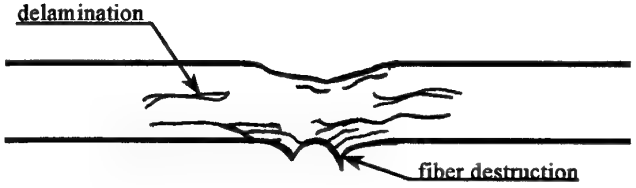

b) MODERATE - ENERGY IMPACT

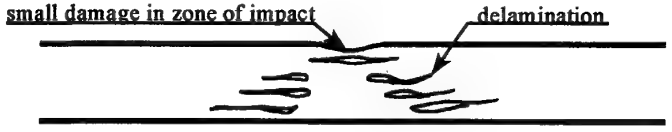

c) LOW - ENERGY IMPACT

COMPRESSION STRENGTH DECREASE WITH IMPACT DAMAGE

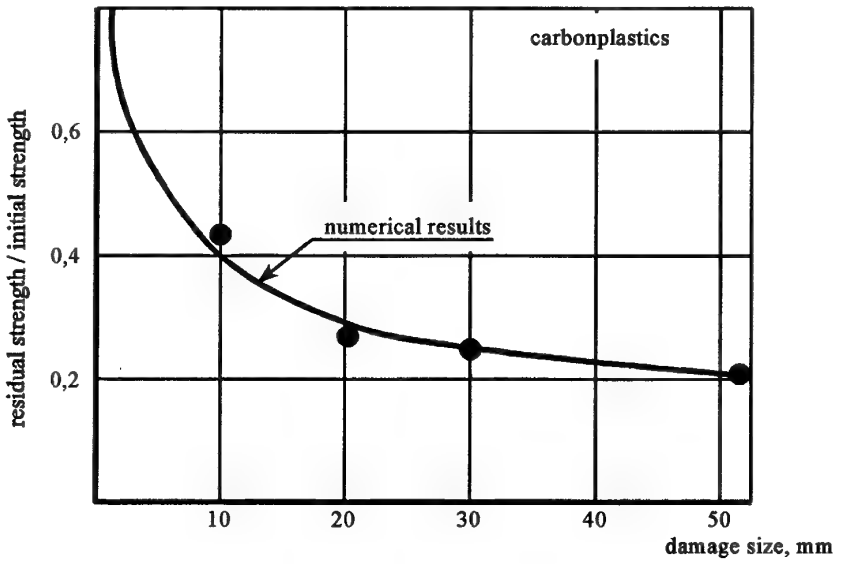

- DESIGN APPROACH - FAIL SAFE STRUCTURE.
- CHOICE OF DESIGN STRESSES IN VIEW OF REGULATED DAMAGES (Kr.d < 1)
- PROVISION WITH RELIABLE CONTRAL:
  a. VISUALLY DURING EXAMINATION BEFORE FLIGHT
  b. INSTRUMENTAL, NONDESTRUCTIVE DURING REGULATIVE EXAMINATION
- TYPICAL EXPLOITATION REPAIR TECHNOLOGIES DEVELOPMENT

Fig. 10

ADVANCED POLYMER COMPOSITES: APPLICATION FOR AVIATION AND AEROSPACE STRUCTURES

BY

T.G. SORINA
VIAM, MOSCOW 107005
RUSSIA

ABSTRACT

Considered in the article are issues related to improvement of properties, fabrication and use of Polymer Matrix Composites based on graphite, organic and glass fibers for aerospace industries of Russia and other countries of the CIS. The best effect is shown to be attained when a partial involvement of these materials (for making certain structures) is transformed into "global" design of large structures out of the PMCs.

SYMBOLS

E	Young's modulus in tension
σ_b	ultimate stress in tension
σ_{-b}	ultimate stress in compression
ρ	mass density
T_g	glass-transition point
G	shear modulus
ε	elongation to rupture

ABBREVIATIONS

CFRP	Carbon Fiber Reinforced Plastic
GFRP	Glass Fiber Reinforced Plastic
PMC	Polymer Matrix Composite
TsAGI	Central Aero-Hydrodynamic Institute, Russia
TsIAM	Central Institute of Aviation Motors, Russia
LII	Flight Research Institute, Russia
NIISU	Research Institute for Automatic Control Systems, Russia
NIAT	Research Institute for Aircraft Manufacturing Processes, Russia
UVZ	Ukhtomsky Helicopter Plant, Moscow region, Russia

Introduction

The Russian Institute for Aviation Materials (the VIAM) is the largest center in the materials science field, unique in respect of the complexy of scientific areas covered. The Institute undertakes research and development for materials of all classes, types and kinds necessary for aviation and space technologies. VIAM is a basis for a certification center accredited by the Gosstandard.

VIAM, in cooperation with other major R&D institutes of the industry (TsAGI, TsIAM, LII, NIISU, NIAT),

- establishes trends in aviation materials development for the far and near time periods,
- takes part in implementation of multidisciplinary scientific research programmes budgeted by the Russian Federation Government,
- conducts basic research intended to form a basis for the future, including advanced materials and new manufacturing processes; at that stage the programmes are undertaken in collaboration with Academy of Sciences institutes, higher education system laboratories, and science centers of other industries.

These studies outline new manufacturing processes and materials (their chemical and "geometric" composition), together with main characteristics evaluation.

When the necessity to prepare a novel aviation technology item appears, we develop and certificate the materials in agreement with specifications prepared by Design Office and approved by TsAGI and/or TsIAM; the work package is usually based on the previous advanced studies and financed by the customer.

VIAM holds a major place in the development and certification of structural Polymer Matrix Composites (PMCs) based on high-strength fibers.

New PMCs (as well as metals) are developed in agreement with requirements of the Aviation Materials Development System (Fig. 1), including

- certification of new materials (prepregs) and manufacturing processes for preparing them,
- development of technical standards for test methods/procedures and amounts of structures made out of PMC'S,
- development of technical standards for manufacturing the semi-finished items and transforming them into final structures,
- developer's supervision.

Paper presented at the AGARD SMP Lecture Series on "Advanced Polymeric & Metallic Composite Materials for Space and Aerospace Vehicle Structures. . .", held in Stuttgart, Germany from 11-12 December 1995; Châtillon, France from 14-15 December 1995 and Ohio, USA from 18-19 December 1995 and published in LS-204.

The stages of development and implementation of new materials are accompanied with a set of documents:

- materials certificates,
- prepreg type certificates,
- prepreg/semi-finished item delivery specifications,
- process-concerned scientific and technical documentation for stages of manufacturing the semi-finished items, transforming them into final structures, and controlling the quality,
- a list of materials utilization restrictions for structures at the design stage,

a conclusion on conformity of materials characteristics with Aviation Regulations requirements.

Advanced Polymer Composites

Polymer-Matrix Composites can be used in various applications; their characteristics can be varied purposefully by simply changing the reinforcing fibers (such as glass, carbon, organic) and the layup sequence; the use temperature range may be widened by utilizing various classes of polymer matrices (including ceramics forming materials); composite structures can be manufactured in highly automated production lines. These, as well as many other qualities ensure great interest in this kind of materials [1].

Table 1 demonstrates structural properties of typical composites -- carbon- and glass-reinforced plastics with quasi-isotropic layups (0/90/±45°) -- in comparison with traditional metals. With respect to fundamental characteristics (the mass density, modulus of elasticity, short-term and long-term static/fatigue tensile/creep strength, damping capability, vibration resistance/ compliance, corrosion resistance) the polymer matrix composites within the -60° through +200°C temperature range are superior to aluminum alloys titanium alloys and steels under certain conditions. As for fracture toughness and interply strength/stiffness, the PMCs do not compete with metals. However, by involving heterofilamentary and hybrid matrix systems the characteristics of the materials in structures can be improved.

PMCs turned out to be effective in military aircraft and rockets; this has been evidenced by long-term successful experience in operations. The utilization of PMCs in military applications enabled the civil aviation industry to widen utilization of these material systems; for instance, the IL-96-300 passenger-carrying airplane incorporates 2.5 t polymer matrix composites, and the AN-124 transport, 5.5 t.

The superiority of reinforcing fibers in elastic behavior and strength characteristics is mainly seen in properties of unidirectional composites, whereas the contribution of the matrix is seen in almost all static, dynamic, serviceability, workability and environmental characteristics of materials; note that, in most cases, it is the matrix and interface properties that are important, especially for cross-ply stacks.

There exists the obvious need to unify PMC structure manufacturing processes, maximize the equipment utilization efficiency, save costs of materials R & D, and fabricate hybrid structural parts; therefore it is common to use a single matrix with fillers of various types (such as graphite, glass and polymer fibers). Derivation of composites with prescribed properties (including workability figures) is based on development of matrices and on investigation into how matrices and interfaces form.

Used as major matrices for structural PMCs are currently epoxies, the materials that provide the highest post-cure characteristics, ensure good adhesion to fibers of various types, and can be cured at relatively low temperatures and pressures with minimal shrinkage.

Thermostable epoxy matrices (such as ENFB and VS-2526) with a maximum use temperature of 150–160°C can be based on epoxy/novolac and polyfunctional epoxy resins to be cured with amines or latent curing agents, e.g., ionizing substances. Such catalysts made it possible to derive epoxy/novolac matrices for prepregs with a room-temperature life time of over a year.

Compositions 5-211B, EDT-69 and UP-2227 with lower glass-transition temperatures (not exceeding 130°C) are based on diane-type epoxies cured by aniline phenol formaldehyde oligomers and urea derivatives.

Thermostable polymers most suitable from the workability point of view include polyimides SP-97 and SP-97M, PAIS series polyamidoimides, and OMI series oligoethermaleinimides; they are currently used in aviation technologies and other machines. The PAIS-104 polyamidoimide matrix ensures a monolithic material (with a 1–3% content of voids) and high mechanical characteristics over a -130° through +250°C temperature range.

Typical thermoplastic agents used to make the matrices of structural PMCs include polysulfon (PSN), polyethersulfon, polyetheramidoimide; they are stable at temperatures of up to 170°C, soluble in commonly used solvents, delivered in films and powders, and transformed into composite materials at relatively low pressures (10–15 kgf/sq.mm) and temperatures (260°–280°C).

It should be noted that behavior of PMCs with a particular matrix depends on the chemical properties of reinforcing fibers. Interaction of the components influences the prepreg life-time, PMC cure temperature/pressure, and variation in characteristics under effects of moisture and heating/cooling. Examples may be seen in Table 2: the influence of fibers on water absorption, cure temperature, and glass-transition temperature.

When combining various fillers in a single structure, the use temperature is prescribed proceeding from the lowest value of T_g.

The pre-cure aggregative state of binding agents is a determinant for semi-finished item fabrication processes. For example, prepregs with the PAIS-104 binder are fabricated by electron/ion-driven deposition of a preparation powder onto graphite fillers followed by the melting of the system in a furnace. Semi-finished items based on binders UNDF-4a, OMI, and VS-2526 are produced by melting. Binders EDT-69, ENFB, and UP-2227 are deposited onto fillers by solution impregnation; and VS-2561 is infiltrated under pressure. The PSN thermoplastic binder delivered in the form of films is added to fabrics and tapes by the lamination technique.

Prepreg certification procedures have been developed employing various state-of-the-art physical, chemical, and mechanical options for validating the materials:

- differential scanning calorimetry,
- X-ray inspection,
- liquid chromatography, etc.

The following parameters are checked:

- weight fractions of resin and fibers,
- adhesion capability,
- excess resin percentage,
- gel formation time,
- fractions of soluble resin and volatile species,
- glass-transition temperature range,
- tensile/compression strength and Young's moduli,
- shear/bending strength of unidirectional composites prior to and after moisture absorption.

Because both a material and a structure are created simultaneously, experts in the materials science and manufacturing processes are being actively involved in works at stages of concept definition, design, and commitment in mass production of structures.

It is generally known that the to-day's wide range of composite materials originated from Glass Fiber Reinforced Plastics (GFRP). Initially, these were for military technologies. The GFRP feature is a very appropriate combination of structural strengths and widely controllable dielectric properties, including permittivity and loss angle being stable throughout life cycle. GFRPs remain irreplaceable for radio engineering applications [3].

As for properties and variety of textile forms, the Russian-produced fillers based on glass fibers are on par with international analogues. GFRPs were improved by developing new matrices (Fig. 2) and are effectively utilized in civil aviation. For example, much work was accomplished to create prop-fans, engines that open prospects for improving the weight/cost characteristics of currently used airplanes; propeller blades are extremely sophisticated designs based on glass fiber reinforced plastics and other composites. The work has been successful in what concerns fatigue strength (250 MPa on the basis of 10 million cycles), noise suppression, engine weight reduction (some 600 kilos), fuel saving, and service life length. An engine with such blades is operated on IL-114 airplane; the fuselage structure and high-lift devices of this airplane are made mainly from PMCs. The wide use of GFRPs is chiefly due to their price which is much less than the prices of CFRPs and organoplastics.

However, glass fiber reinforced plastics play only secondary roles in airframes. These materials are not competitors to metals because of a relatively low modulus of elasticity. Given the high strengths (the ultimate stress σ_b=2000 MPa), GFRPs are only 1 – 4 percent in airframes, mainly within low-stress structural parts. In contrast, helicopter primary structures have up to 35% weight fraction of these materials, utilized in highly stressed elements such as main-rotor spars (Table 3).

The advent of second-generation composite materials (such as organoplastics and CFRPs that are superior to Al and Ti alloys with respect to a set of main properties) has established premises for considerable utilization of composites in airframes.

Graphite/epoxy systems are of special importance in aviation materials science. They possess unique combinations of characteristics and surpass traditional structural materials in respect of specific stiffness, fatigue strength, chemical stability, corrosion/radiation/ fungus resistance, high heat-conductivity, low temperature expansion coefficient; these materials maintain dimensions at high and low temperature; their electric properties may be adjusted to an application type.

CFRPs have a feature that enables designers to consider the materials as a promising substitute for metallic alloys in aircraft construction: high allowable tensile and compression stresses not compromised with a high modulus of elasticity; this is extremely important in maneuverable airplanes [4].

Used as fillers for structural composites are high-strength and high-modulus graphite fibers. The fillers are produced in the form of

- thin tapes (with weak graphite weft filaments), brands LU, ELUR, LZhU and
- untwisted roving, brands UKN, Kulon, Granit, differing in filament percentage (2.5k, 3k, 5k, 6k).

The high-strength and high-modulus graphite filaments for use in load-carrying structures are mandatorily subject to surface treatment, rovings are covered with sizing.

The LUP and ELUR-P CFRP tapes (with P in the brand name symbolizing the surface treatment) have notable

advantages: no sizing on surface, good wettability with various binders, shape-maintaining ability (while in molds) at ply thickness of 0.08–0.1 mm. The tapes are widely utilized to fabricate thin skins and enable manufacturers to implement complex layups with low residual stresses in thin (less than 1 mm thick) stacks.

The UKN-P graphite rovings have been a basis for developing the equally strong fabrics, UT-900, and tapes, UOL-300. In the latter, weft filaments are fine glass and/or organic fibers. Characteristics of the graphite/epoxy systems are represented in Fig. 3.

The GFRPs include thermoset and thermoplastic binders that ensure excellent realization of elastic and strength characteristics of the fillers within the temperature ranges prescribed. As an example, Table 4 represents properties of CFRPs incorporating the EDT-69 matrix and fibers fabricated in Russia, the USA and Japan.

The KMU-7 series CFRPs (with σ_b=1–2 GPa, E=140–240 GPa, τ=9 MPa) can be used in the temperature range from -60 to +150°C wherein the strength characteristics do not fall below 70%. The KMU-7VM high-modulus material (based on the Granit-40 high-modulus braid) has E=240 GPa, the elongation at rupture ε=0.7%, σ_b=1450 MPa, and σ_{-b}=1150 MPa. The KMU-4 graphite/epoxy system based on thin graphite tapes features advanced workability, 1-year life-time (at 20°C) and the maximum use temperature of 160°C.

The KMU-8 thermostable graphite/epoxy system based on graphite tapes and polybismaleinimide matrix is intended for parts that are subjected for a long time to temperatures from -130° to +160°C. This material is suitable for manufacturing shaped parts and integral structures with stiffeners, radiused zones and thickness jumps. Materials KMU-11 and KMU-15 are in wide use within passenger-carrying and sporting airplanes.

Developers of structural materials pay particular attention to their behavior in the course of temperature variation in moist atmosphere.

Studies showed that the safe moisture-content for CFRPs is 0.6–0.7%. If moisture content grows (up to saturation) the material degrades in respect of the maximum use temperature, strength and elastic characteristics. The irreversible loss of component characteristics depends mainly on manufacturing conditions and residual stresses.

When designing graphite/epoxy structural components to be used in moist atmosphere, the developers should change the allowable operating temperature; account must be taken of both the shift in glass-transition temperatures of the moist material and notable degradation of mechanical characteristics in the case of heating over the new value of T_g after moisture absorption.

Studies revealed that T_g of moisture saturated graphite/epoxy materials decreases by 20–30%. A simultaneous impact of alternating temperatures (from -60° to +60°C), moist air, and usual in-service loads ($0.25\sigma_b$ and $0.5\sigma_b$, with 30 cycles being conditionally equivalent to 30 years of operation) worsen the compression and shear strength characteristics by 13–20%.

Performance of CFRPs in natural conditions for 20 years was observed. The study confirmed that the accelerated aging method may be allowed to be involved for predicting the long-term behavior of carbon fiber reinforced plastics.

The very important advantage of the CFRPs is their high fatigue limit that exceeds the fatigue limit of aluminum alloys by a factor of 2 or 2.5 (based on 10 million cycles).

The high fatigue resistance is much dependent on fiber orientation. Unidirectional materials have notably higher characteristics than the cross-ply ones. Fatigue resistance of the cross-ply stacks are much dependent on transverse characteristics of the CFRP. Increasing by 20–30% the ultimate transverse stress and the flatwise tension strength results in two-fold increase of the fatigue limit.

Studies showed that graphite/epoxy materials with thermoset matrices have low resistance against concentrated low-speed loads and dust erosion. In order to improve these characteristics, the formulations of the materials were modified, and special thin coatings were developed on the basis of filaments and discrete fibers that are applied in the usual manufacturing process; the erosion resistance gets increased by a factor of 10 to 20. Table 5 provides data illustrating the CFRP erosion resistance improvement due to application of thin (100 mum thick) coatings, VPT-1 and EPK.

The use of textile forms made of graphite fibers and binary matrices (comprising epoxy and thermoplastic resins) was shown to increase residual strength after impact (by 60–80%), reduce the cracking area, and localize damage, see Table 6.

One of problems in the field of ensuring reliability and safety of aviation technologies is ensuring the lightning strike resistance of airplane structures.

It is known that the probability of airframe damage by lightning depends on the location of a structural component on the airplane. Three basic zones are depicted in Fig. 4:

- Zone A: effects of immediate primary discharge,
- Zone B: high probability of current,
- Zone C: no immediate contact with lightning.

After electric impact, graphite-based materials get considerable damage. Because of the wide use of these materials in airframes, their lightning protection became an important concern to designers.

For Zone A the reusable protection option has been developed; it is an external high-conductivity ply which

ensures multiple protection of graphite-based structures against direct lightning strike, at the 0.99 probability. The 0.22 mm thick conducting layer is applied to the CFRP stack preform surface and bond to the stack during the cure stage. This layer is attached reliably by treating its surface in a special way. The layer takes loads together with the skin, improves erosion resistance, and raises mechanical characteristics of the skin.

For Zone B several versions of lightning protection systems based on special textile forms from graphite filaments with improved conductivity have been prepared. These fillers have physical (and mechanical) characteristics close to those of the graphite fillers of the protected skin, therefore such components take the loads on par, thus the weight increment is extremely insignificant, 100 g/sq.m. A feature of the system is the coating being manufactured and attached to the CFRP skin the through the manufacturing process. Tests showed these protection systems to be appropriate as expendable protection-options for Zone A.

Experimental data suggest that Zone B may be made out of CFRP without protection.

In order to estimate the potential for utilizing the CFRPs in space technologies, mechanical characteristics of these materials were carefully studied after

- radiation-induced aging,
- exposure to combination of temperature gradients, deep vacuum (10^{-6}–10^{-9} atm) and ultraviolet radiation of appropriate intensity, and
- a hold time in space.

Figure 5 demonstrates changes in tensile and in-plane shear strengths of a KMU-4e CFRP sheet with a stacking sequence typical of the BURAN skin; the test conditions corresponded to

- a stay in an intended orbit,
- 80 takeoffs and landings, and
- ground storage/maintenance

over a period of 10 years. Figure 6 shows changes in compression strength for the 150–450 K temperature range. One can see that the ultimate shear stress slightly decreases during the initial 20 cycles then stabilizes, while both the tensile and compressive strengths remain constant; these data evidence serviceability of the material under such conditions.

The efforts for implementing carbon fiber reinforced plastics in domestic aviation technologies were begun in 1976. During the past period we at VIAM have developed more than 20 brands and modifications of structural CFRPs that differ in their mechanical characteristics, workability, operating temperatures, etc.

At stage 1 we adopted and implemented the concept of development of separate composite structures for airplanes AN-24, AN-22, YaK-40, IL-86, and SU-26; performance of the materials in service was thoroughly monitored. Data acquired confirm in-service reliability and weight efficiency of the CFRP structure and have been a basis for introducing composite structures in airframes of newly developed technologies:

- airplanes MIG-29, AN-72, AN-124, TU-160, SU-27, and YaK-42,
- helicopters MI-28 and KA-32,
- gas turbine engines D-36 and D-18, and
- BURAN reusable aerospace vehicle.

For the first time a large series of CFRP structural components were introduced by the Mikoyan Moscow factory – in MIG-29 airframe; 12 items with a total weight of 90 kg provided an overall weight saving of 105 kg.

A modification, MIG-29M, already included 16 parts with a 137 kg total weight that provided a 140 kg overall weight reduction.

In the structure of a new state-of-the-art fighter airplane prepared by Mikoyan factory, the amount of structural CFRPs was 25% of the airframe weight, saving 350 kg of the total weight (Fig. 7).

Simultaneously, the use of CFRPs in structures developed at the Mikoyan Design Bureau made it possible to reduce the total number of load-carrying parts by a factor of 2, to eliminate hole drilling and riveting operations (thus reducing the labor requirements by 12–25%) and to shorten the manufacture cycle (for the parts with CFRPs) by 20–25%. Technical and cost efficiency of CFRPs (KMU-3) may be illustrated by data for the AN-124 passenger airplane. Here, the total amount of composites is 2.2 t (in 200 parts), the weight saving reaches 0.8 t, the materials utilization factor has been increased to 85%; the Al alloy weight saving is 6.0 t.

The industry manufacture of parts and large units out of CFRP made a significant step forward. For the first time these materials have been widely used in structures of passenger airplanes developed by Ilyushin Design Bureau (IL-96-300 and IL-114) and Tupolev Design Bureau (TU-204 and TU-334).

When designing the structures, the industry have to find out a compromise between

- the desire to attain a maximum possible weight-efficiency due to introduction of CFRPs with extremely high mechanical characteristics and
- the structure manufacturing costs.

Therefore, although there exist CFRPs with very high strength (2500 MPa) and elastic modulus (300 GPa), the industry mainly utilizes materials with a ply strength of 1000–2000 MPa. Figure 8 demonstrates dependence of amounts of structural CFRPs on levels of strength, elastic modulus and use temperatures. Over 50% of the presently used structure are fabricated out of CFRPs with the ply strength of 1500 MPa, and only 15%

require a value in excess of 2500 MPa; for 75% the acceptable Young's modulus is 120–150 GPa; only 25% of the materials should withstand temperatures over 300°C.

In parallel with implementation of CFRPs in aviation the work was started to use these in rocket and space vehicles. Similarity of challenges in these two areas resulted in similar stages of efforts.

At the initial stage the CFRPs were introduced in low- and medium-stress parts of rockets: fairings, doors, some units in bodies of launchers. However, pilot structures were also developed, taking advantage of such unique properties as almost zero thermal-expansion and high damping capability: trusses and frames of optical devices, reflectors of aerials, etc. This kind of structure is for operation in real space conditions, which has been a reason for evolving efforts to study the dependence of stability and serviceability of the material on intensity of space factors including deep vacuum, oxygen atoms, cosmic rays and solar radiation, drastic temperature cycles/gradients.

Experiments evidenced the high resistance of the CFRPs to space factors and became a basis for R & D aimed at development and mass production of a set of units from CFRPs:

- frames of reusable solar batteries for "Mir-2" station and many other special items,
- BURAN payload bay doors,
- BURAN on-board manipulator bar,
- a mechanism for deploying the CFRP blind on "Yantar" spacecraft,
- "Energia" launcher fairings of 5000 kg total weight,
- feeders on "Molnia" communications satellites,
- structural parts of automatic interplanetary stations "Luna," "Venera," "Mars," and "Halley comet,"
- parts of telescope on "Almaz" satellite,
- space communications satellite aerial reflectors that are installed on almost all "Kosmos"-type satellites and other space technologies.

The CFRPs in reusable solar batteries made it possible to increase the specific power capability by 30%, simplify (dis)assembly work for replacing out-of-date batteries, and settle the problem of power generation for modules added to the station.

Structural CFRPs are used not only in aviation and space technologies but also in many other branches of the national economy. A growth in the utilization amount is very noticeable in the last three years due to defense conversion and reorientation to civil products.

The organoplastics presently used by the aviation industry are based on the polyheteroarylene fibers, SVM, produced in Russia. The SVM fibers have liquid crystal microstructure and are not inferior to Kevlar-49 (Table 7). Organoplastics are derived from epoxy resins and their modifications based on polyfunctional aromatic compounds that form densely connected thermostable meshes during cure. Utilized as the curing agents are various amines: diamine diphenyl sulfon (DADFS), triethylene amine titanate (TEAT), aniline formaldehyde resins, anhydrides and latent curing agents [5, 6].

The mass production facilities mainly utilize the binder based on the 5-211-BN epoxy aniline formaldehyde resin. This binder is used in textile prepregs for textolite sheets. Long-life adhesive prepregs with good adhesion to honeycomb cores are produced by infiltrating the solutions of epoxies UP-2227 and EDT-69n. Thermostable organoplastics for long service at 150°C have been based on a modification of an epoxy resin cured with aromatic diamine (VS-2526k). In manufacture of metal-organoplastics, use is made of adhesive films from epoxy-sulfon (VK-36) and epoxy-rubber (VK-41).

Table 8 represents the main types of organoplastics, which differ in chemical composition and constitution, properties and major applications. It has been shown that adding glass, graphite or boron fibers to a polymer composition can notably raise the compression strength of organoplastics. The latter are costly materials, so that particular attention is paid to modifying them by adding cheaper glass fibers, VMP. Addition of 40% fraction of glass fibers increases the compression strength by a factor of two (400–450 MPa).

The whole set of mechanical properties of the organoplastics was analyzed, as well as the experience in designing and operating aircraft structures made of these materials. The data available suggest that the highest technical and cost effect is attained in the cases where developers are capable to simultaneously use the following major features of organoplastics as structural materials:

- unique high specific strength and stiffness in tension,
- high fracture toughness,
- low rate of fatigue crack growth,
- capability to accumulate damage for a long time without forming a critical crack,
- low sensitivity to stress concentration,
- high damping ability,
- good impact strength,
- erosion resistance (against dusted air and rain flow).

Moreover, these properties are supplemented with high thermophysical and dielectric characteristics, high chemical stability (in contact with agressive media), ability to retain the properties at both elevated and cryogenic temperatures. Considering organoplastics, they can be involved as structural materials in very diverse applications.

In airplane structures, organoplastics are used as monolithic parts and skins in sandwiches. For the first time in aviation organoplastics were employed to manufacture light-weight trailing edge flap sandwich

panels, wing trailing edge structures, partitions, fairings, etc. in AN-28 transport. In the AN-124 ("Ruslan") the mass of parts with organoplastics has reached 2800 kg; the total area of organoplastic parts is about 1000 sq.m; in particular, the fairing for the landing gear has the area of 155 sq.m and reduces mass by a factor of two as compared with the metallic prototype.

Organoplastics have been used in structural components of passenger airplanes (IL-86, IL-96-300, IL-114, TU-204, TU-334, YaK-42). The most comprehensive utilization is seen in Tupolev airplanes: skins of lowand medium-stress sandwich panels (engine cowl doors, fairings of pylons, fin, fairings between a wing and a landing gear sponson allowing – a weight reduction of 12–26%). Skins for more severely loaded large-size structures are manufactured out of hybrid composites in which the layers with aramid and graphite fibers (in a proportion from 1:3 to 1:1) are intermittent. Of the 4.4 t of PMCs in TU-204 organoplastics are about 3 t; the mass saving is 1.2 t.

Organoplastics are used in helicopter structures: KA-26, KA-32, MI-26, MI-28, MI-38, etc. For the first time, in our joint work with the Ukhtomsky helicopter plant (UVZ), the concept of development of separate PMC elements (in a mainly metallic structure) has been replaced by the concept of manufacturing units with polymer sandwich panels; and further, the manufacturing of modular composite structures. At the first stage the helicopter included more than 400 parts from organoplastics, with 160 of these replacing metallic ones. Almost all external panels (105 pieces) of the helicopter have skins made of organoplastics and OSP with a T-39 combined fabric. These materials are in load-bearing panels of highly stressed units including the cabin, tail unit, wings, trailing edge flaps, and fuel tanks. In main rotors the organoplastic sheets have been successfully used as skins of dynamically loaded tip sections (service life increasing 10–12 times; a better center-of-gravity position due to a weight saving in comparison with a GFRP prototype).

The total material utilization factor has been increased to 0.8–0.9, and the mass of units of the airframe has been decreased by 14%. In addition, damage tolerance was improved, and the service life was raised by a factor of two to three. The wide use of PMCs, and organoplastics in particular, reduced labor requirements and energy consumption by a factor of 1.5 to 3.

Due to the wide implementation of structures made out organoplastics and related hybrid composite material, at the UVZ the concept of partial use of PMCs in separate items has for the first time been replaced with the concept of wide utilization (30–35%) of the materials; furthermore, new helicopter struictures using up to 50 to 60% of PMC's is now prevailing.

Load-carrying skins loaded in tension and submitted to vibrations, acoustic and impact loads are recommended to be fabricated out of multilayer metal/organoplastics. Properties of ALORs are reported in Table 9. These skins made it possible to reduce the structural mass by 20 -25%, improve reliability and service life by a factor of 5 to 10, increase vibration resistance by 30–40%, and improve heat/acoustic isolation by a factor of 1.5–2. The most considerable effect of combining organoplastics with Al alloys is seen when the ALOR is fatigue loaded; the crack growth rate drops down.

Depending on composition of the ALORs, the tensile strength limit is 500–1000 MPa, and the Young's modulus is 70–110 GPa (while decreasing the mass density from 2.4 to 2.2 g/cu.cm). The fatigue crack growth rate gets as low as 0.1–0.4 mm/kcycle.

Owing to the unique set of unique characteristics, this class of materials is much promising for various engineering industries.

With the experience in advanced manufacturing processes gained, the costly special-purpose equipment/facilities available, and highly qualified personnel at hand, it has been possible to organize rather simply the mass production of wide ranges of machine tool/car parts, excellent sporting appliances, gliders, yachts, and medical technologies, in quite a number of Russian Companies.

REFERENCES

1. R.E.Shalin, G.M.Gunyaev. Development of composites -- basis of changes in the structure of usage of materials in industry. J. Advanced Materials, 1994, 1(3), pp. 241 - 245.
2. T.G.Sorina, G.M.Gunyaev. Structural carbon fiber reinforced plastics and their properties. In: Polymer matrix composites, vol. 4. Chapman and Hall, London, 1995, pp. 132 - 198.
3. B.A.Kiselyov. Glass plastics. In: Polymer matrix composites, vol. 4. Chapman and Hall, London, 1995, pp. 229 - 268.
4. G.M.Gunyaev, T.G.Sorina, A.F.Rumyantsev, I.P.Khoroshilova. Aviation materials at the edge of the 21st century. Collection of papers, Printing Office of VIAM, 1994.
5. V.D.Protasov. Organoplastics. In: Polymer matrix composites, vol. 4. Chapman and Hall, London, 1995, pp. 199 - 227.
6. G.P.Mashinskaya, B.V.Perov. Principles of developing organic fiber reinforced plastics for aircraft engineering. In: Polymer matrix composites, vol. 4. Chapman and Hall, London, 1995, pp. 305 - 422.
7. G.P.Mashinskaya, G.F.Zheleznina, O.G.Senatorova. Limited fibrous metal/polymer composites. In: Metal matrix composites (ed. by I.N.Fridlyander), Chapman and Hall, London, 1995, pp. 487 - 568.

Table 1

Comparison of structural materials

Material system	Density ρ, kg/cu.m	Young's modulus E, GPa	Fatigue limit at 10 million cycles, MPa	Log decrement, %	Vibration resistance	Frequency parameter $(E/\rho)^{0.5}$	Specific strength, km
Graphite/epoxy*	1550	58	250	3.2	0.80	62	36
Glass/epoxy*	2000	30	200	4.6	0.65	40	30
Aluminum alloy	2700	72	130	0.65	0.09	51	14
Titanium alloy	4500	120	500	0.03	0.015	52	27

* Layup sequence: (0, ±45, 90)

Table 2

Polymer matrix composites with UP-2227 epoxy resin: moisture absorption (M), diffusion (Dx), and glass point (T_g)

Material	T_{cure}, °C	Forming-pressure, MPa	Porosity, %	M, %	Dx, 10^9 cm^2/s	T_g		Prepreg life time, months
						moist	dry	
Glass/epoxy	150	0.5	1.8	1.9	1.6	140	105	2
Graphite/epoxy	150	0.5	1.2	1.4	1.35	135	100	1.5
	170	0.5	1.0	2.1	1.65	120	80	1
Organoplastic	150	0.5	9	9	2.8	160	135	3

Table 3

Amounts of Glass Fiber Reinforced Plastics in structure of some airplanes and helicopters

Name	Composites percentage in airframe weight	Major parts
Airplanes		
IL-62M IL-86 IL-96-300	2.0 3.9 1.0	Sandwich fairings; internal panels; interior; partitions; floor panel skin; dielectric spacers; etc.
YaK-42	1.5	Auxiliary power unit air duct; air intakes; fairing; container; etc.
TU-154 TU-204	1.6 1.5	Fairings; thermal protection; floor panels; air ducts; etc.
Helicopters		
KA-26 KA-32 MI-28	5.0 16.0 36.0	Main rotor blade spars; sprayers; skins; fairings; equipment containers; partitions

Mechanical properties of PK-11 prepregs

Table 4

UNIDIRECTIONAL PREPREGS					
TYPE OF PREPREG			PK11LR5.0	PK11LT6.0	PK11LA6.0
TYPE OF CARBON FIBER			UKN-P-5K	TORAYKA T300-6K	MAGNAMITE AS-4-6K
TYPE OF MATRIX RESIN			ETD-69N	EDT-69N	EDT-69N
PROPERTIES	UNIT	METHOD			
0 - TENSILE STRENGTH	MPA	AST M D3039	1600	1760	2000
0 - TENSILE MODULUS	GPA	AST M D3039	135	138	138
0 - COMPRESSIVE STRENGTH	MPA	AST M D3410	1250	1380	1290
0 - COMPRESSIVE MODULUS	GPA	AST M D3410	115	119	119
INTERLAMINAR SHEAR STRENGTH	MPA	AST M D2344	82	90	84

Table 5

Erosion resistance*

Material	Coating thickness, mum	Relative depth of erosion (=1 for KMU-4)
KMU-4	—	1
KMU-4 + VPT-1	100	0.1
KMU-4 + EPK	100	0.05

Corundum mass flowrate = 9.6 kg/sq.m·s;
impingement angle = 90°;
impact speed = 65 m/s

Table 6

KMU-7 carbon fiber reinforced plastic: impact resistance

Impact energy, J/sq.mm	Residual compression strength, MPa	
	VS-2526M epoxy matrix	Binary matrix
2	170	330
4	130	260
6	110	210

Table 7

Properties of elementary fibers: comparison

Fibers	γ, g/cu.cm	σ_b, GPa	E, GPa	Elongation at rupture ε, %
Polyheteroarylene (SVM)	1.44	3.8-4.2	120-130	2-4
Poly-n-phenylene-therephthalamid (Therlon)	1.45	3.6-3.8	85-120	1-2.5
Aramide co-polymer (Armos)	1.44	4.5-5.0	145-170	4.0
Poly-n-phenylene-therephthalamid (made in the USA):				
Kevlar-49	1.44	3.7-4.0	130-140	1.9-2.3
Kevlar-149	1.47	3.8-4.2	150-180	2-4

Table 8

Characteristics of organoplastics with 5-211-BN matrix

Name	γ, kg/cu.m	Structural properties, MPa				Reinforcement formula
		σ_b	σ_{-b}	$\sigma_{b.bend}$	E	
Organit 7TL	1370	820	260	510	42000	Satin fabric
Organit 7TO	1300	1500	300	600	70000	Cord fabric
Organit 7N	1300	2000	400	730	95000	Filaments for tape prepreg
Organit 7TKS	1500	1120	400	830	61000	T-89 fabric, SVM : (high-modulus material) = 2:1

Table 9

Dependence of ALOR characteristics on formulation and properties of organoplastics

Organoplastic composition	Organoplastic		Properties of ALORs				
	σ_b, MPa	E, GPa	σ_b, MPa	σ_{02}, MPa	E, GPa	CGR*	LCF**
Fabric	560	30	450	350	62	0.4	$1.05 \cdot 10^5$
Ply 1:1	1000	45	580	400	65	0.2	$2 \cdot 10^5$
Uniaxial tape out of braid	2000	90	840	600	75	0.1	$5 \cdot 10^5$
D16chAT alloy	–	–	430	326	70	5.0	$0.9 \cdot 10^5$

* Crack Growth Rate, mm/kcycle, at stress intensity factor of $31.6 \text{MPa} \cdot \sqrt{\text{m}}$

** Low-Cycle Fatigue, cycles, at a maximum stress of pulsating cycle = 160 MPa

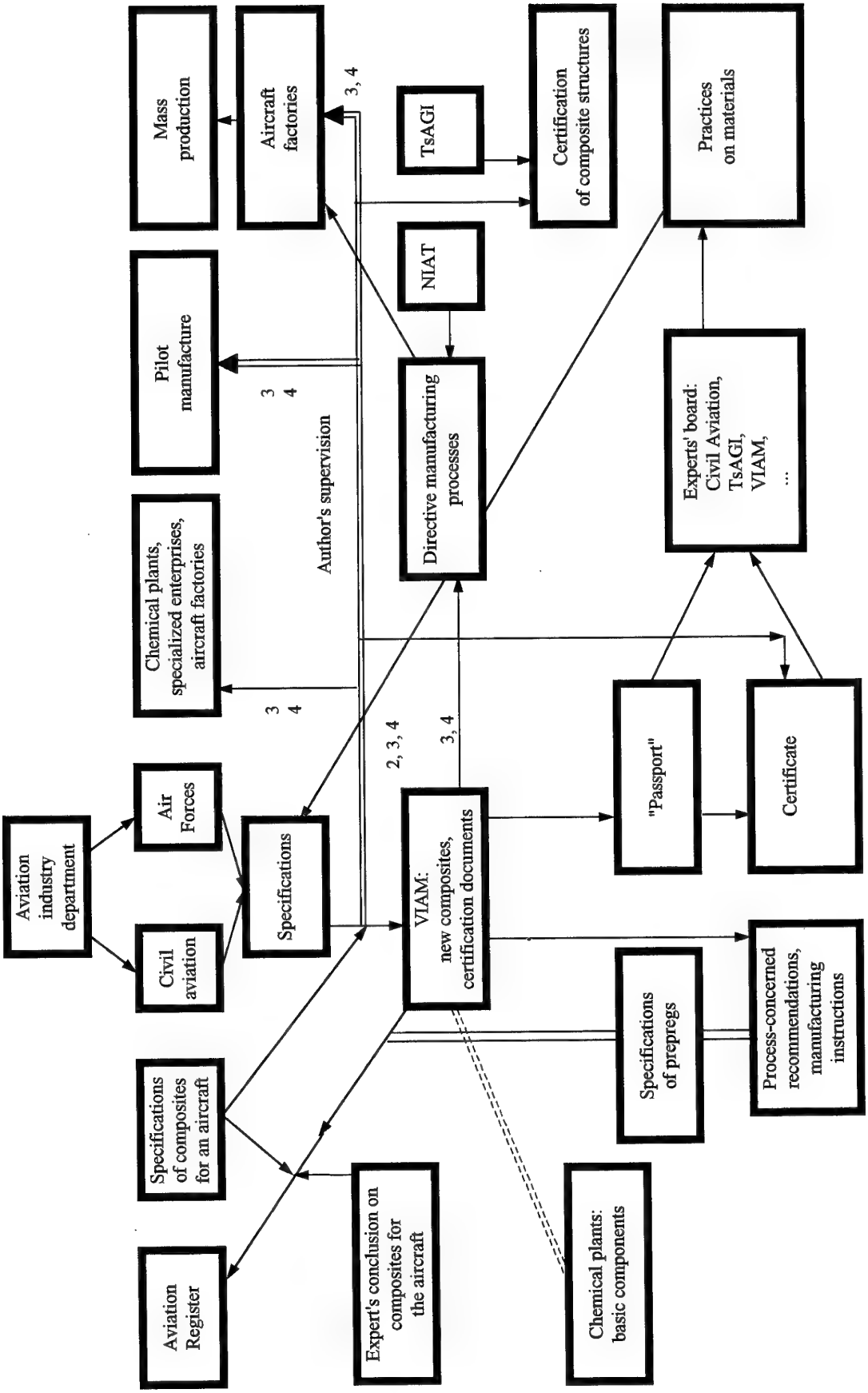
Aviation industry department
Air Forces
Civil aviation
Specifications
Specifications of composites for an aircraft
Aviation Register
Expert's conclusion on composites for the aircraft
VIAM: new composites, certification documents
Chemical plants: basic components
Specifications of prepregs
Process-concerned recommendations, manufacturing instructions
"Passport"
Certificate
Experts' board: Civil Aviation, TsAGI, VIAM, ...
Practices on materials
Directive manufacturing processes
NIAT
TsAGI
Certification of composite structures
Chemical plants, specialized enterprises, aircraft factories
Pilot manufacture
Aircraft factories
Mass production
Author's supervision
2, 3, 4
3, 4
3
4
3, 4

Figure 1.

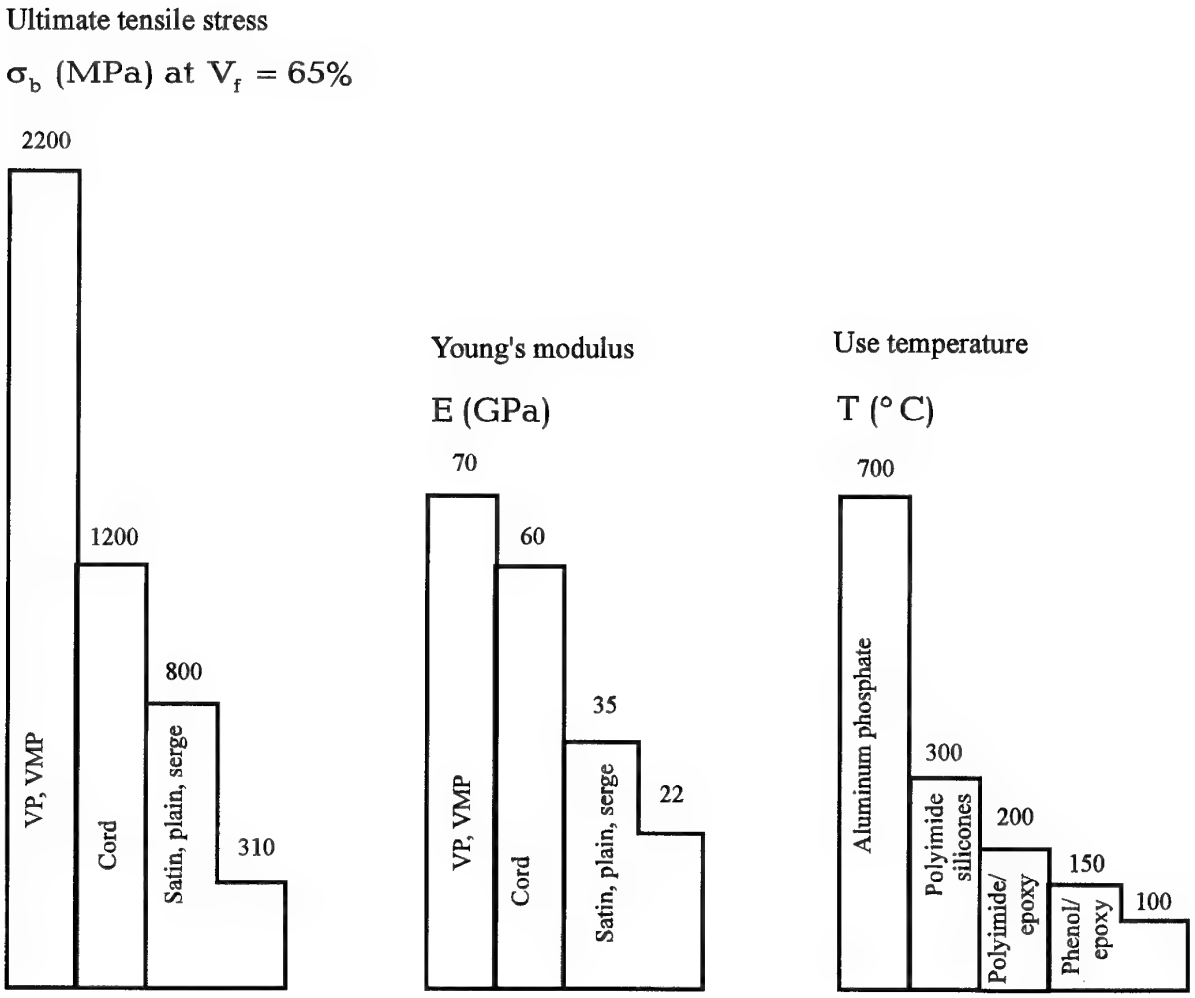

VP (high-strength fibers): σ_b=5000 MPa, E=80 GPa, γ=2560 kg/cu.m
VMP (high-modulus fibers): σ_b=4500 MPa, E=95 GPa, γ=2580 kg/cu.m
E brand glass: σ_b=3500 MPa, E=72 GPa, γ=2520 kg/cu.m

Figure 2. Properties of structural GFRPs

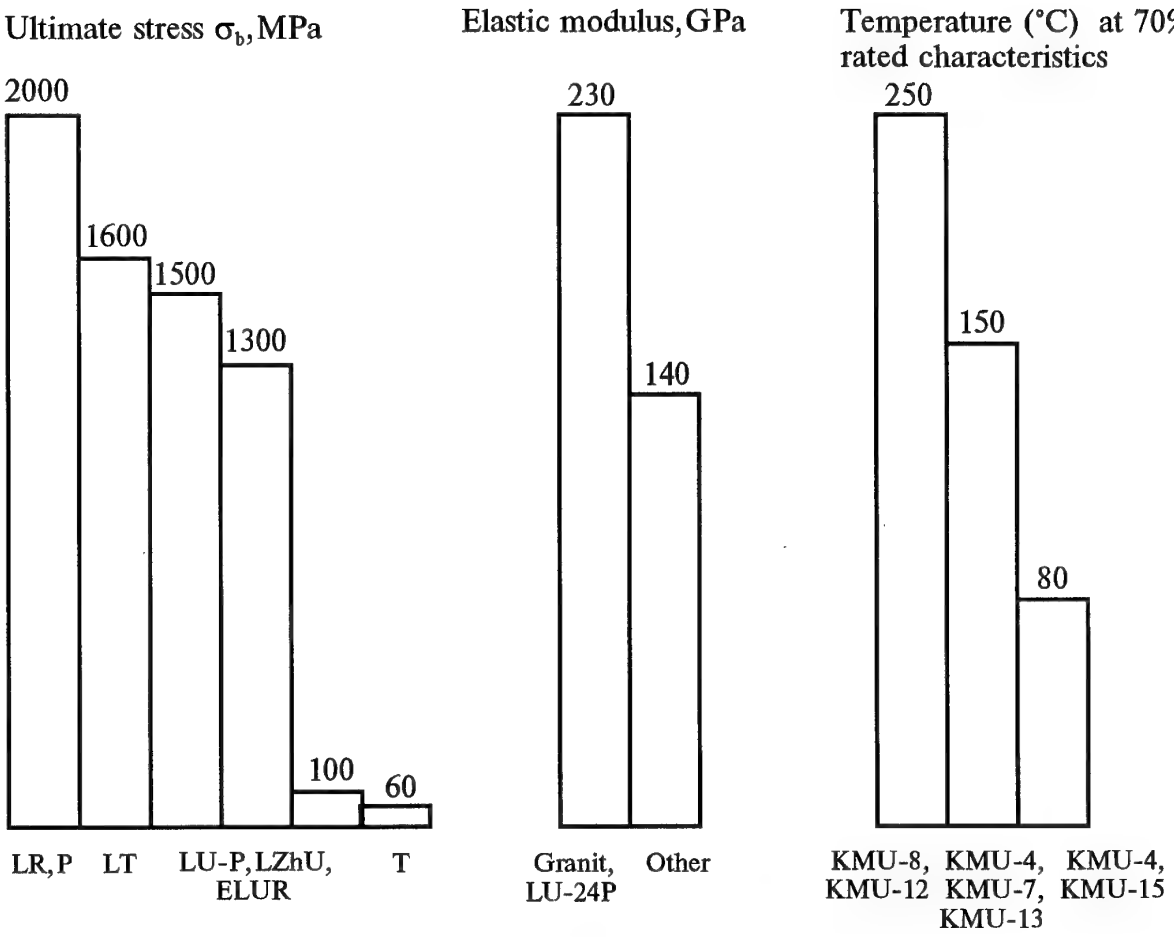

LR	the rolled prepreg tapes (ply thickness of 0.12-0.15 mm) from UKN-P graphite roving
P	the semi-finished items made by pultrusion process
LT	the cord tape with a graphite roving warp and aramide or glass fibers in weft (ply thickness of 0.18-0.22 mm)
ELUR-P, LU-P, LZhU	the cord tape with high-strength graphite warp and weak graphite filaments in weft (ply thickness of 0.18-0.2 mm)
T	the fabric out of graphite roving with plain or serge weave (0.18-0.45 mm ply thickness)

Figure 3. Characteristics of C FRPs used in aerospace technologies (V_f=60%)

Probability of lightning strike = 1 event per 100 passages through Clouds

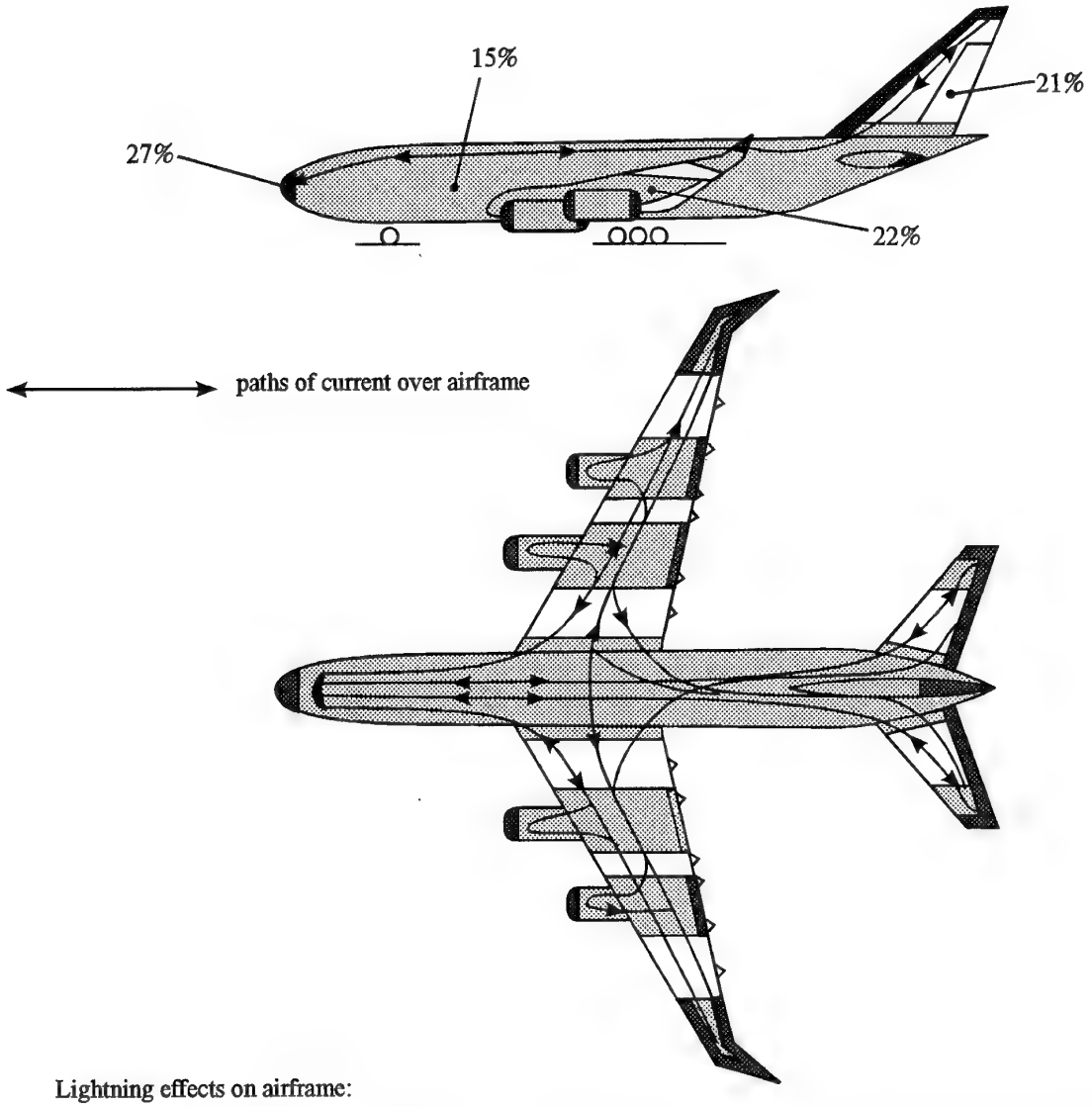

Figure 4. Damage to airframe due to lightning strike

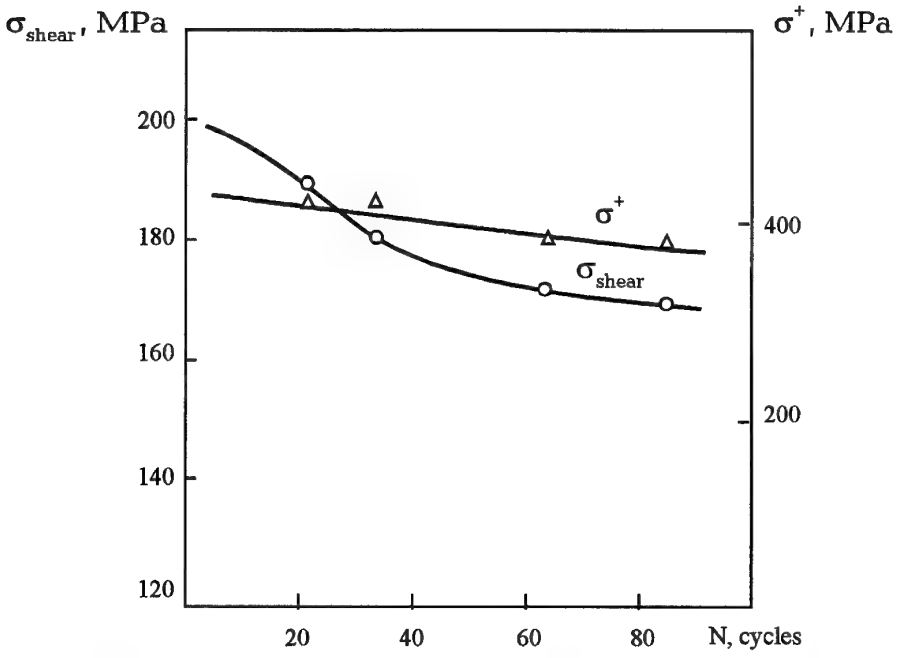

Figure 5. Changes in shear strength of BURAN aerospace vehicle skin (out of KMU-4e CFRP) during ground tests under simulated combined action of space factors.

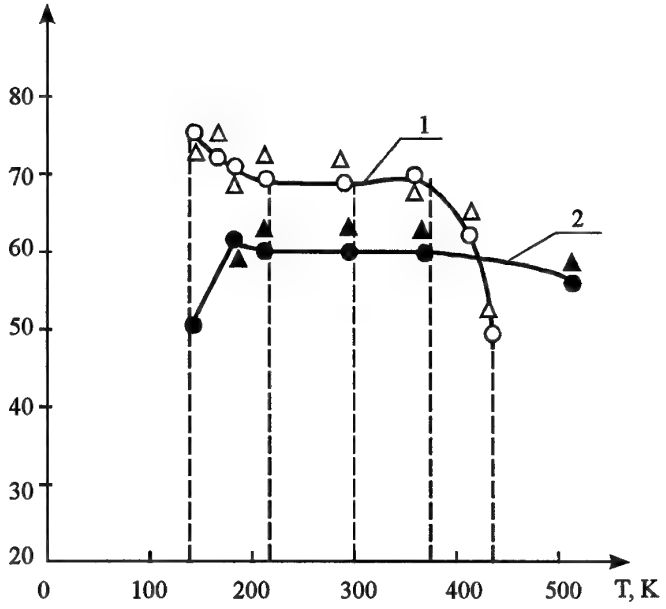

Figure 6. Temperature dependence of ultimate stresses of CFRPs KMU-4 (*1*) and KMU-8 (*2*): prior to (○ ●) and after (△ ▲) exposure to space conditions

TOTAL AMOUNT:
Total surface area= 144 sq.m = 900 kg = 30% of airframe surface

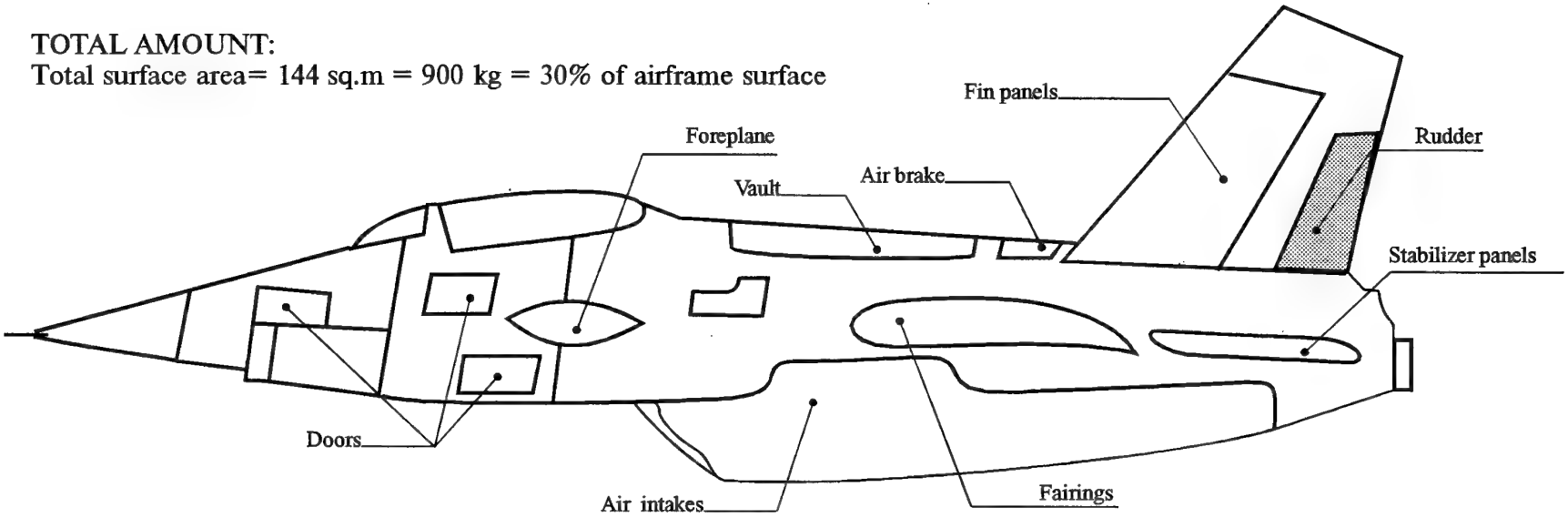

Characteristics of CFRPs

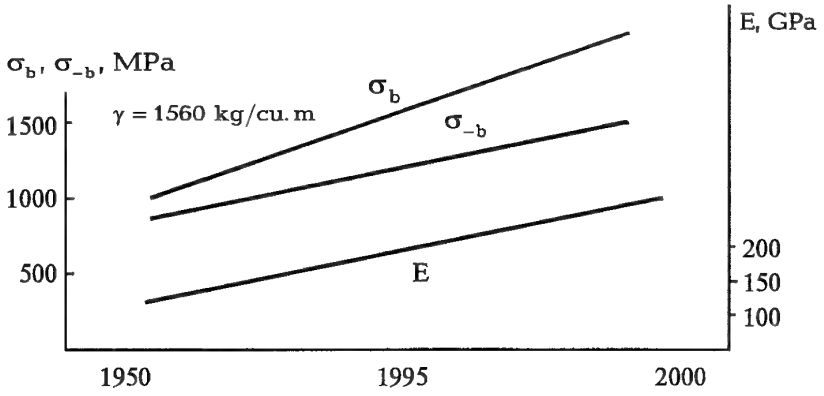

Working temperatures, T (°C)

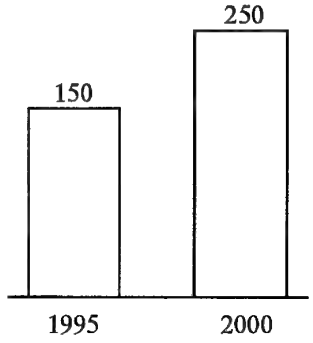

Specific strength, σ_b/γ, %

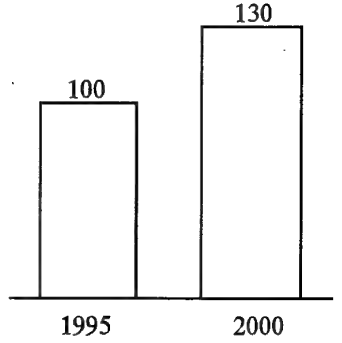

IN 2005 THE TOTAL AMOUNT WILL BE 60% OF THE AIRFRAME

Figure 7. Load-carrying structures out of Carbon Fiber Reinforced Plastics in a fighter airframe.

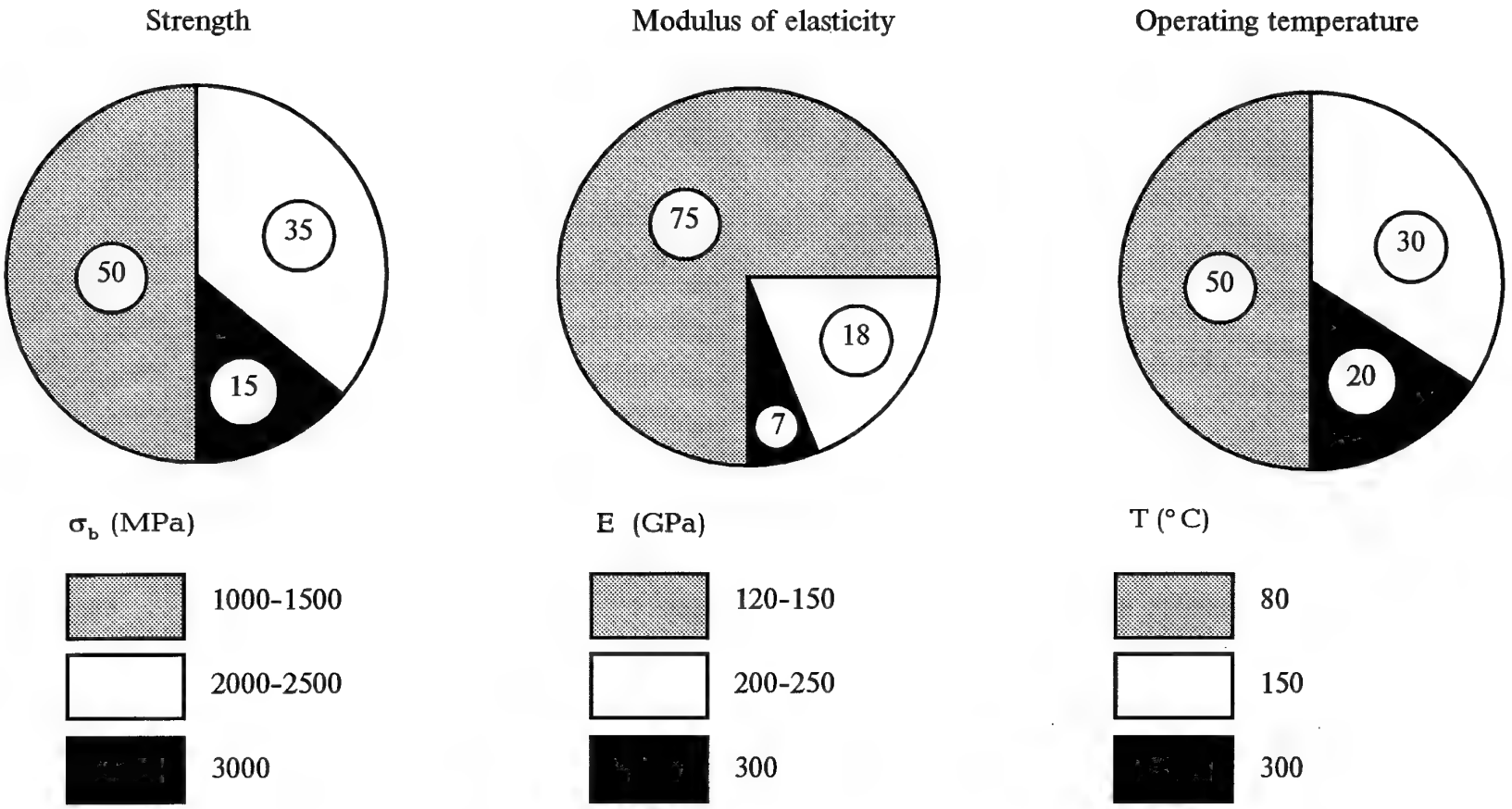

Figure 8. Breakdown of use of CFRPs – weight percentage.

ADVANCED METAL MATRIX COMPOSITES

BY

S.E. SALIBEKOV
VIAM, MOSCOW 107005
RUSSIA

ABSTRACT

The paper is devoted to fabrication and industrial use of metal matrix composites (MMC), in particular, Al/B, Al/C and Al/SiC. Properties of MMCs are considered in relation to microstructures and specific manufacturing procedures.

SYMBOLS:

T	temperature
$\sigma^{\parallel}$	longitudinal tensile strength
$\sigma^{\perp}$	transverse tensile strength
E	modulus of elasticity
δ	elongation at rupture
μ	Poisson's ratio
σ_{100}^{300}	tensile strength after 100 hours at 300°C
σ_{-1}	fatigue limit (load asymmetry factor R=-1)
γ	mass density
α	coefficient of thermal expansion
$\sigma_{0.2}$	yield strength
τ_H	latent period length
Q	process activation energy
R	gas constant
A_H	an experimental parameter

ABBREVIATIONS:

MMC	Metal Matrix Composite
SS-w	Stainless Steel wire

Introduction

For the last 50 years the ultimate stress of aluminum structural materials has been increased from 400 MPa to 650 MPa. As predicted, it will increase to 750 MPa by year 2000. Strength of steels and nickel-based alloys is also expected to raise significantly.

As to elastic moduli, their specific values (related to mass densities) are almost identical for all structural materials -invariably 2400 – 2600 km.

It is obvious that such increases attained by alloying, heat treatment and machining are insufficient and do not satisfy the state-of-the-art engineering.

Only utilization of high-strength fibers for reinforcing the usual alloys is capable to raise drastically and simultaneously:

- the ultimate stress by a factor of over 2,
- the elastic modulus by a factor of over 3,
- the fatigue limit by a factor of over 3,

as well as some other characteristics.

As a rule, increasing the strength of steels and other alloys is associated with simultaneous degradation of their fracture toughness. Composites with fiber-based structure make it also possible to settle this challenge – both characteristics can be upgraded.

In comparison with polymer matrix composites (the Carbon Fibre Reinforced Plastics and Glass Fibre Reinforced Plastics) the metal matrix composites (MMC) have a number of advantages, including:

- a higher operating temperature – 350°C for composites with Al matrix and over 1200°C for intermetallic composites,
- higher static (shear and compressive) and fatigue strength,
- weldability (certain types of welding),
- higher electric and heat conductivity, no indications of radiation -induced destruction.

However, manufacturing processes are much more sophisticated, higher pressures/temperatures are required, and the process must be monitored very carefully. This is caused by chemical activity of components in most MMCs. Their interaction products degrade properties and restrict the material service life.

Efforts of Russian (and VIAM's) specialists in the field of MMCs are directed to the following major problems:

1. Thorough study of physical and chemical processes at component interfaces. The data, thus obtained, make it possible to derive a proper manufacturing process and to use the fiber strength to a maximum possible extent.
2. The development of transformation processes, including cutting, bending, welding etc. – on the usual process equipment, as a rule.
3. Manufacture and evaluation of typical structural MMC parts. This offers a certain experience, makes designers confident, and helps to establish the fields of maximum efficiency for the materials.

Paper presented at the AGARD SMP Lecture Series on "Advanced Polymeric & Metallic Composite Materials for Space and Aerospace Vehicle Structures. . .", held in Stuttgart, Germany from 11-12 December 1995; Châtillon, France from 14-15 December 1995 and Ohio, USA from 18-19 December 1995 and published in LS-204.

Initial components

All MMCs can be conventionally subdivided into three classes, taking into account their matrix alloys:

1) aluminum (or magnesium) based, for use at temperatures not exceeding 350°C,
2) titanium-based, for temperatures up to 800°C, and
3) nickel-based intermetallic and chromium alloys for temperatures as high as 1200°C.

Specific matrix alloy compositions (the alloying elements) are selected taking into account the necessary final properties and the fiber/matrix compatibility requirement.

As for the reinforcing fibers, their ranges in most countries are almost identical: boron and silicon carbide (SiC) fibers, graphite fibers, oxide fibers, steel and tungsten wire, some types of whiskers.

Major characteristics of fibers are represented in Table 1. One can note high strength and elastic modulus of most reinforcing materials, coupled with low density (except the steel and tungsten wire). However, some types of fibers produced in Russia have certain advantages.

Graphite fibers

It is common to reinforce Al alloys with fibers coated with silicon carbide or titanium carbide. This barrier layer prevents intense interaction between fibers and liquid aluminum during the manufacturing process. However, applying carbide coatings is a rather sophisticated and costly process.

Russian industries have mastered the mass manufacture of the "Kulon" graphite tape. Table 1 shows that properties of these fibers insignificantly differ from those of other graphite fibers, but a special chemical/heat treatment makes them more compatible with a liquid Al alloy during impregnation – of course, within a certain temperature/time range. This notably simplifies manufacture of Al-C composites by the vacuum/compression impregnation method.

SiC whiskers

The industries have mastered the mass fabrication of whiskers of silicon carbide, aluminum oxides, zinc oxides, etc. However, acceptable reinforcement for MMCs turned out to be the SiC whiskers only. The manufacturing process is based on pyrolysis of methyl chlorosilane at 1300°C. Crystals are grown using the "vapor→liquid→solid" mechanism [1]. Their strength close to the theoretical limit for solids, is about 10 GPa (Table 1). Production equipment is capable of over 10 t of crystals per year.

Steel wire

The industry has mastered the mass fabrication of high-strength austenitic steel wire (SS-w) of VNS-9 brand (comprising 0.18% C, 15% Cr, 6% Ni and 3% Mo). Hard drawn wire of 0.15 mm diameter has the ultimate stress of 4 GPa [2]. What is especially important, is that the wire remains so strong after being heated to 550°C, that is the temperature for manufacturing the composites by hot pressing.

Boron fibers

Russian enterprises produce 100 and 140 mum dia. fibers on a tungsten core; they have almost the same characteristics as fibers produced by Textron (Avco).

Interrelation of MMC microstructure, properties and manufacturing process

Most components of metal matrix composites form a thermodynamically nonequilibrium system. This means that, during both manufacture and designed utilization at elevated temperatures, there can appear intermediate substances which cause degradation of fibers and the composite material as a whole.

However, in practices it can be sufficient that components are in metastable equilibrium for a long time at the temperature specified.

There exist a number of theories which describe component interaction kinetics. All of them proceed from the assumption of diffusion at interface. They even introduce the idea of a critical (allowable) thickness of a layer of interaction products; with an excessive thickness the properties of the composite degrade drastically.

However, the author has obtained results which certify that most of optimal MMCs do not have continuous layers of interaction products (such as borides, carbides and intermetallic compounds). Moreover, the appearance of a solid layer of the new phase is an indication of excess over the optimal degree of interaction. This can be clearly shown using the boron/aluminum composite [3].

Boron fibers were taken from composites using a selective dissolution of the matrix; surfaces of the fiber have defects such as porosity and cavities (Fig. 1). These are signs of removed aluminum borides that were consequence of component interaction. In numbers the interaction intensity may be evaluated in terms of the ratio of

- the surface s' of the zone spoiled by borides

to

- the entire fiber surface area s_0.

The dependence of this interaction parameter on hot pressing temperature/time is depicted in Fig. 2. It is clear that there exists a latent process period (at any hot pressing temperature) during which no borides form.

Composites obtained with various temperature/time combinations were tested to reveal that the occurence

and development of the boride phase decreases the ultimate stress for both longitudinal and transverse directions. This means that the occurence of borides degrades both fiber strength and fiber/matrix cohesion.

The latent-period duration has also been established not to depend on pressure applied during the hot pressing operation. Both the existence of the latent period and the independence of borides formation from pressure makes it possible to conclude that the boride formation mechanism is governed by diffusion. It is assumed that the latent period corresponds to the time necessary for oxide films or other compounds on the surfaces of the initial components to be dissolved and destroyed.

The latent period length may be assumed to be defined by one of the diffusion-driven processes, so its duration depends on temperature in accordance with the Arrhenius' law:

$$\tau_H \cdot \exp(-Q/RT) = A_H$$

see Fig. 3; here,

τ_H latent period duration,
Q activation energy,
R gas constant,
A_H experimentally obtained parameter corresponding to the end of the latent period.

This means that the microstructure optimum from the viewpoint of composite strength is the one corresponding to the appearance of the first boride formation signs. With the plot obtained, in order to derive the material with the necessary properties, we can vary two main parameters: temperature and duration of hot pressing.

Also, it is seen that hot pressing parameters notably depend on matrix alloy composition. The Figure represents parameters for alloys of brands 1100, 2024, 5052, and 6061.

In composites of systems other than boron/aluminum the values for the end of latent period and optimal bond formation may differ. For example, in dealing with the Al/SS-w system we can proceed from formation of a thin layer of solid solution (but not intermetallics) at the interface. Similarly, for the Al/graphite fiber system we should note the deposition of the first dispersed aluminum carbide (Al_4C_3) particles on the fiber. In this composite the optimum amount of carbides depends on the type of graphite fibers (are these modified or not) and the matrix alloy composition.

In the case of the Al-Zn-Mg matrix and fibers without modification the optimum amount is 0.5% (as referred to fibers), whereas for "Kulon"-type fibers, it is about 0.15%.

Data for this composite (Fig. 4) clearly show how strongly the manufacturing process parameters affect properties. In the upper half, one can see how infiltration time and temperature degrade the residual strength of graphite fibers chemically removed from a matrix alloy; and in the lower half, how these factors improve component bond strength (characterized by the ultimate shear stress) [4].

Optimum parameters are specified so as to reach a compromise between these two trends, taking into account the operating conditions of a structural part.

The matrix alloy composition does influence not only interaction with fibers but also properties of the composite material. For example, the use of high-strength alloys Al-2024 and Al-6061 in the Al/B MMC instead of the plastic, but low-strength matrix Al-1100 improves the boron/aluminum composite properties (including ultimate transverse, shear stresses and fatigue resistance characteristics). However, this substitution decreases the fracture toughness.

Based on this, MMCs should be regarded as complex systems whose strengths are governed by a set of real characteristics of fibers, matrices and their interfaces.

Depending on the manufacturing process adopted, a real composite can have one of the three types of structure.

1. Insufficient interaction of components, poor fiber/matrix bond, if temperature was too low or treatment duration was too short.

   When the material is loaded, fibers disbond from a matrix, and the composite failure follows the mechanism of poorly bonded bundle of fibers.

   In this case the fracture surface shows a number of "distracted" fibers, a disbond of the matrix from fibers, and a "plain" lateral surface of fibers (Fig. 5).

   The material provides very low transverse and shear strength characteristics.

2. Optimal interaction, sufficiently strong bonding of fibers to the matrix, maximum possible extent of the fiber strength use.

   This version corresponds to the end of latent period and appearance of the first points with new phases at component contact areas (interfaces).

   When loading such specimens, only some of the fibers fail, but continue to carry the load over the "entire length" except for two critical zones at fiber ends; the load-carrying capability of the composite as a whole is conserved [5].

   In this case the fracture surface of the specimen exhibits ledges, plastic deformation of both the matrix and fibers (in the Al/SS-w composite), and interface adhesion/cohesion destruction (Fig. 6).

3. Excessive interaction, formation of new substances (borides, carbides, intermetallic compounds) at interfaces; partial degradation of fibers, embrittlement of the matrix.

   The composite is broken by a brittle "trunk crack" at stresses close to the limit for the weakest fibers (Fig. 7).

The breakage surface in this case clearly shows one or several flat projections normal to the fiber axis; brittle fracture; disbond of fibers from the matrix over the intermetallic layer (for the Al/SS-w system).

Such material provides minimum fracture toughness and fatigue resistance.

Thus, it is clear that only material with optimal interaction of components ensures an optimal combination of mechanical properties.

Test methods and properties of MMCs

Methods for evaluating experimentally the mechanical characteristics of MMCs differ insignificantly from those for aluminum alloys and steels. Some differences are due to usual features: anisotropy, low shear and transverse compressive strengths, etc. Specimen shape and dimensions for each material are adjusted individually in order to gain the most reliable information.

However, an important characteristic that should be paid a particular attention is – fatigue resistance. The point is that the usual techniques for estimating fatigue resistance and the low-cycle fatigue limit may not apply to composites.

It is far before the complete failure of a specimen that the latter "produces" a multitude of microfractures which makes the material almost unserviceable. The features include:

- microcracks in the matrix,
- debonding over a matrix/fiber interface and a matrix/matrix surface, and
- failure of separate fibers or groups of fibers.

Contrary to usual metal alloys, the microdefect cumulation stage is a main part of the service life of a composite.

There exist several criteria for estimating fatigue limit:

1) A change in specimen eigenfrequency, where use is made of resonance-based testing. In this case the specimen is regarded as broken when the eigenfrequency reduces by, e.g., 5%, see [6].
2) A change in specimen stiffness [7]. Considered as a fatigue limit is the cycle amplitude stress that reduces the elastic modulus by 20% after 2 million cycles.
3) Specimen failure, as for usual materials (when testing the composite under cyclic tensile loading).

The fatigue strength may be estimated on the basis of residual static strength.

To certificate MMCs, we employ the following criteria for fatigue life estimation:

1) at the cycle number of 20 million, the 5% eigenfrequency decrement or a 50% load-bearing capability reduction;
2) at the cycle number of 0.1 million, failure of a specimen under R 0 cycles.

Boron/aluminum material

The basic mechanical characteristics of the VKA-2 system may be seen in Table 2. It is clear that the boron/aluminum composite features high static and fatigue strengths and a high Young modulus at both room temperature and 400°C temperature [8].

The low-cycle fatigue limit of the boron/aluminum material with a matrix made out of 6061 high-strength alloy is over 0.8 of the ultimate static tensile stress (Fig. 8).

The other feature of the boron/aluminum system is a very high fatigue limit at temperatures that are rather high for Al alloys, see Fig. 9. For instance, the 100-hour strength at 350°C is 750 MPa, which is higher than that of the best Ti-based alloys.

These characteristics make it possible for us to regard the boron/aluminum composite as one of the most advanced materials for aerospace applications, especially the parts loaded with tensile and compressive forces (i.e., alternating stresses) at elevated temperatures.

These materials are fabricated by hot pressing (diffusion bonding) of a stack of plasma-treated prepreg layers. Typical process parameters are 520-560°C temperature and 40 MN/m^2 pressure for 20–40 min. For the material system we have developed current expertise includes bending, cutting and welding the semi-finished items; holes may be drilled.

Various joints (welded, bolted, riveted and adhesive bonded) were tested. Load-carrying panels with stiffeners from the boron/aluminum composite were evaluated by experiment. Some standard shapes and panels are represented in Fig. 10.

The results of tests and analyses conducted by specialists of TsAGI indicate that the use of uniaxial boron/aluminum doublers (of 1.5 mm thickness) for reinforcing the pressurized cabin longeron saves 28% of structural weight, while preserving stiffness and load-carrying capability. Note that similar doublers for a wing spar out of a Ti alloy ensures stiffness increased by 45%, and a weight saving of 42% in comparison with the single-ply spar, the static strengths being equal (Fig. 11).

Full-size AN-77 airplane bulkheads with boron/aluminum stiffeners were tested.

A process for manufacturing tubes and tubular struts with titanium fittings has been prepared; the tubes may be fabricated by either the isostatic pressing or bending and welding of a sheet.

Boron/aluminum tubular transverse rods on "Ruslan" landing gears have been in successful use for several years.

Practices for manufacturing gas turbine engine compressor blades have been developed. In collaboration with specialists of TsIAM, we optimized the reinforcement pattern and conducted tests including an evaluation of fatigue limit at temperature of 350°C.

The blades represented by Fig. 12 were tested in ground conditions.

Graphite/aluminum composites

These properties of VKU-1M composite material are reported in Table 2, compared with the Al-19 castable aluminum alloy and the VT2-1 titanium alloy.

This composite includes

- a matrix of Al/Zn/Mg alloy and
- the reinforcing component, the "Kulon" graphite fibers with modified surface; the elastic modulus is 420 GPa.

One can see that the present material is less strong than the boron/aluminum system, but the difference in specific strength is not so great – due to the mass density of 2.35 g/cu.cm.

We should take into account the following features of the material:

- high modulus of elasticity (250 GPa) and
- very low thermal expansion coefficient (for the fiber direction). These qualities define areas where the composite can be effectively utilized: the structures that should ensure stable forms and dimensions during variation of temperatures and/or loads.

This composite incorporates components with great differences in both elastic modulus and thermal expansion coefficient, so residual stresses appear (tensile in the matrix and compressive in fibers). Therefore the heating/cooling cycle curve has an open hysteresis loop, which means a permanent strain. Various heat treatment procedures were tried for minimizing the permanent strain:

- heating to 350°C and slow cooling,
- cooling at cryogenic temperatures,
- cyclic heating to 120°C, etc.

The best results were obtained by heating the material (at least 4 cycles) to 120°C and slowly cooling in the furnace down to room temperature.

The material under consideration was used to manufacture

- some parts for a platform carrying the research equipment for a space telescope,
- spacers between supports and a reflector of a deep space communications system.

The basic manufacturing process assumes vacuum/suction impregnation of fibers with a liquid matrix alloy at 620-690°C temperature and 4–6 MN/sq.m for 40–120 s.

In one of the versions the vacuum/suction impregnation process makes it possible to fabricate continuous prepreg tapes. Such tape was treated by hot pressing to manufacture the 5 m long sheets, various shapes, and tubes 60 mm in diameter and 1200 mm in length.

Aluminum/steel wire

Table 4 demonstrates characteristics of KAS-1A materials comprising

- a matrix out of the AV aluminum alloy and
- steel wire out of VNS-9.

These materials feature arc an extremely high static strength (about 1500 MPa), high fatigue limit, and high fatigue crack growth resistance. The composite has an insignificant sensitivity to stress concentration. However, it is heavy (the density is comparable to that of Ti alloys).

The most effective applications include reinforcing doublers to be installed in areas prone to fatigue crack occurrence and propagation.

Al/SiC system materials

In recent years many countries succeeded in developing manufacturing processes for fabrication of quasi-isotropic deformable composites – Al/SiC systems. These do not show so high strength and stiffness as boron/aluminum systems but really have a number of other advantages. The materials do not contain costly and deficient components, their thermophysical properties may be varied in wide ranges.

The matrix can be reinforced with either whiskers or SiC powder; two manufacturing processes have been developed, respectively:

- the forced impregnation of whiskers with melted alloy and
- the powder metallurgy process.

There exists a third process, mixing the SiC powder into a liquid Al alloy. Materials obtained in accordance with the latter method (they are named Duralcan) are cheaper, but have a medium strength.

We employ one of the forced impregnation processes – squeeze-casting: the surface of a mat made out of whiskers placed in the mould is covered with a liquid Al alloy, and a hydraulic press plunger forces the alloy within the preform.

However, this process has essential drawbacks. In particular, it turned out that magnesium, present in most aluminum alloys, reacts during infiltration with the SiO_2 film on the surfaces of SIC crystals; this produces magnesium oxide and free silicon. As a result, the central part of the ingot is a zone with almost no magnesium; strength is degraded here (the white zone in Fig. 13).

Therefore we have developed a manufacturing process that ensures unidirectional, "flat-plate" movement of the alloy front (unlike the omnidirectional impregnation of the former case). The zone with less magnesium is displaced to the lower end of the ingot and can easily be removed from the main material.

In addition, the substitution of alloy front flat-plate movement for the omnidirectional impregnation allows the necessary pressure to be reduced from 100–150 to 20–30 MPa.

The percentage of crystals in the composite may be 10 - 25% (depending on production purpose), porosity figure is less than 1%.

Major properties of the composite with an Al/Mg/Si matrix and 17% SiC crystal content are represented in Table 5.

To manufacture the composite materials of Al/SiC system within the solid phase method (out of powders), we use the process and equipment which are usually involved for mechanical alloying (such as attritors). This approach ensures

- strong bonding of components in powders,
- homogeneous distribution of particles or whiskers in a matrix,
- intense comminution of silicon carbide particles, etc.

The method enables adjusting the amount of the reinforcing phase in a wide range (from 5 to 50%).

The subsequent compacting and a deformation treatment of these "composite" powders results in a material with properties reported in Table 6; the latter compares in addition the characteristics of the "SXA" composite having a 20% fraction of SiC.

This material is seen not to be worse with respect to similar materials, but has the following advantages:

1) Machinability with conventional cutting tools. This is due to the SiC particle being less than 1 mum, while materials of other manufacturers have particles with 3-5 mum dimensions.

2) Greater maximum strain, enabling hammer forging of a material with 30% SiC.

3) Lower cost – no higher than 15 $/kg when produced at a 10 t/year rate.

Introducing 20% SiC, for instance, in the Al/Cu/Mg matrix alloy increases the elastic modulus by a factor of approximately 1.5 and decreases the thermal expansion coefficient by about 25%; as well, wear resistance gets improved with static strength and creep resistance remains rather high.

These characteristics outline the most effective applications for this new class of material:

1) Various shapes (including tubes) for load-bearing parts of aerospace technologies. Here, the high strength and stiffness of the material are needed. Weight savings may be as great as 25–30%.

2) Ball supports and ball conveyers in transport-type airplanes, to replace steels with a light-weight material. The structural mass of, e.g., the AN-77 airplane may be reduced by 250–300 kg.

3) Pistons of internal combustion engines. These parts will use such properties of the material as high wear resistance, stability during thermal cycling, low thermal expansion coefficient, creep resistance; the operating temperature in the combustion chamber can be raised, thus increasing the overall efficiency of the engine.

After a proper heat/mechanical treatment the thermal expansion coefficient of the material with a 40% fraction of reinforcing particles can be decreased to $10 \cdot 10^{-6}$ K^{-1}. Such a material can replace beryllium alloys in gyroscopes and other devices of the homing systems.

High-temperature MMCs (for 1300°C) may be based on tungsten wire (W-Mo-Re-Hf, Zr) with reinforcing nitrides, for which a manufacturing process is available. The presence of fine homogeneous dispersion of nitrides (HfN, ZrN) ensures a high temperature of recrystallization and creep resistance levels σ_{100}^{1100}=2000 MPa and σ_{100}^{1200}=800 MPa – while the most advanced tungsten wire with carbide reinforcement has σ_{100}^{1100}=1400 MPa, see [9].

Reinforcing chromium alloys with such wire (30% volume fraction) enables a composite with the allowable stress σ_{100}^{1200}=200 MPa and σ_{100}^{1300}=80–100 MPa.

In addition, VIAM in collaboration with the Solid Physics Institute of Russian Academy of Sciences undertakes development of refractory MMC with an intermetallic matrix (Ni_3Al) reinforced with oxide fibers. The fibers (Al_2O_3 + ZrO_2 + Y_2O_3, a diameter from 50 to 200 mum) are produced by the internal crystallization method [10]. Such material with a density of 6 g/cu.cm does not need antioxidants even at temperatures of 1200°C. Parts not requiring machining may be fabricated by impregnation under pressure.

As for engineering applications, even the well-recognized MMCs (such as Al/B and Al/SiC) are still in a very insignificant demand, as said above. Other MMCs (for example, refractory or Ti/SiC) are now at the lab study stage. The reasons include

- high costs,
- sophisticated manufacturing processes,
- insufficient confidence with respect to behavior of the materials in structures over long periods of time.

Production expansion, mechanization and automation, as well as comprehensive evaluation of MMCs will promote these new, promising materials to their respective areas in engineering.

REFERENCES

1. Gribkov V.N., Isaykin A.S., Portnoy K.I. et al. Metallic composite materials. - Scientific and Technical Information Office of VIAM, 1979, pp. 152-158.
2. Metal matrix composites, J.N.Fridlyander (ed.). Chapman and Hall, London, 1995, pp. 396-485.
3. Salibekov S.E., Sakharov V.V., Romanovich I.V. Metal science and heat treatment of metals. 1978, no. 10, pp. 42-44.
4. Metal matrix composites, J.N.Fridlyander (ed.). Chapman and Hall, London, 1995, pp. 396-485.
5. Zabolotsky A.A. Accomplishments in sciences and engineering, vol.3, VINITI, 1988, 92 pp.
6. Mileyko S.T., Suleymanov F.Kh. Mekhanika kompozitnykh materialov. 1983, no. 3, pp. 427-434.
7. Rabotnov Yu.N., Kogayev V.P. et al. Mekhanika kompozitnykh materialov. 1981, no. 2, pp. 42-49.
8. Portnoy K.I., Salibekov S.E. et al. Composition and properties of composite materials. Mashinostroyeniye, 1979, 242 pp.
9. Petrasek D.W., Signorelly R.A. NASA-TN-777-3, E97931, 39 pp., 1974.
10. Glushko V.J., Mileyko S.T., Kondrashova N.B. J. Materials Science Letters. Chapman and Hall, 12 (1993), 915-917.

Table 1

Characteristics of some reinforcing fibers for MMCs

Type of fiber	Diameter, mum	Density, kg/cu.m	Strength, GPa	Elastic modulus, GPa
B (w)	140	2.5-2.6	3.2-3.6	400
B/SiC (w)	140	2.6	3.0-3.2	400
SiC (c) (SCS-6)	140	3.05	3.8-3.9	400
SiC (Nicalon)	10-20	2.6	2.5-3.2	180-210
SiC, whiskers	0.1-0.2 (ℓ/d=10-20)	3.2	10	550
C, high-strength	8-10	1.7-1.9	5.7-7.5	300
C, high-modulus	8-10	1.8-2.0	2.5-3.7	500-800
C (Kulon)	6.3	1.83	2.5-2.8	450
Si-Ti-C-O (Tyranno)	10-13	2.4	2.5	220
SS-wire (VNS-9)	50, 300	7.8	3.8-4.2	200
W-wire (W-Re-Hf-N)	200-300	19.3	3.2	410

Table 2

Characteristics of Boron/Aluminum composites

Characteristic	T, °C	Al (1100)-B	Al (6065)-B
$\sigma^{\parallel}$, MPa	20	1150	1250
	250	1100	1120
	400	800	830
$\sigma^{\perp}$, MPa	20	100	180
	250	70	145
$E^{\parallel}$, GPa	20	220	220
	300	160	165
$E^{\perp}$, GPA	20	95	100
δ, %	20	0.5	0.5
$\mu^{\parallel}$	20	0.28	0.21
$\mu^{\perp}$	20	0.07	0.1
σ_{compr}, MPa	20	1400	2000
τ_{shear}, MPa	20	47	48
σ_{100}, MPA	100	1100	1150
	250	650	850
	400	500	700
σ_{1000}, MPa	300	550	—
$\sigma_{bend.}$, MPa	20	1450	1700
$a_k^{\parallel}$, J·cm^{-2}	20	30	30
$a_k^{\perp}$, J·cm^{-2}	20	3.0	3.0
σ_{-1}, Mpa*	n=25 Hz N=2·10^7	600	650
Low-cycle fatigue**	n=3 Hz N=2·10^5	900	950

* Bending. Failure criterion: load-bearing capability reduction by 50%.

** Axial pulsating tension, to complete failure of specimen

Table 3

Comparison of properties of carbon-aluminum MMC, Al- and Ti-alloys

Characteristics	Al-C (MMC)	Al-19 (Al-Si alloy)	VT3-1 (Ti-alloy)
Tension: E, GPa	260 (0°) 40 (90°)	70	115
σ_b, MPa	800–900 (0°) 30–40 (90°)	320–370	1000–1200
δ, %	0.45	5	8–10
σ_b at 400°C, MPa	650	60 (300°C)	650
Shear: τ_b, MPa G, GPa	40 22	160 25	700 –
Compression: E, GPa	260	–	–
Fatigue: σ_{-1} ($N=2\cdot10^7$), MPa (bending)	400	75	550–620
Low–cycle fatigue, MPa ($N=1\cdot10^4$)	650	–	–
a_k, kJ/sq.m	1.8–2.0 (0°) 0.4 (90°)	0.8–1.0	2.5–5.0
γ, kg/cu.m	2350	2780	4500
α, 10^{-6} K^{-1} (20–100°C)	2.0–2.5	19–21	9.2

Table 4

Properties of KAS–1A type MMC

Property	Reinforcing element content, % vol.		
	15	25	40
γ, g/cu.cm	3.47	3.98	4.74
σ_b at 20°C, MPa	650	1050	1500
σ_b at 400°C, MPa	560	820	1200
σ_{02}, MPa	490	650	1200
E, GPa	90	100	120
σ_{100}^{300}, MPa	—	—	850
$\alpha^{\parallel}$, 10^{-6} K^{-1}	15.2	15.0	13.5
$\alpha^{\perp}$, 10^{-6} K^{-1}	18.6	17.8	17.6
σ_{-1} ($N=2\cdot10^5$), MPa	22	36	50

Table 5

Mechanical and physical properties of composite based on Al–Mg–Cu–Si alloy reinforced with 17% SiC whiskers*

Ultimate tensile strength	MPa	550–600
Elastic modulus	GPa	100–110
Elongation at rupture	%	1.5–3.0
Density	g/cu.cm	2.8–2.9
Thermal expansion coefficient	10^{-6} K^{-1}	15.2–15.7

* Heat treatment: quenching and artificial ageing

Table 6

Mechanical and physical properties of extruded strip made of composite based on Al–Cu–Mg alloy reinforced with SiC whiskers *

Material	σ_b, MPa	σ_{02}, MPa	E, GPa	δ, %	α, 10^{-6} K^{-1}
Al–15% SiC	500–550	440–480	90–95	5–7	19
Al–20% SiC	600–650	500–550	100–110	3–4	17
Al–30% SiC	600–650	520–560	120–140	1	14
SXA (20% SiC)	645	470	114	—	—

* Heat treatment: quenching and natural ageing

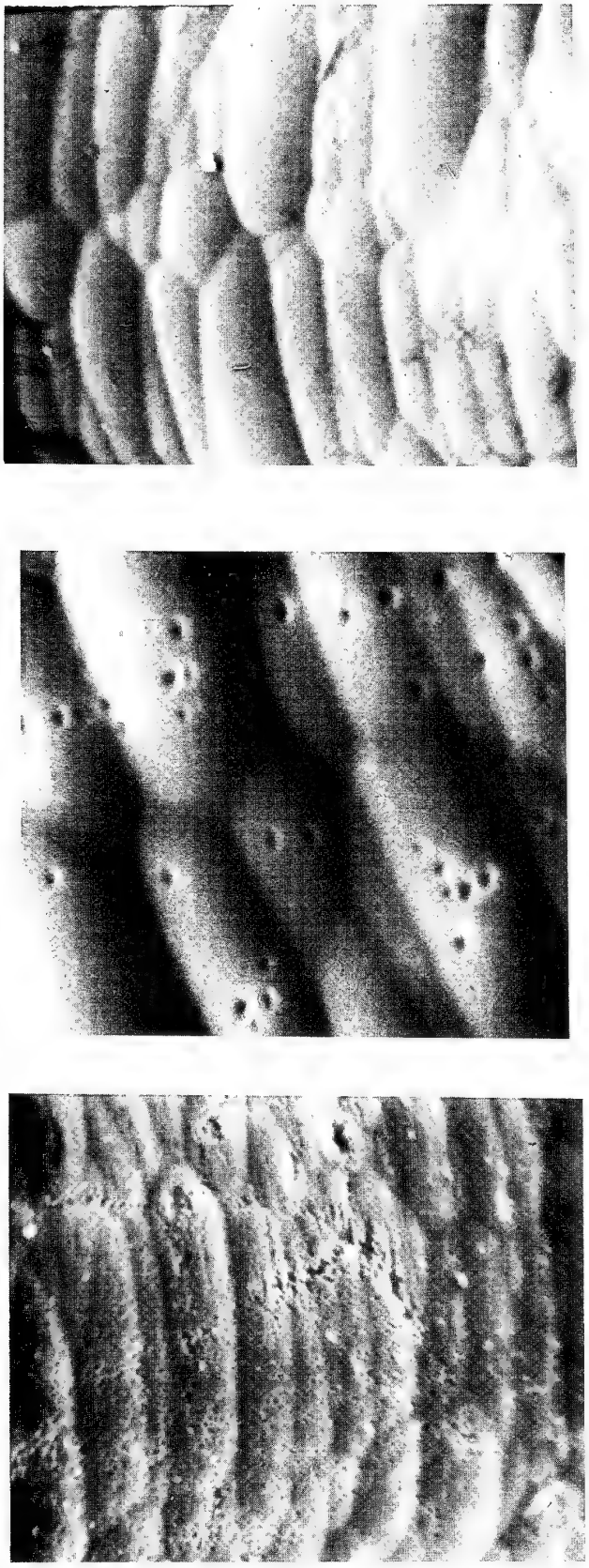

Figure 1. Surface of boron fibers (X2900) in initial state (a) and with signs of borides formed due to interaction with matrix (b, c)

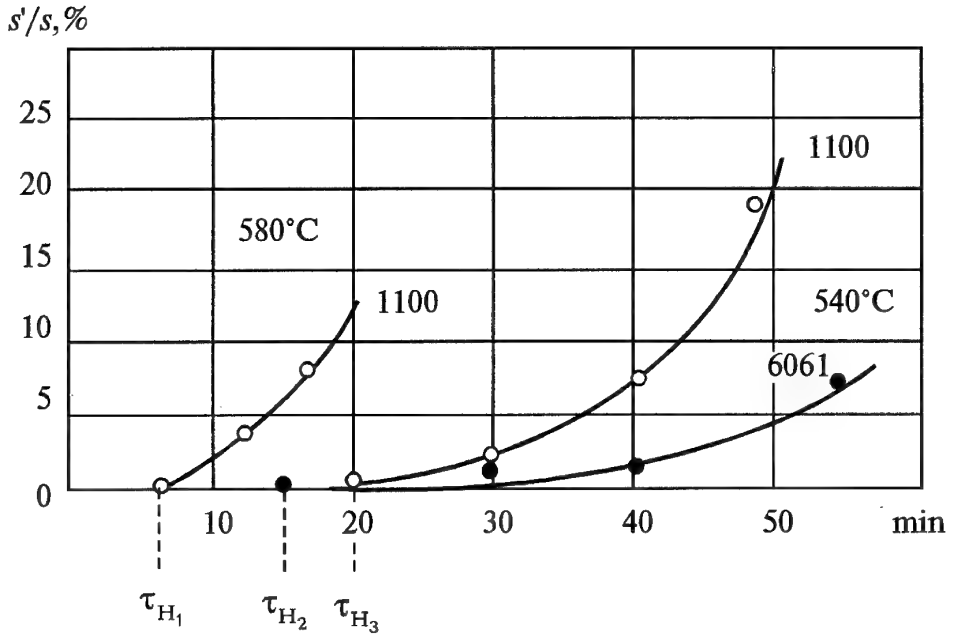

Figure 2. Latent period of boron-aluminum composites with various matrix alloys.

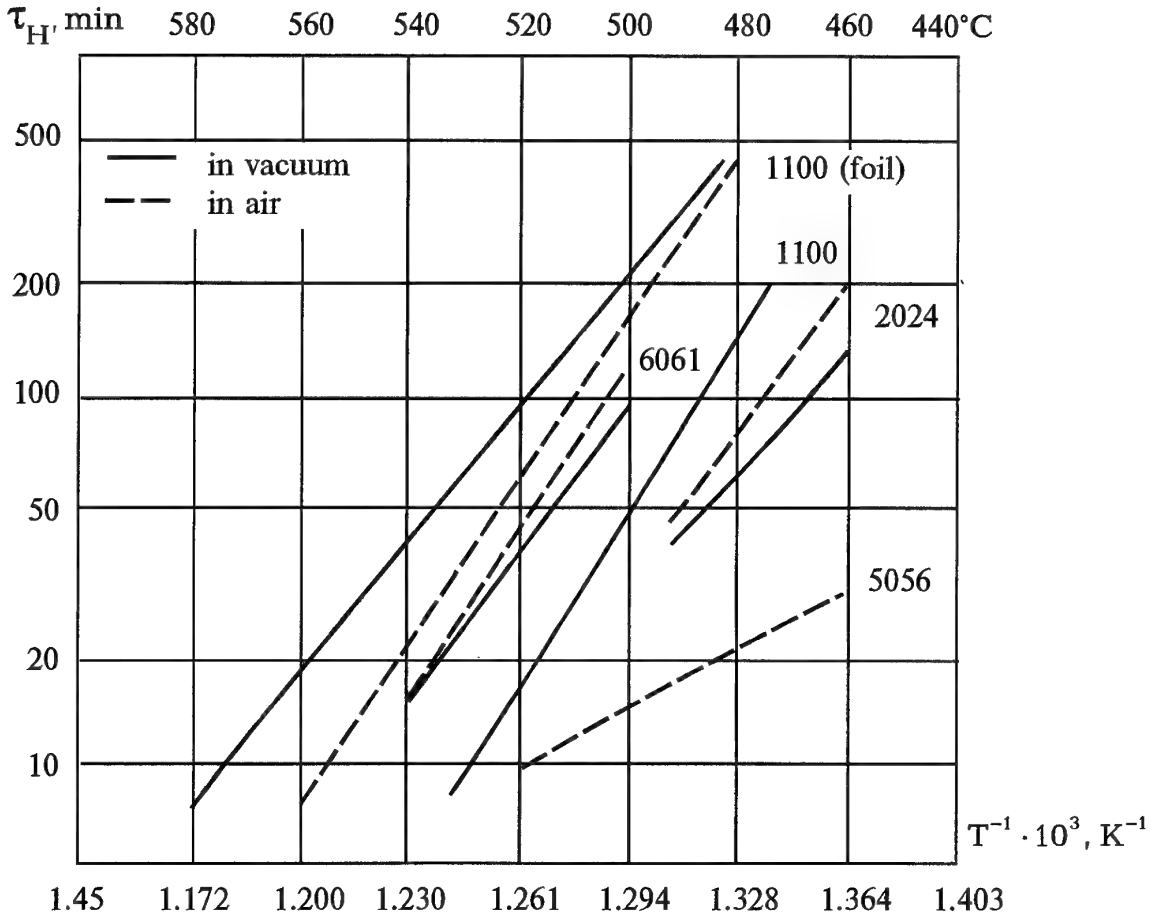

Figure 3. Optimum parameters of diffusion bonding of boron-aluminum composites

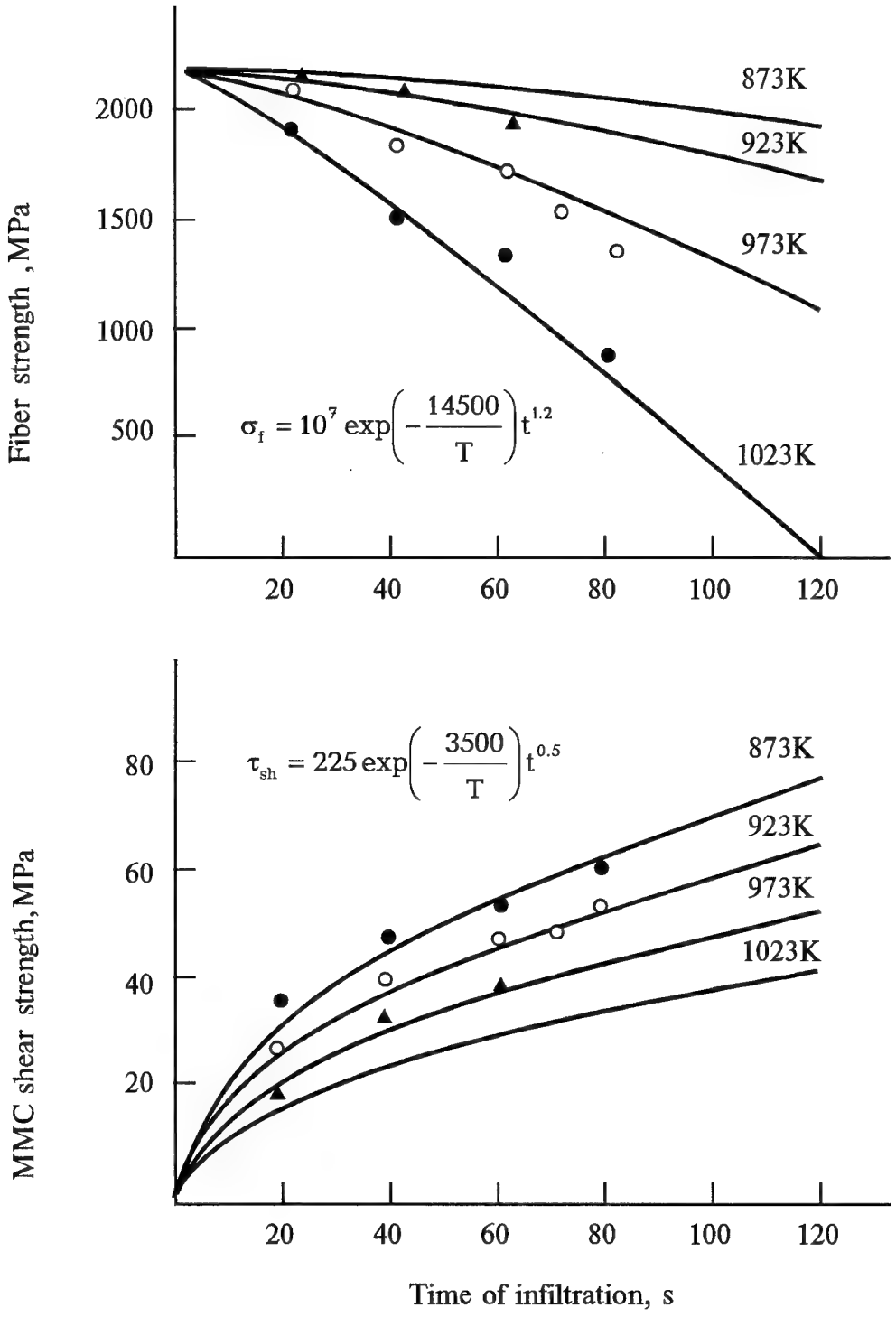

Figure 4. Variation of MMC-extracted fiber strength and MMC shear strength, depending on impregnation time.

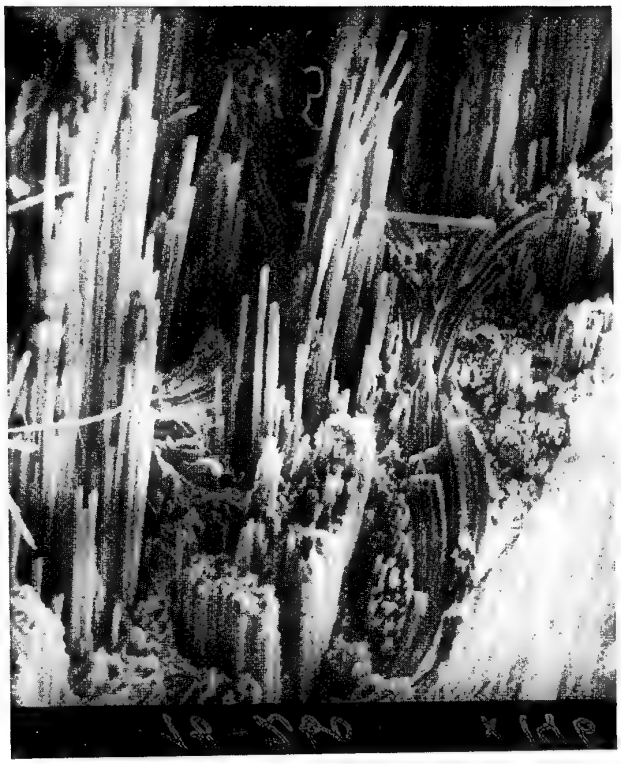

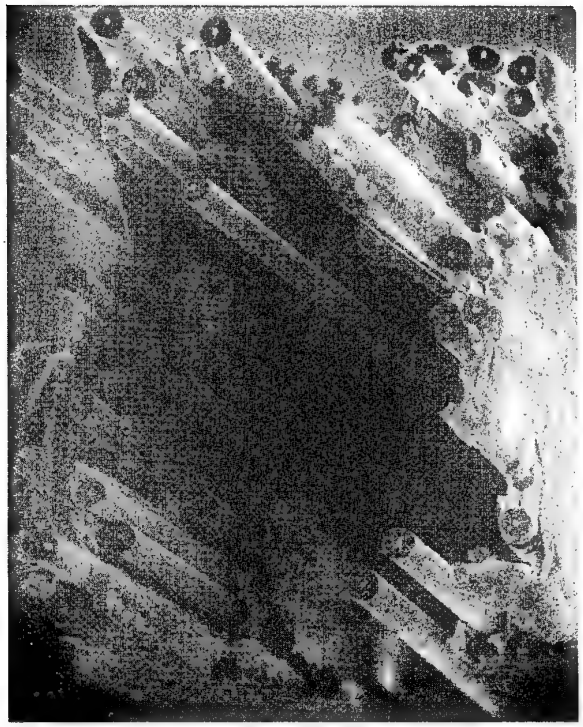

Figure 5. Surface of rupture of MMCs with insufficient interaction of components:
(a) Al-C (×146);
(b) Al-B (×80)

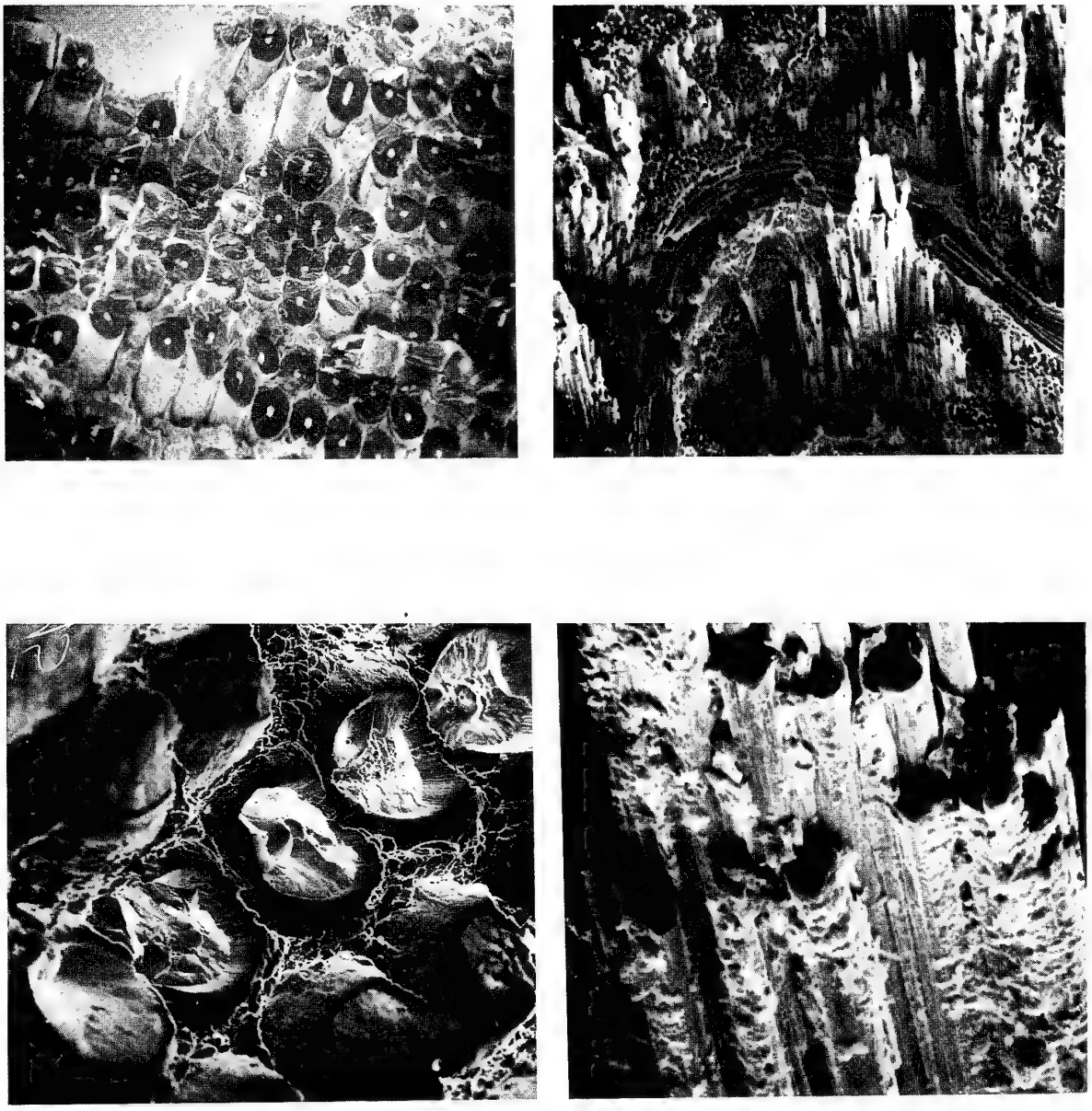

Figure 6. Surface of rupture of MMCs with optimal interaction:
(a) Al-B (×90);
(b) Al-C (×200);
(c) Al-SS-w (×250);
(d) lateral surface of graphite fiber in Al-C composite (×2000)

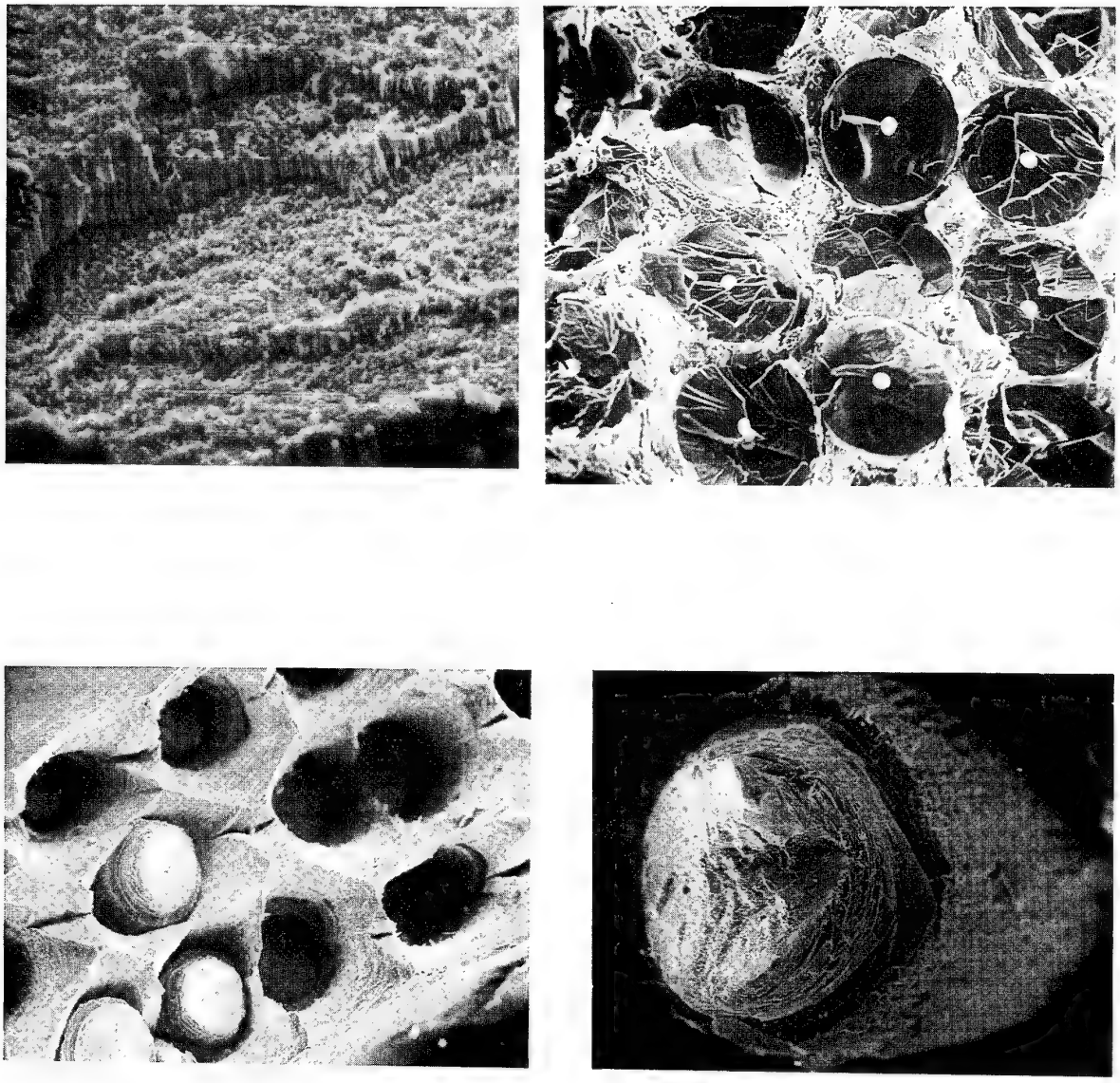

Figure 7. Rupture surface of MMCs with excessive interaction of components:
(a) Al-C (×220);
(b) Al-C (×140);
(c) Al-SS-w (×500);
(d) brittle fracture of steel wire, (×400)

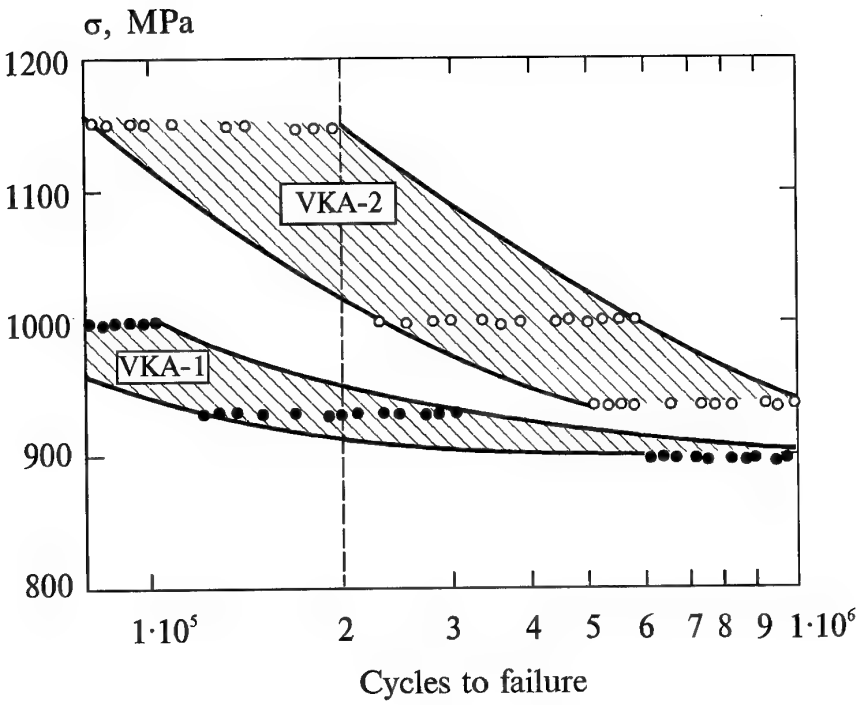

Figure 8. Low-cycle fatigue of boron-aluminum composite: pulsating stress cycle at frequency of 3 Hz

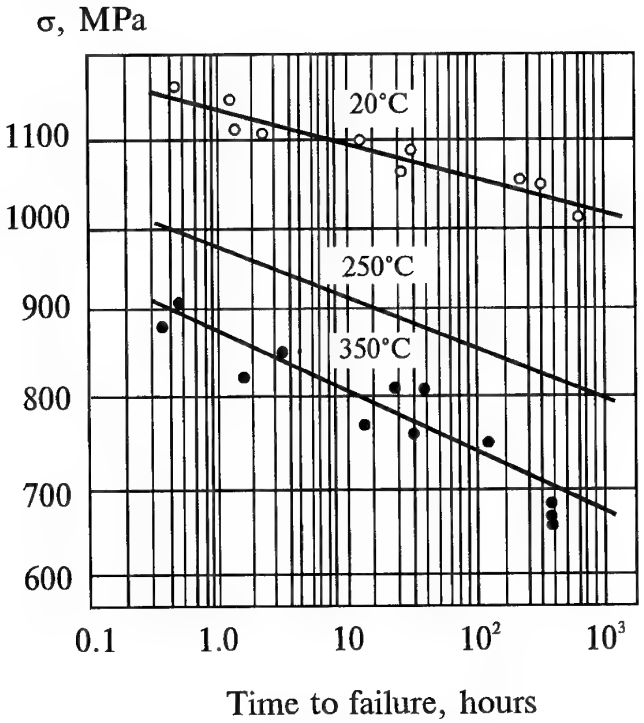

Figure 9. Endurance of AD33-V boron-aluminum composite

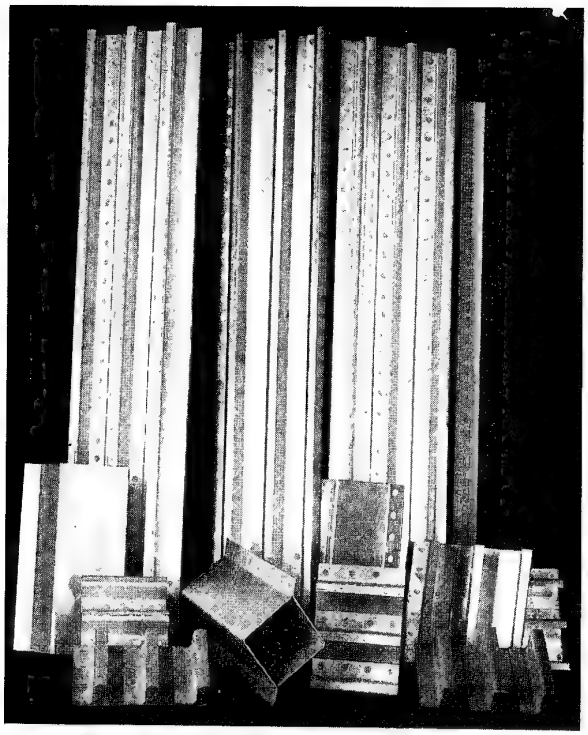

Figure 10. Shapes made out of boron-aluminum composite

PRESSURIZED CABIN LONGERON

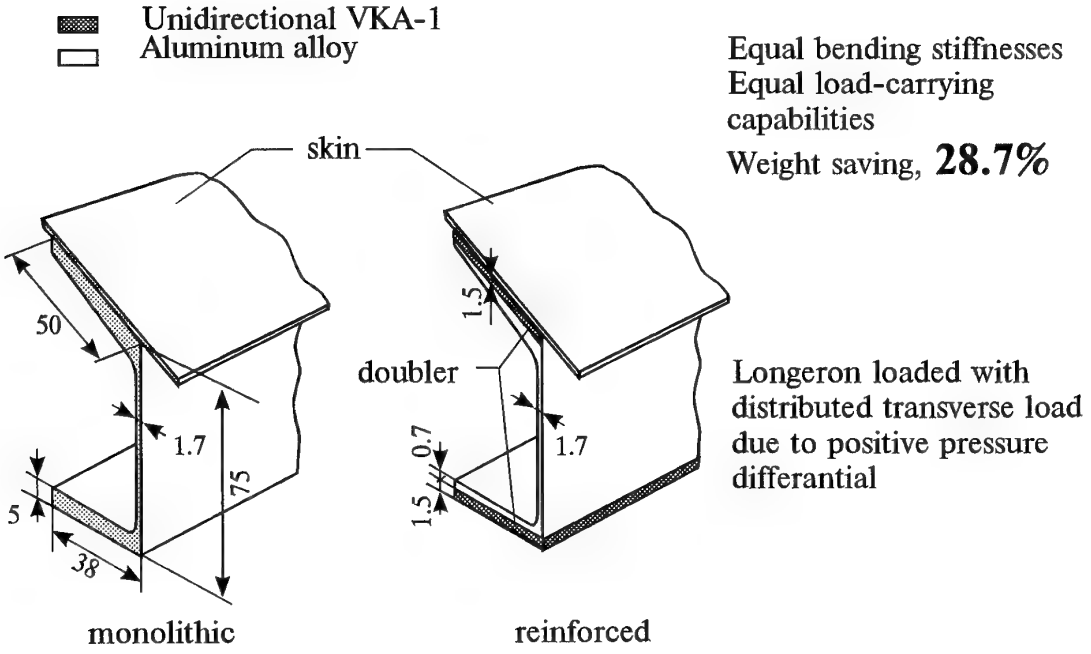

WING SPAR

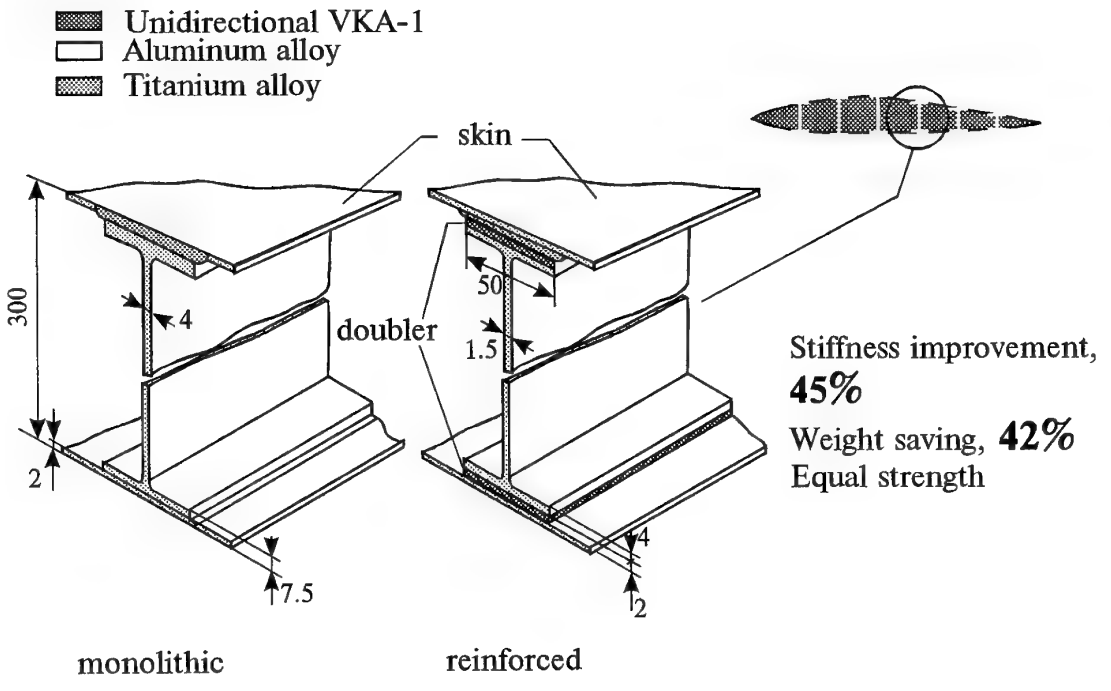

Figure 11. Effectiveness of uniaxial boron-aluminum composite (VKA-1) in doublers within airplane wing and cabin.

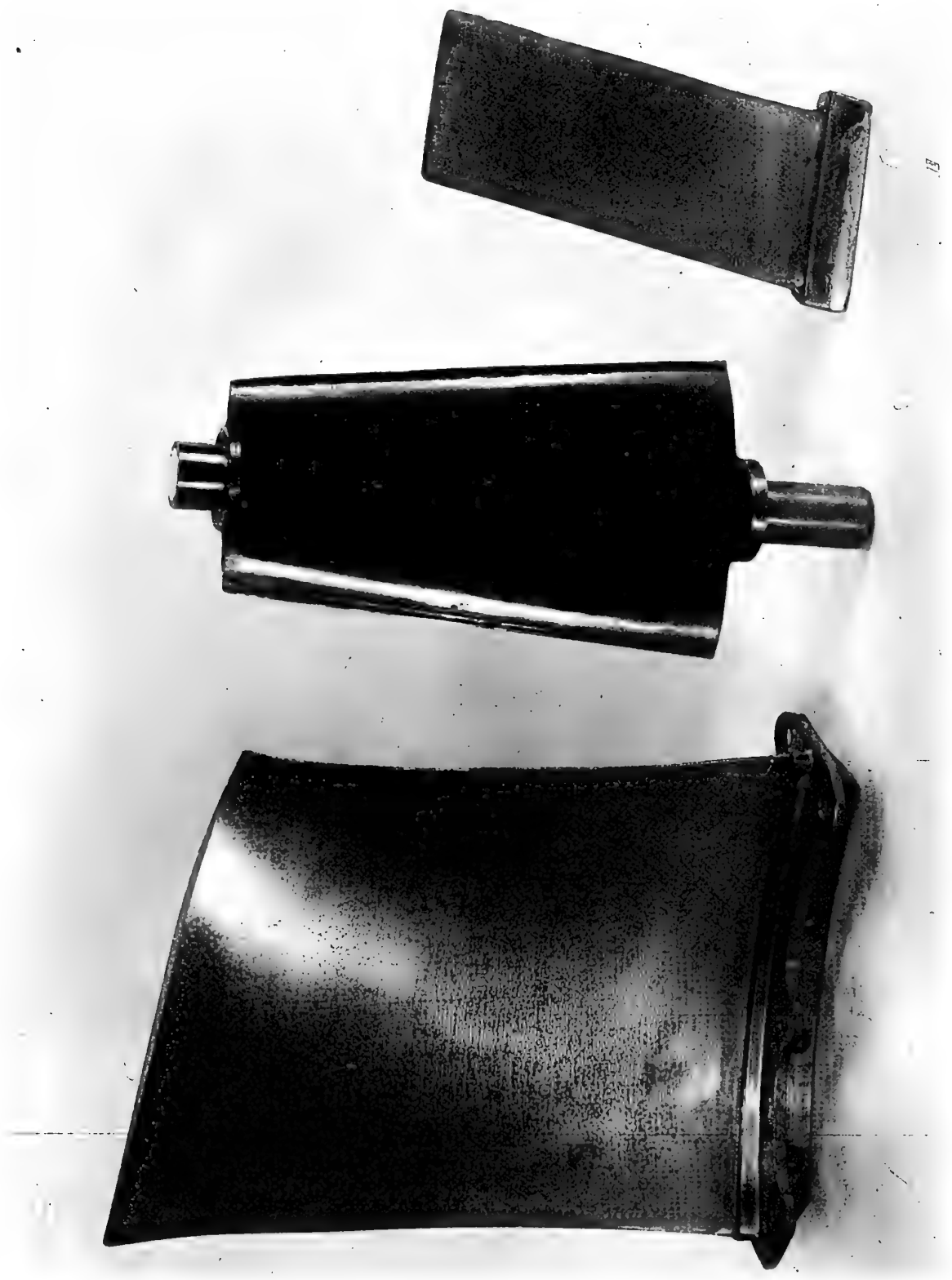

Figure 12. General view of aeroengine compressor blades manufactured from boron-aluminum composite by diffusion bonding

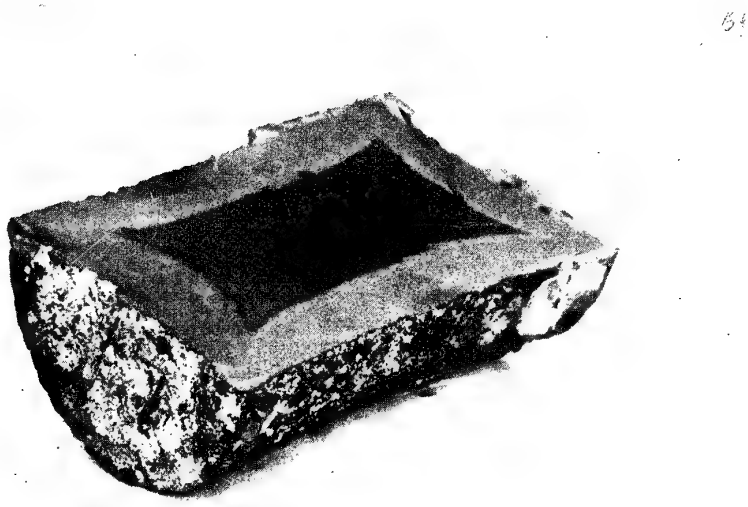

Figure 13. Appearance of Al/SiC (whiskers) MMC ingot after quenching in the air at 400°C

FUTURE GENERATION MATERIALS BY

T.G. SORINA
VIAM, MOSCOW 107005
RUSSIA

ABSTRACT

The paper considers issues for the near future in the development of Polymer Matrix Composites, including: (i) effective use of nano-components and nano-level manufacturing processes for upgrading the physical (and mechanical) characteristics of composites and (ii) ways in development of "smart" materials on the basis of functional components.

The desire to improve the up-to-date technologies requires involving new smart materials whose complex of properties not only exceeds characteristics of the traditional materials but also includes "feeling" the external factors and changing the material characteristics.

Polymer Matrix Composites (PMCs) compare well with metallic alloys; their practical efficiency has been shown by a number of applications. These factors outline clear prospects for composites in the future; the materials consumption breakdown is predicted to change to the benefit of composites.

The technology development process may be said to show a turn from the "structural material" concept to the "functional material" concept, and further to the "smart material" concept. The driving force for creating the smart materials is the ever growing demand of modern civil and military technologies for self-adapting devices and structures (Fig. 1). There are a number of composites in wide use; these may be said to be functional materials. This idea means the possibility to create materials with prescribed properties by selecting certain components, their percentage, and a pattern within the materials. This enables deriving structural materials that in many cases have mutually opposite characteristics (heat insulation/conductivity, radio frequency suppression/transmission, low/high friction), and opens prospects for industries to address functional materials in addition to structural materials.

Functional composite materials may be components of multilayer smart materials combined with diverse devices – sensors, signal processors and actuators – that generate and process the structure condition signals and provide control signals for the very material. The "functionality" of PMC has been used in airframes, space structures and ground devices for a long time.

Structural characteristics of organoplastics and glass fiber reinforced plastics (GFRPs) in combination with dielectric properties adjustable in wide ranges have been used for some 30 years when preparing radio-transparent structures suitable to wide-band transmission.

The high strength of carbon fiber reinforced plastics (CFRP), their ability to maintain initial dimensions, light-tightness, and transparency in the X-ray band are used to manufacture the load-carrying parts of X-ray devices. Figure 2a represents the equivalent aluminum plate thickness as a function of thickness of a high-modulus CFRP based on ELUR tape and utilized for making mammography cassettes and angiography tables.

A study of the deformation type influence on CFRP electrical conductivity shows a linear dependence of resistance R on strain, $R=f(\Delta L)$ (Fig. 2b). When the material is loaded in tension, the function is linear for strains up to 0.9 of the breaking value; and when in compression, linear to 0.6–0.7 of the respective breaking value. Experiments with long-term static and fatigue loading and aging with heating and moisture supply have shown that the CFRP strain sensitivity factor is stable. This property enables monitoring the stress level and damage cumulation in service; so the carbon fiber reinforced plastics may be considered as materials with active self-control.

The industry has developed thin-layer (0.1–1 mm thick) materials based on discrete fibers and polymer matrices (VPT-1, EPK); coating an aluminum alloy with such materials raises (by a factor of 30 to 3000) its acoustic fatigue and erosion resistance, as well as reduces the surface electric charge cumulation.

Experience shows that anisotropy of PMCs (CFRPs in particular) can be used to develop structures that adapt themselves to an air flow due to asymmetry of a stack layup.

The CFRPs have intrinsic adjustable directed electrical conductivity with a clearly pronounced strain sensitivity.

The ability of CFRPs to conduct electrical current offers new options for controlling and monitoring the cure/heat treatment of thick structures when the process involves intense heating by electrical current pulses through the graphite fibers; this facilitates

- complete cure for a short time (of 3–10 minutes, 5–7 pulses),
- development of a high-quality interface, and
- suppression of residual stresses;

the strengths in shear and compression of an oligoetherimide system increase by 20 and 40%, respectively. Using the proper components (the composite layers) of a smart skin, this effect can be employed to adjust damping quality, with feedback being established in a rather simple way.

Paper presented at the AGARD SMP Lecture Series on "Advanced Polymeric & Metallic Composite Materials for Space and Aerospace Vehicle Structures. . .", held in Stuttgart, Germany from 11-12 December 1995; Châtillon, France from 14-15 December 1995 and Ohio, USA from 18-19 December 1995 and published in LS-204.

The major applications and fundamental problems dealt with through the use of smart materials may be grouped as follows:

- monitoring of polymer matrix cure when fabricating a composite material,
- structural condition monitoring, estimation of amount of damage during service of flight vehicles,
- structural oscillation dampers for airplanes and engineering technologies,
- stealth skins (that reduce the effective radar cross section),
- skins that change the aerodynamic surface shapes.

One of the most promising and effective ways for attaining a much higher level of passenger-carrying airplane/helicopter safety and reliability for the 21st century is to develop (and utilize in critical structural areas) the totally new structural materials – the so-called smart materials that "feel" external factors and vary relevant parameters. The development of such materials is a common concern for the materials science, microelectronics, computer technologies and practical manufacturing process field. These materials are used as load-carrying elements and do not only take the in-service loads (the traditional function) but also monitor the occurrence and propagation of fatigue damage, identify and localize damage, and redistribute loads in critical sites [1].

A theoretical foundation of smart materials includes preparation of a comprehensive multifunction system with

- materials components,
- signal-providing and information-processing elements, and
- active components;

these are expected to ensure both improved mechanical properties and the structure condition information (the direct coupling in the system).

In its essence, such material should be composite, comprising the following parts:

- structural, load-bearing material (for instance, a high-strength light-weight CFRP or metal/ organoplastic system like the ALOR),
- a defect sensor (for instance, a fiber-optical system or a metal mesh with highly variable deformation-behavior parameters),
- a logical circuit (based on adaptable modules),
- an actuator (for instance, a shape-memory material).

We conduct the work in the following areas:

- development of "self-monitoring" materials and
- the search for principles to create materials that actively respond to external factors in order to impede a dangerous situation.

Efforts are undertaken to develop feedback in a flight vehicle "smart" skin incorporating "interlaced" layers of aluminum alloys and organoplastic; for determining stress-strain state the stack contains active elements that carry loads and respond to excess of in-flight load.

To localize the sensitive zones in materials, we developed

- a principle for arranging sensors in a sheet and
- a data acquisition system.

The plan is to create materials with feedback that are capable to actively respond to external factors such as dangerous resonance and to change their properties to "mistune" from the dangerous frequency. Such materials may be based on composites including Ti/Ni shape-memory elements that change the geometry of a structure after obtaining a signal from the control system.

Nano-composites and nano-processes

Developers of polymer-matrix composites have a number of common problems for the near future:

- improvement of service characteristics (including extension of use temperature ranges),
- development of new, environmentally friendly manufacturing processes which reduce energy/labour requirements at stages of PMC manufacture and transformation into structures,
- improving components (fillers and matrices), making them cheaper, with due employment of new sources of raw materials,
- improving mathematical methods for optimization of PMCs and structures, taking into account features (and "smartness") of these materials.

Currently, we are studying options for raising the strength and the use temperature of composites by means of nano-level microstructures and manufacturing processes [2].

Nano-composites are materials that contain components in the form of particles, fibers, and layers whose cross-sections measure 3-30 nanometers (remember that 1 nm=0.001 mum) and are arranged in the corresponding matrices. The dimension of such an element differs from that of a traditional fiber (glass, graphite, boron) by a factor of 50 to 3,000.

The positive scale-effect is seen in that the less the probability of surface/internal defects the smaller the element size. This dependence is easily noted in the strength of fibers of a particular compound, e.g., SiC and Al_2O_3 (the whiskers and amorphous and/or polycrystalline fibers), differing by a factor of 100 depending upon their diameter. The ultimate stress of such fibers with a diameter of 20 mum is 1500–2000 MPa, whereas the strength of 0.2–0.5 mum dia.

whiskers (which are "almost nano-level") is 25,000–30,000 MPa. In comparison with traditional microcomposites the nano-composites are anticipated to show higher mechanical characteristics (static and fatigue strength, cracking resistance). The nano-composites are stronger due to the following factors:

- the nano-particles suppress growth of globules in a matrix,
- high surface energy and large total interface length affect the microstructure,
- failure mode changes,
- the nano-reinforcing elements arrest the cracks.

In certain cases the fracture surfaces of CFRPs and organoplastics show the fourth nano-level:

- Level 1 – roving,
- Level 2 – layer,
- Level 3 – fiber, and
- Level 4 – fibril (Fig. 3).

A cross-section of graphite and organic fibers clearly shows the fine fibrils with diameters of 10–50 nm. An interfibrillar substance becomes a matrix for the 4th level, transferring the load to the fibrils. In our opinion, it is there where a strength reserve lies. The difficulty in practice is the necessity to ensure a perfect overall contact between the matrix, microcomposite and fibrils for transferring the load and attaining the potentially high strength.

Studies showed the possibility for creating the second-generation organoplastics on the basis of new high-strength and high-modulus fibers that exceed by a factor of two the initial characteristics of organoplastics with flexible-chain fibers. The current achievement is a material with a 200 GPa elastic modulus, 1300 kg/cu.m density and 350°C maximum use temperature.

Properties of the nano-composites depend on microstructure that is, in turn, governed by the manufacture method. Fillers and matrices can be produced by using various methods:

- from a solid phase,
- from a liquid phase (the colloid deposition, the solvent evaporation), and
- from gases (vaporization, condensation, gas reaction, etc.).

Nano-composites offer great potential for developing a number of materials with many useful sets of properties. By year 2000, the working temperatures of CFRPs are anticipated to be raised to 400°C – due to matrices out of ladder macroheterocyclic polymers which, when cured, contain nano-components; simultaneously, fiber corrosion resistance will be improved; defect-free fiber/matrix interfaces will be attained.

Figure 4 demonstrates a relation between a matrix microstructure and a maximum working temperature of CFRPs based on

- a ladder polymer (curve 1) and
- a PAIS-104 polyimide (curve 2).

The processes prepared for manufacturing the ladder polymers, prepregs and the final CFRP are aimed at forming a fine-dispersion matrix out of diazosymmetric particles* (at the nano-level) with a length-to-diameter ratio of over 10; these particles ensure self-reinforcement and drastic improvement in thermostability; the ultimate stress of the material is 1300 MPa at 400°C, see Table 1.

* The diazosymmetric particles are particles with any cross sectional shape that have the ratio of the length to an equivalent diameter of over 10.

Table 1

Properties of CFRP based on macroheterocyclic polymer

Properties	Test temperature, °C	
	20	400
Ultimate tensile stress, MPa	1450	1350
Elastic modulus in tension, GPa	150	120
Ultimate compressive stress, MPa	900	650
Ultimate bending stress, MPa	1600	1300
Elastic modulus in bending, GPa	140	120

Major efforts are paid to ensuring thermostable systems and to increasing the service life of the material at 350 and 400°C from approximately 30 to about 1000 hours.

A notable stage in the development of PMCs (and, simultaneously, a relatively independent research area) is preparation of advanced thermosetting plastics that can be utilized as ready materials and matrices for PMCs. These have much higher impact tolerance and less weight; structures can be repaired by welding and adhesive bonding. A feature of the structural thermosetting plastics is a high resistance to complex radiation and moisture attack; each can be operated for a long time at temperatures from +150 to -270°C in agressive gases (oxygen and hydrogen). Liquid-crystal thermosetting materials (ZhKT in Russian abbreviation) may be melted to produce three-dimensional parts with 200–300 MPa ultimate stresses (Fig. 5). As for a specific strength, the liquid-crystal thermosetting plastics are competitors to the best Al alloys. These new materials will be utilized in traditional composites (in matrices, fibers, fabrics, etc.) and as a basis for structural plastics. In the latter case the inherent ability of the material to become oriented will ensure reinforcement at the molecular level. Development of liquid-crystal thermosetting plastics is expected to increase the strength of plastics to 2200 MPa (150 MPa in the transverse direction); the working temperature range will be 250 to 300°C; an impact resistance will be raised

by 40%, and a structure mass will be reduced by 25 - 30%.

Clear prospects are view for

- thermostable composites produced by the "polymer-making process" from inorganic binders with a 700°C working temperature (the aluminum phosphates) and
- SiC/SiC composites serviceable at temperature up to 1200°C and suitable for fabrication of sophisticated parts.

A feature of the newly developed ceramics-like SiC/SiC composite is that it is a bulk of chaotically arranged silicon carbide whiskers with dimensions of 0.1–0.3 mum (the nano-level); these crystals are coated with a thin dense layer of a ceramics-like matrix formed by pyrolysis of polycarbosilane or polysilasane. When using the nano-level objects, we form monolithic matrix over a great surface of an ultrafine filler; the matrix remains monolithic after all necessary modifications including high-temperature pyrolysis. The silicon carbide matrix surrounds each fiber and connects the fibers at intersection points. As a result, a porous material appears that can be used at 1200°C (with a strength limit of 150–180 MPa and a mass density of 1450 kg/cu.m); it has a "pseudomonolithic" carcass from β-SiC whiskers with a continuous interface (Fig. 6a). In Fig. 6b one may see a typical microstructure of a SiC/SiC material based on continuous SiC fiber (16 mum in diameter) with a 50 MPa strength limit at a 1600 kg/cu.m density. The precursor material (the plastic without pyrolysis) and the ceramics-like SiC/SiC, both reinforced with SiC whiskers, have identical strengths, whereas strength of the precursor on the basis of continuous fibers decreases after pyrolysis by a factor of 5 to 6. Microphotographs in Fig. 6b clearly show matrix flaws (cracks and fracture origin points) and poor condition at the fiber/matrix interface. The strength of the SiC/SiC material based on traditional fiber may be raised to that of the SiC/SiC nano-composite only after several stages of liquid and/or gas impregnation with intermittent high-temperature treatment; these operations increase the mass density. The present example clearly demonstrates advantages of nano-level SiC fibers in comparison with traditional fibers (like Nicalon) for deriving SiC/SiC composites in accordance with the "polymer-making process."

Examination of nano-level composites confirms the presence of an isotropic skeleton that maintains its physical (and mechanical) properties after high-temperature treatment and the transformation into SiC/SiC ceramics, unlike composites with usual fibers (and usual flaws) – in these materials the matrix is difficult to form because of insufficient specific surface of a filler.

The use of ultrafine fibers offers new options for upgrading materials; this, in turn, raises new problems on predicting the strengths of composites with nano-level components in which the strength, volume fractions, and "spatial" arrangement turn out to be interrelated. Microstructure examination of the ceramics-like composite chaotically reinforced with silicon carbide distinguishes certain structural elements – matrix-coated straight portions of fibers between local intersection areas. A corresponding model has been built; it takes into account the chaotic orientation and the scatter in fiber diameters and matrix layer thicknesses at particular fibers.

Studies produced load-bearing capability estimation algorithms taking into account disorientation and dimensional scatter. A structure modelling technique was prepared to try to evaluate strength of fibers with "supersmall" diameters (at the nano-level). The technique allows for the scale factors in respect of both fiber length and diameter. Computer-aided modeling showed that strengths of materials can be raised by

- increasing the fiber volume fraction and
- using the ultrafine SiC fibers which are greatly effective if loads are properly transferred between the matrix and fibers.

Figure 7 demonstrates the influence of the fiber volume fraction V_f and the fiber diameter d_f on the tensile strength limit of the composite. The numerical experiments revealed that the most efficient method for raising the strength of the final composite is the use of ultrafine SiC fibers: the latter have much higher strength. This numerical experiment methodology can be practically employed in development of composites manufacturing processes – to estimate the attainable strength with due account of process-related restrictions for

- the use of the ultrafine fibers and
- fabrication of materials with greater percentages of fibers.

Owing to new inherent potentialities of composites a tendency to a changeover in aviation materials utilization breakdown may be noted, as Fig. 8 represents. The fraction of aluminum alloys is expected to reduce noticeably (from 70 to 30%); the composites fraction is predicted to increase from 8 to 50%. Similar trends are currently characteristic of many industries.

REFERENCES

1. R.E.Shalin, G.P.Mashinskaya, A.B.Ayvazov, G.F.Zhelezina. Smart materials for XXI-century aerospace structures. International conference "Composite materials under various types of energy attack". VIMI, April 1995, pp. 104 - 107.
2. G.M.Gunyaev, T.G.Sorina. Fibrous nanocomposites based on SiC whiskers. "Nanocomposites and self-alignment in polymers", May 18 25, 1995, St.Petersburg - Moscow.

SMART COMPOSITE MATERIALS WITH VARIOUS LEVELS OF "SMARTNESS"

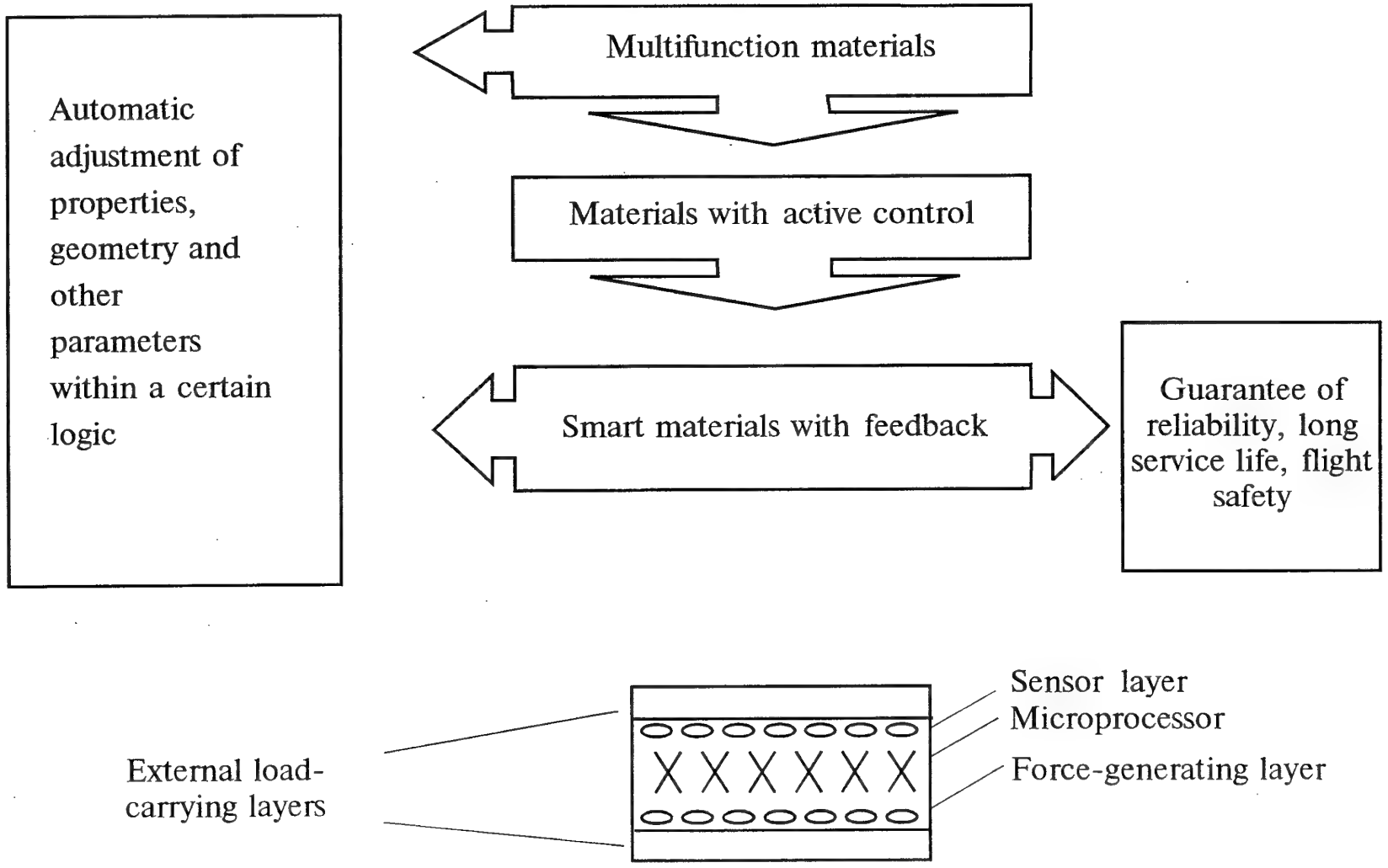

Figure 1.

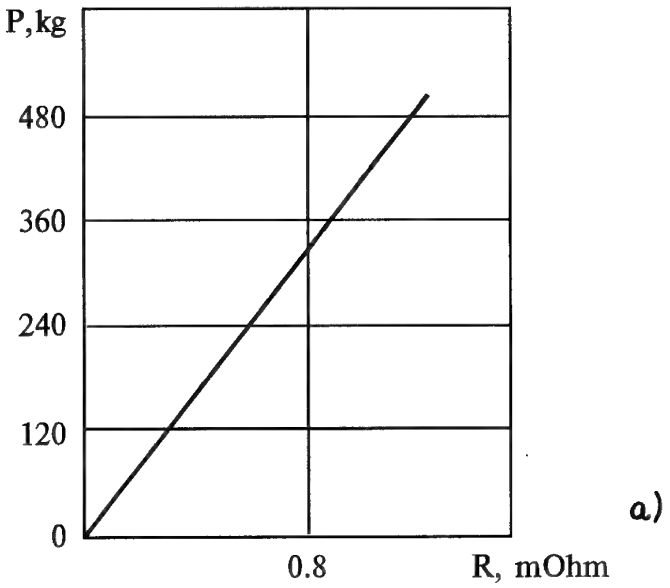

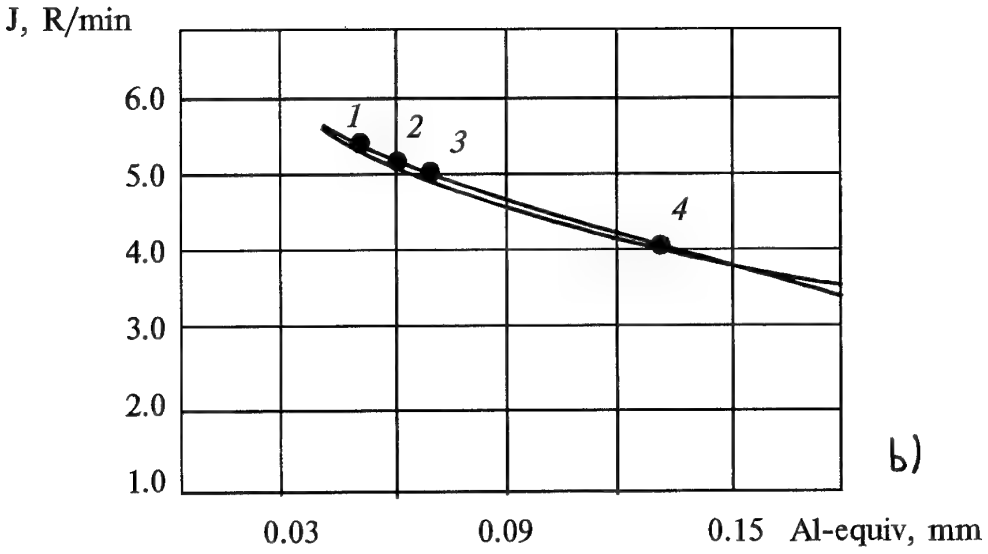

CFRP thickness: 0.4 mm (*1*), 0.75 mm (*2*), 0.9 mm (*3*), 3.0 mm (*4*)

Test conditions: U_a=28 kV, I_a=5 μAmps, distance from source to the plate, 75 cm; source internal filter: 1 mm Be + 0.46 mm Al

Figure 2. Two physical characteristics of CFRPs:

a) dependence of CFRP resistance R on mechanical load;

b) equivalent aluminum plate thickness as a function of CFRP thickness.

NANO-LEVEL IN COMPOSITES MANUFACTURING PROCESS

Composites with fibrils

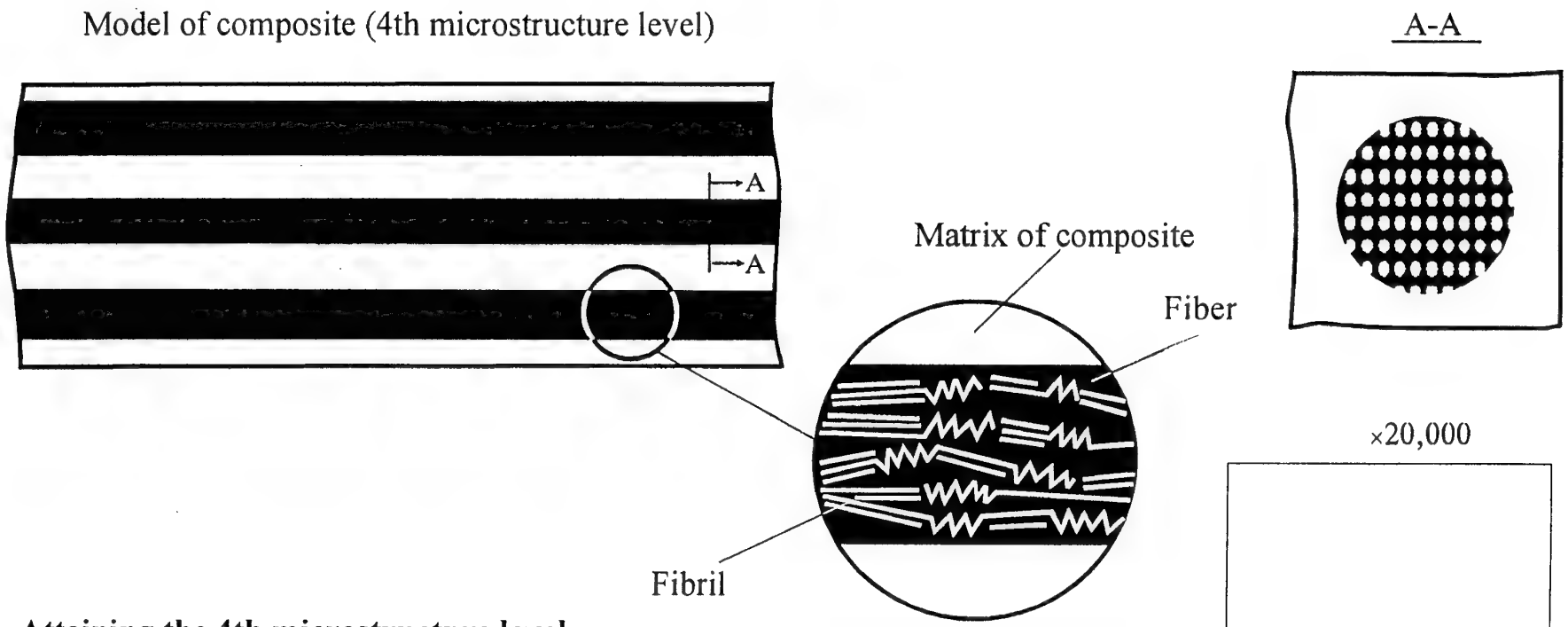

Figure 3.

Attaining the 4th microstructure level

Reaching the fibril percentage $>V_{cr}$

Reinforcing the interfibrillar space in a fiber

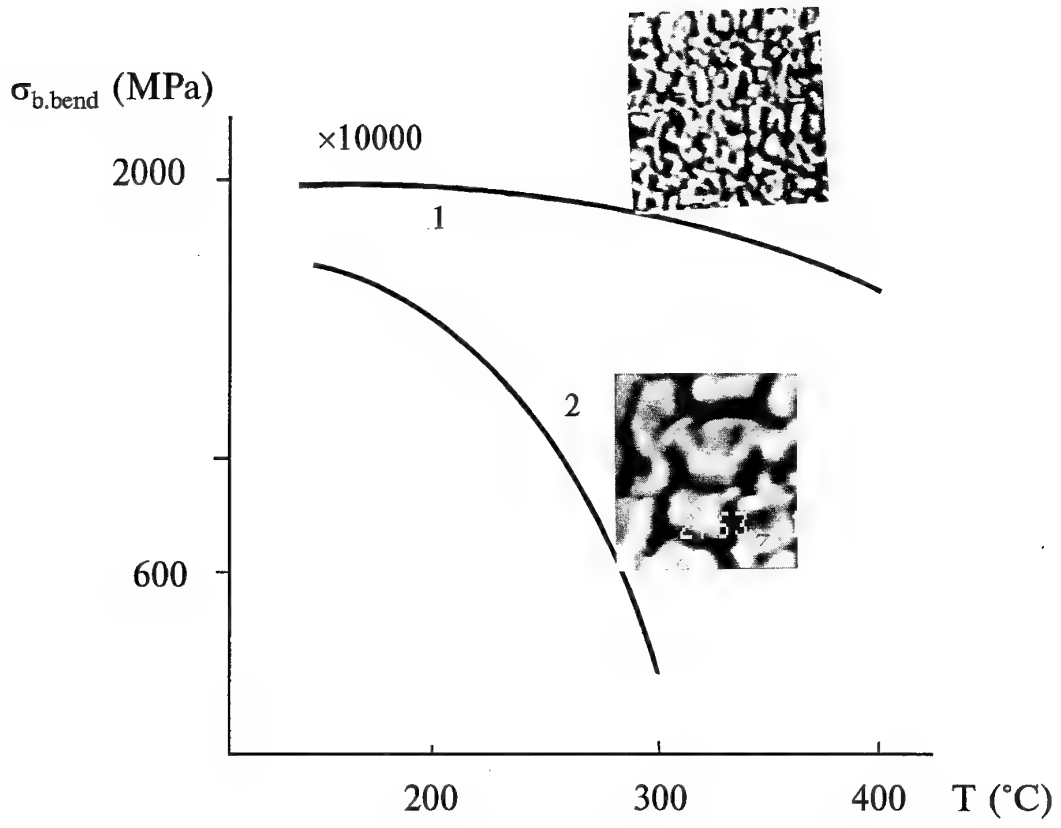

Figure 4. High-temperature CFRPs based on ladder heterocyclic polymers

Figure 5. **Liquid-crystal thermosetting materials:**
the influence of transformation method on tensile strength

Transformation method	Microstructure	σ_b, MPa	
		Type 1	Type 2
Injection moulding	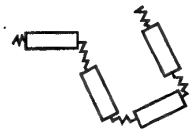	110-120	180-200
Special casting	—	140-160	220-250
Extrusion of films and sheets (thickness ≤ 0.2 mm)	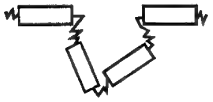	300-350	500
Extrusion of fibers (stretching by 40-200 times)		500-600	2500-3000

Fracture surface

Liquid-Crystal Thermoset Material (type 1) Plastic

Shear strength, MPa

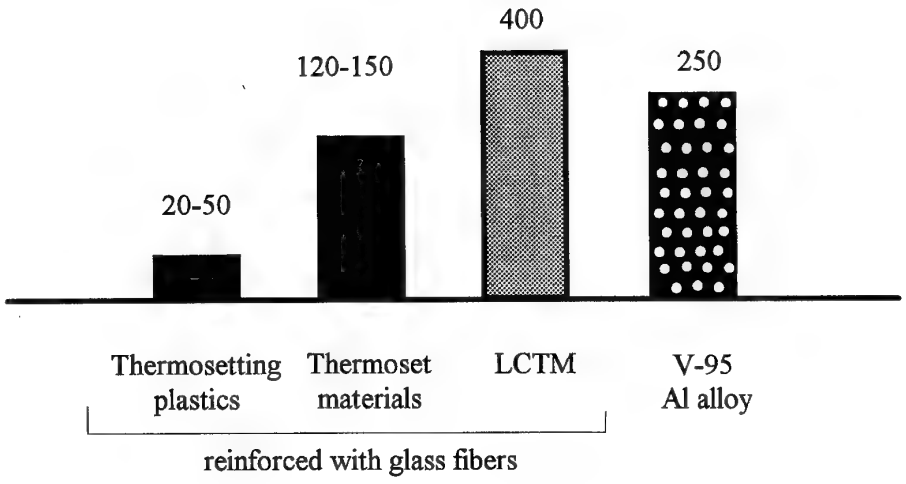

a)

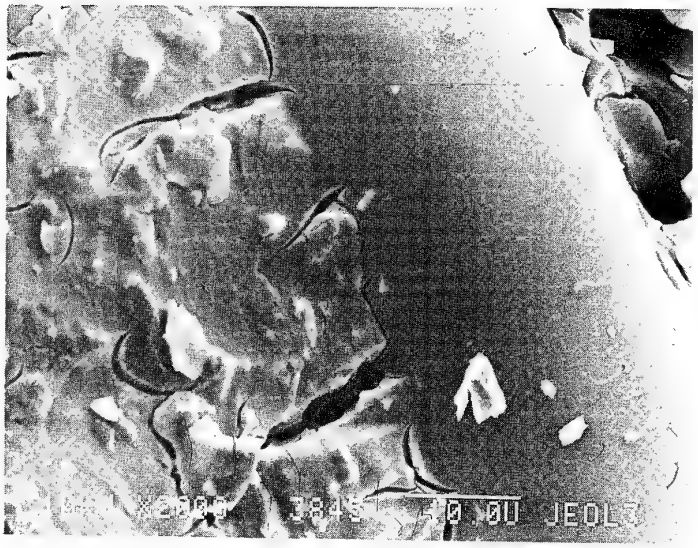

b)

Figure 6.

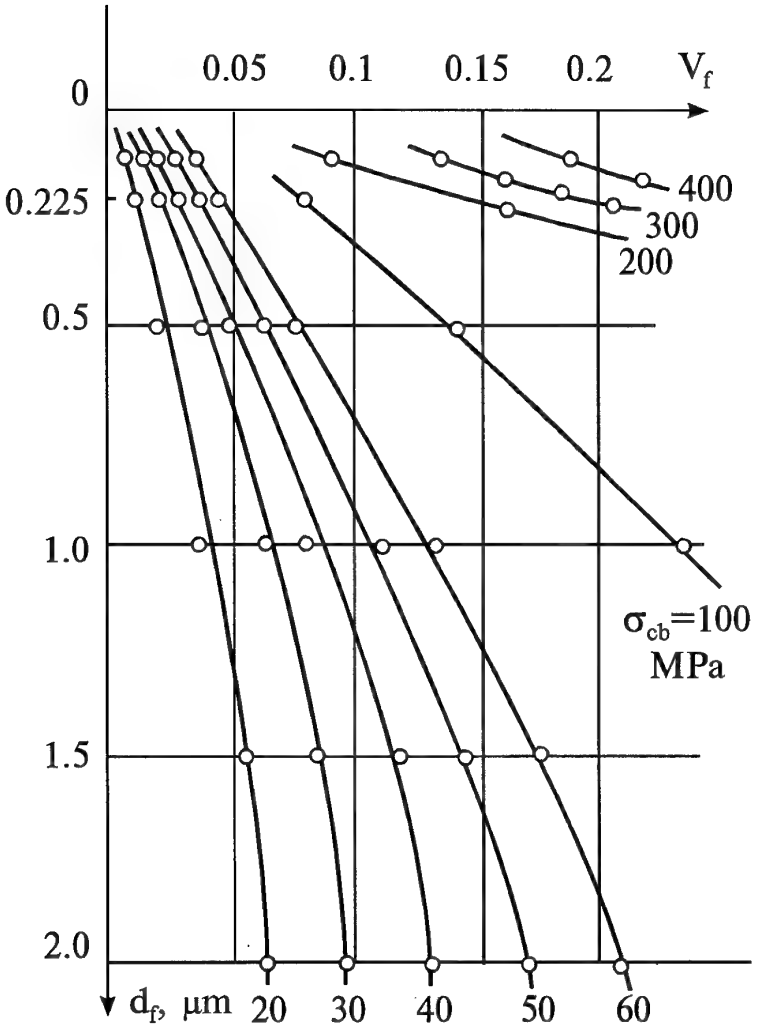

Figure 7. Composites: dependence of ultimate stress on V_f and d_f

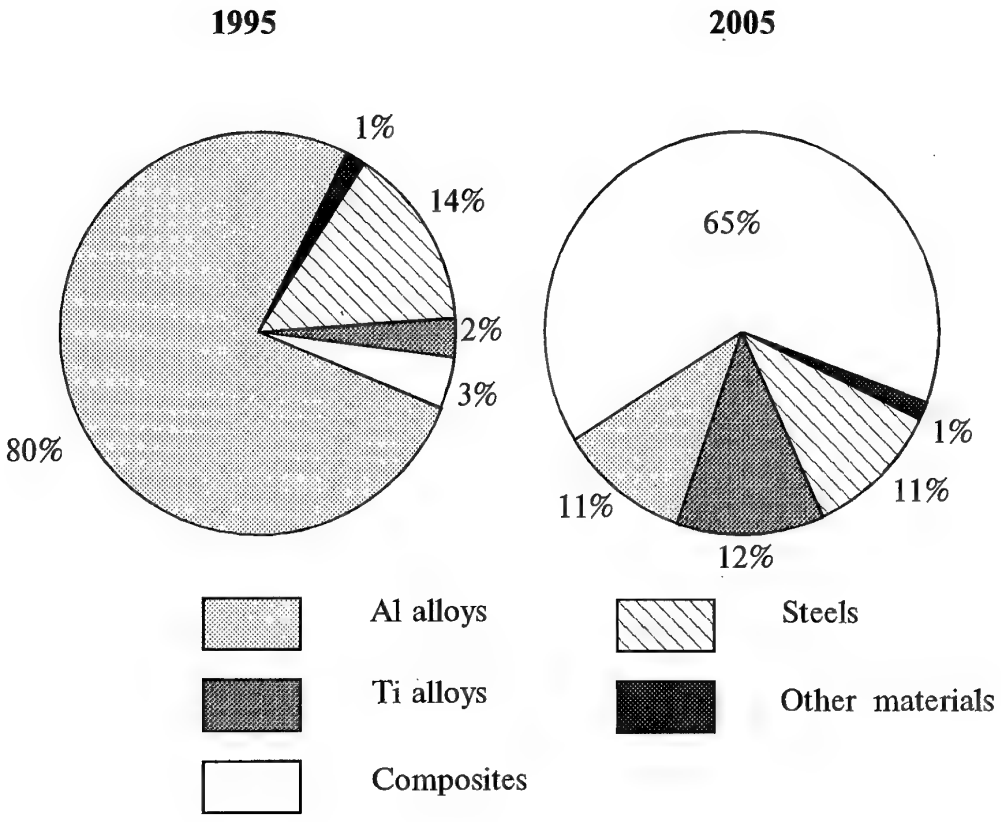

Figure 8. Materials percentage in airframes.

RELIABILITY, MAINTENANCE AND LIFE CYCLES OF COMPOSITE STRUCTURES

A.EU. USHAKOV

CENTRAL AERO-HYDRODYNAMIC INSTITUTE : (TSAGI)
ZHUKOVSKY,140160, MOSCOW REGION, RUSSIA

1. INTRODUCTION

Experience in the development, manufacture and operation of flying vehicles shows that realization of new materials and manufacturing processes is accompanied by notable changes and additions to airframe design methodologies and safety/reliability regulation documents that relate to features of the materials themselves and their behavior. Therefore, to attain the necessary effectiveness, the advantages of PMCs were used practically in accordance with the usual procedure adopted in aircraft industry (Fig. 1):

- "preliminary studies": establishing the factors that influence the airframe static and fatigue strength; formulating the requirements for materials, manufacturing processes, and design methods;
- "development": solving the "three-in-one" problem on development of (i) materials with high production/operational characteristics, (ii) low-cost and high-throughput manufacturing processes, and (iii) methodology for design and safety, taking into account features of the composite materials;
- "materials selection": the materials are chosen under requirements concerned with structural, process, and commercial issues:
  - at the concept definition stage, fulfillment of the following cnteria is verified:
    * the potential for PMCs to be mass-produced in the necessary amount, and
    * stability of materials and/or manufacturing processes;
    * the possibility of predicting the structural behavior from the data and analytical methods available,
  - at the stages of detailed design, manufacture, certification and utilization, the use of new materials is restricted by the standards, specifications and manuals modified to take into account the features of PMCs.

Figure 2 generalizes data on amounts of PMCs in structures of helicopters, maneuverable, cargo- and passenger-carrying airplanes - the ratio of the mass of PMCs, M_{PMC}, to the total airframe mass, M_z. These data evidence that implementation of the composite materials is in line with the procedure above. The range of composite structures and the implementation duration depend on the type of flight vehicle. In the early 1970s, the high requirements with respect to the structural weight and the relatively slack requirements to safety and the manufacture costs made it possible for PMCs to rapidly appear in maneuverable airplanes. In the early 1980s, the acute competition in the market of executive airplanes dictated the necessity to improve airplane performance and cut the manufacturing and operating costs by widely using PMCs, including development of all-composite airframes. However, the much more strict requirements (the low production costs, a longer service/calendar life, high levels of safety and reliability) and larger sizes of passenger-carrying airplanes have been decisive within the last 8-15 years for the use of PMCs in the maneuverable and executive airplanes structures.

By 1980s it was clear that the rate of PMCs replacing the metals depends on

* development of PMCs with necessary characteristics,

* availability of manufacturing facilities and high-rate manufacturing processes,

* effective methods and technologies for designing and testing the composite structures.

Therefore, the efforts related to the use of PMCs in aerospace industries are undertaken in three interrelated areas (Fig. 3):

a) in the field of composite materials science:

- modification of epoxy matrices, development of workable thermostable thermoset matrices, development of thermoplastic matrices,
- development of high-strength graphite fillers,
- increasing the degree of utilization of high characteristics of fillers by improving fiber-matrix interface;

b) in the field of composite structure manufacturing processes:

- the maximum use of technologies for automation and mechanization of
  - impregnation, winding and laying-up of prepregs,
  - formation of separate elements, subassemblies and the structure as a whole,

Paper presented at the AGARD SMP Lecture Series on "Advanced Polymeric & Metallic Composite Materials for Space and Aerospace Vehicle Structures. . .", held in Stuttgart, Germany from 11-12 December 1995; Châtillon, France from 14-15 December 1995 and Ohio, USA from 18-19 December 1995 and published in LS-204.

- structural integrity monitoring;

these are necessary conditions for ensuring stable manufacturing processes (which will result in ensuring the safety/reliability characteristics required);

c) in the field of composite structure design:

- development of advanced analytical and experimental methods for evaluating static and fatigue strength characteristics of composite structures,
- designe's and process enginee's options for ensuring damage tolerance of PMC structural components,
- preparing software for automated design of composite structures under static/fatigue strength and stability requirements.

2. EVOLUTION OF METHODS FOR ENSURING SAFETY AND RELIABILITY OF AIRFRAMES MADE OUT OF PMCs

To substantiate selection of reasonable methods for ensuring safety of composite airframes, let us address (i) the experience in fulfilling airframe service life requirements and (ii) information on in-service damage of composite structure.

Figure 4a shows a typical distribution of metallic structure damage occurence probability density f^{met} in time (T_s = service life). Depending on the way of fulfilling the service life requirernents, the whole range of the fatigue service life can be divided into three zones (I - 3):

- Zone I, where safety is ensured by a practical improbability of structure damage - the so-called safe-life zone;
- Zone II, where emerging damage must be detected in due time during special inspection; in this case a structure should be damage tolerant in service, i.e., it must have either a slow rate of crack growth (damage tolerance) or redundant elements (fail safe);
- Zone III, where operation can be allowed only when the damage does not reduce structure safety (service with structure condition monitoring).

In Table I and in Fig. 5, we see the data on airplane accidents (known by the author) because of fracture of PMC elements. Amongst 12 events, four are serious: two catastrophes and twoo complete failures. One should note that in 8 cases out of 12 the elements failed after being operated for about 40 flighf hours (i.e., for one-hundred or one-thousandth of the design service life); 7 cases were due to rnanufacturing faults not detected at factories; in one case bird strike which damaged the nose fairing, not revealed by the flight crew, and was the cause of catastrophe.

Considering the above features of the PMC behavior and assuming an "equiprobability" of PMC damage due to mechanical impacts dunng the whole senice life, a typical distribution of the damage probability density for PMC airframes, f^{PMC}, may be presented as in Fig. 4b. In this case the service life may be divided into two stages. Attaining the PMC airframe safety on the basis of the safe-life concept is not possible since the structures can be damaged both during manufacture and beginning from the very moment the aircraft enter service. As shown below, this conclusion is in agreement with the service experience.

Figure 6 summarizes values of admissible strains for PMC structures, corresponding to maximum in-service loads; this illustrates the influence of changing the design philosophy for PMC primary aircraft structures. Depending on the way of ensuring safety, it is possible to outline three stages of introducing the PMC structures in airframes.

At the first stage (m^{PMC} / m_{Σ} =1 - 5%) the following problems should be resolved experience accumulation, formulation of requirements to materials, manufacturing processes, operating conditions, weight reduction. Bearing in mind the high fatigue resistance of PMCs, the airframe components were designed based on a safe life concept, while the no-cracking condition for 90-degree layers was used as a criterion for ensuring static strength. The assumption of small probability of PMC is service damage made it possible to achieve a high weight efficiency due to increased composite element load level. E.g., at Σ_{lim}= 0.4% the mass reduction of F-111 prototype stabilizer boren/epoxy skins (which are primary airplane structures) amounted to 26% as compared with the metallic prototype [4].

As an operating experience was gained, it became possible to establish not only the facts that PMC structure in-service damages but also the fact that the provision of safety of damaged PMC structures designed within the safe-life principle is either impossible or economically unjustifiable (for example, in 1975 after two night failures of the F-5 rudders, caused by corroded metallic honeycomb and damage to graphite/epoxy skins due to impacts during scheduled maintenance, 43 remaining units had to be withdrawn from service since rnaintaining the appropriate safety requires frequent inspections involving non-destructive methods and skilled specialists (4)). Therefore, at the second stage the PMC amount was increased (m^{PMC} / m_{Σ} = 5-30% - in secondary and low-load primary airframe components (ligh-lift devices, tail unit, wing and fuselage components) designed under stiffness requirements and possessing considerable strength rnargins. The service safety for such elements is provided by reducing the level of admissible strains Σ_{lim} by a factor of 1.5 - 2 as compared with the stage l; this makes possible (i) long-time service of aircraft structures with damage, (ii) the use of visual inspections only, and (iii) cosmetic repairs, mainly in order to recover aerodynamic characteristics. These provisions correspond to the service of PMC aircraft structures with condition monitoring (Fig. 4b) Implementation of such an approach resulted in (i) reduction of weights of secondary and low-loaded

primary components by 12 - 23% as compared with rnetallic prototypes and (ii) the production cost reduction by 7 - 15%.
At the third stage of and fuselage primary structures of maneuverable and transport airplanes is the principle of ensuring damage tolerant or fail safe structure. Considered as a condition of its realization should be the solution of the three-in-one problem formulated above.
The damage tolvance criterion introduction ($m^{PMC}/m_{\Sigma} > 30\%$) the basis for the development of highly efficient wing makes it possible to increase the allowable strain level to 0.4% at moderate operating costs, and the expected reduction of weight of advanced wing/fuselage structures will arnount to 30 - 45%.

3. LIMITAIION OF UTILIZATION OF PMCs IN PRIMARY STRUCTURES

Experience in design, testing and use of composite airframes shows that the advantages of PMCs are impossible to utilize fully, because the allowable in servicœ stresses of composite structures must be limited in the light of the following circumstances.

3.1 Brittle fracture of PMCs

Brittle fracture of up-to-date PMCs under both dynamic and static loads is due to

- a low value of breakage strains (0.6 - 1.2%) and
- linear behavior up to failure for most types of fillers and matrices. The absence of local plastic deformation in a PMC is a determinant for features of fracture, as compared with failure of metals:
  - notable damage after mechanical impacts,
  - no plastic zone at a tip/corner of a stress concentration area (this results in high stress concentration factors),
  - abrupt propagation of fracture from an origin.

Figure 7 sumrnarizes results of studies undertaken by the author on static strength of specimens and panels of KMU-4 and KMU-9 graphite/epoxy systems after low-speed impacts. The damage (such as delamination, indentation, cracks) more significantly affects compressive strength than tensile and shear strength. It has been established that, depending on a specimen thickness and an impact energy, the damage not detected by inspection reduces compressive strength by 50 - 65% and tensile and shear strength, by 40 - 50%.
In Fig. 8 the author generalized his own data on the influencœ of through defects on compressive, tensile and shear strengths of KMU-3, KMU-4 and KMU-9 graphite/epoxy materials. Studies showed that all types of PMC lay-ups are sensitive to stress concentration. The presence of through cuts whose dimensions correspond to damage revealed in service degrade graphite/epoxy system strength by 35 -80%.

3.2 Environmental attack

Degradation of static/fatigue strength characteristics of PMCs is due to the effects of moisture on fibers, matrix and fiber-matrix interface. The individual contribution of each component depends on load conditions. PMC properties in tension along fibers are governed by fiber characteristics, so moisture effects on them is insignificant. Properties of a PMC in compression and shear depend mainly on matrix characteristics; the latter are affected with the following indications:

a) matrix swelling, extra stress,
b) matrix stiffness drop,
c) less strength of adhesion between fibers and matrix.

The reduction of compression/shear static/fatigue strength characteristics of PMCs in moist air becomes more significant in thermal cycling conditions with elevated temperatures.
Taking into account the variation of PMC properties under environnental attack, the regulations prescribing the procedures for PMC airframe certification in Russia and abroad require demonstration of static/fatigue strength under elevated temperature/moisture conditions by

- accelerated lab envirommental testing of specimens, components, and large-size structures and
- testing thereof in natural conditions.

However, even after such tests are fulfilled in the most severe in-service conditions, the degradation of PMC characteristics over the designed service life should in some cases be taken into account by introducing a safety factor of 1.1 - 1.2, see [5, 6]. Moreover, if the characteristics were determined in normal conditions then the design should be built up with supplementary safety factors which, being multiplied by the above values, result in 1.5 - 2.5 - this in most cases leads designer to a doubt on whether to use the polymer matrix composite materials, or not.

3.3 Scatter of PMC mechanical characteristics.

Figure 9 represents dependencœ of ultimate stresses and elastic moduli in tension (σ_b and E_{tens}) and compression (σ_{-b} and E_{compr}) on the relevant variance coefficients for mechanical characteristics ($\Upsilon\sigma_b$, ΥE_{tens}, $\Upsilon\sigma_{-b}$, ΥE_{compr}); this summarizes the results of the author's testing of specimens from KMU-1, KMU4 and KMU-9 graphite/epoxy materials. The variance coefficients of strength characteristics, as obtained in normal conditions, are larger by a factor of 2 to 3 than those of metals. The coefficients for stiffness characteristics are also larger, but not so significantly.
There exist various methods and procedures for taking into account the uncertainty of the mechanical characteristics. In Russian practice, the regulation recommendations (7) are based on establishment of supplementary safety factors for an intact PMC structure with due account of strength degradation by

10 - 20% over the service life; this approach is based on the idea of a structure failure probability for a certain service length (8). In foreign countries, use is also made of supplementary safety factors to allow for the larger variance, but these are predetermined on the basis of the experience available. For example, the increased strength variation is recommended in (9) to be accounted for by decreasing the PMC allowable stress by 20% in comparison with mean values; whereas Ref. (5) proposes a 10% reduction.

3.4 The influence on PMC efficiency of methods adopted for ensuring airframe safety

The practices and regulations defining the certification procedure and airframe design conditions, formulate the strength requirements for operation safety in the following way:

- the residual strength of the structure in the course of operation under environnental attack and with likely damage must be at a level sufficient for the structure to withstand the maximum in-service loads with due account for the factor of safety.

Airframes designed in accordance with the safe-life principle are not required to be inspected for integrity in service, and the safety factor is set at 1.5. We should bear in mind the above data about dependence of strength characteristics on defects whose dimensions correspond to composite structure damages detected im service (a strength reduction by a factor of 3.3 to 5); we should introduce corrections for degradation of PMC mechanical characteristics (10% for environmental effects and 10% for the greater variance); with this, as Fig. 10 demonstrates, the allowable stress for airframes made out of PMCs is 10 - 20% of the attainable breakage stress shown by the material itself.

For airframes designed in accordance with the damage tolerance principle (that is, those for which visual and instrumented inspections are planned for detecting damage) the safety factor may be decreased to 1.1 - 1.2, see (10, 11). This means that "mere" usual inspection (taking into account that strength of a PMC with damage undetectable in a visual inspection degrades by a factor of 1.7 - 2.2) makes it possible to raise the allowable stress by a factor of 2 or 3 as compared with the case above (Fig. 10). However, implementation of the damage tolerance principle in the PMC airframe design practice requires data on

- manufacturing and in-service damage probability,
- damage development rate, and
- residual strength of damaged composite elements.

4. FEATURES OF DAMAGE CUMULATION AND FRACTURE OF AIRFRAMES MADE FROM POLYMER MATRIX COMPOSITES

We should distinguish causes of damage to a PMC structure:

- manufacturing defects that appear in the course of production and
- in-service damage appearing in structure during operations.

Figure 11 represents the classification; depending on defect relative dimensions, we can distinguish

- microdefects whose sizes are comparable with dimensions of reinforcing elements,
- minidefects whose sizes are cemparable with a ply thickness,
- rnacrodefects whose **sizes are comparable with** characteristic dimensions of the structure.

4.1 Damage to PMC in production

Table 2 shows major manufacturing processes for PMC structures and their related characteristic defects.

The microdefects and minidefects in the form of composition imperfection and ply solidity violation do influence insignificantly the static/fatigue strengths of PMCs, and it is these defects that mainly produces the notable scattering influence in properties.

The PMC mechanical characteristics and structural function-related properties are most notably influenced by macrodefects, including:

- cracks
- foreign inclusions, voids, delamination, disbonded areas,
- surface dents, buckled zones, folds, overlap,
- defects due to impact.

Figure 12 demonstrates histograms of sizes of manufacturing flaws revealed by instrumented inspection of full-scale components on the TU-204 passenger airplane. These were caused by

- poor adhesion between PMC layers,
- the presence of water in the material,
- insufficient forming pressure,
- too rapid heating or cooling,
- isolated mechanical inclusions,
- mechanical impact during the manufacturing process, transportation (from one operation to another), storage, assembly, and/or check test.

4.2 In-service damage

Table 3 represents some data (known by the author) on inservice damage in composite structures of military and civil airplanes; most of the damages have been due to carelessness during ground maintenance (such as impacts at installation/removal and impact by a tool). Causes of the damage included also

- hail impact,
- impact by stones during takeoffs and landings,
- bird strikes,
- lightning strikes.

It should be noted that the author is not aware of cases of PMC fatigue failure under usual in-service loads. This fact shows that, unlike the fatigue failures of metallic structures in stess concentration areas (with cutouts, scratches, etc.), the high fatigue resistance of PMCs under various loading conditions does prevent not only fatigue failure of composite materials but also growth of manufacturing flaws and in-service damage. Indeed, impact-induced damage drastically reduces PMC static strength (Fig 7) but only slightly affects fatigue resistance of

- composite wmgs of LAK-12 ("Lietuva") glider (Fig. 13) and
- CFRP structures of the vertical and horizontal stabilizers of a vertical takeoff/landing fighter (Figs. 14 and 15).

From these data it follows that nondestructive inspection in fullscale fatigue tests did not reveal any growth of preliminarily introduced impact damage in various zones after cycling that corresponded to 1-3 designed service lives.

Thus, causes and mechanisms of manufacturing defects and inservice damage, as well as their development histories differ from those in metals. Although the total number of flight accidents due to damage in composite structures is by a factor of 100 to 1000 less than the number of the very damages, the sensitivity of statically loaded PMCs X defects (damage) requires us to consider each event of this kind as a precondition to a flight incident, since they contain a real threat of catastrophic failure of even the secondary airframe components.

4.3 PMC brittle fracture resistance: models and characteristics

To demonstrate safety and reliability of a PMC airframe at the design and certification stages, one should have the relevant information on the strength of a structure with various stress concentrators (flaws and damage, holes and cutouts etc.). This need required developing analytical methods based on models that enable determination of the strength of damaged PMC on the basis of fracture resistance charactetistics. References (12, 13) provide rather complete reviews of work on PMC fracture mechanics. Therefore we mention the basic models employed for analysing the strength of damaged polymer matrix composites (Fig. 16) :

- the Waddoups Eisenmann-Kaminski (WEK) model (14),
- the two-parameter model (17)
- the Nuismer-Whitney model (16),
- the Wu model (17),
- the Mar model (18).

* Taking this into account, the selection of a fracture model is based on such qualities as
sirnplicity,
* "speed of response",
* compatibility with traditional methods and procedures prepared for designers of metallic structures.

These requirements are best satisfied by the two-parameter model that uses the critical values of stress intensity factors for tension (K_{Ic}), compression (K_{-Ic}), and shear (K_{IIc}) as well as the appropriate corrections for the microcracking zone (a_I, a_{-I}, and a_{II}). The main advantage of this model is the opportunity to employ the force criterion of fracture mechanics in order to establish the correspondence between the lab specimen fracture condition and the full-size structure fracture condition. The critical values (K_{ic}, K_{-Ic}, and K_{IIc}) are material constants for brittle fracture, when the material around the crack tip is elastic until the crack starts developing in an unstable manner. The author mounted tests whose results indicate (Fig.18) that the quasi-brittle fracture condition is obeyed by most structual la-ups. Therefore the introduction of the cracking zone corrections ensures stability of values K_{Ic}, K_{-Ic} and K_{IIc} cover the entire range of defect sizes. This eliminates difficulties associated with dependence of PMC crack resistance characteristics on specimen geometry (such dependence is typical of metals) and enables us to employ the considerable experience in theorical and experimental determination of stress intensity factors (19, 20).

REFERENCES

1. Selikhov A.F. Fulfilling the structure service life requirements (aircraft manufacturing experience). Mashinovedeniye, 1986, no. 5, pp.11 - 18.

2. Soviet Civil Airplane Airworthiness Regulations. 3rd edition, 1979.

3. Selikhov A.F., Raykher V.L., and Khlebnikova I.G. Consideration of multiplicity of critical structural points to evaluate damage tolerance and service life. - Uchenyye Zapiski TsAGI, 1984, vol. 25, no. 2, pp. 72 - 81.

4. Lubin G. and Dastin S.J. Aerospace application of composites. - Handbook of composites, G. Lubin (ed.), van Nastrand Reinhold Co., 1982, pp. 722 - 743.

5. Picard C.A. Use of new materials and new technologies in modern aircraft structures. - L'Aéronautique et l'Astronautique 1988, 5, no. 132, pp.65-76.

6. Bell/Boeing design team maintains V-22 Osprey schedule static test vehicle begin in late January, 1987. - Aviation Week and Space Technology. 1986, March 17, p. 51.

7. Amendment I to Chapter 4 of ENLGS, 1987, 8 pp.

8. Styuart A.V. Method for establishing the safety factor for structures whose load-carrying capability varies in time. - Trudy TsAGI, 1977, no. 1876, 12 pp.

9. Sellars R.J. and Terry G. Sophisticated aircraft structure development - combat aeroplanes - Aeronautical J., 1981, IX, vol. 85, no. 847, pp. 334 - 342.

10. Chaumette D. Certification problems for composite airplane structures. - ICAS Proc., 1984, 3.4.1, pp. 421 - 425.

11. Strength of airplane structures - Design, testing and manufacturing of wide-bodied passenger-carrying airplanes. - G.P.Svishchyov and A.F.Selikhov (eds.), Mashinostroyeniye, Moscow, 1982, vol. II, book 2, 228 pp.

12. Trunin Yu.P. and Yagudina I.M. Fracture of elements of aircraft structure made of composite materials. - TsAGI Printing Office, review no. 562, 1979, 66pp.

13. Backlund J. Fracture analysis of notched composites. Computs and structures, vol. 13, 1981, pp. 145 - 154.

14. Waddoups M.E., Eisenmann J.R., and Kaminslki B.E. Macroscopic fracture mechanics of advanced composite materials. - J. Compos. Mater., 1971, vol. 5, X, pp. 446 - 454.

15. Trunin Yu.P., Chizhova R.I., and Shishmaryova A.S. Study of strength of damaged composite structures and point joints under tension, compression and shear. - Reports of TsAGI, no. 2, 1982, pp. 48 - 50.

16. Whitney J.M. and Nuismer RJ. Stress fracture criteria for laminated composites containing stress concentrations. - J. Compos. Mater., 1974, vol. 8, pp. 253 - 265.

17. Wn E.M. Phenomenological anisotropic failure criterion. - Mechanics of Composite Materials. - Sendeckyj G.P. (ed.) Academic Press, vol. 2, 1974, pp. 403 - 415.

18. Mar J.W. Fracture, longevity and damage tolerance of graphite/epoxy filamentary composite materials. - J. Aircraft, 1984, vol. 21, no. l, pp. M - 83.

19. Tada H, Paris P.S., aad Irwin G.R The stress analysis of crack handbook. - Del Research Corp., Hellertown, 1973, 310 pp.

20. Sih G.C. Handbook of stress intensity factors. - Lehigh University Press, Bethlehem, 1973, 345 pp.

21. Selikhov A.F. and Chizhov V.M. Theory of probability methods in airplane strength analysis. - Mashinostroyeniye, Moscow, 1987, 237 pp.

DESIGN OF DAMAGEABLE AIRCRAFT POLYMER COMPOSITE STRUCTURES WITH A HIGH STRENGTH AND ENHANCED SERVICE LIFE

A.Eu. Ushakov

Central Aero-Hydrodynamic Institute
(TsAGI)
Zhukovsky,140160,
Moscow region, Russia

Part I : General statements

Increased safety and service reliability of engineering structures are very challenging technical and economical problems for whose the solution required the development and practical application activities in the field of the manufacturing of advanced structural materials and products out of them. It becomes most obvious, in the course of the development of modern aircraft systems, when high cost of aircraft make necessary their reasonable long-term service with ever increasing flight frequencies and the provision of required aircraft structure safety and reliability. In this case we have to face two opposite requirements, the minimization of the mass and the increase of the structure service life. Therefore, the best trade-off has to be determined. Strict requirements to airframe mass depending on the need of the fulfilment of specified aircraft performances result in increased airframe structure stresses.

Under veriable loads and corrosive environment it is difficult to realize high operating stresses using only conventional metal materials, that is why an increase in aircraft strength and service life, while decreasing its mass, is associated with the application of polymer composites (PMC) on thermoplastic and thermoreactive matrices reinforced by

- carbon,
- organic,
- glass,
- ceramic

fibers which have high specific strength and stiffness, resistance to crack initiation and development under variable loads.

Increased requirements for structure weight efficiency enabling

- a high level of stresses,
- long service life ,
- great number of
  - operating ,
  - loading cycles

result in limited strengths and service lives of critical primary airframe structures: that means that a structure can approach prematurely its limit load capability.

The provision of the required fatigue resistance of polymer composite structures is not particularly difficult owing to their high fatigue resistance. Properties such as

- PMC brittle failure after mechanical impact,
- sensitivity to stress concentration under static loading,
- diversity of failure modes,
- scatter of mechanical characteristics and their deterioration under environmental attack,

multitude of types of manufacturing defects and in-service damagrs (and low effectiveness of methods for detection thereof) complicated the problem of providing required strength, service life, when designing PMC aircraft structures.

For these reason and regarding the lack of a sufficient design and service experience, necessary data on

- internal damages,
- residual strength,

and particular methodical recommendations, the scope of PMC application has been limited until few years ago to

- secondary,
- low-loaded

aircraft structures for which the level of maximum service stresses σ_{lim} amounts to 10-25% of the material ultimate σ_b series (Fig.1) which prevented the PMC advantages for being applied in full measure. The development of high-efficient primary airframe components from polymer composites has required a methodology to be implemented into the design practice which enables

- prediction,
- preventive

maintenance of PMC aircraft structures under given real service conditions while taking into account

- possible manufacturing defects,
- service damages,
- application of rational structural,
- technological methods

to improve the PMC failure resistance properties.

Data from experiments with PMC aircraft structures and from service records have shown that, considering both the brittle behavior and the high fatigue resistance, the damage initiation and growth mechanisms for the most of the current Polymer composites differ fundamentally from fatigue failure of metals. It has been noted that:

Paper presented at the AGARD SMP Lecture Series on "Advanced Polymeric & Metallic Composite Materials for Space and Aerospace Vehicle Structures. . .", held in Stuttgart, Germany from 11-12 December 1995; Châtillon, France from 14-15 December 1995 and Ohio, USA from 18-19 December 1995 and published in LS-204.

- Damages in polymer composites are not due to periodic airframe loading but to random mechanical impacts, that may occur at any stage of structure manufacturing and service, i.e.
  - ♦ impacts during assembly,
  - ♦ transportation and maintenance,
  - ♦ collisions with
    - * stones ,
    - * hailstones.

  These cases are not typical of metallic structures.
- Unlikely the process of fatigue damage accumulation and main crack growth in metals, the damage incipience in polymer composites due to impacts is of an "instantaneous" nature, therefore the structure strength decreases abruptly.
- There are no hidden damages in metals in they occur in polymer composites when they are manufactured or used, i.e.
  - * matrix cracking,
  - * fibre laminating, breaking.

In many cases such damages can be detected by non-destructive instrumental methods only, while the main means of detecting fatigue cracks in metallic structures are visual inspections.

- Damages in polymer composites under a spectrum of service loads grow extremely slowly.

Fig.2 compares the behavior model for a PMC structure in service including the above noted features with that of a metallic structures. Both types of structures have damages caused by mechanical impacts. A metal structure stress concentrator (scratch, hollow) which can be easily detected visually does not reduce its load capability in any way, but it does initiate the fatigue crack growth.

The growing crack is detected by visual inspections with the interval ΔT_v^{met} being scheduled in accordance with fatigue material characteristics, and a reliably detectable crack length $2L_{det}$. In this case the failure depends on the following events:

- ♦ initiation of a main crack,
- ♦ undetectability during inspections,
- ♦ attainment of a critical crack length $2L_{cr}$,
- ♦ occurrence of a failure load for a structure having a crack of $2L_i \geq 2L_{cr}$.

In polymer structures an "instantaneous" damage of $2L_i \geq 2L_{cr}$ can occur immediately after an impact which results in an abrupt reduction of the component strength below the admissible level. Therefore, unlikely the preceding case, the failure of a PMC damaged structure as well as the interval between its inspections ΔT^{PMC} are determined at the beginning of its entery into service by probabilities of impact after-effects resulting in a damage of

- * a size of $2L_i$,
- * failure load

which increase with service time $_s$.

- The mechanisms of damage initiation and growth found for polymer composites determine special features of system approaches to provide strength and service life of critical primary PMC aircraft structures with taking into account their damages during manufacturing and service. While for metallic structures the main factors limiting their service life and strength are
  - * the fatigue of main primary structures,
  - * corrosive damages ,
  - * wear of moving elements,

then for PMC aircraft structures those factors are damages due to

- ◊ mechanical impacts,
- ◊ sensitivity to stress concentration ,
- ◊ brittle failure behavior under static loading,
- ◊ scatter of mechanical properties,
- ◊ deterioration under environmental exposures.

The most dangerous cause of probable failures of PMC aircraft structures regarding to its sudden and disastrous nature are their damages due to in-service mechanical impacts resulting in a drastic (up to 50-60%) reduction of the structure load capability /1/, as well as some defects not detected during manufacturing. The stochastic nature of

- ♦ service loads,
- ♦ mechanical impacts,
- ♦ failure resistance

properties of PMC necessitates the application of a probabilistic failure model to solve the problem of providing

- * strength,
- * service life

of PMC aircraft structures, which ensures necessary safety factors resulting from the methods used to increase

- * residual strength,
- * damage "undetectability".

The main criteria of this problem applied to passenger aircraft are as follows /2/:

I. The failure of aircraft structures having non detected defects during manufacturing or service damages under repeated loads during regular service including seldom extreme values of these loads must be practically improbable. "Normalized" probability of this phenomenon is $P_N = 10^{-9}.....10^{-10}$ (1/f.h.)/3/.

II. The damage at which the aircraft failure probability $\beta_{d.s} > P_N$ must be detected in due time during specifically scheduled inspections using required non-destructive test methods. The detection reliability should provide the required structure.

III. The failure probability of damage aircraft structures must meet the requirements for the flight readiness (the probability of flights $P_{f.r.} = 0.97.....0.99$)

IV. The structure check- and maintability, the rate and procedure of inspections must satisfy the requirements

of serviceability determined by the number of man-hours required for maintenance and running repair.

The above criteria are constraints in the problem when the required strength and service life of PMC aircraft structures are provided while taking into account their damages at minimum consumption of mass. This problem is solved by taking and fulfilling a combination of measures during

- design,
- manufacturing,
- certification,
- service.

The first of them is the choice of design considerations to provide the required strength and service life which, alongside with a set of operation conditions, must include principles of ensuring the structure safety.

This philosophy governs both the requirements to residual strength of a damaged structure and necessary measures of a timely detection of damages.

In order to validate the choice of a rational way for ensuring the safety of PMC structures accounting for their damages we can turn to the experience of providing airframe service life and introducing polymer composites in aircraft manufacturing. Fig. 3a shows a typical distribution of metallic structure damage occurrence probability density f^{met} in time (T_s = service life). Depending on the way of fulfilling the service life requirements, the whole range of the fatigue service life can be divided into three zones [1 - 3]:

- Zone I, where safety is ensured by a practical improbability of structure damage -- the so-called safe-life zone;
- Zone II, where emerging damage must be detected in due time during special inspection; in this case a structure should be damage tolerant in service, i.e., it must have either a slow rate of crack growth (damage tolerance) or redundant elements (fail safe);
- Zone III, where operation can be allowed only when the damage does not reduce structure safety (service with structure condition monitoring).

In Table 1 and in Fig. 5, we see the data about the airplane accidents (known by the author) because of fracture of PMC elements. Amongst 12 events, four are serious: two catastrophes and two complete failures. One should note that in 8 cases out of 12 the elements failed after being operated for about 40 flight hours (i.e., for one-hundredth or one-thousandth of the design service life); 7 cases were due to manufacturing faults not detected at factories; in one case the bird strike has damaged the nose fairing, has not been revealed by a flight crew, and has been the cause of catastrophe.

Considering the above features of the PMC behavior and assuming an "equiprobability" of PMC damage due to mechanical impacts during the whole service life, a typical distribution of the damage probability density for PMC airframes, f^{PMC}, may be presented as in Fig. 4b. In this case the service life may be divided into two stages. Attaining the PMC airframe safety on the basis of the safe life concept is not possible since the structures can be damaged both in manufacture and beginning from the very moment the aircraft enter service. As shown below, this conclusion is in agreement with the service experience.

Figure 6 summarizes values of admissible strains ε^{lim} for PMC structures, corresponding to maximum in-service loads; this illustrates the influence of changing the design philosophy for PMC primary aircraft structures. Depending on the way of ensuring safety, it is possible to outline three stages of introducing the PMC structures in airframes.

At the first stage (m^{PMC}/m_{Σ}=1 - 5%) the following problems should be resolved: experience accumulation, formulation of requirements to materials, manufacturing processes, operating conditions; weight reduction. Bearing in mind the high fatigue resistance of PMCs, the airframe components were designed based on a safe life concept, while the no-cracking condition for 90-degree layers was used as a criterion for ensuring static strength. The assumption of small probability of PMC in-service damage made it possible to achieve a high weight efficiency due to increased composite element load level. E.g., at $\varepsilon_{lim} = 0.4\%$ the mass reduction of F-111 prototype stabilizer boron/epoxy skins (which are primary airplane structures) amounted to26% as compared with the metallic prototype [4].

As the operating experience was gained, it became possible to establish not only the facts of PMC structure in-service damage but also the fact that the provision of safety of damaged PMC structures designed within the safe-life principle is either impossible or economically unjustifiable (for example, in 1975 after two flight failures of the F-5 rudders, caused by corroded metallic honeycomb and damage to graphite/epoxy skins due to impacts during scheduled maintenance, 43 remaining units had to be withdrawn from service since maintaining the appropriate safety requires frequent inspections involving non-destructive methods and skilled specialists [4]). Therefore, at the second stage the PMC amount has been increased (m^{PMC}/m_{Σ} = 5 – 30% -- in secondary and low-load primary airframe components (high-lift devices, tail unit, wing and fuselage components) designed under stiffness requirements and possessing considerable strength margins. The service safety for such

elements is provided by reducing the level of admissible strains ε_{lim} by a factor of 1.5 - 2 as compared with the stage 1; this makes possible (i) a long-time service of aircraft structures with damage, (ii) the use of visual inspections only, and (iii) cosmetic repairs, mainly in order to recover aerodynamic characteristics. These provisions correspond to the service of PMC aircraft structures with condition monitoring (Fig. 4b). Implementation of such an approach resulted in (i) reduction of weights of secondary and low-loaded primary components by 12 - 23% as compared with metallic prototypes and (ii) the production cost reduction by 7 - 15%.

At the third stage of introduction ($m^{PMC}/m_{\Sigma} \geq 30\%$)the basis for the development of highly efficient wing/fuselage primary structures of maneuverable and transport airplanes is the principle of ensuring damage tolerant or fail safe structure. Considered as a condition of its realization should be the solution of the three-in-one problem formulated above.

The damage tolerance criterion makes it possible to increase the allowable strain level to 0.4% at moderate operating costs, and the expected reduction of weight of advanced wing/fuselage structures will amount to 30 - 45%. On of the structural methods to provide the fail safety of PMC aircraft structures is special stoppers preventing these structures from a disastrous growth of damage cracks which are built in the composite skin by a local change of stiffness and toughness /6,7/. Fig.5 gives the ways for forming low- and high-modulus crack stoppers in graphite-epoxy skins.
In order to achieve the required PMC aircraft structure strength and service life, a number of measures should be taken from the very beginning of aircraft design, during its manufacturing and service. A combination of these measures is an organizational and technical system whose structure and main takes are presented in Fig.6 /2/.The typical features of this system are as follows:

- the formulation of conditions to provide strength and service life before designing, accounting for damage tolerance and fail-safe requirements when statistic strength and service life are considered starting from the earlier design stages; the unity of models and methods to analyze and predict structure service life characteristics;

- the existence of constant feedbacks permitting required corrections of models and methods on the basis of laboratory and flight test results and service experience.

The realization of this system assumes that a number of structural and technological measures should be used to ensure required survivability (Table 1).
Particular attention is given to the so-called regular structure zones including,

- alongside the skin itself,
- longitudinal joints of the skin with
  - spars,
  - ribs.

Because of extended and, hence, non-efficient local reinforcements, the failure resistance characteristics of the regular zones determine

- the level of admissible operational stresses

and, in a decisive way,

- structure masses

as well. The main means of ensuring the required survivability of the regular zones are as follows:

- the choice of the material and layup schemes providing respective toughness and PMC failure resistance under mechanical impacts;
- the joint of the PMC skin with PMC reinforcing elements in a non-cured state by means of cross-linking, and the use of "buffer-strips" in the joint zone in case of mechanical fasteners;

the application of integral structures where reinforcing elements are used as crack growth stoppers and special formation of crack stoppers in PMC skins.
The implementation of

- automated technological processes,
- monitoring,

control of service conditions
reducing the level of PMC structure damages in

- manufacturing ,
- service

are very important additional means of increasing the weight efficiency of regular zones of PMC aircraft structures.
The main task for a wide spectrum of structural and technological measures aimed to

- provide
  - strength ,
  - survivability

of nonregular zones (Table 1),

- minimize
  - the volume of structure-designing ,
  - reinforcement

during

- certification,
- serial production,
- service

related to its premature failure caused both by

- a high PMC sensitivity to structural stress concentrators (fastener holes, cut-out etc.) ,
- technological defects ,
- service damages in these zones as well.

The possibilities given by the whole complex of the structural and technological measures of providing the service life of PMC aircraft structures are realized and verified while providing and improving the survivability along the following main directions.

A) The definition of PMC aircraft structures damages during manufacturing and service. Analytical and experimental procedures of predicting PMC damage parameters under mechanical impacts at laboratory conditions and statistic methods of their determination based on results of PMC structure inspections during
- manufacturing,
- repair,
- service.

make it possible, respectively, to select structural and technological means of reducing structure damages while designing and to determine the survivability and safety in order to actively control the processes of product manufacturing and technical service. At present, methodical criteria of damage considerations for the PMC aircraft structure classification are being formulated.

B) The analysis of general and local stress-strained stated of regular and nonregular structure zones. For these purposes use is made of modern powerful computing complexes bases on the finite element method and which ensure the prediction of stress-strained states of complicated structures having arbitrary forms and the optimization of the structural scheme from the conditions of static strength, service life and aeroelasticity.

C) The prediction of the damage size growth and residual strength of PMC aircraft structures using the data of the damages and stresses in elements and joints. The current design technique is based on a two-parameter model of fracture mechanics of composites with idealized through defects (slot, hole). Accounts for
- the effects of PMC failure modes,
- structural , technological, service factors on the residual strength

provide the prediction of the failure under
- ◊ combined loading
- ◊ the PMC structure strength with crack stoppers.

At the same time the variety of PMC damage types (defects) shows that it is necessary to further
- develop ;
- implement
  - * models ,
  - * methods

of the composite fracture mechanics in order to determine more precisely the residual PMC structure strength with
- typical manufacturing defects;
- service damage (laminations, matrix cracking, layer break etc.).

D) The determination of survivability based on probabilistic methods of predicting the failure of damaged PMC aircraft structures which account for scatters of
- service loads,
- damage sizes,
- residual strength,
- srructural sheme used. The level of
- admissible stresses,
- safety factors with respect to residual strength,
- inspection periodicity.
- required efficiency of strength recovery methods (repairs) ,

which are established for various strategies of PMC structure service from the condition of providing the required survivability at a specified failure probability accounting for constraints on admissible service manhoures.

E) Testing of structural schemes during
- preliminary and detailed design,
- the verification of their efficiency during Certification using test results of
  - * specimens,
  - * structural elements,
  - * units,
  - * fragments (Table 2).

The Russian and foreign experience shows that a timely experimental verification of the solutions is an extremely efficient method of avoiding premature failures during full- scale tests and in service. The tests results of component
- specimens of regular zones (skins, spar, rib walls and booms),
- zones of loading nonregularities (lugs, suspension units)

give the characteristics of PMC
- ◊ strength,
- ◊ stiffness,
- ◊ toughness

that are required for verification calculations, and find the scatter of these characteristics and the environmental influence on them as well. The tests of more complicated structural elements (units, fragments) are used to obtain the information on their
- * strength,
- * service life,
- * survivability

in laboratory conditions and in extreme service conditions and to improve and certificate manufacturing methods, control and repair techniques.

F) Full-scale static and fatigue laboratory tests of damaged PMC aircraft structures which are a means of a final survivability verification to formulate

conditions providing service safety and reliability within a specified aircraft service life. From survivability point of view the strength and service life of PMC aircraft structures must be verified in full-scale tests for main design cases of loading:

* in the presence of manufacturing defects and service damages that will not be detected during the whole service life;
* in the presence of service damages that will be detected during scheduled special -purpose visual and instrumental inspections;
* in the presence of "obvious" service damages of large sizes with which the structure can be operated during a short time period (a-2 flights).

The above procedure is performed using two full-scale articles, one of which is intended for static and the second one for fatigue and residual strength tests. Table 3 gives recommendations for the sequence of full-scale structure tests, which were realized, e.g., during the certification of the PMC aileron structures of the passenger aircraft Tu-204, wing and stabilizer of the performance-type glider LAK-12 /8/. The size of damages and the type of the defects simulating them, the value of applied loads for each damage case are determined in a special analysis using the service experience, control- and maintainability of PMC aircraft structures, their failure after effects on general aircraft reliability and safety.

Part II : Probabilistic model of failure

The provision of survivability implies the determination of the level of admissible service stresses, intervals between inspections and repair efficiency when a required level of service safety of polymer composite (PMC) aircraft structures is achieved while taking account of their damages. This problem can not be considered without accounting

- for the effects of a combination of structural,
- technological and service aspects,
- stochastic nature of service loads and mechanical impacts,
- scatter of damage (defect) sizes and failure resistance characteristics of polymer composites.

That is why the methodical background for its solution is a probabilistic model of the failure of damaged PMC aircraft structures which services as a basis for applying required safety factors, the choice of which is governed by the efficiency of the methods used to improve survivability, control and inspections during manufacturing, service and repair. In doing so, use is made of the methods of the reliability theory, based on terms of structure failure probability during a certain service life.

Taking the admissible probability of failure during the whole service life β_{Σ}^{adm} as a criterion, we can write the condition of structure failure with an admissible damage of $2L_{adm}$ as follows

$$\beta_{\Sigma}^{adm} = \beta(2L_{adm}, P_c^{adm}, f_{P_c}, \Delta T, \varphi) \qquad (2.1)$$

where $\beta(2L_{adm}, P_c^{adm}, f_{P_c}, \Delta T, \varphi)$ is the failure probability of a damaged structure with accounting for inspections, carried out with interval ΔT , and repairs with efficiency $\varphi = \frac{P_c^{rep}}{P^{design}}$ (P_c^{rep} is the structure strength with a repaired damage; design strength of an undamaged structure P^{design}).

Based on the analysis of the mechanisms of PMC damage incipience and growth /9/ and accounting for their detection peculiarities during inspections, we take as design sizes of admissible damages $2L_{adm}$ with which the structure must retain admissible residual strength P_c^{adm} the following ones:

$2L_{adm}^{a}$ - for manufacturing defects and service damages that will not be detected during the whole service life;

$2L_{adm}^{b}$ - for service damages that are detected in special-purpose visual and instrumental structure inspections;

$2L_{adm}^{c}$ - for obvious damages to be detected during an overall structure inspection.

Admissible damages $2L_{adm}^{b}$, $2L_{adm}^{c}$ relate to regular structure zones with an ensured free access for inspections.

Fig.7 shows an interrelationship between P_c^{adm} and $2L_{adm}$ for three given design damage cases. The values of P_c^{adm} and f_{P_c} are determined in accordance with the possibilities to detect damages and the time of their existence.

When studying such a complex random event as a failure of a damaged structure we can resort to "partitioning" it in simpler ones so that the relationship for the final result in the combination of "elementary" event results should be defined using sufficiently obvious assumptions.

Then the analysis of the complex event might be replaced by a study of its constituents with a subsequent estimation of probabilities of final results based on the assumptions taken. Applying the above approach to eq.(2.1) and neglecting the values of the second, third and forth order in view of their smallness, we obtain the relationship between β_{Σ}^{adm} and all design cases as a sum of independent summands:

$$\beta_{\Sigma}^{adm} = \beta_{ds}^{a} + \beta_{ds}^{b} + \beta_{ds}^{c} + \beta_{ds}^{rep} \qquad (2.2)$$

where

β_{ds}^{a} - is the failure probability of a damaged structure during the whole service life;

β_{ds}^{b} - is the failure probability of a damaged structure in the intervals between inspections during the whole service life;

β_{ds}^{c} - is the failure probability of a damaged structure in flight;

β_{ds}^{rep} - is the failure probability of a repaired structure.

Eq.(2.2) establishes an unambiguous correlation between the requiredments to

- level of safety,
- value of PMC toughness,
- effectiveness of the methods of increasing survivability,
- methods of recovering structural strength in repairs,
- quantity and quality of inspections.

The specific determination of safety factors, intervals between inspections and the choice of repair techniques at the stages of technical proposals and design are carried out on the basis of the eq.(2.2) using constraints of specific labor volume for inspections and repairs, as well as from the condition of achieving a minimum mass, which are design criteria.

In order to account for the scatter of the residual structural strength and limit loads during the determination of safety factors and the period between inspections use is made of the dependence of failure probability β_t for a flight f_{P_c} hour on safety factor γ_c and residual strength variation factor of the type presented in Fig.8. for transport aircraft /9/. In the case under discussion a normal distribution of probabilities of

random values with variation factor $\gamma_c = 0.08$ is taken for limit loads. In case of the absence of damaged structure tests for residual strength the value of variation factor γ_c is taken to be equal to the value of variation factor of toughness ($\gamma_{K_{1c}}$) under respective loading conditions. The test experience /10/ shows that, as a rule, this value for PMC does not exceed 0.08-0.1. The dependencies presented allow us to value of safety factors at a known value of γ_c and a specified level of β_Σ^{adm} (now it is β_Σ^{adm} = 0.0001-0.0005) for transport airframe determine the structures).

1. The determination of safety factors f_{Pc}^{*} and f_{Pc}^{c}. For structures undamageable during their service or for which $2L < 2L_{adm}^{*}$ (i.e. $\beta_{ds}^{b} = \beta_{ds}^{c} = \beta_{ds}^{rep} = 0$) eq.(2.2) has the form $\beta_\Sigma^{adm} = \beta_{ds}^{*} = \beta_f T_s$. It follows from Fig.8, that for this damage case the safety factor $f_{P_c}^{*} = 1.5$ yields $\beta_\Sigma^{adm} \le 0.0005$ for a transport aircraft with service life of $_s$ = 50000 flighthours at $\gamma_c \le 0.08$.

A component with an "obvious" service damage $2L_{adm}^{c}$ is operated during a short time period when the probability of a limit load is negligible. Therefore, if the moment of the damage appearance is not fixed by the pilot during the flight, then is taken, and if the moment of the damage is fixed during the flight or is detected in a pre-flight aircraft inspection, then, according to A.V. Stuart, is taken. The given values of $f_{P_c}^{c}$ =0.67 provide the non-equality $\beta_{ds}^{*} << \beta_\Sigma^{adm}$ since the actual value $f_{P_c}^{*}$>1.5. It should be noted that the given values of safety factors $f_{P_c}^{*}$, $f_{P_c}^{c}$ coincide with recommendations of the Boeing /11/ and Dassault-Breguet /12/ companies for similar cases of damages of PMC aircraft structures.

2. The determination of safety factor $f_{P_c}^{b}$ and intervals between inspections.

The safety factor $f_{P_c}^{b}$ and the interval between inspections ΔT are determined with taking into account the multiple PMC structure damages and the scatter of the occurrence moments and possible sizes $2L_{adm}^{b}$ under the following assumptions:

* The damages occur independently of each other and produce their effect on the structure strength independently either.
* During equal time periods the number of damages N in each structure of this type is the same for the whole aircraft fleet.

In determining $f_{P_c}^{b}$ and ΔT we use the model of providing the service survivability of PMC aircraft structures whose basic components will be both random and determinate values. The first group includes:

- admissible damage size $2L_{adm_i}$;
- limit service load during time period between inspections P_{lim} ;
- residual structure strength $P_c(2L_{adm_i})$.

The second group includes the values subject to determining: intervals between inspections ΔT , safety factors $f_{Pc_i}^{b}$.

1. The structure without crack stoppers

The service survivability of structures without crack stoppers is provided according to the principle "damage tolerance". While determining the value of β_{ds}^{b} let us use the linearization with respect to rare events, i.e. we shall account for only main terms in the relationships which establish the probability of their occurrence. Then considering that in this case the residual strength of the structure with N damages is governed by the size of the largest one, the expression for the failure probability during the intervals between special-purpose inspections for the whole service period is as follows:

$$\beta_{ds}^{b} = \sum_{m=1}^{M}\left\{\sum_{i=1}^{L}\beta_{fi}\Delta T_{Nm}\chi_i(N,\Delta T_{Nm})\sum_{n=1}^{m}P_{n.d.}^{n-1}(2L_i,1)\right\} \quad (2.3)$$

where

M - is the number of special-purpose inspections including visual and instrumental methods (i.e. the intervals between visual and instrumental inspections are taken to be equal);

m - is the number of inspection,

β_{fi} - is the probability of structure failure with damage $2L_{adm_i}$ for a flight hour;

$\chi_i(N,\Delta T_{NM})$ - is the probability of such a combination of N damages during the period between inspections ΔT_{Nm} for which the largest one has the size of $2L_{adm_i}^{b}$.

Expression (2.3) is obtained providing that the probability of the non-detection of the damage during one inspection $p_{n.d.}(2L_i,1)$ is independent of the number of inspections.

The values of $\chi_i(N,\Delta T_{Nm})$ are found from the equation

$$\left[\sum_{i=1}^{L}\chi_i(1,\Delta T_1)\right]^{N} = 1,$$

where

ΔT_1 - is the service time during which a damage of any kind and size appears in each components of this type in the whole aircraft fleet;

$\chi_i(1,\Delta T_1)$ - is the probability of the occurrence of damage $2L_{adm}^{b}$ during time period ΔT_1

$$\chi_i(1,\Delta T_1) = \quad (2L_i)\Delta T_1,$$

where $(2L_i)$ - is the intensity of the service damage occurrence under mechanical impacts.

If not more than one damage of any kind and size appears in each component of this type in the intervals between special-purpose inspections for the whole aircraft fleet then we have

$$\beta_{ds}^{b} = \sum_{m=1}^{M}\left\{\sum_{i=1}^{L}\left\{\beta_{f1} \quad (2L_i)\Delta T_m^{2}\sum_{n=1}^{m}p_{n.d.}^{n-1}(2L_i,1)\right\}\right\} \quad (2.4)$$

For "absolutely reliable" special-purpose inspections with a period of $\Delta T = \frac{T_s}{M}$ we have

$$\beta_{ds}^{b} = M \sum_{i=1}^{I} \{\beta_{fi} H_i(2L_i)\Delta T^2\} \qquad (2.5)$$

Equations (2.3-2.5) based on known values of $H_i(2L_i)$, $p_{n.d}(2L_i,1)$ allow us to establish the values of $f_{P_{ci}}^{b}$ for a given schedule of special-purpose inspections which provide the required level of the failure probability of a damage structure β_{ds}^{b} and, inversely, to determine the required periods between inspections for ΔT taken and PMC toughness (K_{ic}). The calculation procedure is as follows:

the whole range of possible sizes of admissible damages $2L_{adm}^{a} < 2L_{adm}^{b} < 2L_{adm}^{c}$ is divided into I segments $\Delta 2L_i$ where, in each segment, the residual strength is assumed to be a constant value and equal to the value of the residual strength of the PMC structure with maximum damage for this segment- $\sigma_c(2L_i^{max})$. Then based on values of $f_{P_{ci}}^{b} = \dfrac{\sigma_c(2L_i^{max})}{\sigma_{lim}}$ and variation factor γ_c the values of β_{fi} are found from Fig.8 which are substituted into eqs.(2.3-2.5) to determine β_{ds}^{b} for a given schedule of inspections ($\Delta T_{Nm}, \Delta T_m, \Delta T$).

In those cases when the period between inspections required to provide the safety of the structure with "admissible damages" is too short and does not meet the requirements with respect to the admissible level of labor volume for servicing either service loads should be reduced or PMC failure toughness increased or constraint applied to the intensity of the damage occurrence and their sizes. When the listed measures do not allow us to attain the specified weight efficiency and serviceability, then using structural and technological methods of forming crack stoppers one should resort to a fail-safe type of PMC structures.

2. The structure with crack-stoppers

In this case the structure with crack stoppers or elements of the same destination is divided into d cells so that when there appears a damage in the structure it could develop only within q cells damaged, at the moment of the impact, without prejudice to the remainder.

For a fail-safe element with crack stoppers predicted admissible damages are:

a) a damage of the size of one insterstopper distance provided that one cell ($q_{adm}^{a} = 1$) fails as a result of the crack development from damage $2L_{adm}^{a}$;

b) a damage of the size of one-two interstopper distances provided that one or two cells fail as a result of damages $2L_{admi}^{b}$;

c) a damage of the size of more that two interstopper distance that occurs when a crack develops from an "obvious" damage $2L_{adm}^{c}$ ($q_{adm}^{c} > 2$).

When the period between inspections and safety factors $f_{P_{ci}}^{b}$ are determined the following data are used:

- intensity of the occurrence and possible sizes of admissible damages $2L_{admi}^{b}$, which cause failures corresponding to predicted admissible damage q_{adm}^{b};
- controllability expressed through the probability of damage non-detection for one visual inspection of the damage whose size is equal to one or two interstopper distances $p_{n.d.v}$ (1.1), $p_{n.d.v}$ (2.1);
- admissible damage number N^{mf} at which the condition satisfies the damages influence independently of the structure strength.

The value of N^{mf} depends on the total area of the element and the location of damages with respect to each other.

Fig.9 illustrates possible cases of damages which lead to multiple failures in a section of the skin with crack stoppers at $N = 2$. The probability of each of these events is assessed from the ratio of

$\dfrac{F_{fail}}{F_{\Sigma}}$ - type, where

F_{Σ} -is the total area of the skin surface;

F_{fail} - is the area where an "off-design" damage leading to a premature disastrous structure failure, can occur when damages $2L_{adm}^{b}$, $2L_{adm}^{b}$ causing failures of an admissible number of cells appear.

The probability of a structure failure within the intervals between inspections during the whole service life is established as follows:

$$\beta_{ds}^{b} = \beta_1(\Delta T) + \beta_2(\Delta T) + \beta_{mf}(\Delta T), \qquad (2.6)$$

where $\beta_1(\Delta T), \beta_2(\Delta T), \beta_{mf}(\Delta T)$ - are the probabilities of structure failures in the intervals between inspections during the service life in the presence of a damage whose size is equal to one or two interstopper distances and at multiple failures, respectively.

We assume that during the period between special-purpose inspections the number of visually undetectable damages for each structure of this type and for the whole aircraft fleet is equal to N^{mf}. In the intervals between these inspections visual inspections with periods ΔT_{mN}^{V} are conducted in order to reveal visually detectable damages including failed cells.

In compliance with assumptions adopted the values of $\beta_1(\Delta T)$, $\beta_2(\Delta T)$ -are found from equations of the form; (2.7)

$$\beta_K(\Delta T) = M \sum_{m=1}^{M^V} \left\{\beta_{fk}^{st} \Delta T_{Nm}^{V} \theta_{Ki}(N, \Delta T_{Nm}^{V})\right\}$$

$K = 1;2$ is the number of failed interstopper distances corresponding to the size of the admissible damage ;

M - is the total number of special-purpose inspections during the service life;

M^V - is the number of visual inspections during the period

between special purpose inspections;

$\beta^{\#}_{f_K}$ - is the probability of a failure during a flight hour of the structure with a damage whose size is equal to interstopper distances;

$\sum_{i=1}^{I}\{\beta_{fi}\Delta T^{V}_{Nm}\theta_{Ki}(N,\Delta T^{V}_{Nm})\}$ - is the probability that in the interval between visual inspections ΔT^{V}_{Nm} the strength of a damaged structure is determined by the damage size that is equal to K interstopper distances (i.e. the size of one of N damages is equal to K instopper distances and the remainder of damages are less or equal to this size and they influence the strength independently of each other);

$\theta_{Ki}(N,\Delta T^{V}_{Nm})$ is the probability of the occurrence of such a combination of N damages during ΔT^{V}_{Nm} for which the growth of the maximum one leads to a damage of the size that is equal to K interstopper distances and the remainder of the damages are less or equal to it and influence the strength independently of each other.

$$\sum_{i=1}^{I}\theta_{Ki}(N,\Delta T^{V}_{NM}) = \sum_{i=1}^{I}\xi_{Ki}(N,\Delta T^{V}_{NM})\times$$

$$\times\frac{F_{\Sigma}-\sum_{P=1}^{P}F_{fail}}{F_{\Sigma}},$$

where

$\sum_{P=1}^{P}F_{fail.P}$ - is the area of the structure surface where the appearance of a damage of the size that is more than K interstopper distances is possible as a result of a damage that fails K cells.

$\xi_{Ki}(N,\Delta T^{V}_{Nm})$ - is the probability that the structure with N damages would have K failed cells when there $2L^{b}_{admi}$ appears at least one of them. In the case under discussion the possible number of damaged cells, when damage appears, is equal to $K=1;2$, the values of $\xi_{K_i}(N,\Delta T^{V}_{Nm})$ can be found from the equation:

$$\left[\sum_{i=1}^{I}\xi_{1i}(1,\Delta T_{1m})+\sum_{i=1}^{I}\xi_{ri}(1,\Delta T_{1m})\right]^{N}=1,$$

where

$\xi_{1i}(1,\Delta T_{1m}),\xi_{2i}(1,\Delta T_{1m})$ - are the probabilities that the structure with a damage of the size of $2L^{b}_{admi}$ would contain, respectively, one and two damaged cells.

ΔT_{1m} - is the service time corresponding to the m-th visual inspection during which there appears one damage of any kind and size in each structure of this type for the whole aircraft fleet.

$$\sum_{i=1}^{I}\xi_{1i}(1,\Delta T_{1m})=\sum_{i=1}^{I}\{H_t(2L_i)\Delta T_{1m}\times F_1(2L_i)\}$$

$$\sum_{i=1}^{I}\xi_{2i}(1,\Delta T_{1m})=\sum_{i=1}^{I}\{H_t(2L_i)\Delta T_{1m}\times F_2(2L_i)\}$$

where

$F_1(2L_i),F_2(2L_i)$ - are the probabilities that a damage of the size of $2L^{b}_{admi}$ would lead to one and two damaged cells, respectively. The values of $F_1(2L_i),F_2(2L_i)$ are found from the equation:

$$F_1(2L_i)=1-\frac{h^{\#}+2(2L^{b}_{admi}-h^{\#})}{2\times 2W+3h^{\#}}=1-F_2(2L_i),$$

where

$2W,h^{\#}$ - are the width of the interstopper distance and the width of stoppers, respectively. If we take the probability of a structure failure in the presence of a multiple failure to be the period between inspections $\beta^{\#}_{fmf}\times\Delta T^{V}_{NM}=1$, then

$$\beta^{b}_{mf}=M\sum_{m=1}^{M^{V}}\sum_{i=1}^{I}\left[\beta_{fi}\Delta T^{V}_{Nm}\theta_{mf_i}(N,\Delta T^{V}{}_{Nm})\right] \qquad (2.8)$$

where $\theta_{mfi}(N,\Delta T^{V}_{Nm})$ - is the probability of the occurrence of such a combination N of damages during ΔT^{V}_{Nm} when the growth of a maximum one could lead to a damage of the size that is large than two interstopper distances.

$$\sum_{i=1}^{I}\theta_{mfi}(N,\Delta T_{Nm})=\sum_{i=1}^{I}\xi_{Ki}(N,\Delta T^{V}_{Nm})\frac{\sum_{P=1}^{P}F_{fail.P}}{F_{\Sigma}}$$

When during the period between inspections there appears no more than one damage, of any kind and size, in each structure of this type for the whole aircraft fleet, its failure probability is established without accounting for the failure multiplicity $(\beta_{mf}(\Delta T))=0$. In this case, visual inspections conducted in the aim of revealing completely failed cells are the prime control method.

The probability of a structure failure in the intervals between "absolutely realiable" visual inspections in expressed as follows (2.9):

$$\beta^{b}_{ds}=\sum_{k=1}^{2}\beta^{\#}_{fk}T_s\sum_{i=1}^{I}\left\{\beta_{fi}\Delta T^{V}\left[H_t(2L_i)\Delta T^{V}F_K(2L_i)\right]\right\}$$

The probability of a structural failure in the intervals between visual inspections with accounting for the damage nondetection, provided that the values of $p_{n.d.v}(1.1)$, $p_{n.d.v}(2.1)$ do not depend on the number of inspections, is established from the equation (2.10):

$$\beta^{b}_{ds}=\sum_{m=1}^{M^{V}}\sum_{k=1}^{2}\{\beta^{\#}_{fk}\Delta T^{V}_{m}\sum_{i=1}^{I}\left\{\beta_{fi}\Delta T^{V}_{m}\left[H_t(2L_i)\Delta T^{V}_{m}F_k(2L_i)\right]\right\}\times$$

$$\times\sum_{n=1}^{m=n}p^{n-1}_{n.d.v}(k,1)\}$$

Using eqs.(2.6-2.10) and known values of $H_t(2L_i),\beta_{fi},\beta^{\#}_{fk},p_{n.d.v.}(k,1)$ it is possible to establish at a given β^{b}_{ds} the required period between inspections or to assess β^{b}_{ds} with specified inspection schedule and efficient methods of increasing the residual strength of a damaged structure. The prediction procedure is as follows:

the whole range of possible values of $2L^{b}_{admi}$ is divided into I segments and the values of f^{b}_{Pci} and β_{fi} are found for each of them in the same manner as in case of "damage tolerance".

When $f^b_{PCI} < 1$, then the safety factor is supplemented by the probability of the crack propagation from damage $2L^b_{admi}$ in the structure with crack stoppers during the period between inspections $\beta_{fi}\Delta T = 1$. Then the residual strength of the structure in the presence of K failed cells and the value of safety factors $f^b_{P_{CK}} = \frac{\sigma_c(K)}{\sigma_{lim}}$ are determined. Based on the values of $f^b_{P_{CK}}$ and residual structure strength variation factor γ_c found from full-scale component tests or from tests of small-scale panels with crack stoppers the values of β^d_{fk} are determined from Fig.8 which are used in expressions(2.7-2.10) at a known value of β^b_{ds}.

3.The determination of the level of admissible limit stresses

In accordance with the found safety factors $f^a_{Pc}, f^b_{Pc}, f^c_{Pc}$ the following values are established:

σ^a_{lim} - admissible structure limit stresses in the presence of undetectable damages $2L^a_{adm}$;

σ^b_{lim} - admissible structure limit stresses in the presence of damage detectable during inspections $2L^b_{adm}$;

σ^c_{lim} - admissible structure limit stresses in the presence of "obvious" damages $2L^c_{lim}$.

The level of admissible limit stresses for a PMC structure from the conditions of providing survivability is taken to be equal to:

$$\sigma^{adm}_{lim} = \min\begin{Bmatrix}\sigma^a_{lim}\\ \sigma^b_{lim}\\ \sigma^c_{lim}\end{Bmatrix}$$

Fig.10. compares the analysis results of the effect of the PMC fracture toughness on the value of admissible limit stresses σ^{adm}_{lim} with the existing experience of the design, certification and service of PMC aircraft structures. Solid and dot lines present admissible limit stresses corresponding to design damages considerations of PMC aircraft structures. The results in Fig.10.a show that the suggested damage criteria are satisfied by those aircraft units as

* horizontal stabilizer of F-16, whose survivability is verified by the exiting service experience,
* vertical stabilizer of B-1,
* horizontal stabilizer of B-737,
* horizontal stabilizer flap of "Alpha-Jet", whose survivabilities are confirmed by certificate full-scale tests /13,14/.

High survivability characteristics of the above structures are provided owing to adequate margins for static and residual strengths which are ensured by the respective design requirement for aircraft structure stiffness.

The data in Fig.10b indicate that the level of admissible limit stresses is increased in order to attain the required survivability of PMC structures, various structural technological methods can be used, the choice of which is made on the basis of the

* weight efficiency,
* manufacturing costs,
* maintenance etc.

The effectiveness of unidirectional carbon fiber strips used as crack stoppers and formed in booms of carbon fiber spars and ribs and which reinforce the low-modules carbon fiber skin is verified by survivability tests and service experience of the wing and forebody section of AV-8B /15/, of the A 300/A 310 fin /16/. The same effectiveness in providing survivability possess high-modules stoppers formed of boron fiber layers in the carbon fiber skin of the test horizontal stabilizer of B-1 /17/.A high tension effectiveness of low-modules crack stoppers formed of unidirectional glass fiber layers makes it possible to increase the level of admissible limit stresses for the lower wing surface up to $\sigma^{adm}_{lim} = 250 - 320$ MPa which is verified by wing box model tests of F-4 /18/.

4. The determination of the required efficiency of repair method.

Aircraft structures are repaired in which damages of the sizes of $2L^b_{admi}$ and $2L^c_{adm}$ are detected during inspections. In choosing the repair method it should be taken into account that the failure probability of an aircraft structure with damages of small sizes assumed during its service life could be neglected in case it is considerably less than β^b_{ds}.

Hence, it is possible not to repair the damages of the sizes of $2L^{n.rep}_{admi} < 2L^{rep}_{adm}$ or to apply only a "cosmetic" repair, e.g., in order to recover the aerodynamic efficiency of the skin surface. The size of damages $2L^{n.rep}_{admi}$ not to be repaired is established depending on the level of admissible limit stresses from the following condition:

$$\left(\beta^b_{ds}\right)^{n.rep} = \sum_{i=1}^{c} \beta_{fi} T_s \chi_i(N, T_s) << \beta^b_{ds} \qquad (2.11)$$

where $(\beta^b_{ds})^{n.rep.}$ is the failure probability of a structure with damages of the size of $2L^{n.rep.}_{admi}$ during the service life.

$\chi_i(N, T_s)$ is the probability of the occurrence during the service life of such a combination of N damages for which the damage governing the value of the residual strength has the size of $2L^{n.rep.}_{admi}$. If there appears no more tan one damage of the size of $2L^{rep.}_{admi}$ subject to repair in each structure of this type during the service life for the whole aircraft fleet, the required efficiency of the repair method φ in case of "absolutely reliable" inspections with period ΔT is found from the following condition:

$$\beta_{ds}^{rep} = \sum_{i=C+1}^{I} (H_t(2L_i^{rep})\Delta T \beta_c^{rep} \Delta T \sum r << \beta_{ds}^{b}) \quad (2.12)$$

where β_{ds}^{rep} is the failure probability of a structure with repaired damages of the size of $2L_{admi}^{rep}$ during the service life of $_s$;

$r = 1,2,3...M - 1$ is the number of the repair;

$M = \frac{T_s}{\Delta T}$ - is the number of inspections;

β_c^{rep} - is the failure probability of a repaired structure during a flight hour;

$H_t(2L_i^{rep})$ - is the occurrence intensity of damages of the size of during a flight hour.

In case a multiple structure failure the conditions for determining φ have the following form:

$$\beta_{ds}^{rep} = \sum_{i=C+1}^{I} (H_t(2L_i^{rep})\Delta T \times \beta_c^{rep} \Delta T \times \sum r +$$

$$+ \beta_c^{rep}(T_s - \Delta T^{rep}{}_1) << \beta_{ds}^{b}$$

$$\text{if } \Delta T = \frac{\Delta T_1^{rep}}{M} \quad (2.13)$$

$$\beta_{ds}^{rep} = \beta_c^{rep}(T_s - \Delta T_1^{rep}) << \beta_{ds}^{b}, \text{ if } \Delta T \geq \Delta T_1^{rep} \quad (2.14)$$

where $\Delta T_1^{rep} = \frac{1}{H_t(2L_i^{rep})}$ is the service period during which a damage of the size of $2L_{admi}^{rep}$ appears in each structure of this type for the whole aircraft fleet.

$M > 2$ is the number of inspections during the time period of ΔT_1^{rep}.

The value of β_C^{rep} is determined from conditions (2.12-2.14) and based on this value, safety factor $f_{PC}^{rep} = \frac{\sigma_c^{rep}}{\sigma_{lim}}$ is found from Fig.8 when the repaired component strength variation factor is known γ_c^{rep}. Then the required efficiency of the repair method $\varphi = \frac{\sigma_c^{rep}}{\sigma_{ultim.}} \times 100\%$ is established. It should be noted that expressions (2.12-2.14) are obtained assuming that the values of φ do not depend on damage sizes. The required efficiency of the method of repairing the damages occurring at the very beginning of the service, including "obvious" damages $2L_{adm}^{c}$, is established from the following conditions:

$$\beta_{ds}^{rep} << \beta_{ds}^{a} \quad \text{at} \quad \beta_{ds}^{a} = \beta_{\Sigma}^{adm}$$

$$\beta_{ds}^{rep} \approx \beta_{ds}^{a} \quad \text{at} \quad \beta_{ds}^{a} << \beta_{ds}^{b}, \beta_{ds}^{a} << \beta_{ds}^{c}$$

Fig.11 gives the analysis results establishing the required efficiency of the method of repairing the tension carbon fiber skin presented as dependencies of stresses on the PMC fracture toughness at the following specified conditions:

$_s = 60000$ flight hours;

$\beta_{\Sigma}^{adm} = 10^{-3}$

$\Delta T = 2500$ flight hours;

$\gamma_{K1c} = 0.08$

$2L_{adm}^{a} = 20mm$

$20mm < 2L_{admi}^{b} < 75mm$

$2L_{adm}^{c} = 250mm$

$H_t(2L) = 2 \times 10^{-3} e^{-2L/15} + 1.25 \cdot 10^{-5} e^{-2L/20}$

$f_{Pc}^{c} = 0.67$

$\gamma_c^{rep} = 0.08$

$f_{Pc}^{a} = 1.5$

The dependence characterizing the variation of the required strength of repaired components σ_c^{rep} at an increased fracture toughness of the skin material is shown by a dash-dot line.

Comparing it with given values of ultimate stresses σ_{ultim} for an undamaged skin, which are taken as a PMC ultimate strength in the first approximation it becomes clear that in order to provide the required service safety level the repair methods applied must have an efficiency of $\varphi = 38 - 46\%$

References

1. A.Ye. Ushakov, V.V. Kireev. Determination of load capability of compressed carbon fiber shells in case of absence and presence of stress concentrators under increased temperatures. -Mekhanika kompozitnykh materialov, 1988, N2, s.299-305.

2. A.F. Selikhov Provision of structure service life (aircraft manufacturing experience). -Mashinovedenie, 1986, N5, s.11-18.

3. Airworthiness requirements for Soviet civil aircraft. Third edition,1979.

4. A.F. Selikhov, V.L. Raykher, I.G. Khlebnikova Consideration of the
multiplicity of critical structure places to evaluate survivability and service life. -Uchenye zapiski TsAGI, 1984, t.XV, N2, s. 72-81.

5. G.Lubin, S.J. Dastin. Aerospace application of composites. - Handbook of composites, ed. By G.Lubin, van Nastrand Reinhold Co.1982, s.722-743.

6. Bell/Boeing design team maintains V-22 Osprey schedule static test vehicle begin in late January, 1987. - Aviation Week and Space Technology. 1986, March 17, p. 51.

7. Amendment I to Chapter 4 of ENLGS, 1987, 8 pp.

8. Styuart A.V. Method for establishing the safety factor for structures whose load-carrying capability varies in time. - Trudy TsAGI, 1977, no. 1876, 12 pp.

9. Sellars R.J. and Terry G. Sophisticated aircraft structure development -- combat aeroplanes. - Aeronautical J., 1981, IX, vol. 85, no. 847, pp. 334 - 342.

10. Chaumette D. Certification problems for composite airplane structures. - ICAS Proc., 1984, 3.4.1, pp. 421 - 425.

11. Strength of airplane structures -- Design, testing and manufacture of wide-bodied passenger-carrying airplanes. - G.P.Svishchyov and A.F.Selikhov (eds.), Mashinostroyeniye, Moscow, 1982, vol. II, book 2, 228 pp.

12. Trunin Yu.P. and Yagudina I.M. Fracture of elements of aircraft structure made of composite materials. - TsAGI Printing Office, review no. 562, 1979, 66 pp.

13. Backlund J. Fracture analysis of notched composites. - Computers and structures, vol. 13, 1981, pp. 145 - 154.

14. Waddoups M.E., Eisenmann J.R., and Kaminski B.E. Macroscopic fracture mechanics of advanced composite materials. - J. Compos. Mater., 1971, vol. 5, X, pp. 446 - 454.

15. Trunin Yu.P., Chizhova R.I., and Shishmaryova A.S. Study of strength of damaged composite structures and point joints under tension, compression and shear. - Reports of TsAGI, no. 2, 1982, pp.
48 - 50.

16. Whitney J.M. and Nuismer R.J. Stress fracture criteria for laminated composites containing stress concentrations. - J. Compos. Mater., 1974, vol. 8, pp. 253 - 265.

17. Wu E.M. Phenomenological anisotropic failure criterion. - Mechanics of Composite Materials. -- Sendeckyj G.P. (ed.) - Academic Press, vol. 2, 1974, pp. 403 - 415.

18. Mar J.W. Fracture, longevity and damage tolerance of graphite/epoxy filamentary composite materials. - J. Aircraft, 1984, vol. 21, no. 1, pp. 77 - 83.

Table 1

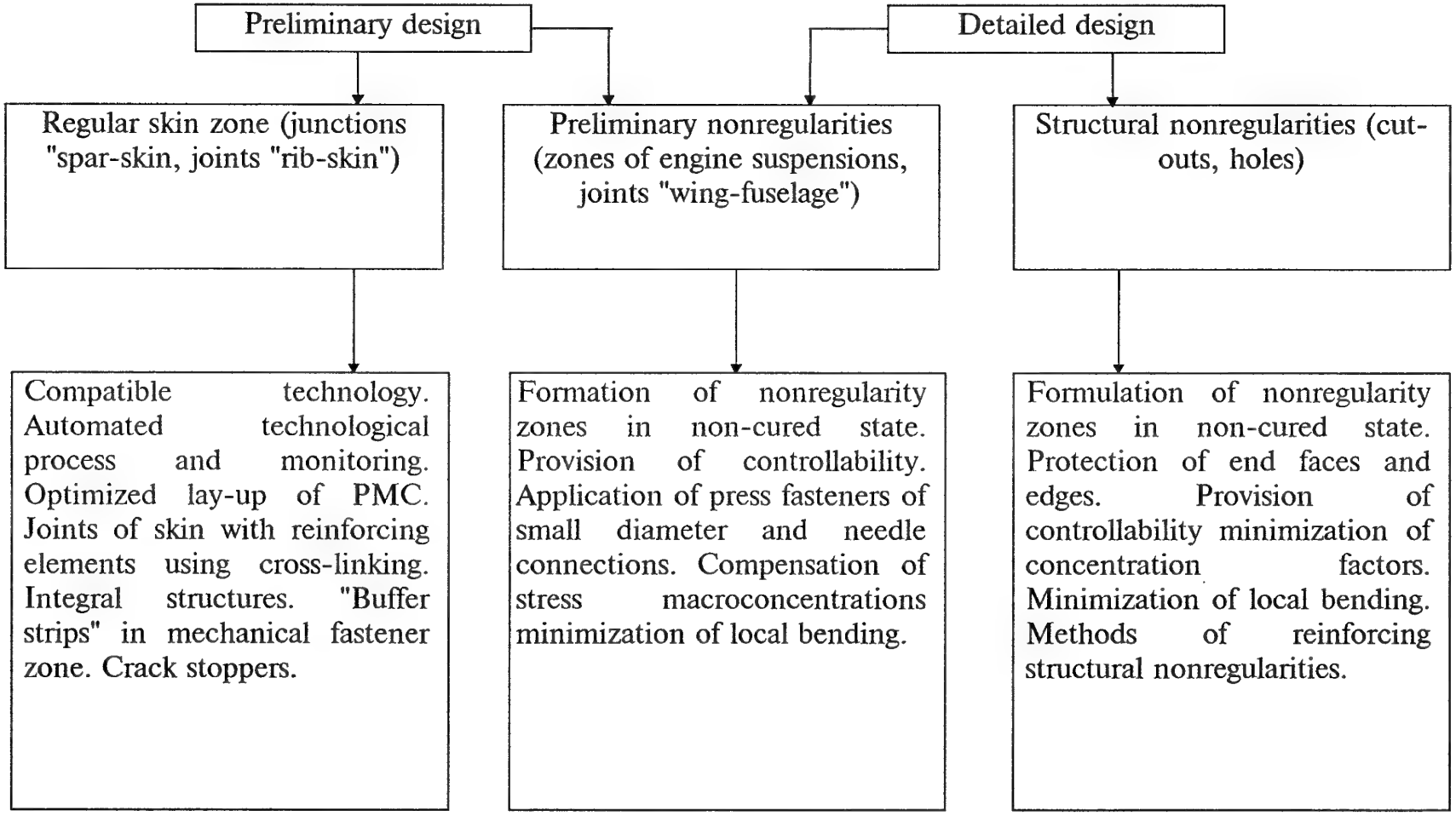
Preliminary design
Detailed design
Regular skin zone (junctions "spar-skin, joints "rib-skin")
Preliminary nonregularities (zones of engine suspensions, joints "wing-fuselage")
Structural nonregularities (cut-outs, holes)
Compatible technology. Automated technological process and monitoring. Optimized lay-up of PMC. Joints of skin with reinforcing elements using cross-linking. Integral structures. "Buffer strips" in mechanical fastener zone. Crack stoppers.
Formation of nonregularity zones in non-cured state. Provision of controllability. Application of press fasteners of small diameter and needle connections. Compensation of stress macroconcentrations minimization of local bending.
Formulation of nonregularity zones in non-cured state. Protection of end faces and edges. Provision of controllability minimization of concentration factors. Minimization of local bending. Methods of reinforcing structural nonregularities.

Table 2

Test object	Specimen or element type	List of tests
Specimens	skin panels	statics (compression, shear, combined, loading) fatigue tests survivability tests ("damage tolerance" and "failsafe")
	spar walls	strength and survivability tests at static shear
	spar booms	strength and survivability tests at static tension and compression
	mechanical joints	strength and survivability tests at static loading fatigue tests
	skin panel with rib fasteners (spar)	- " -
	suspension assenablies (lugs)	- " -
Element (unit, fragments)	root spar box	Static tests; fatigue tests; survivability tests; tests of repaired structures; climatic tests
	box segment	
	root skin panel with fastener fitting	

Table 3

N structure example	Test type	Damage cases	Test purpose
I	Static	$2L^{a}_{allwbl}$	Verification of ultimate static load in the presence of damages undetectable during whole service life
	Fatigue (correspond to whole service life)	$2L^{a}_{allwbl}$	1. Study of metallic structure element fatigue. 2. Study of PMC damage growth undetectable during whole service life
	Fatigue (correspond to the interval between inspections)	$2L^{b}_{allwbl}$	Study of growth of damages detectable in intervals between special-purpose inspections
	Static	$2L^{b}_{allwbl}$	Verification of required residual strength in the presence of damages detectable in special purpose inspections
	Static	$2L^{c}_{allwbl}$	Verification of required residual strength in the presenceof "obvious" damages
	Fatigue	repaired damages	Verification of fatigue life of repair zone
	Static		Verification of required repair efficiency

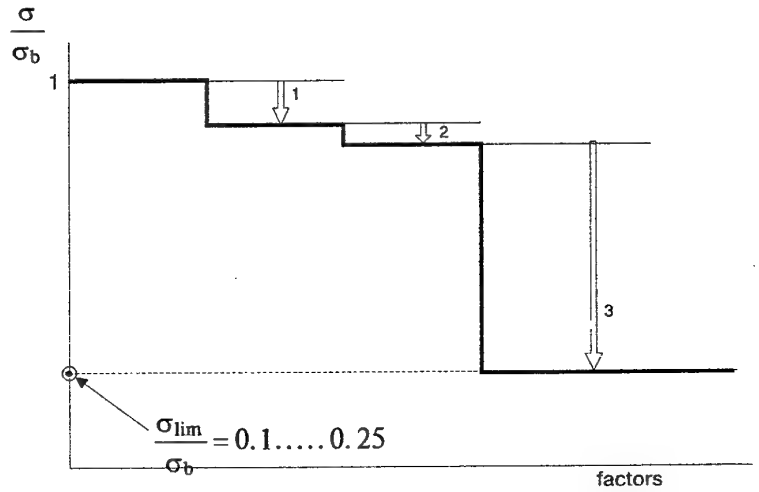

Fig.1. Influence of the scatter of characteristics (1), moisture saturation (2) and stress concentrators (3) on the level of relative service stresses $\frac{\sigma_{lim}}{\sigma_b}$

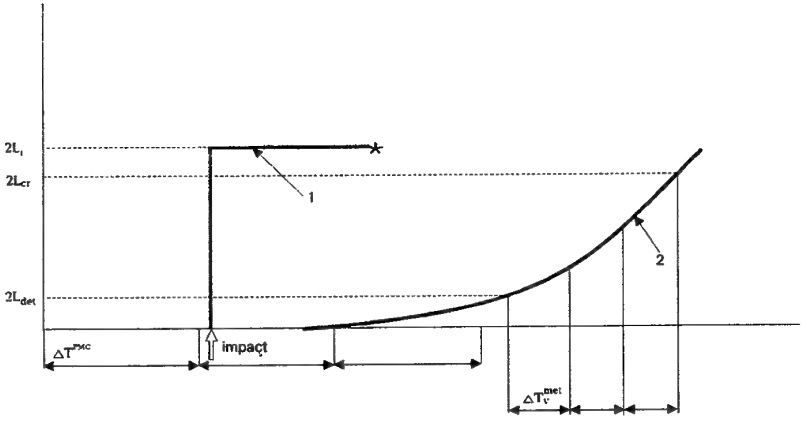

Fig.2. Comparison of service behavior of polymer composite element (1) and metallic structure (2) damaged under mechanical impacts (* is failure).

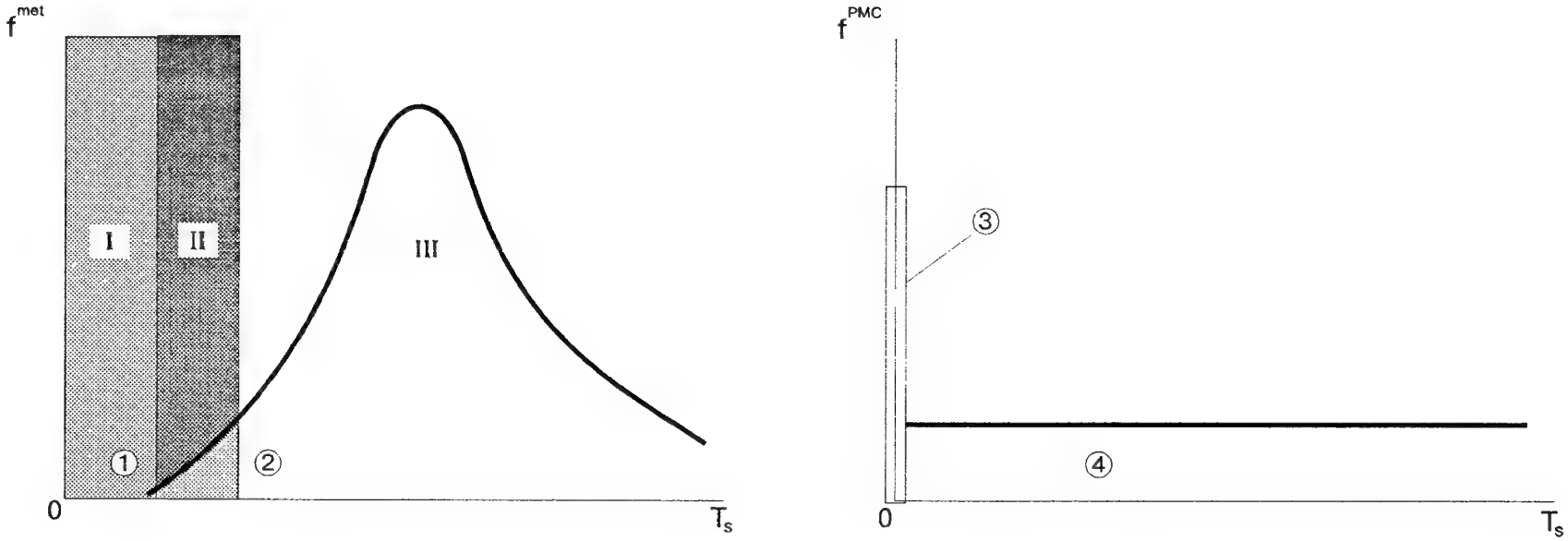

Fig.3. Damage probability densities during service life of a metallic structure (a) and a PMC element (b) with different methods of providing their service life (1-safe service live; 2- "damage tolerance" or "fail safe"; 3- manufacturing defects; 4 - service damages).

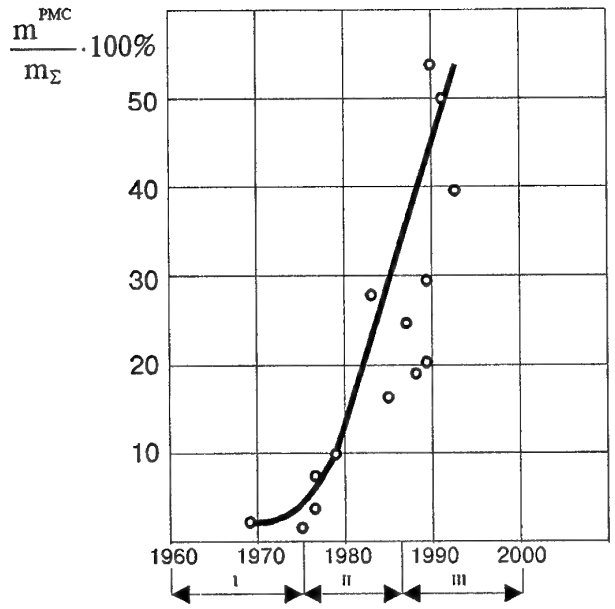

a)

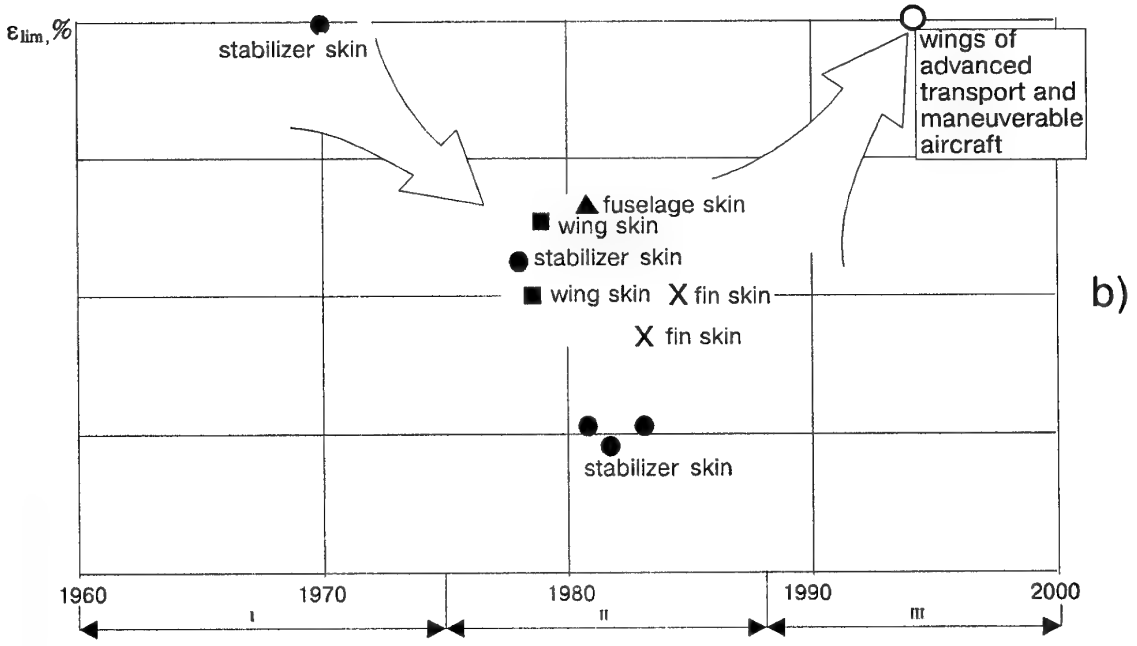

b)

Fig.4. Trends of the variation of the relative PMC mass in the airframe structure of a manoeuverable aircraft $\left(m^{PMC} / m_\Sigma \right)$ and of the level of admissible strains ε_{lim} for PMC structures.

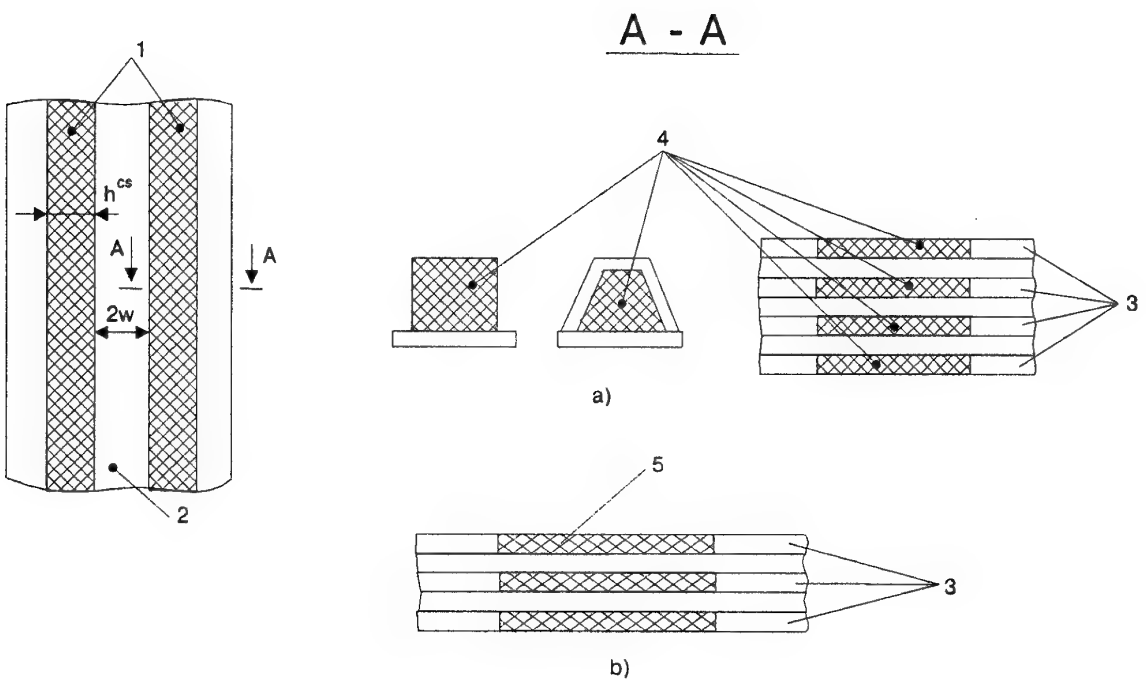

Fig.5. Methods of forming high-modules (a) and low-modules (b) crack stoppers in carbon fiber skins (1-stoppers, 2-basic material; 3- 0^0 - layers of carbon fibers; 4- 0^0 -layers of boron or carbon fibers; 5- glass or Kevlar layers).

Fig. 6 Interrelation of design / process measures for ensuring damage tolerance
(using safe-life and fail-safe principles)

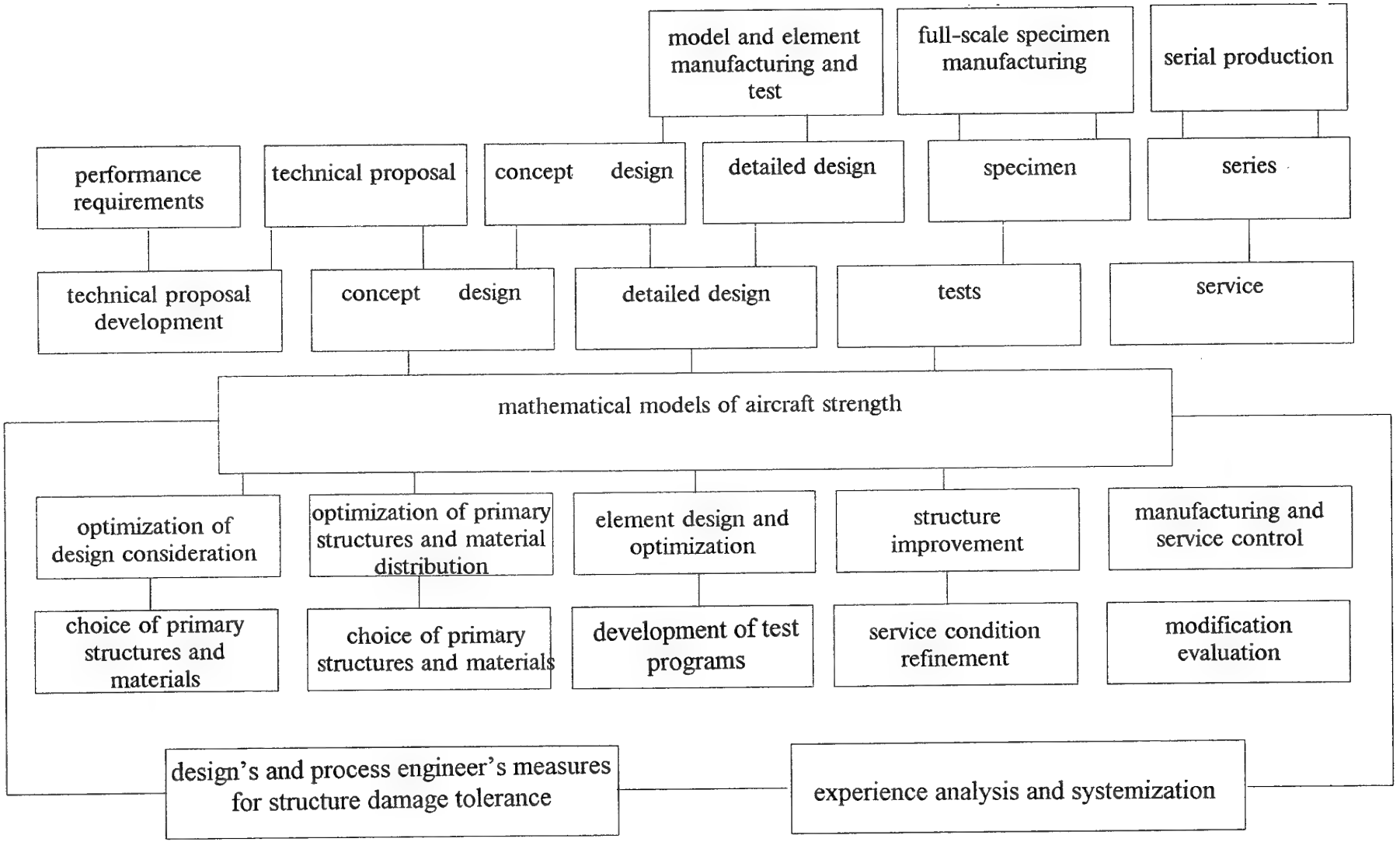

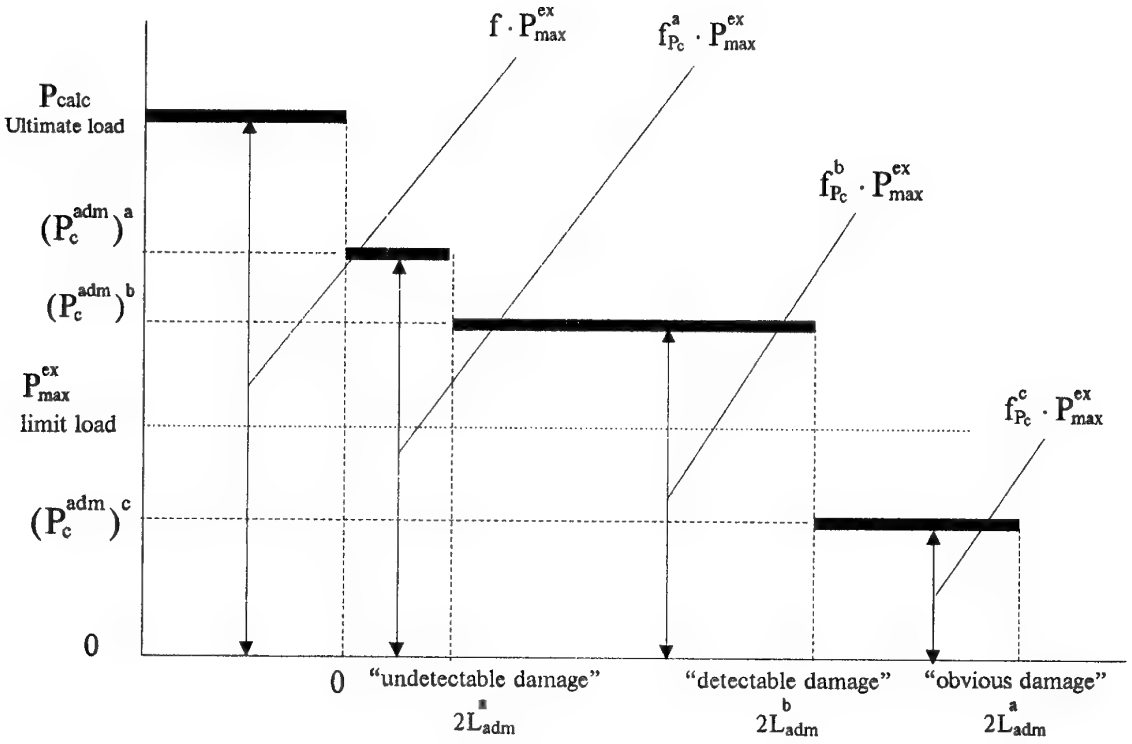

Fig.7. Interrelation between P_c^{adm} and sizes $2L_{adm}$ for design damage cases of PCM aircraft structures (P^{ult} is the design strength of an undamaged aircraft structure).

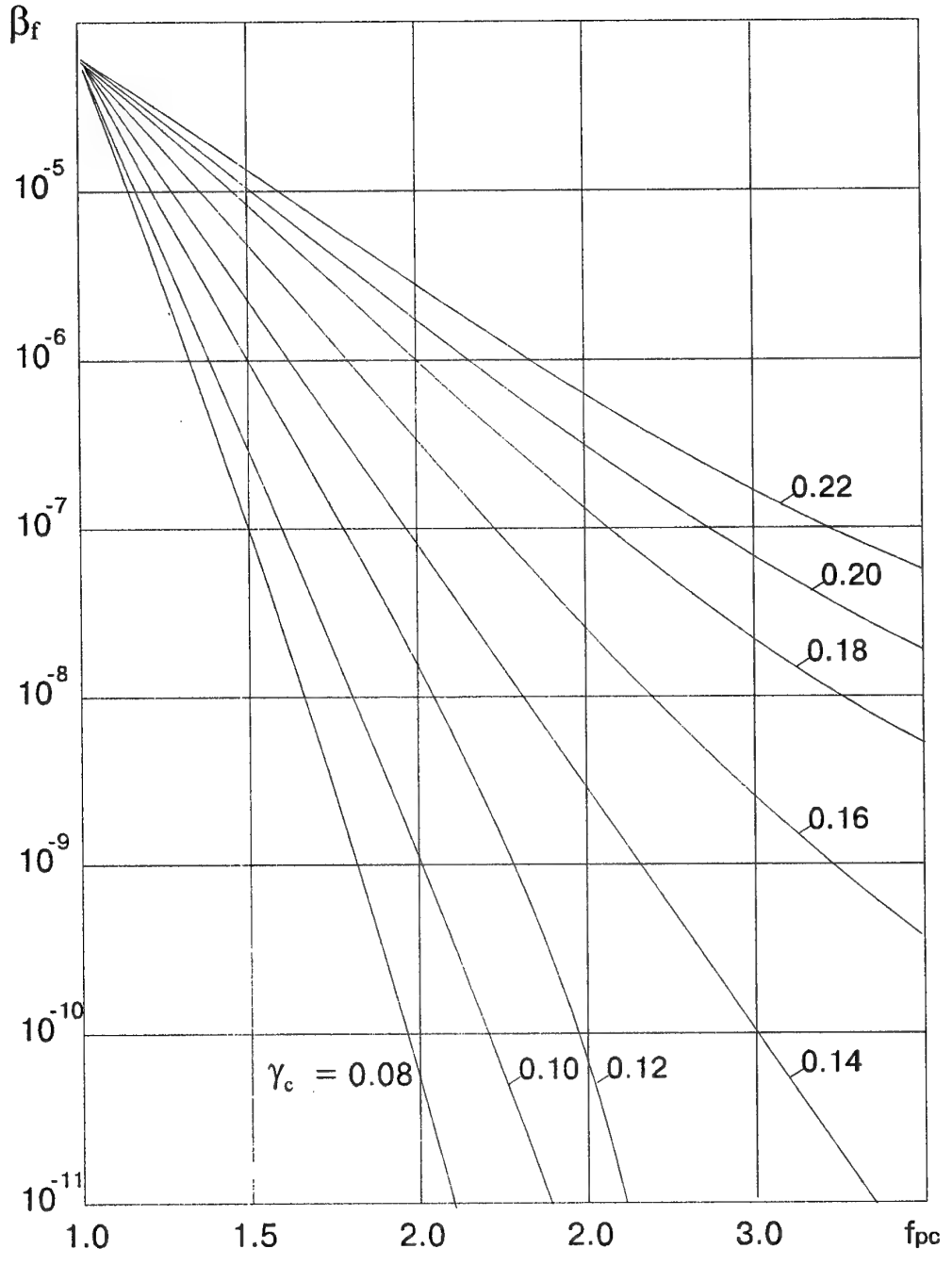

Fig.8. The dependence of the failure probability during a flight hour β_f on safety factor f_{pc} and residual strength variation factor γ_c.

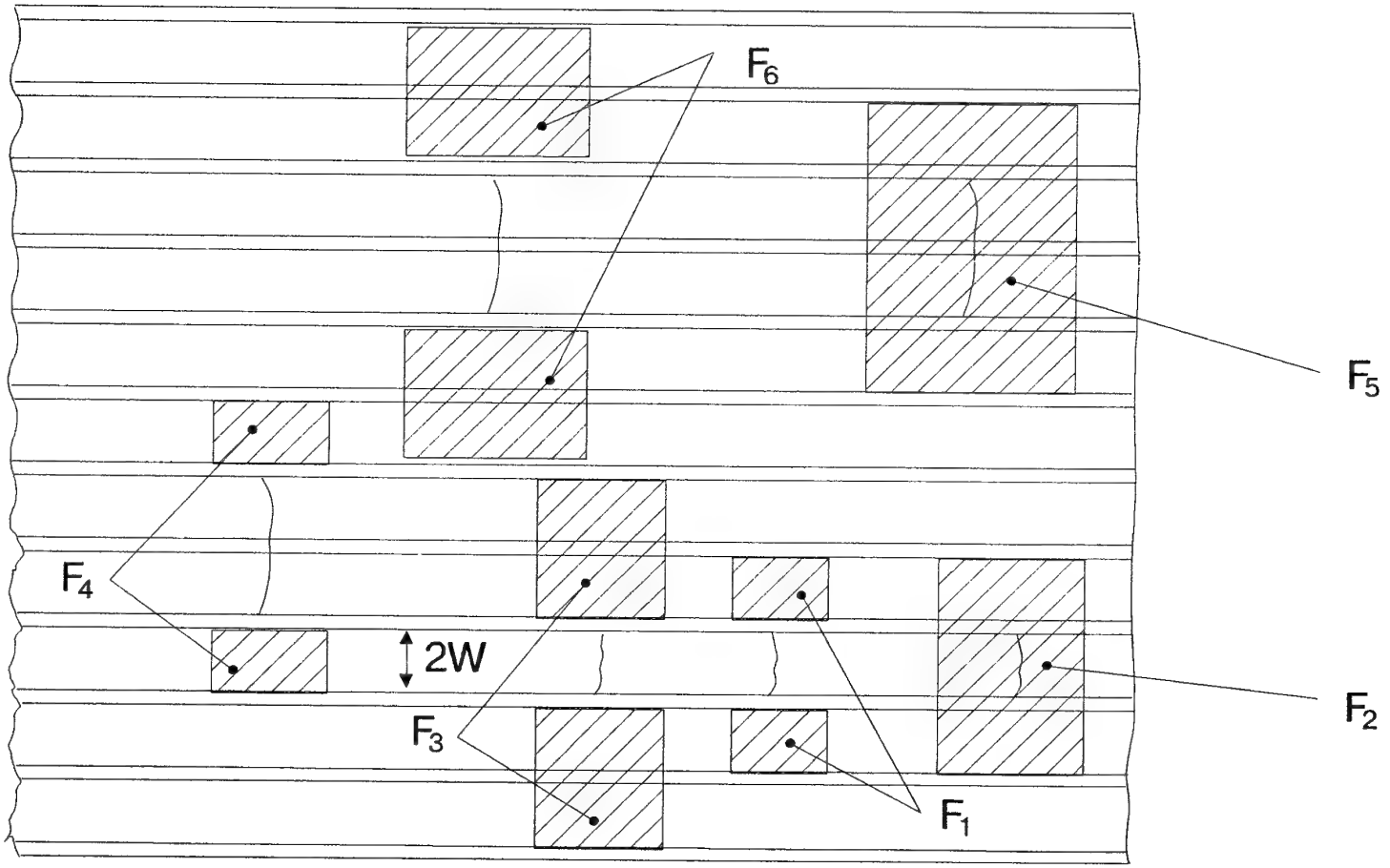

Fig.9. Damage cases resulting in multiple failures of the skin with crack stoppers at N =2 (F_1, F_2 - are the areas where the occurrence of damages $2L^{a}_{adm}, 2L^{b}_{adm}$ leads to damages q^{b}_{adm}, q^{c}_{adm} ; $F_3 - F_6$ - are the areas where the appearance of damages $2L^{a}_{adm}, 2L^{b}_{adm}, 2L^{c}_{adm}$ results in "off-design" damages.

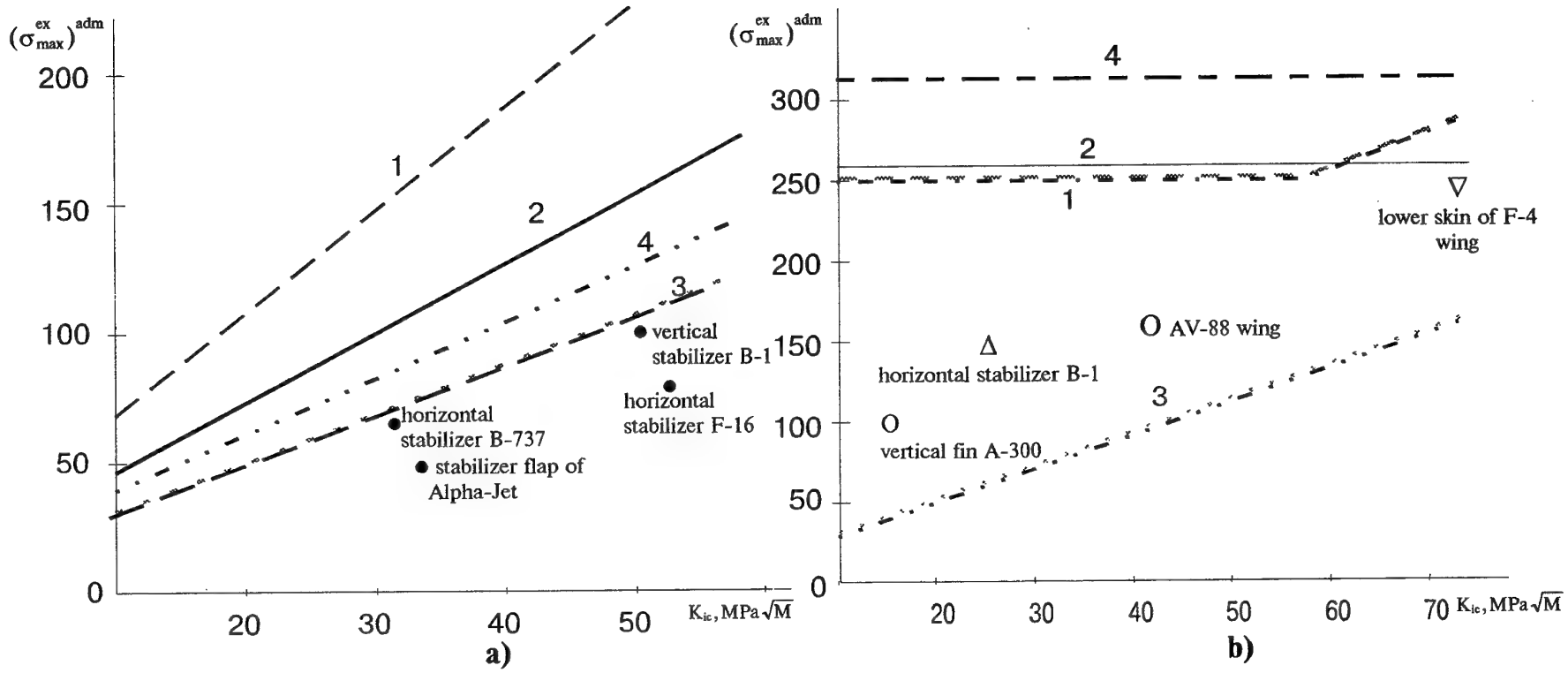

Fig.10.Comparison of the analysis results for predicting the effect of fracture toughness of PCM aircraft skin K_{ic} on the level of admissible service stresses with design experience;

a) "damage tolerance";

b) " fail-safe";

- damage $2L^{a}_{adm}$;
2 - damage $2L^{b}_{adm}(H_t(2L) \le 10^{-5} e^{-24/b}$;
3 - damage $2L^{b}_{adm}(H_t(2L) \ge 10^{-3} e^{-24/b}$;
4 - damage $2L^{c}_{adm}$;

∇ - low-modules stoppers of 0^0- fiber glass layers;
O - high-modules stoppersof 0^0-carbon fiber layers;
Δ - high-modules stoppers of 0^0 - boron fiber layers.

COMPOSITE MATERIALS IN AIRCRAFT STRUCTURES (DESIGN, OPTIMIZATION and CERTIFICATION)

V.I. Biryuk
TsAGI, Zhukovsky 140160
Moscow Region, Russia

ABSTRACT

This report presents the scientific problem of composite structure optimization and their certification. The approach to optimization of a lifting surface (as a wing and empennage) is studied. The use of arbitrary anisotropic models in designing is shown. There are some examples of designing composite structures. It's briefly considered sertification problems including the design conditions and means of complience.

NOMENCLATURE

$\sigma_x,\sigma_1,\sigma_y,\sigma_2$ - normal stresses

τ_{xy},σ_{12} - shear stresses

$[\sigma],[\sigma_p],[\sigma_c]$ - allowable tensile or compressive stresses

K_{ix},K_{iy},K_{2xy} - stress intensity factor for tension if i=I, for compressive if i = -I and for shear.

K_{icx},K_{icy},K_{2cxy} - critical stress intensity factor.

1. STAGE OPTIMIZATION OF POLYMERIC AND METALLIC STRUCTURE ELEMENTS.

Primary structure design to a specified set of loads is traditionally performed through selecting the values of structural design variables to provide the minimum weight under various constraints. The use of composites makes the designer's possibilities wider since there are options to control the properties of the anisotropic material in course of designing. The deformational behaviour of a lifting surface (e.g. a wing, an empennage) of the same structural concept may be changed by introducing "unbalanced" layups; them, the aerodynamic loads and aeroelasticity parameters are controlled. These "unbalanced" panels are known to have fibers laid at an angle θ (with respect to some axis) and not to have fibers at an angle $-\theta$ (with respect to the same axis). Fig. 1 represents an example panel which models a uniformly loaded wing the " unbalanced " symmetric panels (Fig. 1,b ang 1,c) become not only bended but twisted about the longitudinal axis.

The noticeable growth in the best amount of versions of composite structures due to the increase in the number of both the design parameters and constraints complicate the work and necessitate the application of numerical optimization methods, the processing of numerous data on materials, and the use of complex techniques for structural strength analysis. Further difficulties are associated with the sophisticated interaction of anisotropic structures with a low plasticity and low breaking strains; this improvement necessitates a more detailed elaboration and the accuracy of analytical models.

For the best solutions, non-linear programming methods are usually involved, with iteration procedures requiring a number of analyses for attaining the minimum mass structure or the extremum of another objective function. Reduction in solution in the time is achievable through both the choice of the simplest model (with a minimum allowable number of DOFs) and simplification of design procedures. This approach is obviously in contradiction with the requirement of detailed elaboration of analytical models. This conflict can be overcome by dividing the design procedure into stages as presented in Fig. 2 for composite lifting surfaces.

In the first stage, use is made of beam/plate (Level I) models in order to preliminarily specify parameters of a minimum-weight structure. Constitutive equations of the Level I model are of low dimension, which makes it possible to organize a multidisciplinary analytical support of design. After the first stage, a coarse discrete finite-element model can be constructed for the second stage.

Based on the methods developed for structure optimization the program package for the optimum design of structures simulated by the finite element method was realized. The package consists of the following programs:

1) structure optimization and analysis;
2) preparation of the initial data;
3) checking of the initial data;
4) generation of programs for the required problem parameters [1].

One of the major elements of structure design is its calculation using the finite element method. It comprises the following basic phases: input of the initial information on the structure, calculation of the elements stiffness matrices, synthesis of the structure stiffness matrix and solution of the linear algebraic equations system, calculation of the stresses and forces in the elements.

The initial data may be input in two ways depending upon the wish of the user:

1) through the data file,
2) as the on-line entry.

Paper presented at the AGARD SMP Lecture Series on "Advanced Polymeric & Metallic Composite Materials for Space and Aerospace Vehicle Structures. . .", held in Stuttgart, Germany from 11-12 December 1995; Châtillon, France from 14-15 December 1995 and Ohio, USA from 18-19 December 1995 and published in LS-204.

If the data are input in the on-line mode the user may initialize the protocol, and the data input from the display will be adequately written to the protocol file. As the input information we can consider the structure topology, nodes coordinates, setting up the material properties, distribution of the finite elements thicknesses (areas), method of the structure fixing, setting the loading cases.

During the structure optimization it is necessary to additionally input data on the optimization criteria, maximum permissible stresses, minimum cross sections of the elements, number and types of constraints for displacements, description of the merging of elements of the finite-difference scheme (structure model). The user obtains the possibility of generating the so called "weight elements", i.e. merging of the finite elements, the total weight of which shall be calculated for the optimized structure (for instance, weight of the coating, weight of the spar, weight of the rudder etc.)

Elements of two types are used in the program: diaphragms and bars.

When filling the stiffness matrix of the whole structure its symmetrical and band characteristics are taken into account. To save memory in the program only its upper part is stored, which does not contain any zero elements exceeding the half-width of the band. When the system of linear algebraic equations is solved Gaussian elimination is used which takes into consideration the band and symmetrical methods of the stiffness matrix storage.

The stress matrices are multiplied by the displacements obtained to determine the stress-strain state of the structure (i.e. stresses and forces in the elements).

Structure optimization may be performed using the algorithm of equistrength and equistability.

Several types of criteria for the lifting properties by the elements are used:

1) static and residual strength criteria

equivalent breaking stress in the diaphragm elements according to the criteria of the forming energy

$$\sqrt{\sigma_x^2 + \sigma_y^2 - \sigma_x\sigma_y + 3\tau_{xy}^2} \le [\sigma \quad ;$$

different permissible compressive and tensile stresses for the bars

$$s_p \le [s]_p \,, \; s_c \le [s_c].$$

The Tsai-Hill static strength criteria for the elements made of the orthotropic material

$$(s_1/[s_1])^2 + (s_2/[s_2])^2 - s_1 s_2 / ([\,s_1][\,s_1]) + \\ + (s_{12}/[s_{12}])^2 \le 1;$$

equivalent breaking stresses in the diaphragm elements according to the criteria of the full strain energy

$$\sqrt{\sigma_x^2 + \sigma_y^2 - 2\nu\sigma_x\sigma_y - 2(1-\nu)\tau_{xy}^2} \le [\sigma$$

Strength of laminate according to failure of the matrix and the fiber in the most loaded layers.

The Tsai-Hill residual strength criteria

$$(K_{ix}/K_{icx})^2 + (K_{iy}/K_{icy})^2 - K_{ix}K_{iy}/(K_{icx}^2) + \\ + (K_{2xy}/K_{2cxy})^2 \le 1;$$

2) stability criteria:

local buckling of the skin for m-element

$$F1 = -N_x/(h\, s_{xm}) - N_y/(h\, s_{ym}) + (N_{xy}/(h\, \tau_{xym}))^2 \le 1,$$

where s_{xm}, s_{ym}, s_{xym}, are the critical stresses for the skin under the independent action of distributed forces N_x, N_y, N_{xy} ($N_y = 0$ is taken at $N_y > 0$);

local buckling of the stringer element

$$F2 = E_{.st}\,(\nu\, N_y - N_x)/(E\, h\, s_{.st}) \le 1 \,,$$

where $s_{.st}$ is the critical stress for the stringer element; general buckling of the panel reinforced by the stringer in the direction X

$$F3 = -N_x/(h\, s_{x0}) - N_y/(h\, s_{y0}) + (N_{xy0}/(h\, s_{xy}))^2 \le 1,$$

where s_{x0}, s_{y0}, s_{xy0} are the buckling critical stresses for the panel with the respect to the independent action of the distributed forces N_x, N_y, N_{xy} ($N_x = 0$ is taken at $N_x > 0$, $N_y = 0$ is taken at $N_y > 0$).

The design variables are an integral part of the structural model. Four types of unions are envisaged: free unions, common-thickness unions, initial-thickness unions (the thickness cannot be changed in the course of optimization), and thickness-proportion-keeping unions (thicknesses are changed in proportion to original values). A union can include finite elements of various groups of diverse types. When dealing with stress constraints, thicknesses of finite elements are modified by dividing current values by the minimum safety coefficient for each of them (on the basis of all loading cases); the safety margin is defined hereafter as the ratio of allowable stresses to the current value. The thickness of a finite element is modified, if needed, in conformity with the type of union. After a specified total number of iterations the user has the possibility to manually modify the design variables. In order to optimize the structure under strength and stability constraints, the

user can create panels comprised of membranes and bar finite elements. Implemented in the present version of the program is the procedure for optimization of:

- unstiffened plates and
- panels stiffened (in one direction) by stringers.

In the event that a panel planform differs from a rectangle, the panel is automatically transformed into an effective rectangle, the direction of the stringers being taken for the direction of the X- axis of a new coordinate system (where components of critical stresses are computed). The effective rectangle is formed by:

- two straight lines parallel to the stringers and drawn through midpoints of longitudinal edges, and
- two straight lines drawn through midpoints of transverse edges.

When the actual panel length is less than the length envisaged in the finite element analytical model (say, when the finite element mesh is coarser than the primary structure concept) then the length partition parameter may be introduced, i.e. the number "N" of intermediate additional webs. In this case the panel will have a reduced length, a/(N+1), on computation of the critical stresses.

The program implements several optimization problems including strength and buckling constraints.

Problem 1. The optimization employing the criterion of "equal stability" with respect to the general buckling of the panel and the local buckling of both the stringers and the skin (F1 = F2 = F3 = 1) with strength and side constraints. For isotropic material, here and in the subsequent problems, material nonlinearity is taken into account (by means of the plasticity coefficients to be determined from the material stress-strain diagram).

Problem 2. The optimization of a panel with a buckled cover skin, with assumption of simultaneous buckling of the panel and the stringer (F2 = F3 = 1) with stength and side constraints. In this approach the buckling of the cover skin between stringers is permitted (F1>1). The skin thickness is governed by the strength requirements with due account for the increase in the skin normal stress Sx' max which takes place over the area of reducing the skin to a stringer. The critical stress for a local buckling of the skin is determined through the loading parameter r:

$$s_x' = r\, s_x, \quad s_y' = r\, s_y, \quad \tau_{xy}' = r\, \tau_{xy},$$

where s_x , s_y , τ_{xy} are the applied stress components in the skin, corresponding to the ultimate loads. The program derives the loading parameter from the skin buckling constraint written as an equality:

$$\mathbf{F1(r)} = -(s_x'/s_{xm}) - (s_y'/s_{ym}) + (\tau_{xy}'/\tau_{xym})^2 =$$

$$= -r\,((s_x/s_{xm}) + (s_y/s_{ym})) + r^2\,(\tau_{xy}/\tau_{xym})^2 = 1$$

The value of the parameter indicates what factor should be applied to the current stresses in the skin to make it buckle. A formal solution of this problem is of sense only in the event that the loading parameter $r < 1$. If $r > 1$ or $r < 0$ the cover skin cannot buckle in response to the current ultimate loads. The increase in the normal stress Sx'max is determined from the total compression stress resultant conservation in the laminate prior to and after the buckling. The strength of stringers is estimated with correction for increased stresses in the skin.

Problem 3. The optimization of a panel with a buckled skin at a prescribed f load level with assumption of "equal stability" with respect to the panel general buckling and the stringer local buckling (F2=F3=1) with strength and side constraints.

Here the parameter $f >= 1$ specifies the panel load level under the loads which are a certain fraction of the ultimate stress results Nx, Ny, Nxy. For example, at $f = 1{,}5$ the local buckling constraint is given by :

$$\mathbf{F1}\,(N_x/f,\ N_y/f,\ N_{xy}/f) = 1$$

it means that skin buckling occurs under loads which are 1.5 times less than the ultimate ones.

To solve this problem the optimization process is built so that the design variables at the convergence point provide the value of the loading parameter r being the inverse to the "f" (which is indicative of the load level). A solution of this optimization problem can be derived by analogy with the problem 2, the result being different if $0 < r < 1$ / $f < 1$. In this case the skin on the width reduction portion will have a safety margin under the increased normal stresses s'_{xmax}. A general solution for a primary structure, at every stage of a global iteration process, is formed as envelope of the solutions obtained on the basis of the fully-stressed design concept and by one of the approaches using the "equal stability" criterion. In all algorithms, attainment of the prescribed accuracy, in respect of the stress constraints, is used as a convergence criterion. The optimization process can be terminated after a specified total number of iterations.

The goals of the second stage are (i) to formulate a reasonable structure concept, (ii) to interface the basic units, and (iii) to improve parameters including the "microstructure" of materials. The coarse FE model serves as a basis for investigation into alternative primary structure concepts; best one should be of minimum mass and meet the specified requirements and constraints. Then there is a possibility to return to the continuum-mechanics model (defined at the first

stage), to correct the loads, and to thoroughly examine the aerodynamics and aero-elastic behaviour of the structure (with the changes introduced at the second stage). The result of the second stage is the airframe finite-element model.

In the third stage, individual structures are treated by appropriate optimization methods so that the entire model is upgraded.

Stage 3 (i.e., an individual treatment and optimization of structural elements) is implemented in the TsAGI-developed COMPOSITE program package [2].

The next Figures represent some applications of the COMPOSITE programme:

- computation of strengths and stiffness characteristics, evaluation of load-carrying capability and stability of panels (Fig. 3) and
- optimization of the panels and shells to withstand the general loads shown (Fig. 4).

Finally, in the fourth stage , the airframe structural analysis is carried out using the FE model of high dimension.

At TsAGI, methods of all four stages are implemented in several programs. They are up to practical application. In the present report, most attention is paid to the first and the second stages.

Techniques for these stages are implemented in "ARGON". Thepurpose of this programme is to preliminarily design the minimum-mass thin-walled airframes made of metallic and/or composite materials. Optimization can be performed under strength, displacement, and fatigue resistance constraints with due account for the aerodynamics and aeroelastic behaviour, criteria of stability and controllability of the airplane under study. A schematic diagram of "ARGON" is presented in Fig. 5.

The following information on the flight vehicle: utilized as input data is the outline, operational specifications of control surfaces, the limit maneuvering parameters (the flight envelope), weight breakdown, the list of the materials to be applied, static and fatigue strengths, allowable displacements at test sections, arrangement of principal load-bearing structures, the side constraints. Using these input data the aerodynamic and dynamic models for the first stage of optimization are being synthesized. The cycle of aero/strength/dynamic design on the first stage includes the following analyses:

- evaluating airloads within the bounds of a linear theory with account for inertia forces and aeroelasticity;
- revealing the extreme load conditions among provisions of Civil Aircraft Airworthiness Requirements complete with the limit maneuvering parameters specified;
- determining the most severe loads for airframe units (to be judged by values of equivalent stresses, displacements, and/or weight);
- evaluating the aeroelastic behavior and flutter speed margins.

The vector of design variables for composite structures is comprised of thicknesses and fiber orientation angles. Their values are proposed to be determined in the iteration procedure based on the fully-stressed design (FSD) concept.

The cycle of a multidisciplinary, aero/strength/dynamic design begins with analyzing the rigid airplane loads. Next, the structural optimization is performed, stiffnesses and the weight breakdown are updated. The data obtained go in to the dynamic model. The computation of loads to be applied to the elastic airplane is carried out, and so on until the iteration process converges. With this, the possibility to interrupt the cycle is envisaged, in order to examine characteristics of interest and to specify new allowable modifications.

If the minimum-weight version is selected amongst the versions considered, the FE model for the second stage can be created. There are options for computing the nodal forces; the algebra involved preserves the strain energy. The comprehensive set of one- and two-dimensional isoparametric finite elements available allow construction of a model which properly represents the structural features.

The FEM analysis includes determination of stress-strain states and optimization with regard to the strength and displacement constraints. Both the FSD concept and reliable buckling analysis criteria are used.

After extensive studies on the level II model, the stiffnesses can be transferred back to the level I model so that the aerodynamics could be computed and the airplane aeroelastic behavior analuzed. The transfer matrix which relates stiffness matrices of models of the first and the second stages is derived from requirements for equal displacements at common nodes and equal potential energies of both models.

If the load convergence criteria are met and the aeroelastic behavior satisfies the constraints, the design is considered to be finished.

At the first stage of composite structure optimization one can use the anisotropic model of plates. We seek to attack a problem of creating a mathematical model of an unrestricted anisotropy for elastic media [3].

There is the formulation of an elastic unrestricted anisotropic body topological structure optimization problem with constraints on the mission function at this stage.

The problem is solved for a set of elastic bodies, which may be represented as a system of thin anisotropic plates. These plates are loaded in bending; the Kirchhoff hypothesis and the Hooke's law are assumed to be obeyed. The work by S.G.Lekhnitskii is used in problem solution. A plate

with general anisotropy may be described in the following way.

The plate is loaded in bending, with both an out-of-plane displacement and a plate thickness being small values in comparison with other dimensions.

In a general case the bending deformation is due to

- a load q distributed over the surface and being normal to the undeformed plate mid-surface, and

- loads applied at the edge; these are bending moments m and forces p being normal to the undeformed plate mid-surface (Fig. 6a);

these moments and forces are either specified or calculated as reactions at support areas.

Let us regard the undeformed mid-surface as the 0XY plane; the 0Z axis runs towards the unloaded external surface. Body forces are neglected. With this, the generalized Hooke law is assumed to be applicable.

We will employ the simplified plate bending theory based on the following assumptions:

1) straight lines that were normal to the mid-surface of the undeformed plate remain straight and normal to the bent mid-surface,

2) pressure from layers parallel to the mid-surface (the stress σ_z) is negligible in comparison with stresses in cross sections (σ_x, σ_y, τ_{xy}).

Assume that a plate of general planform has a general distribution of stiffnesses. Let us tie this plate to an external coordinate system 0XY (Fig. 6a) and subdivide the plate into N elements (n=1, 2, ..., N); within each of these we assume all stiffnesses to be constant. An n-th element is described as follows:

the n-th element has

- a local Cartesian coordinate system $0^nX^nY^n$ rotated through an angle θ^n with respect to the external system 0XY and

- a local oblique system $0^n\xi^n\eta^n$ with an angle β^n between axes, the $0\xi^n$ axis running along the $0X^n$ axis (angles are positive in the counterclockwise direction), see Fig. 6b.

"Directions" of principal moduli of elasticity, E^n_1 and E^n_2, coincide with the $0\xi^n$ and $0\eta^n$ axes, respectively. Values of β^n, θ^n and the principal moduli E^n_1 and E^n_2 can change in going from one element to the other one. In this model we have additional elastic constants which describe the behavior of an arbitrarily anisotropic body:

- $E_{\xi\xi}$ and $E_{\eta\eta}$, the Young moduli that are related to linear displacements along the 0ξ and 0η axes, respectively,

- $G_{\xi\eta}$, the shear modulus,

- $\mu_{\xi\eta}$ and $\mu_{\eta\xi}$, the Poisson's ratios that characterize a decrease in transverse dimensions along one of the axes when the plate is elongated in the direction of the other one,

- $\nu_{\xi\eta,\eta}$ and $\nu_{\xi\eta,\xi}$, the coefficients of interaction of the first kind; each of these denotes a ratio of shear in the $0\xi\eta$ plane to a strain along the 0η axis (or the 0ξ axis, respectively), the axis being a direction of a normal stress,

- $\nu_{\xi,\xi\eta}$ and $\nu_{\eta,\xi\eta}$, the coefficients of interaction of the second kind; each of them is a ratio of an elongation along the 0ξ axis (or the 0η axis, respectively) to shear in the $0\xi\eta$ plane under a shear stress Ξ_η.

For the n-th element we introduce additionally a Cartesian system $0^nX^nY^n$ such that

- origins of the systems $0^nX^nY^n$ and $0^n\xi^n\eta^n$ coincide,

- axes 0^nX^n and $0^n\xi^n$ coincide, and

- the unit lengths for the axes are identical (Fig. 6c).

In this case the coordinates ξ^n and η^n relate to the coordinates X^n and Y^n through usual transformation equations.

A strain tensor ε_{pq} in the oblique system $0^n\xi^n\eta^n$ is related to a strain tensor ε_{kl} in the Cartesian system $0^nX^nY^n$ via a transformation matrix.

A stress tensor σ^{ij} in the system $0^n\xi^n\eta^n$ is related to a stress tensor σ^{rs} in the system $0^nX^nY^n$ in a similar way.

It is known that any linear homogeneous transformation of coordinates has a related generalized Hooke law with a matrix E^{ijkl} (which is a multiplier for strains). So one can easily write a relation between the stress tensor σ^{ij} and the strain tensor ε_{kl} in the local Cartesian system $0^nX^nY^n$, this relation being based on elastic constants specified for the oblique system $0^n\xi^n\eta^n$.

For obtaining components of the stiffness matrix of the arbitrarily anisotropic plate in the external Cartesian system (0XY), use can be made of usual transformation equations [4].

This means that we can explicitly write components of stiffness matrices of arbitrarily anisotropic plates.

In so doing, we have derived a "closed-form" mathematical model of an arbitrarily anisotropic plate, and this model utilizes conventional material characteristics.

Thereafter the optimal control theory and gradient methods are used for solving optimization problems.

Let us refer to examples which demonstrate the effectiveness of such models in the problem of forming a structural concept of an aircraft.

We have prepared a procedure for optimizing the thicknesses in a structure where the

anisotropy angles are allowed to be varied. A computation result is a structure "equally strong" in respect of multiple loading cases. Comparison shows that a thoughtful variation of anisotropy angles enables a decrease in notably the structural weight. The example is an undercarriage well in a wing, for which two models were employed: one with isotropic elements, and the other, with anisotropic elements. Results evidence that the weight of the anisotropic structure can be less. Figure 7 depicts "paths" of optimum moduli.

One can see these paths concentrate on the force application point of the "undercarriage loading case."

The other example is optimization of a swept-forward wing and a swept-back wing. In the former case the concept is governed by the no-divergence requirement, and in the latter case, the aileron effectiveness requirement. The trajectories of the maximum modulus (i.e., the greater modulus amongst the two principal moduli) can be considered to be locations of reinforcement components; in the first case these ensure a maximum authority of ailerons, and in the second case, a maximum critical speed of divergence. With no gain in the structural weight the swept-forward wing critical speed has been increased by 30% due to anisotropy optimization. The authority of lateral control surfaces has been increased by 50% (Figs 8 and 9).

This suggests that the introduction of anisotropy widens the class of reasonable structural concepts and makes it possible to additionally reduce weight and/or raise the stiffness characteristics. After that one can solve the problem of defining the fiber orientation in composite plate with optimal modulus and the optimal angle between moduli.

Let us illustrate the use of "ARGON" in application to some large structures.

The vertical stabilizer of a high-technology aircraft. Adopted as an analytical model for the first stage was a sandwich panel (with a shear-rigid core) clamped on the fuselage. The "microstructure" of the skin material is specified as a four-layer stack wich 0, 90, +45, and -45 degree plies. The vector of lamination parameters includes relative thicknesses of the layers and the main layer fiber direction (with respect to the assumed longitudinal axis of the vertical stabilizer). Optimization would provide a minimum-mass structure subjected to the constraint concerning the tip section rotation angle.The iteration procedure has given dependency of the mass and the rotation angle on the main layer fiber direction: plots are represented in Fig. 10. The minima are both seen to be at the same fiber orientation angle.

In the second stage, several alternative primary structure concepts were considered, all having composite cover skins and metallic spars and ribs. Howerer, they differed in both arrangement of spars and the stabilizer-to-fuselage attachment interface. For every version, use was made of the lamination parameters obtained at the first stage. Design investigations on the basis of coarse finite-element models were a reliable source of optimum (minimum-mass) thickness vectors. All versions of the structure were considered under identical conditions, as loads and constraints. A comparative analysis made possible to find the minimum-mass primary structure concept shown in Fig.10. Next, for the selected primary structure concept, the finite-element model (including the box, the leading edge, control surfaces, and a neighbouring part of the fuselage) has been built, and analyses were carried out to refine the vector of design variables. The analytical model of the vertical stabilizer contained over 2000 displacements and 1000 design parameters. When optimization was completed, dimensions and lamination parameters were obtained for all parts of the vertical stabilizer:cover skin, booms and walls (of spars and ribs), attachment fittings etc. The resulting relative thicknesses of layers are plotted in Fig. 11.

Swept-forward wing. The present programme was used in optimizing a swept-forward wing. The skin panels were designed as "unbalanced" laminates. The objective was to minimize the wing mass under constraints on structural strength, the roll moment efficiency of the control surfaces, and the divergence speed.

The wing under study has a sweep angle of -30 degrees (Fig. 12) and is equipped wich ailerons and eilevators. The level I model was comprised of anisotropic "unbalanced" composite load-carrying skins and a shear-rigid core.

In the first stage, a general layup and unbalanced layer orientation were determined to satisfy the stress, displacement and controllability constraints. Parametric investigations within the cycle of aero/strength/dynamic design made it possible to calculate an optimum angle of the unbalanced load. As Fig.12 shows, the maximum efficiency of the roll control surfaces ($X_x = X_{x\ aileron} + X_{x\ ailevon}$) corresponds to the angle =-30deg. The wing root bending moment and the wing mass are increased insignificantly (about 10%).

The lamination parameters derived were used as a basis for the second stage. The design procedure was generally the same as in the previous case:

- coarse FE models are constructed for several (alternative) structural concepts and analyzed under identical load conditions and constraints;
- among these versions the minimum-weight design is chosen;
- a detailed FE model of the best candidate version is coupled with a model of the neighbouring area of the fuselage and is optimized under all the above constraints.

Fighter foreplane. The canard configuration was analyzed by using level I (beam/plate) model to define the foreplane displacement requirements from the airplane stability/controllability parameters desired. Computation showed that the present comfiguration would have a flexible foreplane where airloads could be reduced to place the aerodynamic centre at a favorable point. The stiffness requirements were formulated in terms of a tip section rotation angle.

A reasonable version of a structural concept was sought on the basis of coarse FE models; the mass and stiffness were criteria in this work. Among the versions depicted in Fig.13 the maximum flexibility is demonstrated by a single-spar configuration; the fan of spars at the foreplane root increases stiffnesses in this area.

Thereafter, the concept adopted was analyzed using an FE model of large dimension to refine the spar position with the composite laminate principal axis fixed; then the spar position was fixed and the lamination parameters were optimized. Fig.14 represents the results obtained. The minimum mass and the maximum flexibility correspond to the spar axis angle, j , of 60 degrees. Varying the lamination parameters affects the structural mass only slightly but the tip section rotation angle can change significantly. The optimum angle of the laminate principal axis is j =90 degrees.

The examples reported indicate that the procedure suggested can help to establish the best structural parameters taking into account to stiffness/aerielasticity constraints.

2. CERTIFICATION OF AIRCRAFT COMPOSITE STRUCTURES

The existing approach for airframe certification has been perfected; it assumes the structural analyses and theoretical evaluations of the strength properties, should be validated by flight test [5].

The diagram in Fig.15 represents the amounts of certification works for the composite structures; the shaded cells indicate additions caused by the replacement of metals by composites. In comparison with the metallic structure, the composite structure must be shown to be able to meet the static and fatigue strength requirements after introduction of standardized damage in the most severe environments; complementary efforts are undertaken to substantiate

- fail-safe operation capability,
- damage tolerance,
- inspectability, and
- repairability.

The analytical estimation of the strength includes:

- a theoretical computation of stresses and strains by means of state-of-the-art methods; currently, finite element methods are widely employed;
- the use of data available in handbooks and from the experience of designing and operating similar structures.

The estimates are validated by certification tests that envisage large amounts of testing for static and fatigue strength of various specimens. The range of specimens may be categorized in types (Fig. 16 which differ in sizes, total numbers of specimens, and values of interest.

Elementary specimens are usually small-size and can easily be tested in prescribed environmental conditions. These tests supply mean values of characteristics and the scatters. Experimenters determine degrees of the influence of various service factors in various combinations; the worst conditions by strength degradation are outlined.

Some "fragments" being medium-size portions of a structure are used to evaluate technological concepts and/or to obtain the strength limits. Such specimens are too large to be used for evaluating the scatter, but the strength degradation under real environmental effects can well be estimated.

Units which are important parts of an airframe can be very large. The experimentation usually involves one or two copies. The principal problem in this case is to evaluate the concepts and manufacturing processes by strength. For these tests two approaches are possible:

- direct tests with simulation of service conditions and
- an "analysis and experiment" approach that envisage tests in conventional environment and a subsequent extrapolation of the data to the most severe conditions.

The entire airframe with composite parts are tested in agreements with the test amount requirements adopted for "all-metal" airframes. The full-size airframe is tested in normal environment and the results are corrected for in-service factors; here, reliance is made on analytical procedures and the data obtained from testing of specimens of other types.

The aim of the full-size tests is to comprehensively validate the airplanes put into service and to ensure their strength and long operational life.

3. DESIGN CONDITIONS FOR PASSENGER-CARRYING AIRPLANES

3.1. The influence of environmental conditions

As to the passenger-carrying airplanes, the environment parameters are as defined in Fig. 17. Extreme conditions are simulated during static tests and/or residual strength tests, whereas the long-term

strength parameters are determined by exposing the airframe during the fatigue strength tests.

3.2. Fail-safe design requirements

The impact may be prescribed in terms of an impact energy or a damage area size -- these values are interrelated. An in-service damage to a full-scale structure is modelled by a notch or a spherical indentation. The size of a design limit in-service damage is defined on the basis of a value at which the damage will be reliably (at a probability of not less than 90%) detected by the usual inspection technologies and inspector's skill.

An airplane operated within the fail-safe design principle must remain strong with in-service damage. The design limit conditions establish a relation between a standardized damage and the factor of safety.

Figure 17 demonstrates fail-safe conditions; the abscissa axis represents ranges of the damages, and the other axis corresponds to the necessary strength margins which must be substantiated. Specific parameters of the standardized damages depend on a number of aspects (a type of a structure, a material, skills, etc.) and should be established via statistical data and/or special tests for damage inspectability.

4. MEANS OF COMPLIANCE

To demonstrate the correspondence of real strength characteristics of a structure to the certification requirements, the means of compliance are developed. Let us cite some of these methods that were used for certifying the composite assemblies of TU-204 passenger-carrying transport.

4.1.Nondestructive inspection method validation

Using a certain nondestructive inspection technique (specifically, the ultrasound impedance method), the damage sizes are determined and compared with actual dimensions measured on a microsection of the damage area. The comparison makes it possible to estimate acceptability of the method and introduce the proper corrections (Fig. 18).

4.2. Damage detectability

Boundaries of reliably detecting a damage by means of instrumented and visual inspection were outlined via detectability tests. The upper and lower surfaces of an aileron were damaged by impacts with various energy levels, and the damage area sizes were measured. In so doing, the plot of a characteristic length of a damage area versus the impact energy level have been generated, Fig. 18; thereafter, boundaries of reliable detection by instruments and visual inspection were outlined.

4.3. Damage growth rate

This value is necessary to assess the inspection schedule and the structure life capability. The damage growth rate determination method is as follows: during the life evaluation the structure is systematically inspected with instruments to measure the visible damage sizes. These measurements are a basis for plotting the size variation versus the number of cycles; damage growth rate is computed. This method is illustrated in Fig. 19.

REFERENCES

1. E.K.Lipin, D.D.Evseev and others. Multi-disciplinary Analytical Support of Aircraft Design. ARGON. (Report of TsaGI). 1994.

2. Mishulin I.B. and others. Package of Interrelated Programs for Analyzing the Composite Structures. Report of TsAGI.1994.

3. Biryuk V.I., Shumilova I.N. Structural optimization technique in aeroplane design problem. First World Congress of Structural and Multidisciplinary Optimization. Extended Abstracts - Lectures. May 28 - June 2. 1995. Goslar, Germany.

4. Lekhnitskii S.G. Anisotropic plates. - OGIZ, Moscow, 1947.

5. Birjuk V.I., Kut'inov V.F. The Certification Technique of Composite Civil Aircraft Units. Report of TsAGI. 1992.

Symmetric unbalanced layups

Balanced laminate

Unbalanced laminates

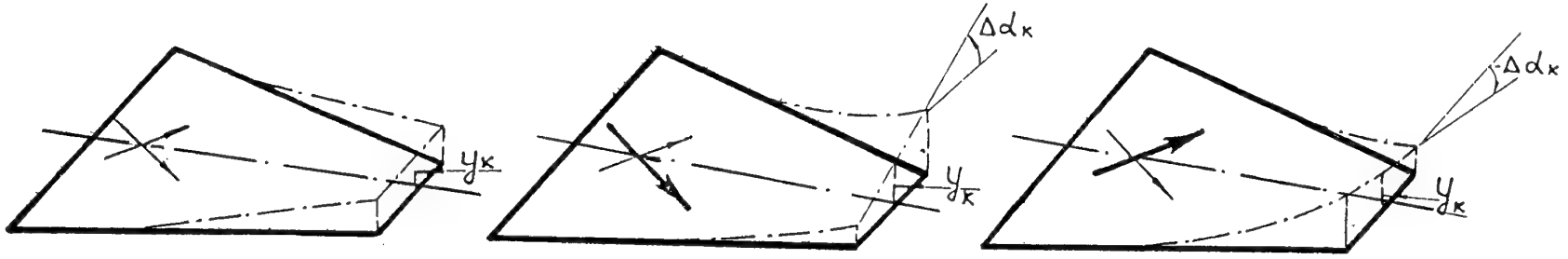

Fig. 1.a

Fig. 1.b

Fig. 1.c

Uniform load

Fig. 1

MAIN STAGES IN DESIGNING THE COMPOSITE AIRFRAMES

ARGON

1 STAGE	
Aim	Determination of thicknesses and lamination parametres
Model	Continuum mechanics: roads, beams, plates
Design variables	Thicknesses, ply angles
Constraints	Strength, displacements, aeroelastic behaviour, min/max thickness

2 STAGE	
Aim	Upgrading the thickness distribution and structural concept
Model	Coarse, discrete, finite-element
Design variables	Thicknesses, ply angles, structural concepts
Constraints	Strength, stiffness, etc.

COMPOSITE

3 STAGE	
Aim	Optimization of joints and individual components
Model	Roads, beams, plates. Finite Element Model
Design variables	Microstructure of material Structural concept
Constraints	Strength, stiffness. Mass

MARS

4 STAGE	
Aim	Structural analysis
Model	Detailed discrete model
Design variables	-
Require-ments	Check for all constraints and restrictions

Fig. 2

COMPOSITE

CALCULATION OF STRENGTH PARAMETERS

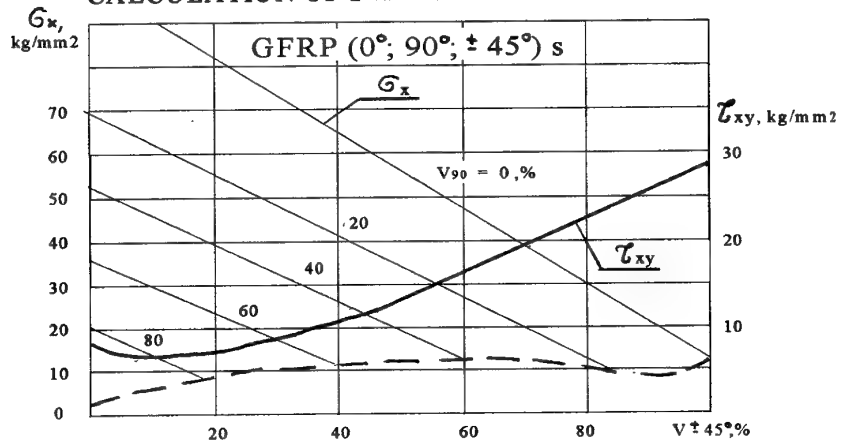

CALCULATION OF ELASTIC PARAMETERS

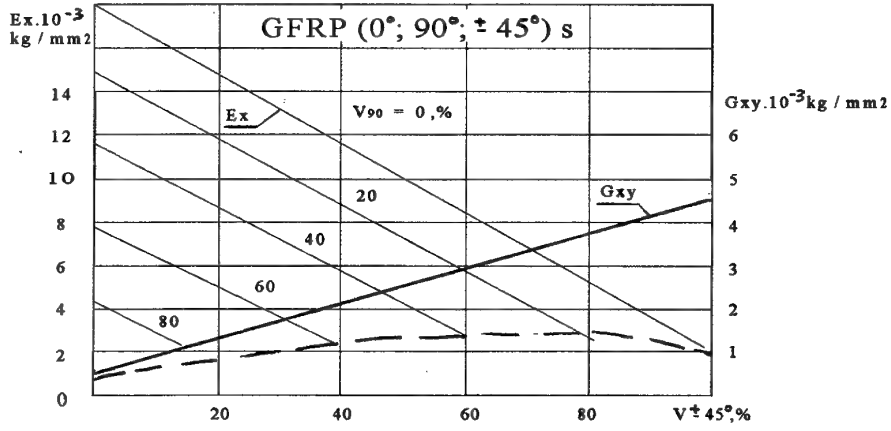

PACKAGE OF INTER-RELATED
PACKAGE OF INTER-RELATED
PROGRAMS FOR ANALALYZING
THE COMPOSITE STRUCTURES

ANALYSIS OF STRUCTURAL MEMBERS

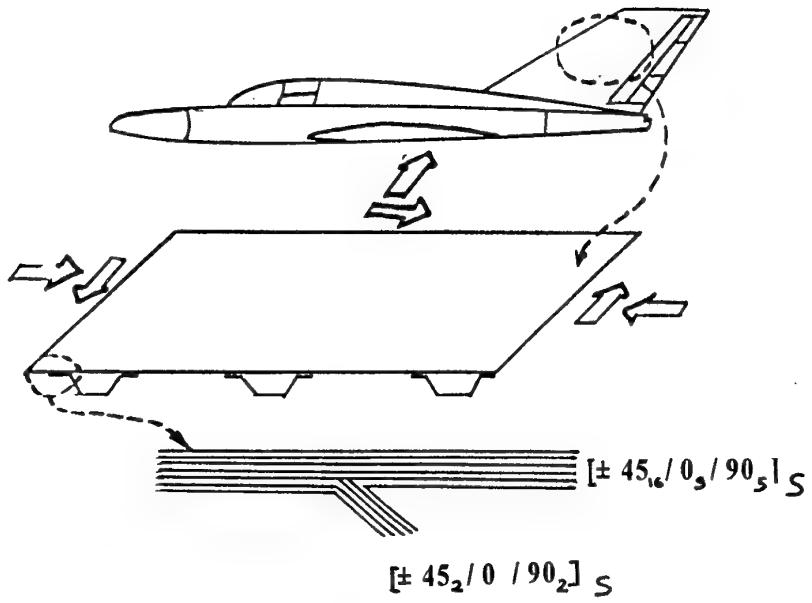

COMPOSITE is a convenient means for designers to use at their working stations.

Fig. 3

OPTIMAL DESIGNING OF COMPOSITE

PANEL / SHELLS

Problem formulation

Initial data	Objective function	Constraints
Load : Pcompr Geometry : R, L	Min Weight : G min	Stress : $\sigma_1 <= \sigma_b$; $\sigma / <= \sigma$ crit Manufacture : (t_i / t_{pam}) = integer

Design variables
Detailed geometry skin, web, str, fr...

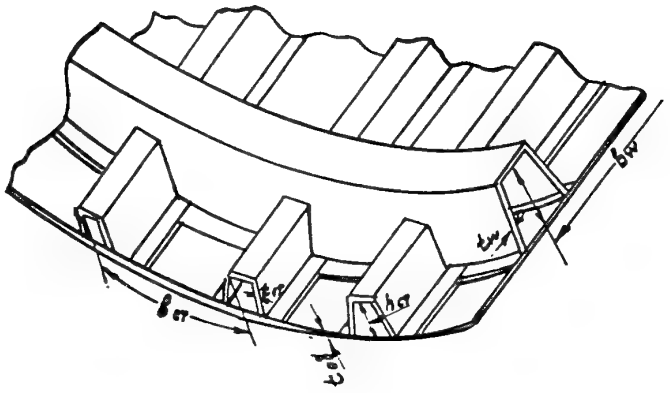

Type of material

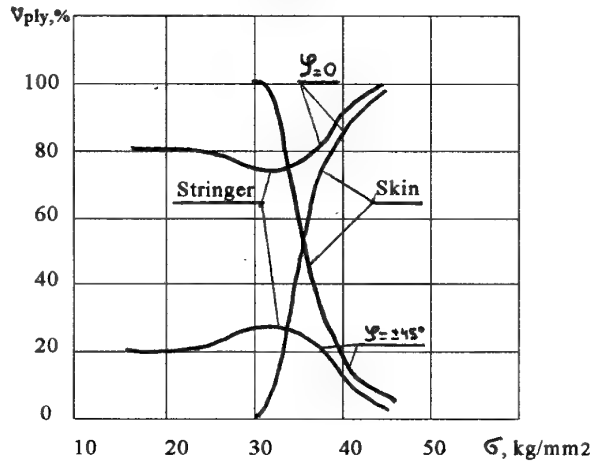

Parameters of panel members

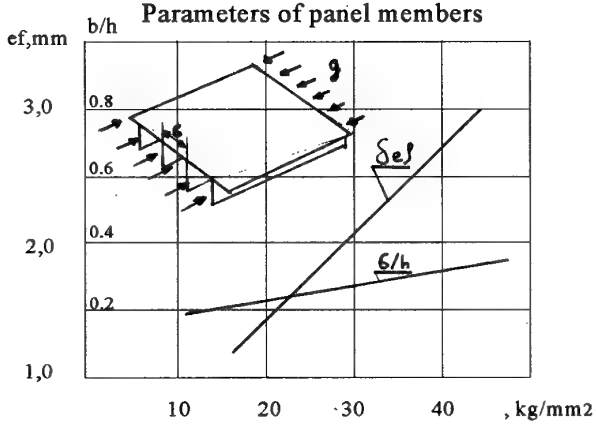

Fig. 4

Data flow in ARGON during aero/strength/dynamic designing of the composite lifting surfaces

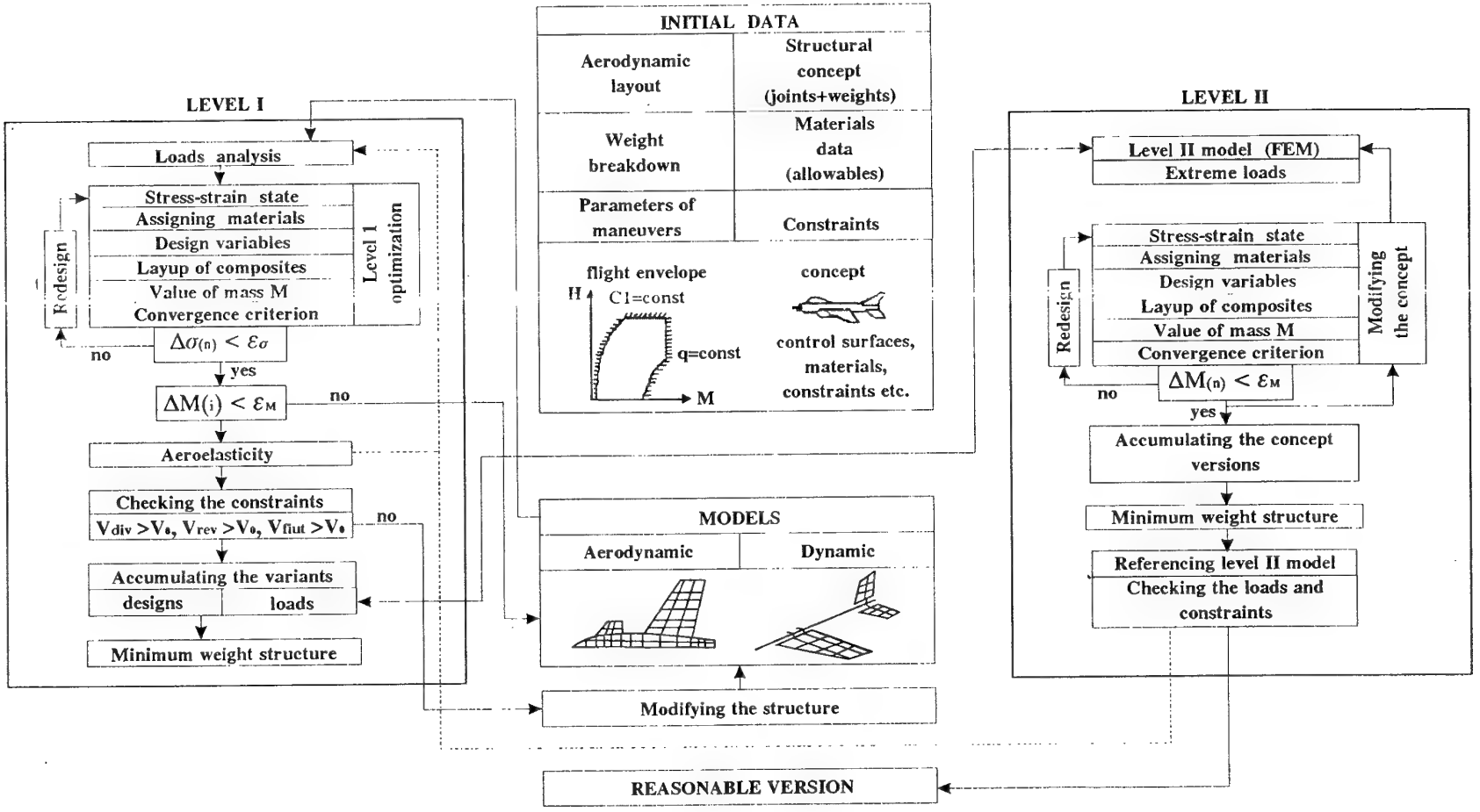

Fig. 5

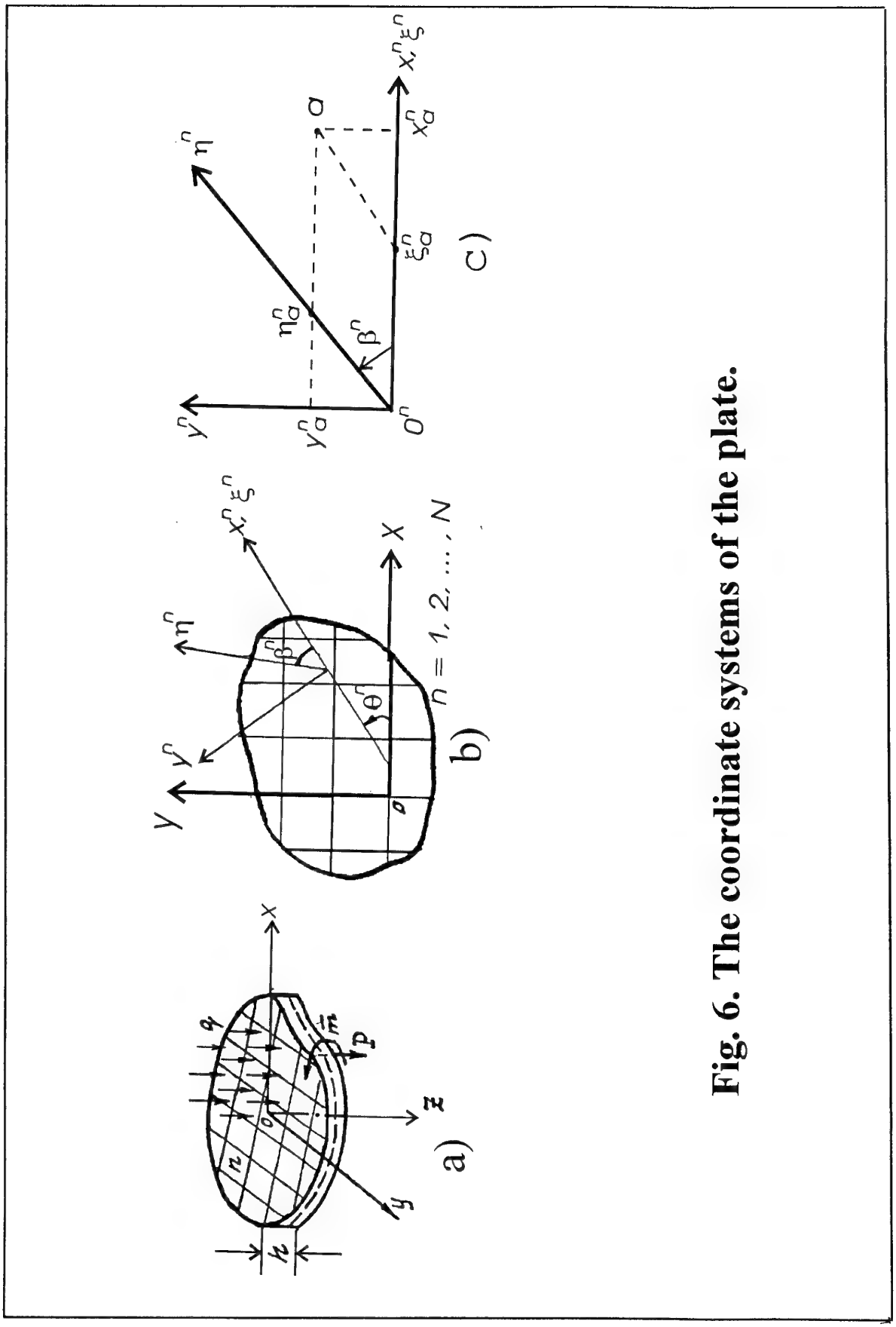

Fig. 6. The coordinate systems of the plate.

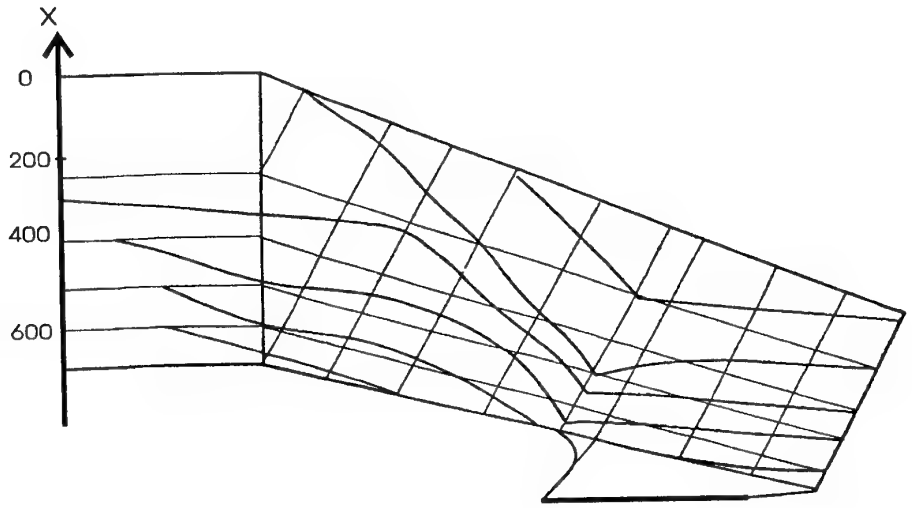

Fig. 7. Optimum trajectories of maximum module for the undercarriage well.

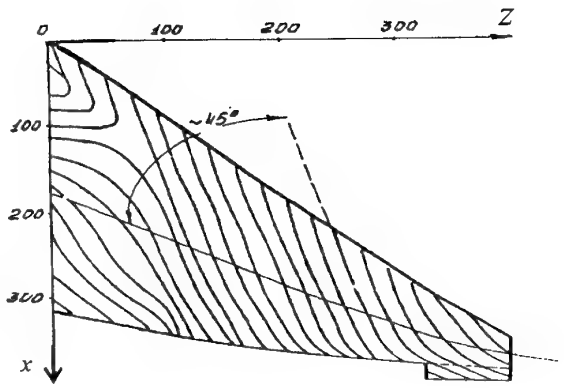

Fig. 8. Paths of optimum moduli for maximum authority of aileron.

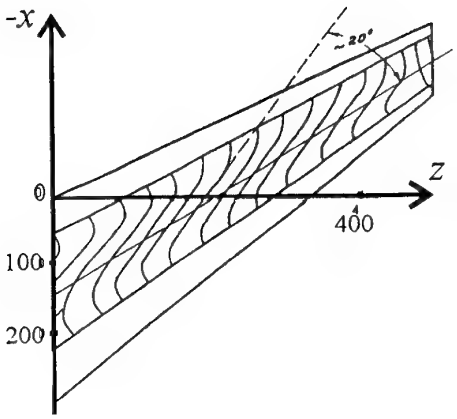

Fig. 9. Paths of optimum moduli ensuring maximum critical speed.

VERTICAL FIN OF A HIGH-PERFORMANCE AIRCRAFT

Level I model

A - A

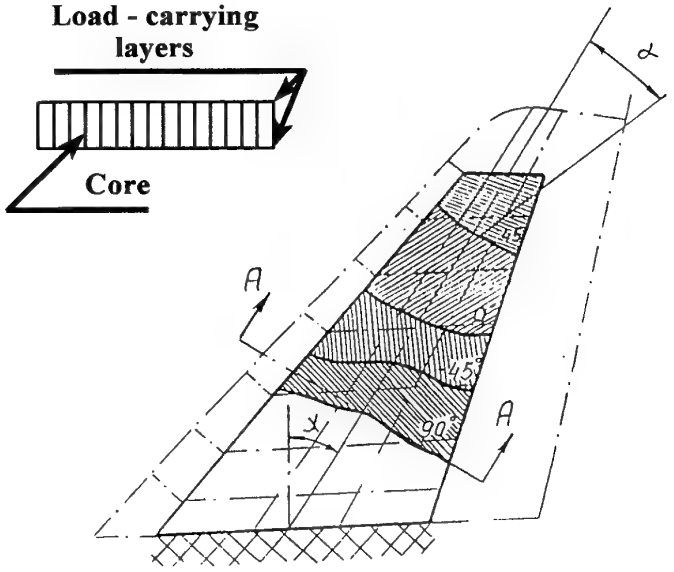

Mass M and fin tip rotation angle φ_K vs. laminate principal axis angle α

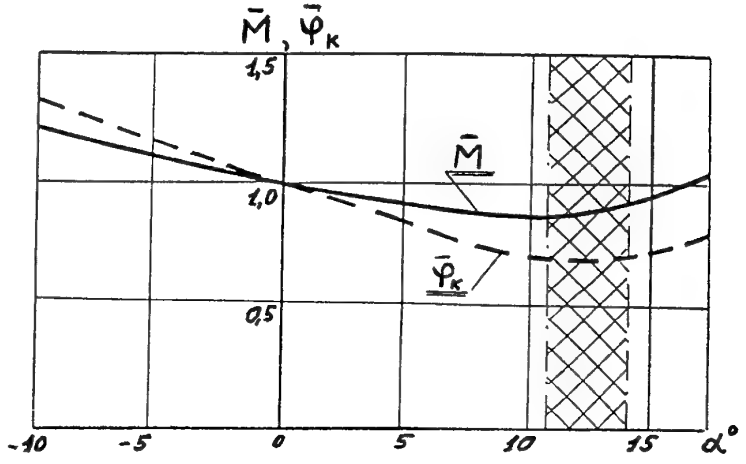

$$\bar{M} = \frac{M}{M_{\alpha=0}} \qquad \bar{\varphi}_K = \frac{\varphi_K}{\varphi_{K,\alpha=0}}$$

Fig. 10

VERTICAL FIN OF A HIGH - PERFORMANCE AIRCRAFT

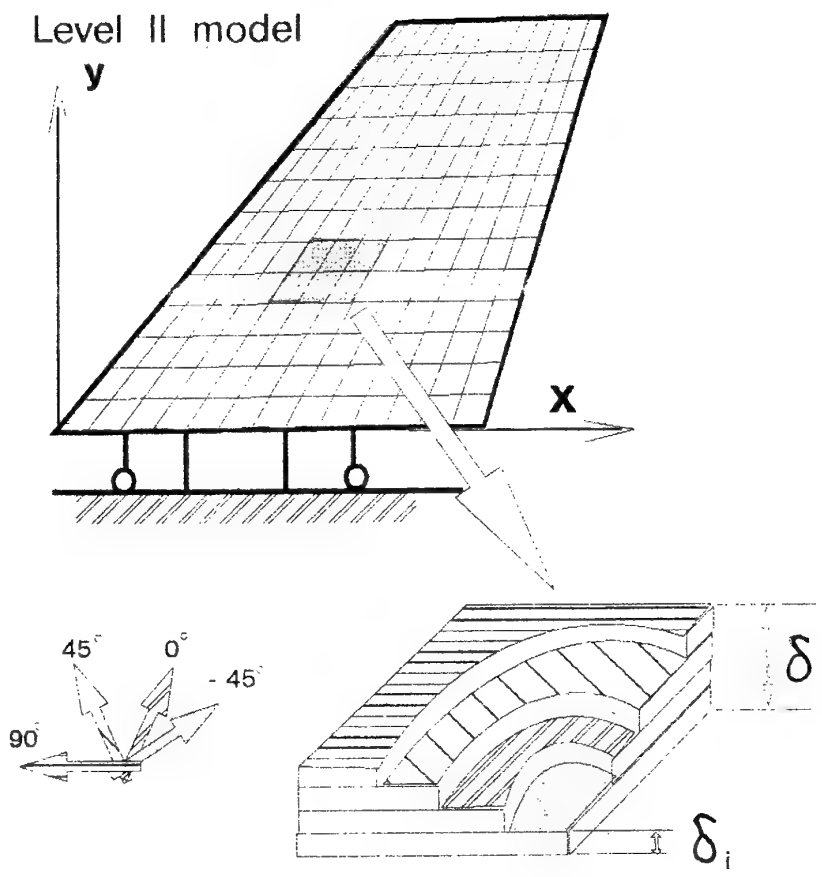

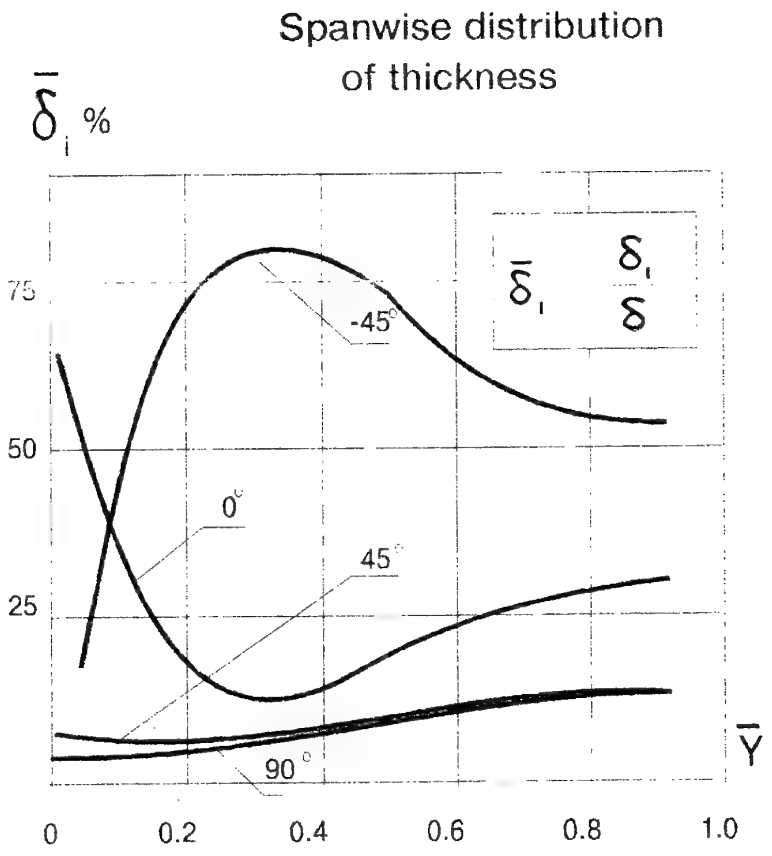

Fig. 11

SWEPT-FORWARD WING

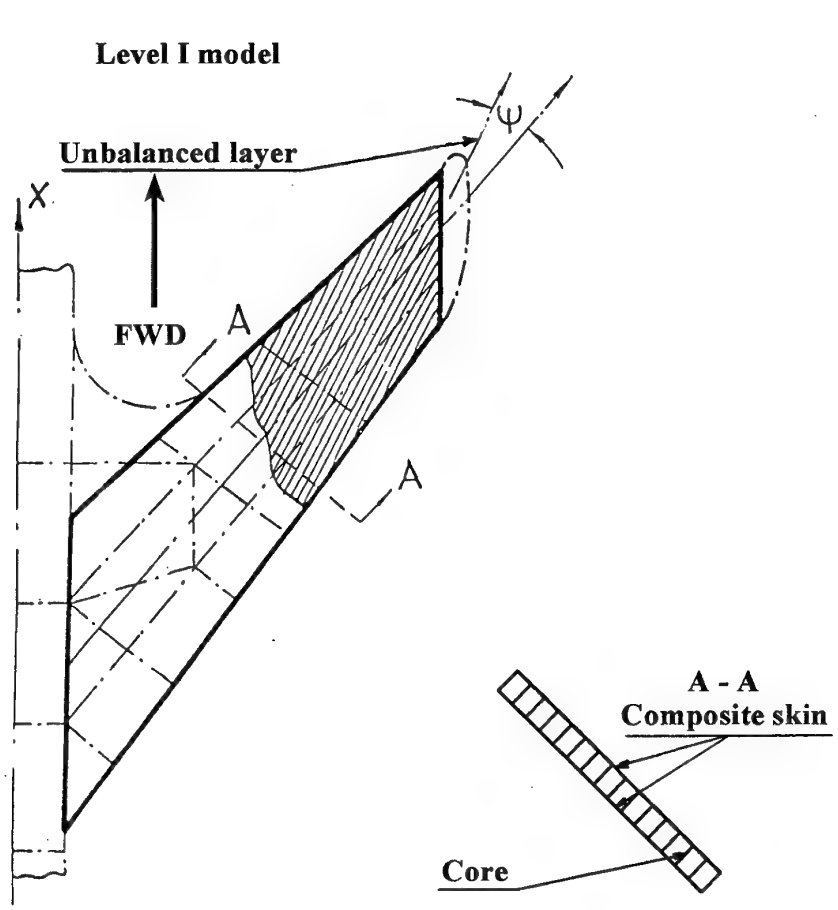

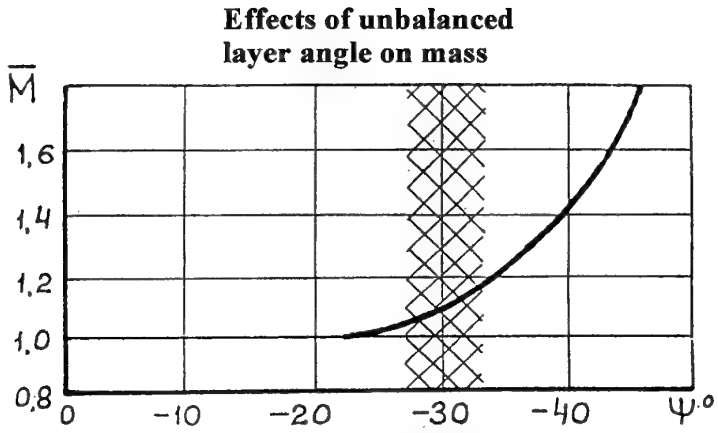

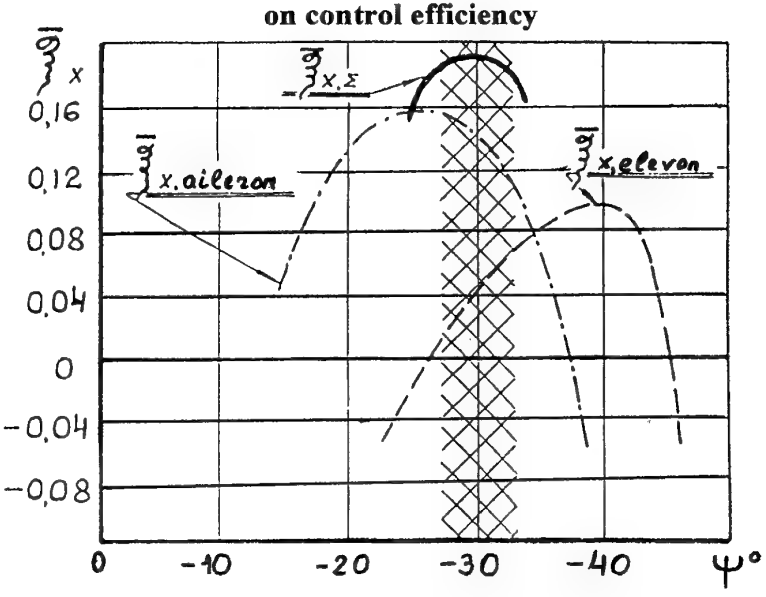

Fig. 12

Optimizing the foreplane structure concept

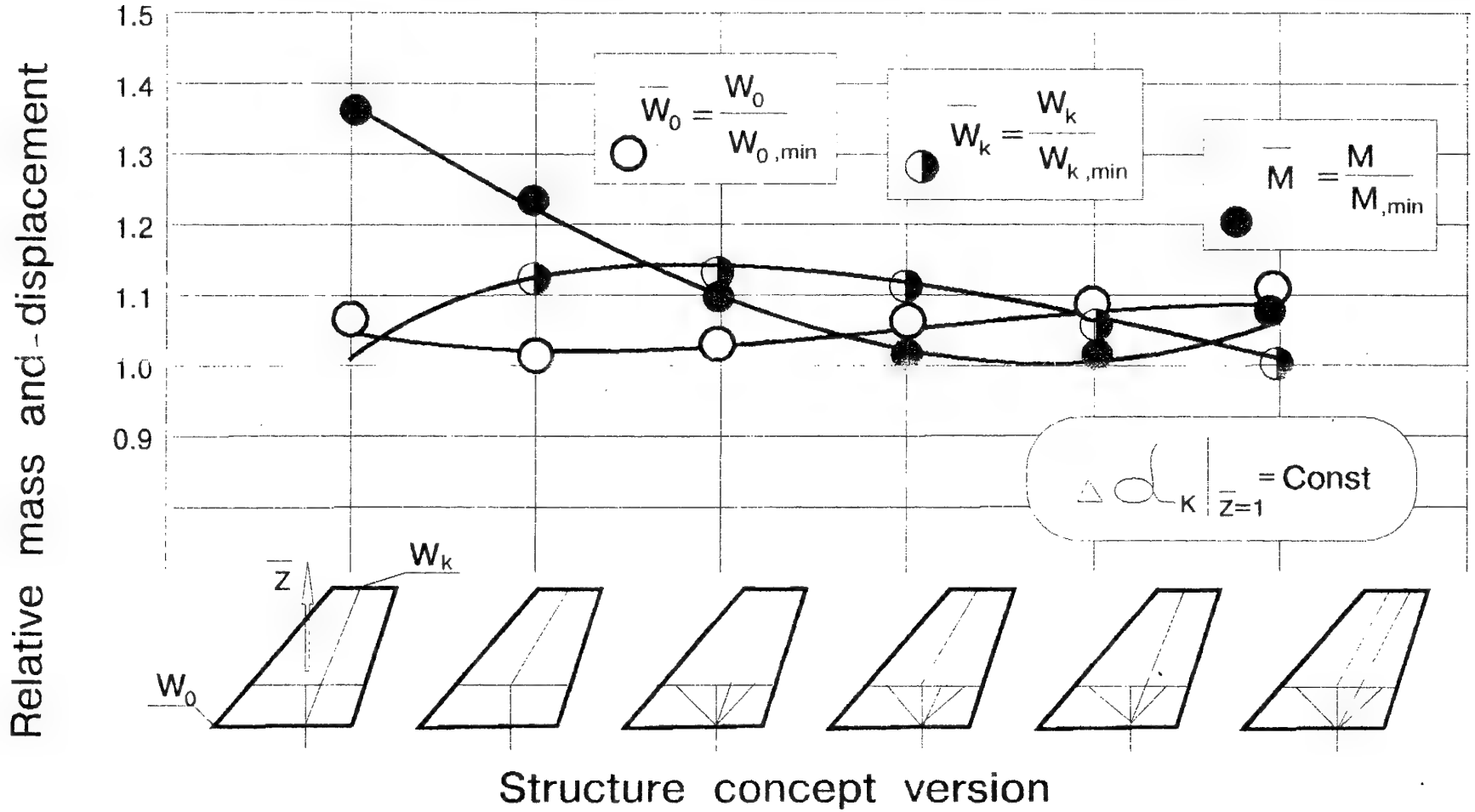

Fig. 13

Spar position angle optimization at Ψ = const

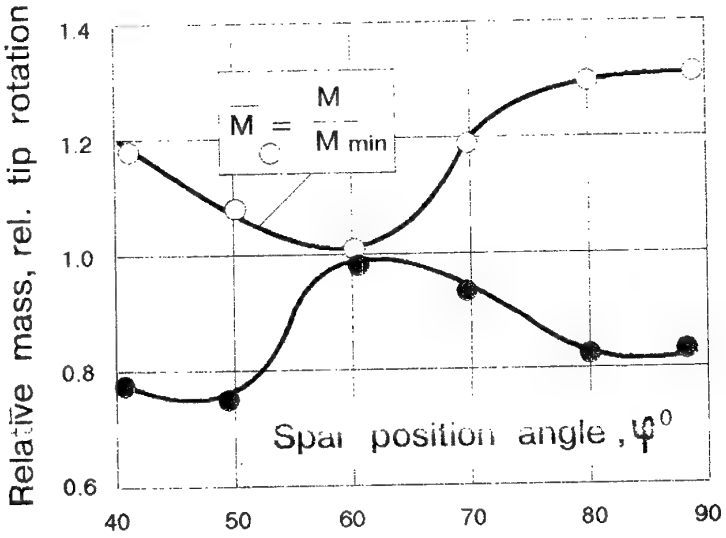

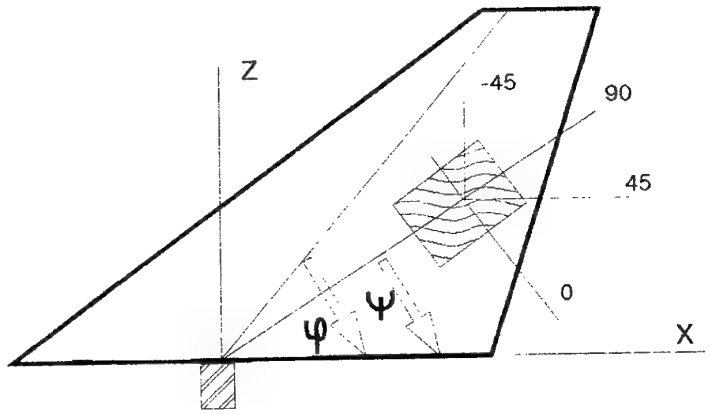

Optimization of principal direction angel of composite laminate at φ const

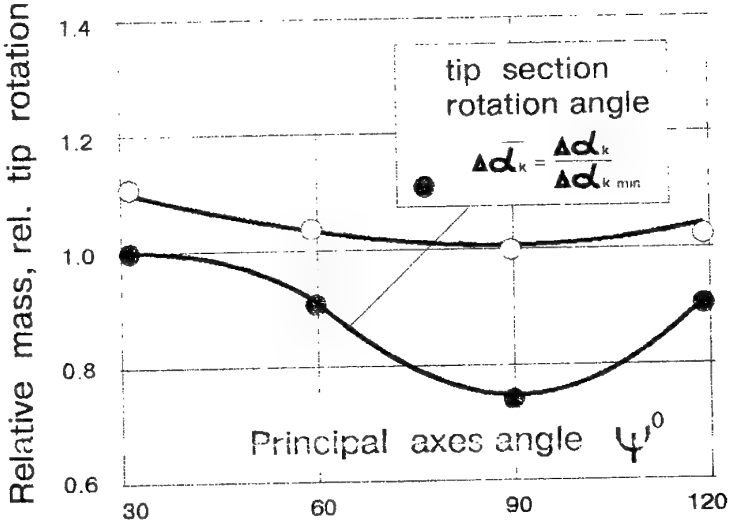

Foreplane design

Principal axis	spar	φ =90
	laminate	Ψ =60
Laminate layup	90 layer	0.1 δ
	|45| layers	0.8 δ
	0 layer	0.1 δ

Fig. 14

CERTIFICATION OF COMPOSITE AIRFRAME STRUCTURES

CERTIFICATION APPROACH
- THEORETICAL STRENGTH ANALYSIS. - TESTS OF STRUCTURE SPECIMENS OF COMPLEXITY

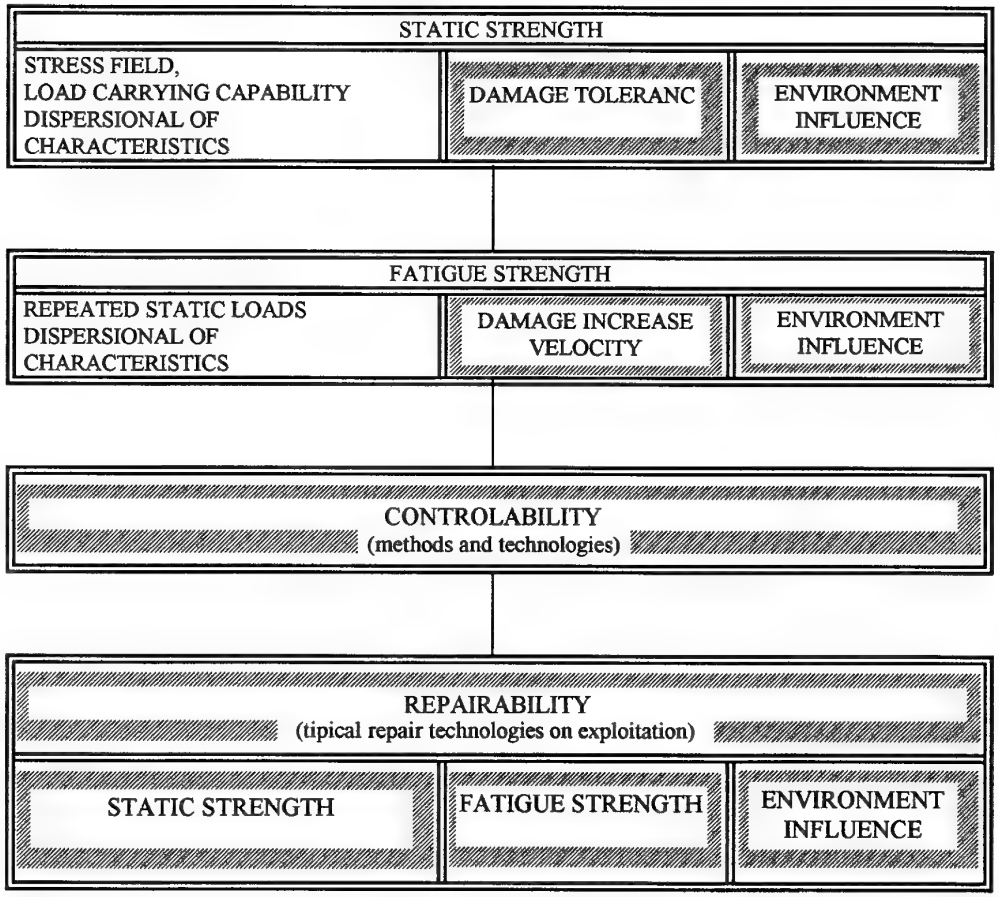

Fig. 15

SPECIMEN TYPES FOR CERTIFICATION TEST.

N	TYPE	EXAMPLE / ——— L ——— /	L, M	NUMBER OF SPECIMENTS	PURPOSE	CORRESPONDENCE DETERMINATION METHOD
1	COUPON	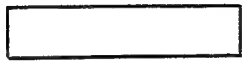	UP TO 0,3	LARGE	STRENGTH CHARACTERISTIES; MEAN ONES, DISPERSION, INFLUENCE OF EXPLOITATION CONDITIONS (HUMIDITY, TEMPERATURE IMPACT DAMAGES ECT...)	TESTS IN CONDITIONS WHICH ARE CORRESPONDED TO EXPLOITATION ONES
2	STRUCTURAL DETAIL	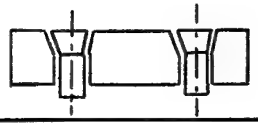	UP TO 1,0	LARGE		
3	SUB-COMPONENT		UP TO 3,0	MODERATE (5 -10 pieces)	REAL STRENGTH AND FATIGUE CHARACTERISTIES. TECHNICAL SOLUTIONS CHECKING...	TESTS IN CONDITIONS WICH ARE CORRESPONDED TO EXPLOITATION ONES. OR TEST IN NORMAL CONDITIONS WITH RECALCULATION TO EXPLOITATION ONES.
4	COMPONENT	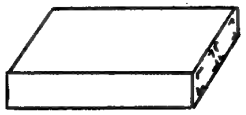	UP TO 10,0	1 - 2 pieces	TOTAL CHECK OF ALL TECHNICAL SOLUTIONS AND PROCESSES RELATED TO AIRFRAME CREATION.	
5	FULL SCALE AIRCRAFT		UP TO 30,0	1 piece		TEST IN NORMAL CONDITIONS WITH RECALCULATION TO EXPLOITATION ONES.

TEST FOR ALL SPECIMENT TYPES ARE OBLIGATORY
PART OF AIRPLANE FLIGHT MAINTENANCE CERTIFICATION.

Fig. 16

ENVIRONMENT INFLUENCE.

PARAMETERS / AIRCRAFT	EXTREME PARAMETERS Tmax,C	Tmin,C	Wmax,%	DURATION OF EXPOSITION T,C	F,%
TU - 204	80	- 60	1.0	35	70
B - 737	82	- 56	1.0	21	70
A - 310	70	- 50	1.2	20	80
	STATIC TEST			FETIGUE	

W - moisture content level
F - humidity in exposition

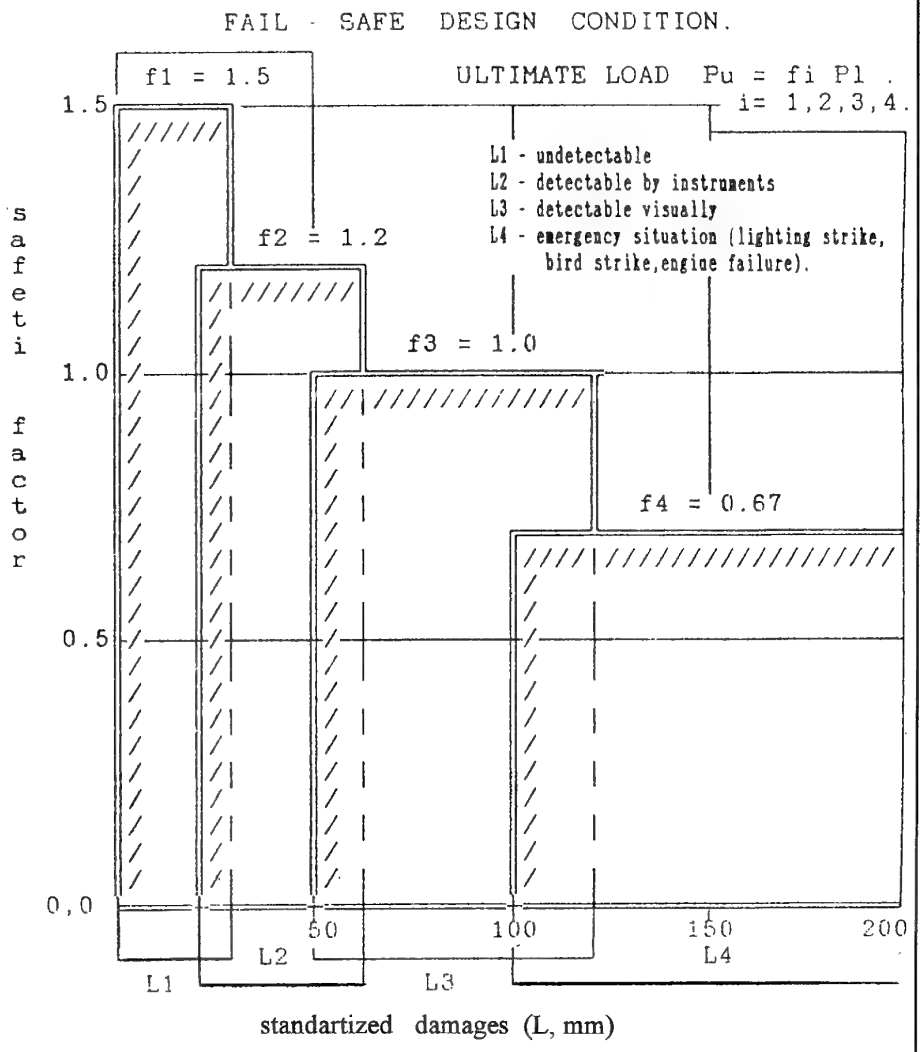

Fig. 17

DAMAGE DETECTABILITY TEST

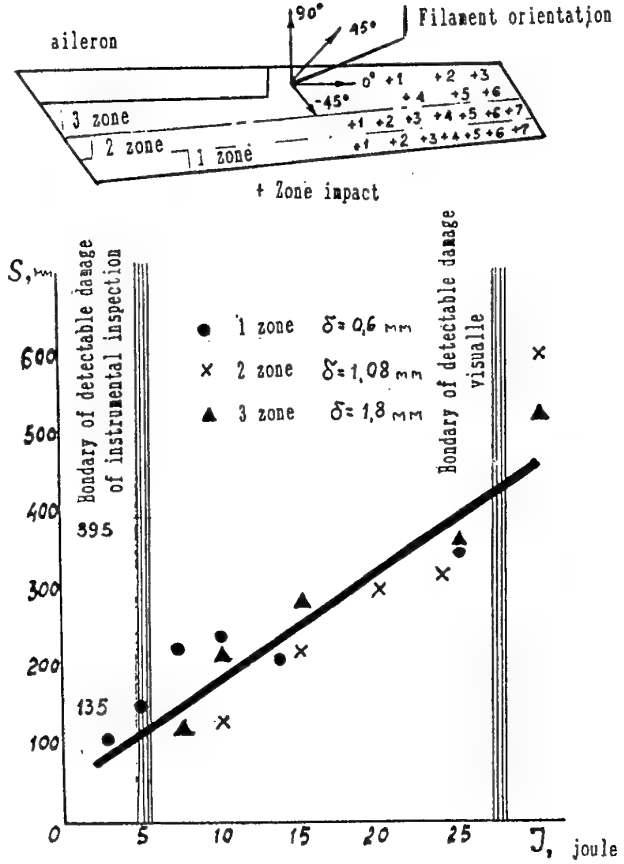

VERIFICTION OF ACUSTIK METHOD

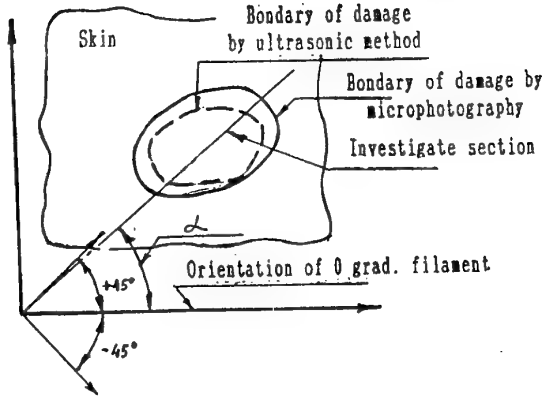

Fig. 18

GROWTH RATE OF DAMAGES AND DEFECTS

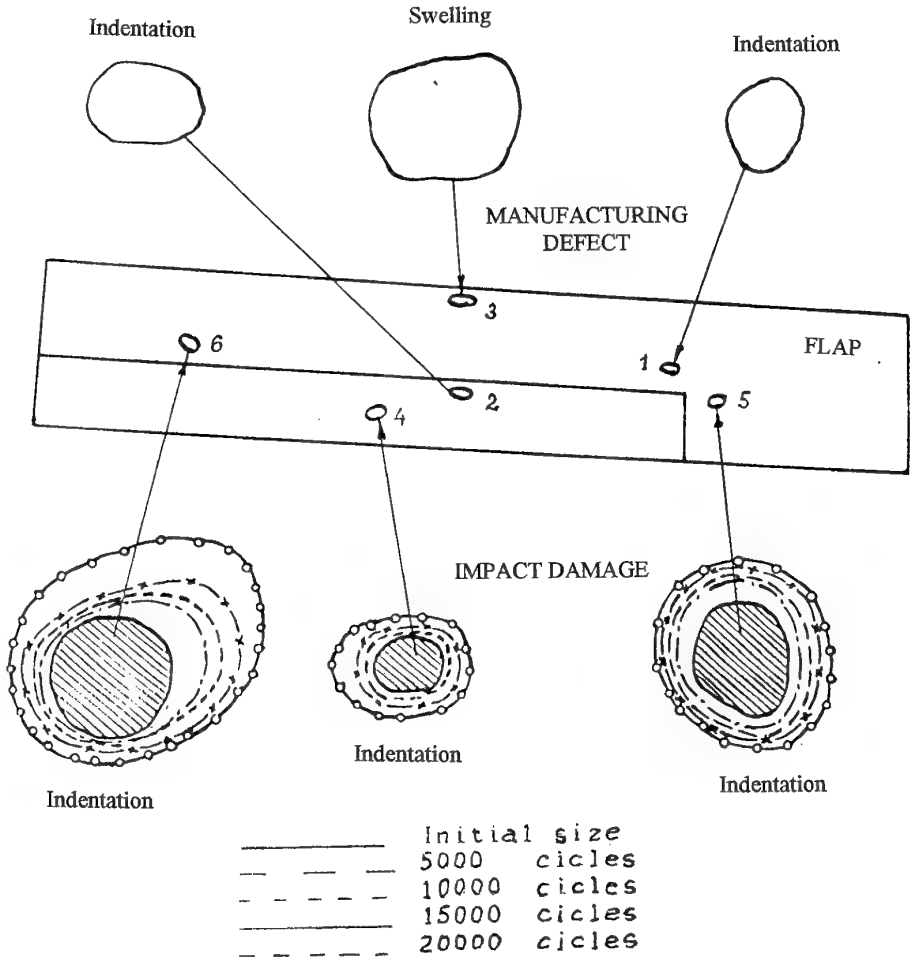

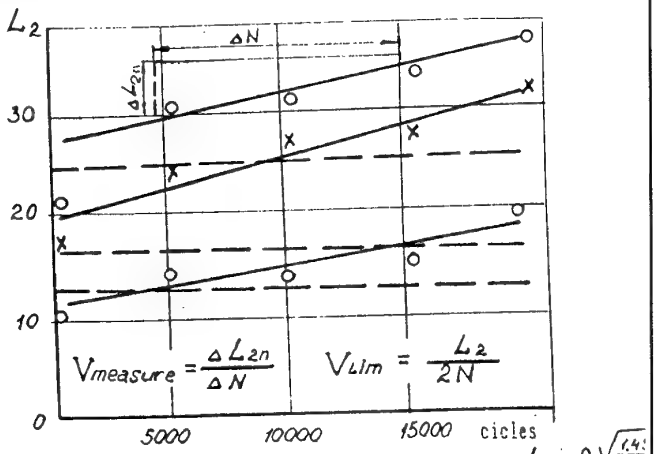

$L_2 = 2\sqrt{\frac{1.4}{\pi}}$

N point	Type of damages	Damage growth rate, мм/с Measure	Limit
1	Indentation	0	
2	Indentation	0	
3	Swelling	0	40 E -4
4	Indentation	3.4 E -4	
5	Indentation	5.6 E -4	
6	Indentation	5.9 E -4	

V measure = V limit

Fig. 19

CERTIFICATION OF PREFORMS AND STRUCTURE ELEMENTS OF COMPOSITE MATERIALS

Yuri P. Trunin
Central Aero-Hydrodynamic Institute, Zhukovsky 140160
Moscow Region, Russia

Abstract

The cost-efficient approach for certification of preforms and elements of composite materials is presented. The criterion of certification is the requirement that A- or B-values of a characteristic concerned are not less than the design values for a typical zone considered. The most critical typical zones are the ones with manufacturing defects, in-service impact damages and structural stress risers. Unlike the usual guidelines our method does not require testing specimens from all general population. The approach relies on static and fatigue tests of specimens from one material batch which has the worst average properties. As the worst material batch it is suggested to consider that which will be produced with critical per ply thickness from the allowable range of per ply thickness alteration. The A- or B-values may be determined on the basis of experiment and/or analysis in consideration of environmental effect. The experimental and analysis substantiations of the suggested approach are presented.

List of Symbols

A -	basis value - a 95% lower tolerance boundary for the upper 99% of a specified population.
B -	basis value - a 95% lower tolerance boundary for the upper 90% of a specified population.
p, p_n	actual and nominal per ply thicknesses
t, t_n	actual and nominal specimen thicknesses
n_p	ply number in specimen
t_f	thickness of dry fabric (tape)
$\overline{p} = t / p$	ply packing density
V	volume content of i-th ply
α	angle of orientation of i-th ply
k	layup coefficient
σ_t, σ_c	static failure stresses at tension and compression in specimen
σ^1_t, σ^1_c	static failure stresses at tension and compression in longitudinal plies
$\dot{\sigma}$	loading rate
K_{Ic}, K_{-Ic}	critical stress intensity factor (SIF) at tension and comprehension
σ_m, σ_a	mean stress and stress amplitude of cycle
$\sigma_{min}, \sigma_{max}$	minimum stress and maximum stress of cycle
r	asymmetry coefficient
f	frequency of cycle
N	life duration
N_0	life threshold
m	exponent of fatigue curve
d	exponent of long-time curve
s	exponent of curve of rate influence on static and fatigue strengths

1. Certification approach

As the certification criterion of preform material, element and detail the requirement is suggested that A- or B-values of its strength and service life will not be less than the design values. It should be shown takin into account environmental effects on the design values that component and items have: (i) the ultimate load and the service life in presence of flaws and damage which will be detected during manufacturing and major repairs by the inspection procedure selected; (ii) the residual strength of 80% of the ultimate load and the service life part (equal to the flight number between capital repairs in presence of the fatigue and impact damages which are to be detected during the visual pre-flight inspection). The residual strength at the end of the service life and the part of service life between capital repairs should not be less than the limit load. As allowable flaws and damage detected during manufacturing and major repairs it is advisable to take the part-through thickness crack, the delamination and the indentation by size of 10-20 mm, but under pre-flight inspection it is advisable to take the through-thickness gaps. The allowable gap size is established depending upon the inspection conditions.

It is known that a great quantity of specimens manufactured from several prepreg batches must be tested for estimating the design values of material, structural element and structural detail. For example, below five batches it is not necessary to determine the A- and B-value for material properties [1]. If the question concerning the evaluation of design values of preform materials, elements and units of aircraft structure with such confidence degree is raised, then the test extent becomes extremely large, because the number of elements and units that influence flight safety is too longe. Therefore, the proposed suggestion [2] concerning tests of the worst batch of preform material, component and items from the acceptable range is an attractive prospect.

The selection of the worst material batch is suggested to be chosen on the basis of the relation between strengt and per ply thickness. These relations are established by the supplier or the user on results of strength and fatigue tests of lamina or laminate under tension and compression. These tests are more reliable to carry out in advance. For obtaining the relations between a strength and per ply

Paper presented at the AGARD SMP Lecture Series on "Advanced Polymeric & Metallic Composite Materials for Space and Aerospace Vehicle Structures. . .", held in Stuttgart, Germany from 11-12 December 1995; Châtillon, France from 14-15 December 1995 and Ohio, USA from 18-19 December 1995 and published in LS-204.

thickness alteration in preform material, the between-batch variance and the critical per ply thickness [3] which is equal to one from two range bounds. As the worst material batch having the worst average properties we suggest to consider those which will be produced with critical per ply thickness. The test specimens of preform material, component and items (they are called the model specimens below) designated for estimation of the batch mean properties and the within-batch variance should be manufactured with the critical per ply thickness or close to it. In the last case a per ply thickness deviation is taken into consideration during the test result analysis. The procedure for A- and B-value estimation is given in Ref.[3]. The estimation of A- and B-values is suggested to be conducted only on model specimens which have been subjected to environmental exposure and have been tested at the most critical temperature. Influence of different factors on strength and fatigue of model specimens is suggested to be evaluated on the basis of the averages. Model specimen tests could be conducted under the loading selected from the in-service loading. In this case the A- and B-values should be estimated by the analysis. The analytical procedure should be substantiated by tests including tests of the model specimens.

2. Substantiation of certification approach

2.1. Influence of per ply thickness upon strength and fatigue of composite

The present section is devoted to experimental substantiation of the approach to certification of preform materials and structure elements.

The autoclave curing method is being generally used in the fabrication of fiber-reinforced composite parts. The curing parameters typically lie within ranges of pressure of 0.2-1 MPa and temperature up to 200° C. The material and process specifications set the procedures and the requirements for the resin content in prepreg, the storage of prepreg and the operating parameters for autoclave. In spite of this the experience of fabrication of numerous parts have demonstrated that the per ply thickness in the process control specimens and the elements can be alter over a wide range. The per ply thickness alteration results in a change of strength and fatigue of composite materials and structures.

The influence of per ply thickness upon strength and fatigue of composites should be considered in two aspects. At the stage of material and process development, the optimum per ply thickness and the allowable range of per ply thickness alteration are needed to determine the maximum of unit static and fatigue strengths that are equal to the ratio of static failure stress or fatigue failure stress under given life to unit weight of composite. In this case the static failure stress and the loads for fatigue tests should be calculated under the actual thickness in the specimen failure area.

The second approach to an estimation of the per ply thickness influence on resistance of a composite to failure is proper to the step of the structure certification. In this case the static failure stress and the loads for fatigue tests should be calculated under the nominal per ply thickness under which the analysis of stresses acting in service have been conducted. The nominal specimen thickness is equal to the nominal per ply thickness multiplied by the ply number ($t_n=p_n \cdot n_p$). On application of the nominal per ply thickness the static and fatigue failure loads will be directly proportional to corresponding stresses. The relations between the static failure stress and life versus per ply thickness within the allowable range need to be established the fit curves and the between-batch variances.

The static and fatigue test results of specimens of different composites are presented below to demonstrate the influence of per ply thickness on the resistance to failure and to draw some useful conclusions. Most of complete investigation of per ply thickness influence have been performed with glass/epoxy [4]. The thickness of dry fabric of 8 harness satin weave construction is equal to 0.23±0.02 mm. After removal of the coating glass fibers by burning out the fabric, thickness from equal to t_f=0.25 mm. This is explained by the fact that the coating helps to be stuck together the fibers. The lay-up type is [0]. The maximum pressure during the curing is equal to 0.8 MPa.

The tension strength values σ_t of unnotched glass/epoxy specimens under their actual thickness versus per ply thickness are given in Fig. 1 [5]. The strength of specimens cut from plates is shown by small points and the strength of the ones cut from helicopter rotor blade spars is shown by large points. The fitted curve are correspondingly, σ=618+1205p-6351p and σ=827-1295p and glass/epoxy unit weight curve are also presented in Fig. 1.

The life values for unnotched specimens of the same material versus per ply thickness are given in Fig. 2 [7]. The mean stress, the stress amplitude and the frequency of cycle are equal to σ_m=100 MPa, σ_a=120 MPa and f=12 Hz. The data are approximated by curve of lgN=-26.8+278p-587p^2 that is represented in Fig. 2.

The unit static failure stress and the unit stress amplitude that are obtained on the basis of above mentioned test results are presented in Fig.s 3 and 4 versus per ply thickness. For comparison the curves for static failure stress and stress amplitude under nominal specimen thickness are also demonstrated in Fig.s 3 and 4. It can be seen in Fig.s that the maximum values of unit static and fatigue strength are attained under per ply thickness of 0.21 mm and 0.23 mm, correspondingly. The maximum nominal stresses at static and fatigue failures and, consequently, the corresponding maximum loads take place under per ply thickness of 0.25 mm.

The fatigue tests of glass/epoxy with fabric by thickness of t=0.3 mm showed that the maximum unit fatigue strength is attained under per ply thickness of p=0.3 mm.

Thus, under $p<t_1$ when compression of fabric sheets occurs the glass/epoxy resistance to failure decreases.

This describes carbon/epoxy test results. The mean values of tension strength under nominal per ply thickness of p_n=0.157 mm for unnotched carbon/epoxy specimens versus per ply thickness are presented in Fig. 5. Unlike above mentioned glass/epoxy, the per ply thickness decrease resulted from the pressure increasing from 0.1 MPa up to 1 MPa. The thickness of dry carbon tape is equal to t_1=0.157 mm. It can be seen that under $p<t_1$ the composite strength decreases.

The batch mean compression strength for hybrid composites with three close layups of carbon/epoxy and aramid/epoxy versus carbon/epoxy per ply thickness are shown in Fig. 6. The unnotched specimens, (five pieces in one batch) were taken away from components of acrobatic aircraft as process control specimens. The thicknesses of dry carbon tape and dry aramid fabric are equal to 0.115 mm and 0.25 mm, respectively. The nominal per ply thickness for carbon/epoxy is equal to 0.09 mm. The maximum pressure during the curing is equal to 0.6 MPa. Measurement of dry carbon tape under pressure of 0.6 MPa have given the average value of 0.067 mm. The strength is evaluated by nominal failure stress in longitudinal carbon/epoxy plies by the relation

$$\sigma_n^{'}=\sigma_n/k$$

where σ_n is the nominal failure stress of specimen under compression;

k is the layup coefficient that is determined by the rough relationship

$$k = \sum_{i=1}^{n_1} V_{1,i}\cos^4\alpha_{1,i}+\frac{E_2^{'}}{E_1^{'}}\sum_{j=1}^{n_2} V_{2,j}\cos^4\alpha_{2,j} \qquad (1)$$

Here n_1 and n_2 are the numbers of carbon/epoxy and aramid/epoxy plies;

$V_{1,i}$ and $\alpha_{1,i}$, $V_{2,j}$ and $\alpha_{2,j}$ are the volume content and the orientation angle of i-th carbon/epoxy ply and j-th aramid/epoxy ply.

E'_1 and E'_2 are the elasticity modulus of carbon/epoxy and aramid/epoxy of longitudinal plies.

In the per ply thickness range of p=0.065÷0.115 mm the test results presented are approximated by linear equation of σ =-149÷12804p. The batch average not meeting the acceptance criteria are shown by large points in Fig. 6. The acceptance criteria is equal to material allowables under compression that have been chosen for element strength analysis.

Rejection of elements with poor strength produces truncated distribution. The empirical truncated distribution that is plotted on the batch averages of the process control specimens for accepted elements (demonstrated in Fig. 6) is presented in Fig. 7. Truncated distributions can also appear when the per ply thickness limitations are introduced for specimens. The empiric distributions for logarithm of life are presented in Fig. 8 for the above mentioned glass/epoxy with different ranges of per ply thickness alteration.

The Weibull formula fits with a good approximation the distribution of logarithm life for specimens with the most large range of per ply thickness alteration of p=0.18÷0.27 mm:

$$F(lgN) = 1 - \exp[-(lgN/\alpha)^{\beta}]$$

$$\alpha = 6.062 \qquad \beta = 12.79$$

The narrowing of per ply thickness range down p = 0.19÷0.27 mm provides lognormal distribution with average value of lgN = 5.825 and variance of S^2 = 0.308. But narrower per ply thickness rang produces truncated lognormal distribution:

$$F(N-N_0) = \frac{1}{\sqrt{2\pi}S_{lg(N-N_0)}}\int_{-\infty}^{lg(N-N_0)}\exp[-\frac{(x-a)^2}{2S^2_{lg(N-N_0)}}]dx$$

where N_0 is the life threshold.

Decreasing per ply thickness range induces both the increase of life threshold and a decrease of variance (Ref. Table I).

The narrowing of per ply thickness range at the average value of p = (1 ÷ 1.05) t_1 also promotes a decrease of between-batch variance up to an insignificant value in comparison with the variance of batch average. This last result testifies the lack of physical cause for appearance of between-batch variance.

The influence of per ply thickness on static and fatigue strength was presented for unnotched specimens. The most critical zones for structures are the ones with different stress risers. Experience of the analysis and experimental strength studies of composite structures with stress concentrators such as cutouts, mechanical joints, delaminations and impact damages has shown that characteristics of fracture toughness can be used for the analysis of a structure strength. In the case of fracture under plane stress state the critical stress intensity factors (SIF) under tension, compression and shear are the fracture criteria and, consequently, the design characteristics.

The critical values of SIF for carbon/epoxy laminates with close layups versus a failure stress of unnotched specimens under tension and compression are presented in Fig.9. All strength and fracture toughness characteristics are evaluated in longitudinal plies of carbon/epoxy by means of k-coefficient presented previously (1). As it can be seen, there is nearly linear relation between these characteristics.

The tension test results of glass/epoxy flat specimens with hole with d_0 = 5 mm (Fig. 10) confirm that their ratio to the unnotched specimen strength does not practically depend on per ply thickness. The specimens were fabricated from above mentioned glass/epoxy laminates. The life values of flat specimens with central hole versus per ply thickness are shown in Fig. 11. The test loads were calculated under actual thickness of specimens. It is necessary to note that the specimens with per ply thickness of p = 0.24 ÷ 0.26 mm were heated in the riser zone up to temperature of T = 60° C. This leads to a drop of life duration by a factor of 2.5. The test results are approximated by quadratic equation of lgN = -57.45 + 559.3 p ÷ 1237 p^2. The maximum life is attained under per ply thickness of p = 0.227 mm. This value is near to the corresponding value for unnotched specimens p = 0.237 mm (Fig. 10).

Thus, considering the stage of preform material and element certification it should be noted that (i) the maximum values of static and fatigue strength take place under per ply thickness equal to per ply thickness of dry tape or fabric where fibre coating has been removed, (ii) function of distribution of strength and life depends on per ply thickness range and the range narrowing promotes the threshold appearance, (iii) total and between-batch variances decrease under the range narrowing and their most small values take place under the mean per ply thickness of p = (1 ÷ 1.05) t_l.

2.2. Substantiation of analysis procedures for certification

2.2.1. Special requirements for polymer composite materials and to its test conditions

The results of the fatigue investigations stated below are concerning the composites, containing the longitudinal plies in the direction of load and the resin that corresponds to the fiber. The criteria of this correspondence for the fatigue conditions can be formulated as follows:

1) The absence in the resin of chemically active components, which can promote destruction of the fiber material.

2) The inadmissibility of global delamination of composite under cyclic loading up to total fatigue fracture.

In the fatigue tests the self-heating of composite specimens may occur due to the hysteresis energy loss in the process of cyclic deformations. Depending on load frequency and stress amplitude the rise of specimen temperature can be transient (non steady-state temperature). The specimen temperature can rise up to a relatively high level, leading to a decreasing in life if comparised to the life reached with lower load frequency or with cooling of the specimen.

Since the continuous rise of structural temperature due to self-heating is not inherent to the structure in operation, the study of the fatigue resistance should be conducted at given constant specimen temperature. For majority of structural composites the conditions of specimen loading is assumed to be satisfactory, if the material temperature rise from ambient temperature is less than 10°C.

2.2.2. Effect of loading rate

The rate of sinusoidal loading ($\dot{\sigma}$) is usually described by an averaged value, which is equal to the product of a double stress amplitude $2\sigma_a$ and a double cycle frequency $2f$:

$$\dot{\sigma} = 4\sigma_a f .$$

As is shown in Fig. 12, the restricted fatigue limit (σ_{aw}) of glass/epoxy fabric laminates is increased with the increase of the rate of cyclic loading of unnotched and notched specimens [6]. The mean stress of cycle was equal to σ_m = 100 MPa, σ_m = 200 MPa, and σ_m = 300 MPa. The majority of specimens were tested at temperature T = 15-35°C. One set of specimens was tested at an elevated temperature T = 55°C that leads to decrease of fatigue resistance. The ultimate strength is also hising with increasing loading rate. It is shown in Fig.13 for mentioned above glass/epoxy and carbon/epoxy laminates under the condition of uniform tension loading. The dependence of the ultimate strength and the restricted fatigue limit on the loading rate are rather well approximated by the exponential function:

$$\left| \begin{matrix} \sigma_t \\ \sigma_{aw} \end{matrix} \right| = \left| \begin{matrix} A \\ D \end{matrix} \right| \dot{\sigma}^S$$

The values of the exponent s are nearly equal (Fig. 14) for static and fatigue specimens and are dependent on the ply packing density $\bar{p}$ which is defined as the ratio of the thickness of dry fabric or tape to per ply thickness.

Long-time strength under constant stress can be also described by the power function:

$$t = C\ \sigma^d$$

where t is the time to fracture of the unnotched specimen.

Using the linear hypothesis of damage accumulation the relation between the ultimate strength and the loading rate can be deduced in following form:

$$\sigma_t = [C(1-d)\dot{\sigma}]^{1/(1-d)} \qquad (2)$$

For example, the mean ultimate strength for cord-glass-fabric/epoxy laminates in tension at loading rate S = 50 MPa/sec at temperature T = 20°C and T = 100°C are σ_t = 940 MPa and σ_t = 810 MPa, respectively, while values predicted using the equation (2) are σ_t = 927 MPa (d = -57.0) and σ_t = 794 MPa (d = -47.2). Fig. 14 shows the values (2) of the exponent s obtained for this

glass-fabric/epoxy laminate from equation:

$$s=1/(1-d) .$$

2.2.3. Effect of amplitude and mean cycle stress

If fatigue curves were plotted at fixed loading rate rather than fixed loading frequency, then these curves are well approximated by the power function for both constant mean stress (σ_m = const) and constant coefficient of cycle asymmetry (r = const) .

$$N = B\,\sigma_a^{-m}$$

The coefficient of cycle asymmetry r is defined as $\sigma_{min} / \sigma_{max}$, where σ_{min} and σ_{max} are minimum and maximum stress of the cycle, respectively.

The fatigue curves for glass-fabric/epoxy laminates with various values of ply packing density are shown at Fig.15. These curves were obtained for the unnotched specimens. If for N = 1 the realization of the static failure is assumed, then

$$B = \sigma_a^m = (\sigma - \sigma_m)^m$$

where σ is the stress of the static failure ($\sigma = \sigma_t$ in tension and $\sigma = \sigma_c$ in compression).

Then:

$$N = [(\sigma - \sigma_m)/\sigma_a]^m \qquad (3)$$

If parameter σ of fatigue curve (3) is estimated in static tests, it is necessary, that the rate of static loading is equal to the rate of cyclic loading. The equations describing the fatigue curves for tension-tension cycle (r = 0), compression-compression cycle (r = -∞), and symmetrical cycle (r = -1) can be written in the following manner [6]:

$$N = (\sigma_t / \sigma_{max})^{m_{r=0}} \qquad for\ r = 0$$

$$N = (\sigma_c / \sigma_{min})^{m_{r=-\infty}} \qquad for\ r = -\infty$$

$$N = (\sigma/\sigma_a)^{m_{r=-1}} \qquad for\ r = -1$$

where: if $\sigma_t < |\sigma_c|$ then $\sigma = \sigma_t$; if $\sigma_t > |\sigma_c|$ then $\sigma = |\sigma_c|$.

The values of σ_t, σ_c, $m_{r=0}$, $m_{r=-\infty}$ and $m_{r=-1}$ are considered as the design values of material.

The relation between the m exponent of fatigue curve with arbitrary average stress and the exponent m_r either for tension-tension cycle (if $\sigma_m > 0$) or compression-compression cycle (if $\sigma_m < 0$) was deduced.

If $\sigma_m / \sigma \geq 0.05$, then

$$m = m_r \frac{lg(\sigma/2/\sigma_m)}{lg(\sigma/\sigma_m - 1)} \qquad (4)$$

If $\sigma_m/\sigma < 0.05$, then

$$m = m_{r=-1} + 20(m_{0.05} - m_{r=-1})\sigma_m/\sigma \qquad (5)$$

Where: If $\sigma_m > 0$, then $m_r = m_{r=0}$ and $\sigma = \sigma_t$;

if $\sigma_m < 0$, then $m_r = m_{r=-\infty}$ and $\sigma = \sigma_c$;

$m_{0.05}$ is the exponent determined by formula (4) at $\sigma_m / \sigma = 0.05$.

If the average stress is approaching zero, the values of m, obtained from the equation (4), are restricted to value of $m_{r=-1}$.

The special feature of the fatigue fracture of composites under the alternating sign loading cycle and with S = const, is that the fracture can occur due to both the action of tensile stress and that of compressive stress of the cycle depending on stress amplitude. Then the fatigue life will be equal to the minimum of two values: the first value being determined by equation (3) with σ_t (if $\sigma_m > 0$) or σ_c (if $\sigma_m < 0$): the second value being determined by equation (3) with $m = m_{r=-1}$ and σ_c (if $\sigma_m > 0$) or σ_t (if $\sigma_m < 0$).

Fig.16 shows the test results and the analytical relations of restricted fatigue limit of glass-fabric/epoxy laminates versus the mean cycle stress. The design properties of material used for analytical prediction were as follows:

- at $\bar{p}$ = 1.08 and $\dot{\sigma}$ =4800 MPa/s: σ_t = 677 MPa, $m_{r=0}$ = 14, σ_c = -460 MPa,
  $m_{r=-\infty}$ = 19.8 and $m_{r=-1}$ = 13.8

- at $\bar{p}$ = 1.05 and $\dot{\sigma}$ = 4800 MPa/s : σ_t = 655 MPa, $m_{r=0}$ = 14.6.

The ply packing density has a significant influence upon the fatigue resistance of composites.

2.2.4. Fatigue resistance of hybrid composites

Carbon/glass/epoxy and carbon/aramid/epoxy composites are the most important materials for the practical application among all hybrids. The static and fatigue properties of their components are quite different. Therefore, depending on the conditions of cyclic loading the first fracture may occur either in the plies of glass/epoxy (aramid/epoxy) or in the carbon/epoxy plies. It is called here the first fracture. Then the second fracture is the fracture of the remaining component.

There is a significant difference between fatigue fracture of hybrid composites in comparison with the static fracture. The static fracture begins in the plies of material with the lower ultimate strain (material denoted by subscript 1). The remaining material with the higher ultimate strain (denoted by subscript 2) may fail under the load acting in that moment, or may withstand a higher load, depending on its strength and content . Hence the static strength of hybrid composites will be equal to the maximum of two values of strength, calculated for the first and second fractures. Analytical model of static ultimate strength of hybrid composite shall take into account the first kind of hybrid effect, i.e. the increase of ultimate strength of plies of first material when these plies are uniformly distributed among plies of second material.

The relative strength of plies in hybrid composite with respect to carbon/epoxy composite tensile strength is shown in Fig. 17 vs. glass plies contents in hybrid. The load, at which the fracture of first material occurred, was determined from the stress-strain diagrams and by the acoustic emission method.

The analytical model for the fatigue resistance of hybrid composites must allow the fatigue life determination for both first and second material. The life until complete fracture is equal to the sum of the minimum of these two values and the life of the remaining material, determined by taking into account the possible fatigue damages, occurred in it at the first stage. The experimental results and the analytical fatigue curves for carbon/glass/epoxy composite under tension-tension cycle are shown in Fig. 18. The design properties of material used for analytical prediction were as follows:

- for carbon/epoxy at $\bar{p}$ = 1.27, $\dot{\sigma}$ =10 MPa/s and nominal lamina thickness 0.15 mm: σ_t'= 710 MPa, $m_{r=0}$ = 65, s = 0.0128, E'= 120000 MPa

- for glass/epoxy at $\bar{p}$ = 1.27, $\dot{\sigma}$ = 10 MPa/s and nominal lamina thickness 0.27 mm: σ_t'= 1200 MPa, m = 7.49, s = 0.046, E'= 59000 MPa.

The 90% confidence interval for ratio of the measured strength to the predicted strength , estimated from the results of the analytical prediction and the static strength tests of graphite/glass/epoxy with glass content of Vg = 53.6 - 83.4% are equal 0.966 - 1.058. The similar values for restricted fatigue limit are 0.976 - 1.09.

2.2.5. Fatigue resistance of composites under complex loading

The investigations of the effect of complex loading upon the fatigue resistance of composites are usually carried out with tubular specimens. The dependence of fatigue life on the minimum tangential cycle stress for unnotched glass/epoxy tubular specimens and graphite/glass/epoxy specimens shown in Fig. 19 for conditions of in-phase compression and torsion (r = -∞). The results of tests are in satisfactory agreement with the analytical prediction. The predicted fatigue life was determined as minimum from three values, calculated according to the action of the normal stress along axis X and Y and the tangential stress in the plane XY. The effect of complex stressed state is accounted for by decreasing of static strength. In considered loading conditions the influence of the tangential stress upon the static ultimate strength was estimated by quadratic relationship:

$$\sigma_{Cx} = \frac{\sigma_x}{\sqrt{\left(\frac{\sigma_x}{\sigma_{ux}}\right)^2 + \left(\frac{\sigma_{xy}}{\tau_{uxy}}\right)^2}}$$

$$\tau_{Cxy} = \frac{\tau_{xy}}{\sqrt{\left(\frac{\sigma_x}{\sigma_{ux}}\right)^2 + \left(\frac{\tau_{xy}}{\tau_{uxy}}\right)^2}}$$

where σ_x and τ_{xy} are extreme values of the axial and tangential stress in full cycle.

It is assumed, that critical stress (here σ_{Cx} or τ_{cxy}), which provides maximum value of the ratio to the corresponding ultimate strength, is responsible for the static fracture. However for cyclic loading this condition may be insufficient. In this view the concept of the corrected stress of static fracture is introduced in the model of the fatigue fracture for the directions of loading, where the above-mentioned ratios are less than maximum. This concept helps to answer the question: at which stress the static fracture in the direction considered should occurr if it had not occurred in the most critical direction (according to static conditions) for a given ratio of cycle extremes of load directions? In the considered mode of loading the most critical direction with respect to static fracture conditions was axial compression. Therefore, the corrected value of static strength under shear was determined from equation

$$\tau^*_{Cxy} = \frac{\tau_{xy}}{\sqrt{2\left(\frac{\tau_{xy}}{\tau_{uxy}}\right)^2}}$$

2.2.6. Models of static strength and transverse crack propagation.

A two-parameter model of static fracture under tension of composite specimens with the through macrocrack was suggested in [7] . According to this model a critical value K_{Ic} of the stress intensity factor (SIF) is used as the fracture criteria. This value is

determined accounting for the correction for the intense energy zone A_1 in the crack tip. The fracture criterion in a point was obtained in [8]. According to this criterion the fracture of the specimen with initial crack occurs when the stress in distance b from the crack tip exceeds the ultimate strength of composite. The authors established a relation

$$b = A_1 / 2$$

Thus it was shown, that the zone of width A_1 near the crack tip has a strength equivalent to that of the unnotched specimen onk made of the same composite. It is possible to assume that this equivalence remains valid for fatigue conditions. In accordance with this assumption the crack under cyclic loading may propagate either discretely by steps of size A_1, or continuously at the constant value of the actual SIF in considered zone of size A_1. The last way of the crack propagation seems to be quite possible if one takes into account that: 1) In contrast to metals the crack front in composite is spread owing to, firstly, the crack propagates in composite in a form of matrix cracking and, secondly, the fibers in the macrocrack tip may not be destroyed simultaneously.

2) In case of rather high values of A_1, the most part of cycles will be spent to fracture of the first region by length A_1.

For both cases the transverse crack growth rate is:

$$V = A_1 / N$$

where N is the fatigue life of the unnotched composite specimen, which can be determined by the above-mentioned procedure.

In this case it is expedient to determine the static fracture stress and the loading cycle stress and the gross cross-section.

The static fracture stress in the specimens with central location of the stress concentrator (notch or the crack of size $2L$) for discussing below cases of uniaxial tension which is given by equation

$$\sigma_t = \frac{K_{IC}}{\sqrt{\pi(L + A_1)}\, f\left(\frac{L}{B}\right)}$$

where

$$f\left(\frac{L}{B}\right) = \frac{1}{\sqrt{\cos\left(\frac{\pi L}{B}\right)}}$$

is the factor taking into account the finite specimen width [9]:

$$f\left(\frac{L}{B}\right) = \frac{2 + \left(1 - \frac{d_0}{B}\right)^3}{3\left(1 - \frac{d_0}{B}\right)}$$

is the correction for specimen width with central hole of diameter d_0 [10]:

$$K_{IC} = \sigma_t \sqrt{\pi A_1}$$

$$A_1 = \frac{L}{\left(\frac{\sigma_t}{\sigma f\left(\frac{L}{B}\right)}\right)^2 - 1} \qquad (7)$$

Application of the two-parameter model of fracture for the analysis of static strength a mechanical joint loaded in tension and compression without bending [11, 12] have given the following relation

$$\sigma = \frac{K_{IC}}{\sqrt{\pi(0.5d_0 + A_1)}\left[+_{(}1 - k_1) + k_1 \frac{B}{2d_0 n_1}\right] f\left(\frac{L}{B}\right)}$$

where "+" - under tension, "-" - under compression, n_1 and k_1 - the fastener number in the first row of joint and the coefficient of loading of the first row.

If the values of K_{Ic} and A_1, obtained for the specimens in initial state, are used to predict the fatigue life, the result can be conservative in comparison with an experimental evaluation. It is due to the rapid matrix cracking in the beginning of cyclic loading, which leads to a reduction of the stress concentration and an increase of the static strength. For example, the static strength of glass-fabric/epoxy laminates with a central hole (d_0 = 8 mm) was increased after cyclic tension by factor 1.2 due to the growth of the longitudinal cracks. Hence it is necessary to take into account this static strength increase, if more exact evaluation of the fatigue resistance of composite specimen with the stress concentrator is needed.

The comparison of predicted and experimental values of fatigue life of glass-fabric/epoxy specimens with central hole (d_0 = 8 mm) under uniaxial loading is shown in Fig. 20. The value of the correction for the cracking zone under tension is equal to A_1 = 5.47 mm (although this value for similar specimens which have experienced a pre cyclic loading was equal to A_1 = 2.67 mm). The values of other properties are given in the figure inscriptions.

The above mentioned analytical procedures have been used during certification of preform materials, elements and units of aircraft components.

Certificate content

Certificate of preform material and element contains the following sections:

1. Brief description of preform and element (trade--marks of applicable composites and other materials, aircraft component, design values).

2. Input materials for preform processing (trade--marks of input materials, fabric or tape thickness).

3. Processing and main parameters of process (pressure, temperature, curing time).

4. Preform batch for certification (natural or model preform, copy number, geometry, layup, average and variation coefficient of per ply thickness, nominal per ply thickness).

5. Batches of model specimens and process control specimens for certification (specimen type and property, fabrication, number).

6. Acceptance criteria for strength of process control specimens (calculated under nominal per ply thickness) and for per ply thickness.

7. Physical properties of preform material (unit mass, fiber volume, void content, equilibrium moisture content at given relative humidity and temperature, actual moisture content in model specimens, glass transition temperature of dry material and material with equilibrium moisture content).

8. Within-batch and between-batch variation coefficients for analysis of A- and B-values.

9. Table of properties (specimen type, property, specimen state, test temperature, batch average, within-batch variation coefficient, specimen number, A- and B-values).

All sections of certificate should be provided by references on documentation.

Conclusion

The cost-effectiveness approach to the certification of preform materials and structural elements is suggested. The approach relies on static and fatigue tests of specimens from one material batch that has the worst average properties. The per ply thickness effect on strength and fatigue of polymer composite materials lies in substantiation of the certification approach. The procedures of analytical estimations of strength and service life of structural elements are outlined.

References

1. Military Handbook "Polymer Matrix Composites", MIL-HDBK-17-3C,1992.
2. Райхер В.Л., Сеник В.Я. и Трунин Ю.П. "Сертификация заготовок и элементов конструкций из композиционных материалов", Тезисы доклада на Международной конференции"Экспериментальноеоборудование и сертификация авиационной техники", 22-27 августа 1995г., Жуковский, Россия.
3. V.Y.Senik "Determination of A- and B-values of strength and fatigue resistance for preforms and elements of composite structural materials" Lecture Series TCP 04, AGARD-NATO, 1995.
4. Трунин Ю.П. "Исследование выносливости стеклотекстолитов для лонжеронов лопастей несущего винта вертолета", кандидатская диссертация, 1973.
5. Трунин Ю.П. "Зависимость прочностных характеристик стеклотекстолита от коэффициента армирования", Труды ЦАГИ, выпуск 1239, Изд. отдел ЦАГИ, Москва, 1970.
6. Трунин Ю.П. "Влияние плотности упаковки стеклоткани и условий нагружения на выносливость стеклотекстолита", Труды ЦАГИ, выпуск 1417, Изд. отдел ЦАГИ, стр.114-120, Москва, 1972.
7. M.E.Waddoups , J.R. Eisenmann and B.E. Kaminski - Macroscopic Fracture Mechanics of Advanced Composite Materials.-"J. of Composite Materials", 1971, vol.5, 10, p.446-454,ill. Bibl.
8. Whitney J.M. and Nuismer R.J.- Stress Fracture Criteria for Laminated Composites Containing Stress Concentrations.-"J. Composite Materials", vol.8., p.253-265, 1974.
9. Tada H., Paris P.C., Irwin G.R., The stress analysis of crack handbook, Del Research Corporation, Hellertown-Pennsylwania, 1973.
10. Peterson R.E.- Stress concentration Design Factors.- Wiley and Sons, New York, 1974.
11. Ю.П.Трунин "Методика расчета статической прочности точечных соединений композиционных материалов", РТМ "Проектирование, расчет и испытания конструкций из композиционных материалов", Труды ЦАГИ, выпуск 10, стр.90-108, Издво ЦАГИ, 1984.
12. Ю.П.Трунин "Модели статической прочности конструкции с концентратором напряжения, изготовленной из полимерных композиционных материалов со встроенными стопперами трещин", "Ученые записки ЦАГИ", том 24, No1, стр.145-156, 1993г.

Table I

Specimen number	Per ply thickness range, mm	$\overline{lgN}$	$S^2_{lg(N-N_0)}$	N_0
213	0.2 ÷ 0.26	5.95	0.154	29060
112	0.21 ÷ 0.25	6.109	0.121	87370
45	0.22 ÷ 0.24	6.235	0.098	180100

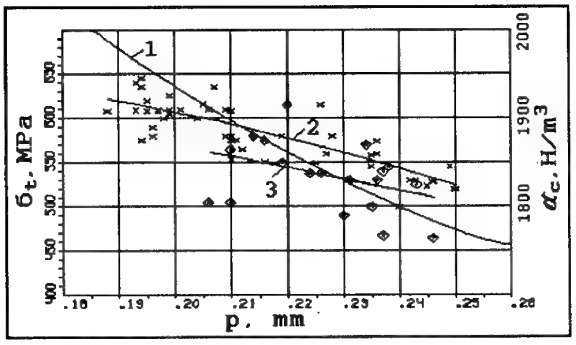

Fig. 1. Unit weight d_c (1) and actual tension failure stress σ_t of unnotched specimens cut from sheets (2, small points) and from helicopter rotor blade spars (3, large points) versus per ply thickness of glass/epoxy.

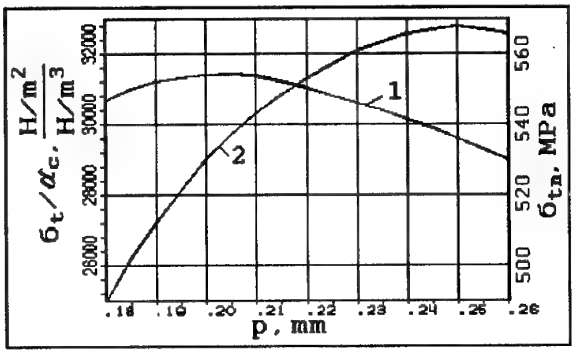

Fig. 3. Variation of unit tension failure stress (1) and tension failure stress under nominal thickness (2) of glass/epoxy unnotched specimens with per ply thickness.

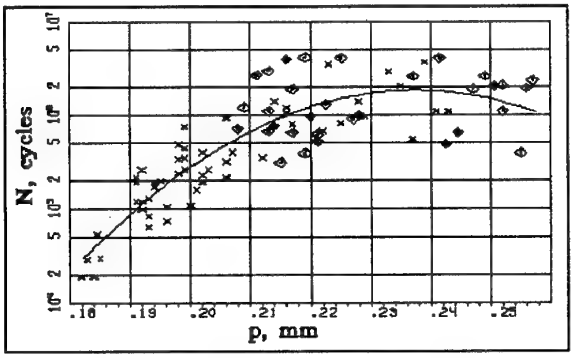

Fig. 2. Life of glass/epoxy unnotched specimens cut from sheets (small points) and helicopter rotor blade spars (large points) versus per ply thickness. Cycle stress under actual specimen thickness are σ_m = 100 MPa and σ_a = 120 MPa.

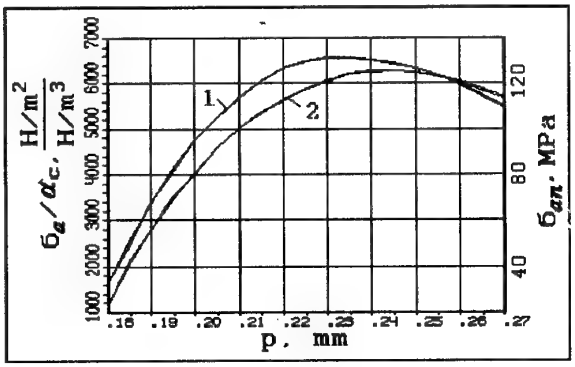

Fig. 4. Variation of unit stress amplitude (1) and stress amplitude under nominal thickness (2) of glass/epoxy unnotched specimens under $N = 10^6$ cycles and stress mean of σ_m = 100 MPa with per ply thickness.

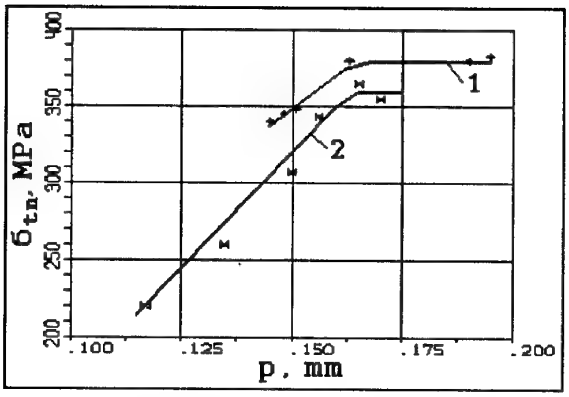

Figure 5. Variation of average tension failure stress under nominal per ply thickness of p_n = 0.157 mm for carbon/epoxy on the Lu-3 tape (1) and the Lu-3P tape (2) with per ply thickness. Layup type is [0/90].

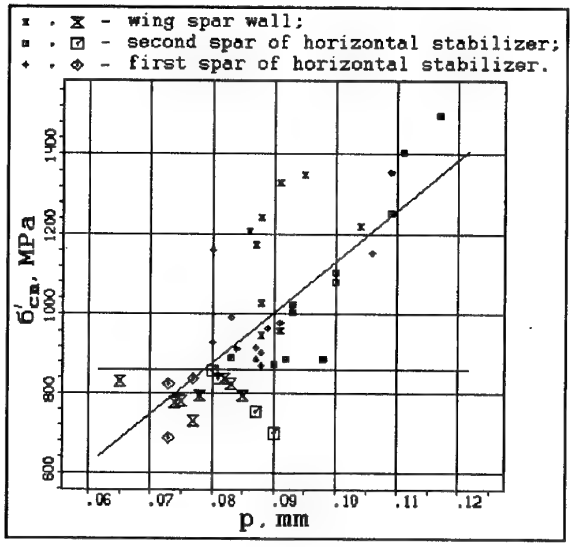

Figure 6. Batch average values of nominal failure stress in carbon/epoxy longitudinal plies of hybrid composite versus per ply thickness. The bakch mean compression strength obtained from process control specimens for wing spar which do not meet requirements are shown by large points

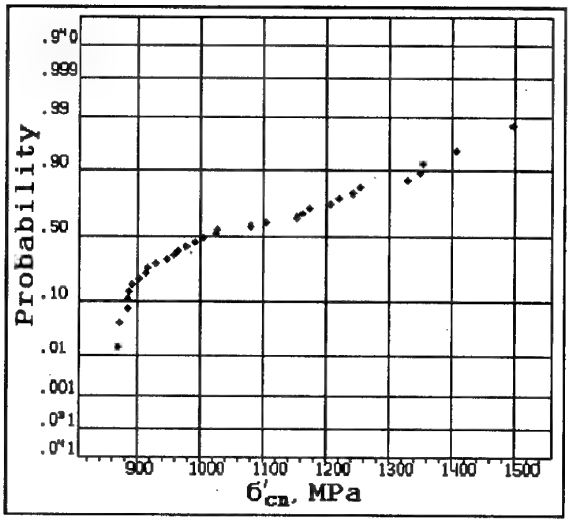

Figure 7. Empiric distribution of batch average values of nominal failure stress in carbon/epoxy longitudinal plies of hybrid composite (small points in Figure 6)

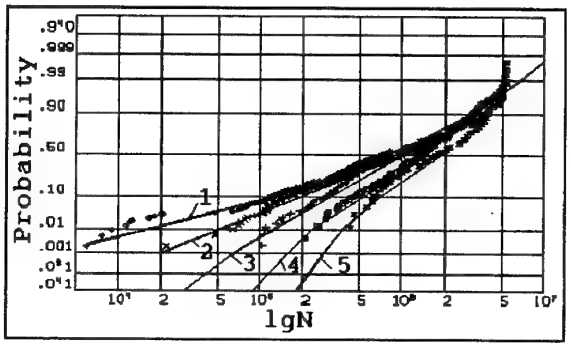

Figure 8. Empiric distribution of life logarithm for glass/epoxy unnotched specimens tested under the actual stresses of σ_m = 100 MPa and σ_a = 120 MPa.
1 - p =0.18 - 0.27 mm, n=270 specimens
2 - p =0.19 - 0.27 -"- 253 -"-
3 - p =0.20 - 0.26 -"- 213 -"-
4 - p =0.21 - 0.25 -"- 212 -"-
5 - p =0.22 - 0.24 -"- 45 -"-

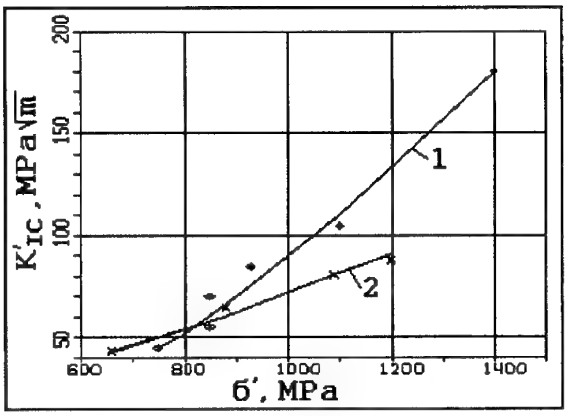

Fig. 9. Critical values of SIF for carbon/epoxy under tension (1) and compression (2) versus strength of unnotched specimens. All values are evaluated in longitudinal carbon/epoxy plies.

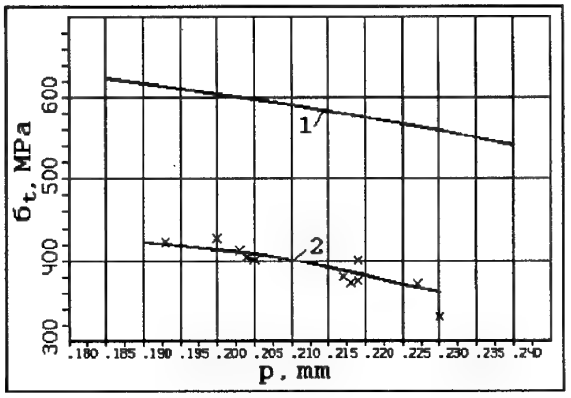

Fig. 10. Actual tension failure stress (brutto) of glass/epoxy flat unnotched specimens (1) and specimens with hole of d_0 = 5 mm and by width of 25 mm (2) versus per ply thickness.

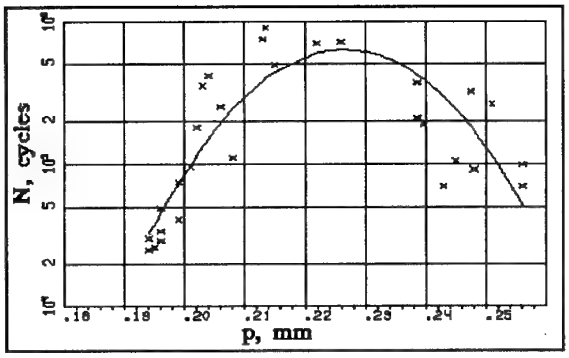

Fig. 11. Life of glass/epoxy flat specimens with hole of d_0 = 8 mm and width of 50 mm versus per ply thickness. Actual test stresses (brutto) are σ_m = 80 MPa and σ_a = 96 MPa. T = 30 - 60°C under alteration of per ply thickness from p = 0.195 mm up to p = 0.255 mm.

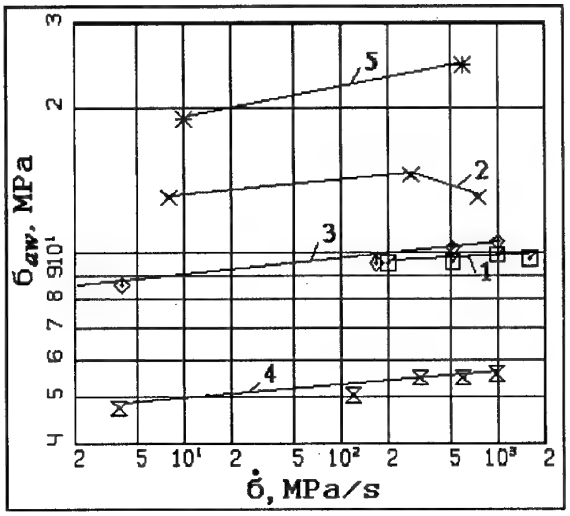

Fig.12.Effect of loading rate on the restricted fatigue limit for satin-glass-fabric/epoxy laminates (1, 2, 3, 4; t_1 = 0.23 mm) and the cord glass fabric/epoxy (5; t_1 = 0.3 mm). T = 15 ÷ 23 °C.

1, 2, 3, 5 - unnotched specimens of width B = 50 mm.

4 - specimens with central hole, d = 8 mm, L/B = 0.16.

1. σ_m=100 MPa N=7000000, $\bar{p}$ = 1.12
2. σ_m=100 MPa N= 300000, $\bar{p}$ = 1.12
3. σ_m=200 MPa N= 100000, $\bar{p}$ = 1.12
4. σ_m=200 MPa N=100000, $\bar{p}$ = 1.125
5. σ_m=300 MPa N = 10000, $\bar{p}$ = 1.33

*) net stress corresponds to the actual per ply thickness.

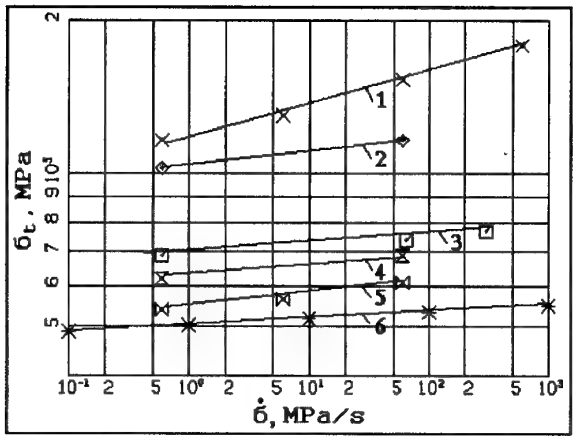

Fig.13. Effect of loading rate on ultimate strength for the satin-glass-fabric/epoxy laminates (3, 4, 5; t_1 = 0.23 mm) cord glass fabric/epoxy (1, 2; t_1 = 0.3 mm) and for carbon/epoxy laminates (6)

1. $\bar{p}$ = 1.335; 2. $\bar{p}$ = 1.08; 3. $\bar{p}$ = 0.94; 4. $\bar{p}$ = 1. 15; 5. $\bar{p}$ = 1. 15; 6. p_1 = 0.09 mm.

*)For 1, 2, 3, 4 and 5 the stress correspond to the of actual per ply thickness and for 6 - to nominal one.

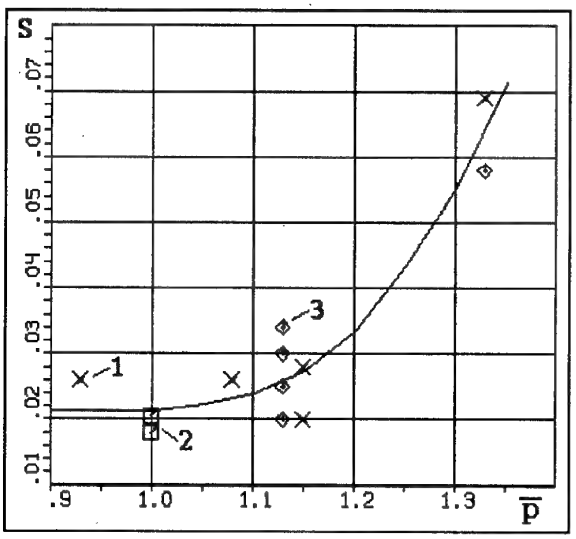

Fig.14. Effect of the ply packing density on the exponent s for ultimate strength (1,2) and fatigue limit (3).

× - 1,

□ - 2,

◇ - 3.

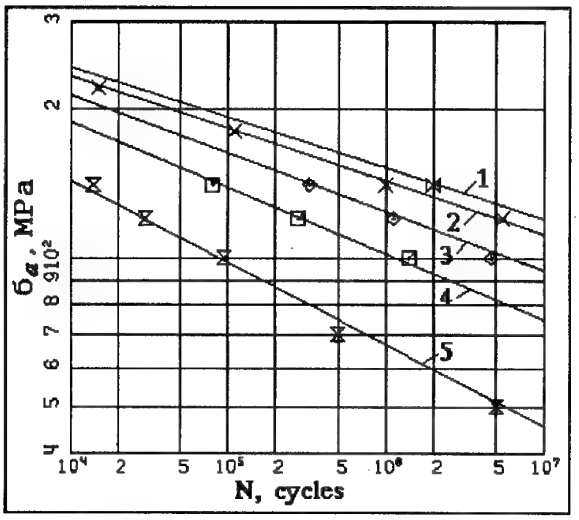

Fig.15. Fatigue curves for unnotched specimens of glass-satin-fabric/epoxy laminates: σ_m = 100 MPa, T = 15 ÷ 35°C, $\dot{\sigma}$ = 4500 MPa/s,

1. $\bar{p}$ = 1; 2. $\bar{p}$ = 1.08; 3. $\bar{p}$ = 1.12; 4. $\bar{p}$= 1. 18; 5. $\bar{p}$ = 1.24; t_1 = 0.23 mm.

*) stress corresponds to the actual per ply thickness.

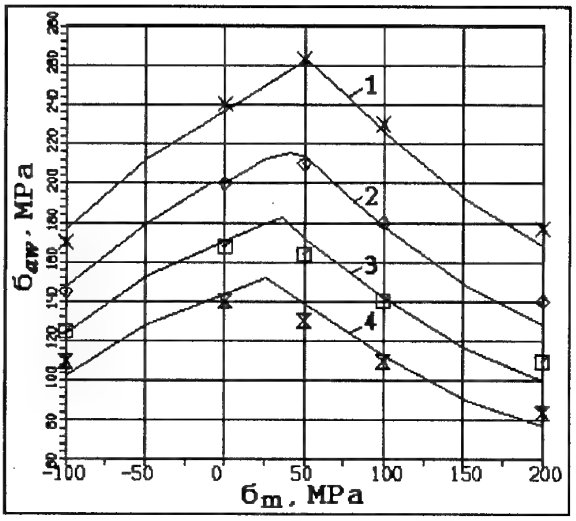

Fig.16. Predicted diagram "stress amplitude -mean stress" for the unnotched specimens of glass-satin-fabric/epoxy laminates: $\dot{\sigma}$ = 4800 MPa/s, $\bar{p}$ = 1.08 and $\bar{p}$ =1.05 (σm = 200 MPa); t_1 = 0.23 mm.

1. N = 10 000; 2. N = 100 000; 3. N = 1 000 000; 4. N = 10 000 000 t_1 = 0.23 mm

*) the stress corresponds to the actual per ply thickness.

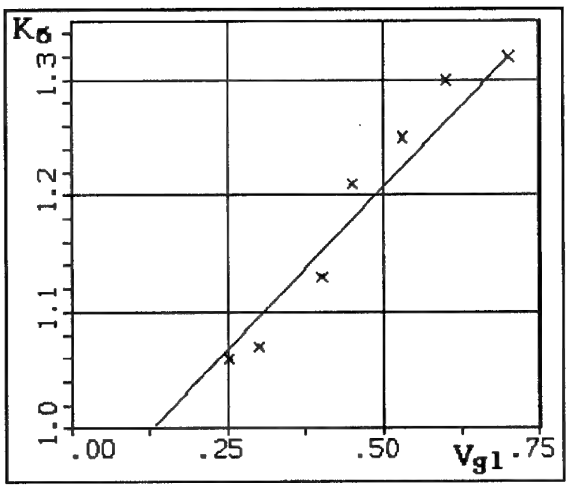

Fig.17. The relative strength of carbon layers in hybrid composite with respect to carbon/epoxy composite tensile strength vs. glass layers contents in hybrid.

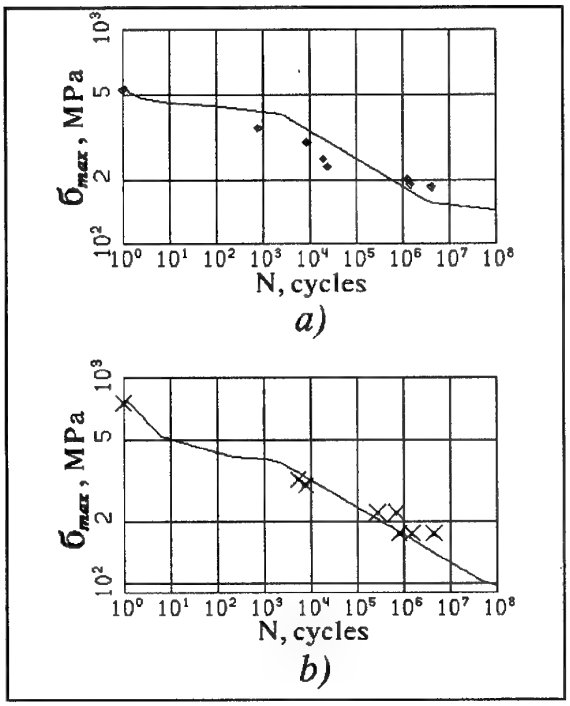

Fig.18. The experimental results and analytical fatigue curves for carbon/glass/epoxy composite under tension-tension cycle. $\dot{\sigma}$ =4000 MPa/s;

a)layup $[90_{gl}/O_{gl}/+45_{gl}/O_{gr}/O_{gl}/O_{gr}/O_{gl}/O_{gr}/-45_{gl}/0_{gr}]_s$, V_{gl} = 75.5%

b)layup $[90_{gl}/O_{gl}/+45_{gl}/O_{gr}/O_{gl}/O_{gl}/O_{gr}/O_{gl}/-45_{gl}/O_{gr}]$s, V_{gl} = 83.4%

*)stress corresponds to the nominal values of the per ply thickness: 0.15 mm for carbon layer 0.27 mm for glass layer

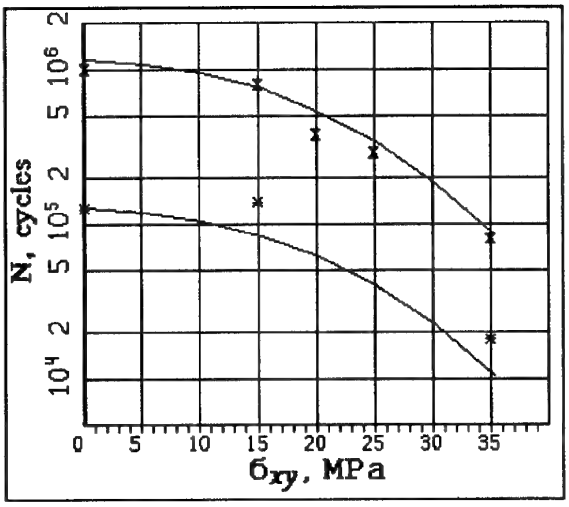

Fig.19. The dependence of fatigue life on the minimum tangential cycle stress for the unnotched glass/epoxy tubular specimens and carbon/glass/epoxy specimens for conditions of in-phase compression and torsion ($r = -\infty$):
1)glass/epoxy:layup[0]8, σ_{min}=-355 MPa
2)carbon/glass/epoxy:
layup $[O_{gl}/O_{gr}/O_{gl}/O_{gr}]_s$, σ_{min}=-390 MPa
*)stress corresponds to the nominal values of the per ply thickness 0.3 mm for all plies.

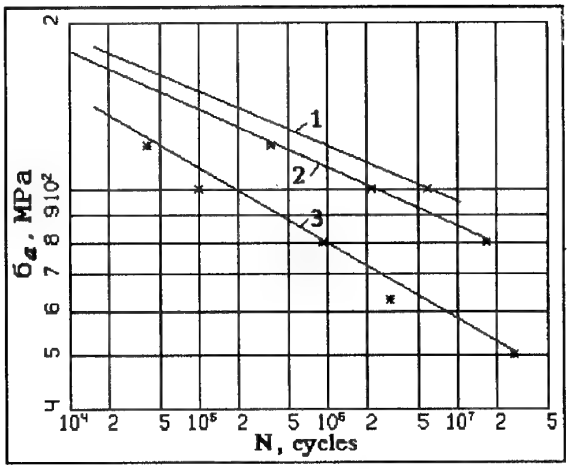

Fig.20.Comparison of predicted and experimental values of fatigue life of glass-fabric/epoxy specimens with central hole under uniaxial loading, d=8 mm, B=50 mm,

A_f=5.47 mm, $\dot{\sigma}$ =4500 MPa/s, σ_m=100 MPa (net);

1) p = 0.23 mm, σ_f=580 MPa, $m(r=O)$ = 14.8, s = 0.024;
2) p = 0.21 mm, σ_f=600 MPa, $m(r=O)$ = 13.5, s = 0.024;
3) p = 0.195 mm, σ_f = 615 MPa, $m(r=O)$ = 10.4, s = 0.03.

DETERMINATION OF A- AND B-VALUES OF STRENGTH AND FATIGUE RESISTANCE FOR PREFORMS AND ELEMENTS OF COMPOSITES STRUCTURAL MATERIALS.

V. Ya. Senik.

Central Aero-Hydrodynamic Institute
(TsAGI),
Zhukovsky 140160
Moscow Region, Russia

For estimation of A - and B -values TsAGI use a joint analysis of (i) the coupon test results for process verification and (ii) test results of model specimens for certification of preforms and structure elements. The model specimens are fabricated from one prepreg batch. The procedure is based on a normal distribution or a truncated normal distribution of strength and fatigue resistance characteristics and other hypotheses validated by experimental studies.

Nomenclature.

A - -value;
B - value;
b_i - random effect for ith batch;
$F_s(y)$ - Student distribution function;
i - ith batch (ith element);
k - batch number of process control specimens;
k_{eq} - equivalence coefficient that is equal to the ratio of the process control specimen strength to the model specimen strength;
M - realization number for process of modeling;
m , - fatigue curve parameters;
n - process control specimen number in batch;
n_1 - model specimen number in batch;
N - life;
p - per ply thickness;
p_s - batch mean value of per ply thickness for model specimens;
p_c - sample mean value of per ply thickness for accepted batches;
S_b, γ_b - between-batch standard deviation and between-batch variation coefficient of property for model specimens;
S_{bk} - between-batch standard deviation of property for all batches;
S_{bkc} - between-batch standard deviation of property for accepted batches;
S_e - within-batch standard deviation for model specimen property;
S_{eki} - within-batch standard deviation of property for process control specimens;
S_{ek} - average for within-batch standard deviation of process control specimen property;
$S_{\lg N}$ - logarithm life standard deviation;
$t_{A,0.95,\delta_A}$, $t_{B,0.95,\delta_B}$ - 0.95 quantile of the non-central distribution with noncentrality δ_A (δ_B) and with f_A (f_B) degrees of freedom;
x - random variable;
x_{ij} - test result of jth specimen in ith batch;
$\bar{X}$ - estimation of the overall average of population for model specimen property;
$\bar{X}_{ki}$ - batch mean property for process control specimens of ith batch;
$\bar{X}_k$ - sample mean property for all batches of process control specimens;
$\bar{X}_{kc}$ - sample mean property for accepted batches of process control specimens;
$\bar{X}_s$ - batch mean property for model specimen;
$\bar{X}_{oki}$ - batch mean property for process control specimens of ith batch under modeling;
$\bar{X}_{0l}$ - estimation of the overall average of population for model specimen property under lth model realization;
$\bar{X}_0$ - generalized estimation of the overall average of population for model specimen property;
y - random variable having the Student distribution with $n - 2$ degrees of freedom;
γ_e - within-batch variation coefficient for model specimen property;
ε_{ij} - random error which represents variation within each batch;
μ - overall average of population;
τ - normalized difference of random variable from batch mean;
σ - repeated stress at fatigue tests;

Paper presented at the AGARD SMP Lecture Series on "Advanced Polymeric & Metallic Composite Materials for Space and Aerospace Vehicle Structures. . .", held in Stuttgart, Germany from 11-12 December 1995; Châtillon, France from 14-15 December 1995 and Ohio, USA from 18-19 December 1995 and published in LS-204.

Introduction

The certification procedure of preforms, elements and details of aircraft composite structures is based on the application of the statistically-based values of static and fatigue properties. The statistical aspects of this procedure are presented in Ref.[1]. The application of the design values with a confidence of 95% assures that the actual properties of all the composite structures manufactured in accordance with the fixed process will exceed the design values with a sufficiently large probability. Two probability levels of 99% and 90% have been chosen for the evaluation of material properties used for analysis of strength and service life of elements and details with alternative levels of responsibility.

For computation of A- and B-values for preform material, components and elementary items a great extent of experimental data is required because the information should be representative, i.e. it should contain the possible alterations of material properties and structures produced at different times by diverse manufacturers. So, for computation of B-value of one property it is required to test not less than 30 specimens even in the case of stable production (5 batches of material and 6 specimens in each batch). In other cases the test extent required should be significantly larger.

Taking into account the great list of preforms, components and elementary items and also of their properties under different conditions the cost and time expenses are too large. Therefore the search for a cost-effective certification approach is an urgent problem. The experimental regularities received in Ref.[2] under analysis of the material and element test results offer the possibility of estimating A- and B-values with an acceptable accuracy. The suggested approach relies on static and fatigue tests of coupons and elements from one material batch that has the worst average properties. As the worst material batch it is suggested to consider that which will be produced with critical per ply thickness from the allowable range of per ply thickness alteration.

1. TIME-EFFECTIVE PROCEDURE OF A- AND B-VALUE ESTIMATION FOR PROPERTIES OF PREFORM MATERIAL AND ELEMENT.

1.1 Applicable information.

The time-effective procedure for A- and B-values estimation is based on application of the test results of lamina and/or laminate and/or process control specimens from different material batches and also on test results of model specimens from one material batch. In addition it is considered that the regularities received on the basis of generalization of investigation results of strength and fatigue of composite coupons and elements [2].

The process control specimens are cut from the preform or from the special test panel to be laid up and cured along with production element. Panel and element are produced from one prepreg batch. Five process control specimens are tested in tension and five are tested in compression. The thickness of each element and each specimen are measured and the per ply thickness is calculated for each element and each specimen. The failure stress is calculated at the nominal thickness of specimen that is equal to the product of the nominal per ply thickness by the ply number.

The batch mean values are calculated for tension and compression test, for per ply thickness of element and process control specimens. If the per ply thickness mean value of specimens and element is not equal, then the specimen mean strength mean should be evaluated under the element per ply thickness mean using the relationship "tension (compression) strength multipied by per ply thickness" that are established on the basis of test results of lamina and/or laminate and/or process control specimens [2]. The allowable per ply thickness range is also established on the basis of this relationship. The process control specimens mean strength received are compared with acceptance criteria. If both mean strength per batch exceed the corresponding acceptance criterions then the element is taken. If at least one batch mean strength is less, than the acceptance criterion and the preform per ply mean thickness does not meet the allowable per ply thickness range, then the preform is rejected. The tests are repeated, if at least one batch mean of strength is less, than the acceptance criterion and the preform per ply thickness meets the allowable per ply thickness range.

The model specimens are used for the certification static and fatigue tests. These specimens model the most critical zones of elements and elementary items of structure, namely, the zones with stress risers caused by local construction feature or manufacturing or service usage. The model specimen state must correspond to the element state in conditions of in-service environment. The model specimens should be manufactured with one prepreg batch with the critical per ply thickness or close to it [2] in accordance with the fixed process. If allowable range of per ply thickness alteration is restricted or per ply thickness influence is not significant then the model specimens can be produced with any prepreg batch. Static and fatigue failure stresses for model specimens are calculated at nominal per ply thickness in specimen failure zone. The actual per ply thickness in specimen failure zone is also determined. The model specimen number must not be less than the number of process control specimens in one batch. For A- and B- value estimations the model specimen number should be equal to 10-15 and 5-7 pieces, respectively.

Above described tests supply us with the following data for computation of A- and B-values:

- batch number k of process control specimen;
- process control specimen number n in each batch

- nominal failure stress and actual per ply thickness of each process control specimen;
- model specimen number n_1 ;
- nominal failure stress (life) and actual per ply thickness of each model specimen.

2. *BASIC ASSUMPTIONS*

2.1 As appears from the Ref. [2] the widely used autoclave process does not permit to control the per ply thickness in specimens and elements. As a consequence the per ply thickness values can vary over a wide range. Per ply thickness alteration may enhance alteration of static and fatigue strength of preform material and element. Therefore, the per ply thickness is the random controllable parameter which impacts over the influence upon the between-batch dispersion of static and fatigue strengths in comparison with other factors. If per ply thickness range is restricted or the relationship of strength fatigue with per ply thickness is insignificant, then the influence of this factor on dispersion of strength fatigue characteristics becomes comparable with the influence of other parameters. In both cases the variance model satisfies the requirements of the one-way variance model with balanced random effect. This model presents each observation as the sum ofthree components

$$x_{ij} = \mu + b_i + \varepsilon_{ij}, j = 1, \ldots\ldots\ldots, n$$

2.1.1 The error terms ε_{ij} are assumed to be independently distributed normal random variables with a mean of zero and a variance of S_e^2 (within-batch variance). It is considered that the variance S_e^2 is the same for all batches.

2.1.2 The random effect b_i are assumed to be independently distributed normal random variables with a mean of zero and a variance of S_b^2 (between-batch variance). If the large preform number was rejected on the basis of the test results of process control specimens, then the distribution of b_i describes by truncated normal distribution (Fig.1).

2.2 The ratio of static (fatigue) strength values for the process control specimens and for the model specimens does not depend upon per ply thickness. The example of experimental substantiation of this assumption is presented in Figure 2. The value of proportion coefficient keq depends upon riser efficiency and environment.

2.3 In accordance with assumption 2.2 it follows that the between-batch variation coefficients of static strength (fatigue strength) for the process control specimens and the model specimens are the same.

2.4 The fatigue curves for the element can be described by power function with the constant exponent (Figure 3 and 4).

$$N * \sigma^m = C \qquad (1)$$

2.5 The logarithm life of element with unlimited range of per ply thickness has two-parameter Weibull distribution (Fig. 5). Hence in consequence of rejection of preforms not meeting the acceptance criterions the distribution for logarithm life approximates to the normal distribution. With the more large narrowing of the allowable per ply thickness range the distribution of logarithm life becomes by three-parameter normal distribution (Fig. 5). Because as a rule the extent of truncation is not great, we shall limit self by the consideration of the two-parameter lognormal distribution for life.

3. *COMPUTATION PROCEDURE OF A- AND B-VALUES.*

The one-way variance model with random effect is used for computation of A- and B-values. Taking into account of the limited extent of certification tests, the parameters that are necessary for computation of A- and B-values by this method are estimated step by step in sequence of test result analysis of the process control specimens and the model specimens.

3.1 Analysis of test results of process control specimens.

The test results of process control specimens are used for validation of some assumptions and definitions:

- relationship "nominal failure stress - per ply thickness";
- empirical distribution of failure stress means;
- between-batch variance;
- overall per ply thickness average of the population of taken batches.

The assumptions 2.1.1 and 2.1.2 are verified. The Leman criterion [1] is used to test the hypothesis that the within-batch variance is the same from batch to batch. The hypothesis 2.1.2 about the normal distribution of the failure stresses in within batch is tested on the whole complex of batches. Because the information represents the large number k of the small batches of the same extent n , then for test of hypothesis the criterion used is based on random value

$$y_i = \frac{\tau_i \times \sqrt{n-2}}{\sqrt{n-1-\tau_i^2}},$$

which has the Student distribution with $k-1$ degrees of freedom and on the statistics ω^2 [4]. The term $\tau_i = (x_{ij} - \bar{X}_{ki}) \Big/ S_{eki}$ is the difference, normalized by standard deviation, of the random value in ith batch from the batch mean. The standard deviation is calculated on the basis of the same batch.

$$\omega^2 = \frac{1}{12k^2} + \frac{1}{k}\sum_{i=1}^{k}\left[F_s(y_i) - \frac{2i-1}{2k}\right]^2$$

On the basis of test results of the process control specimens the relationship "failure stresses - per ply thickness" is approximated by polynome

$$x = a_0 + a_1 \times p + a_2 \times p^2 + \ldots + a_r \times p^r + \ldots \quad (2)$$

The linear regression method is used for coefficient computation (see section 8.5.8 [1], [3]). All test results are used including the ones of the rejected preforms. The experience of analysis have shown that these relationships are approximated by the quadratic equation under
the sufficient wide per ply thickness range. With narrowing the per ply thickness range it is advisable to use a linear equation. The approximation curves are shown in Figures 6, 7, 8 and 9. In addition the overall average of population $\bar{X}_k$, the average of the within-batch variance S_{ak}^2 and the between-batch variance S_{bk}^2 are estimated for the process control specimens.

The between-batch variance and the distribution of the batch means are calculated on the basis of test results for the accepted batches. The analysis is conducted in full extent in accordance with ANOVA- method ([1], [3]). Afterwards the between-batch variation coefficient is calculated as the ratio of the between-batch standard deviation S_{bkc} for failure stresses to the overall average for the accepted batches $\bar{X}_{kc}$. The Anderson-Darling method is used for verification of hypothesis of the normal distribution of batch means.

3.2 Analysis of certification test results.

The basic goal of certification tests is to estimate the A- and B-values for strength and fatigue properties for preform materials and elements.

3.2.1 Estimation of distribution parameters of strength and life for model specimens.

On the basis of the static test results the mean $\bar{X}_s$, the standard deviation and the variation coefficient γ_e are calculated by standard methods. They characterize the distribution of property for one batch. On the basis of fatigue test results the fatigue curve parameters are calculated (1) by the linear regression method [1, 3].

The average of the fatigue limit is estimated for the given life on the fatigue curve. Then the mean value and the standard deviation of the logarithm of life are calculated under the cyclic stress close to the fatigue limit. The variation coefficient of the fatigue limit is estimated as follows

$$\gamma_e = \sqrt{\exp((S_{\lg N} / m)^2 / 0.189) - 1}$$

where $S_{\lg N}$ is the estimation of the standard deviation for logarithm life, m is the exponent of fatigue curve function (1).

3.2.2 Estimation of the overall average of population for element strength (life).

i) Case of significant influence of per ply thickness.

The certification tests are conducted on the model specimens with the per ply thickness mean close to the critical per ply thickness. The model specimens are manufactured from one material batch. The batch mean value will characterize the property of structure element received that has the same per ply thickness p_s . The calculation of the following values are necessary to implement for estimation of the overall average of population for strength (life) of the preform material and the element:

- the sample mean p_c for accepted preform per ply thickness that is the estimation of the overall average of population of per ply thickness for all elements;
- the strength $X(p_s)$ of process control specimens under the batch mean for per ply thickness of model specimens p_s (on the basis of the relationship 2);
- the equivalence coefficient k_{eq} which is equal to the ratio of the process control specimen strength $X(p_s)$ to the batch mean of strength for model specimens $\bar{X}_s$;

$$k_{eq} = X(p_s) / \bar{X}_s$$

- the process control specimen strength $X(p_c)$ under the sample mean p_c for per ply thickness in accepted preforms (on the basis of the relationship 2);
- the estimation of the overall average of population for model specimen strength by division of $X(p_c)$ into the equivalence coefficient k_{eq}

$$\bar{X} = X(p_c) / k_{eq}$$

ii) Case of insignificant influence of per ply thickness.

The empirical distribution for the batch means of the process control specimen strength is used the for estimation of the sample mean $\bar{X}$. The probability P corresponding to the batch mean of strength of the process control specimens for the model specimen preform is determined on the basis of this distribution. The quantile $_p$ of normalized normal distribution is determined for the probability P .

Then the standard deviation of the batch mean for the model specimen strength is calculated

$$S_{\bar{x}_s} = \sqrt{S_e^2 / n_1 + S_b^2}$$

The estimation of the overall average of population for model specimen strength is calculated as

$$X = X_s - u_p \times S_{\bar{X}_s}$$

3.3 Estimation of A- and B-values.

3.3.1 Normal distribution of random effect.

It is suggested to use the procedure recommended in Ref. [1]. Under this:

1. The within-batch variance S_e^2 for model specimens is equal to the estimation received on the basis of certification test results.
2. The between-batch variance S_b^2 is calculated as the product of the estimation of the overall average of population for model specimen strength $\bar{X}$ and the between-batch variation coefficient for accepted batches γ_b.
3. It is proposed that the batch number for model specimens is equal to the accepted batch number of process control specimens.
4. The effective extent of batch is equal to the model specimen number in batch n_1 at the test.
5. The ratio of the between-batch variance to the within-batch variance is calculated as
$$R = S_b^2 / S_e^2$$
6. The upper 87.75% and 80% confidence bounds for this ratio are calculated
$$R_A = \left[(1 + R \times n_1) / F_{0.1225} - 1\right] / n_1,$$
$$R_b = \left[(1 + R \times n_1) / F_{0.2} - 1\right] / n_1$$
where $F_{0.1225}$ and $F_{0.2}$ are the 0.1225 and 0.2 quatiles of an F-distribution with $k-1$ numerator degrees of freedom $(n_1 - 1)k$ and denominator degrees of freedom. If $R_A (R_B)$ is negative, then set this value equal to zero.
7. The A- and B-values are calculated
$$A = \bar{X} - T_A \times \sqrt{S_e^2 + S_b^2}$$
$$B = \bar{X} - T_B \times \sqrt{S_e^2 + S_b^2}$$

where $_A$ and $_B$ are the tolerance limit factors defined by the following approximated expressions [1]

$$_A = \sqrt{\frac{n_1 \times R_A + 1}{n_1 \times k \times (R_A + 1)}} \times t_{f_A, 0.95, \delta_A}$$
$$_B = \sqrt{\frac{n_1 \times R_B + 1}{n_1 \times k \times (R_B + 1)}} \times t_{f_B, 0.95, \delta_B}$$

$_{f_A, 0.95, \delta_A}$ and $_{f_B, 0.95, \delta_B}$ are the 0.95 quantile of non-central distribution with noncentrality parameter

$$\delta_A = 2.326 \times \sqrt{n_1 \times k \times (R_A + 1) / (n_1 \times R_A + 1)},$$
$$\delta_B = 1.282 \times \sqrt{n_1 \times k \times (R_B + 1) / (n_1 \times R_B + 1)}$$

and degrees of freedom

$$f_A = \frac{(R_A + 1)^2}{\frac{(R_A + 1/n_1)^2}{k-1} + \frac{(1 - 1/n_1)^2}{k \times (n_1 - 1)}},$$
$$f_B = \frac{(R_B + 1)^2}{\frac{(R_B + 1/n_1)^2}{k-1} + \frac{(1 - 1/n_1)^2}{k \times (n_1 - 1)}},$$

3.3.2 Truncated normal distribution of random effect.

The statistical modeling is used for the estimation of the tolerance limit factors. The parameters at modeling are the test results of process control specimens

– the batch number k of process control specimens and the process control specimen number in batch n,

– the sample mean of property $\bar{X}_k$ for all batches of process control specimens, the average for within-batch variance of process S^2_{ek} control specimen property and the between-batch variance S^2_{bk} of

– property for all batches,
– the acceptance criterion,
– the model specimen number in batch n_1.

The modeling is conducted in the following sequences:

1. The k averages $\bar{X}_{0i}$ from the normal distribution with parameters $(\bar{X}_{0i}, S_{bk})$ are modelled.
2. The k batches by extent n from the normal distribution with parameters $(\bar{X}_k, S_{ek})$ are modeling. The batch means are calculated. The batches with batch mean not meeting the acceptance criterion are rejected.
3. The k_c batch means meeting the acceptance criterion are used for the modeling of batches by extent n_1 of the normal distributed random variable with parameters $(\bar{X}_{0i}, S_{ek})$. The values received are united in one sample that is used for estimation the 0.01 and 0.1 quantiles ($X_{0.01}$,and $X_{0.1}$) and the overall average of population for model specimen property under lth model realization $\bar{X}_{01}$.
4. The steps 1, 2 and 3 are repeated many times (M). The generalized estimation of the overall average $\bar{X}_0$ of population for model specimen property is calculated. The $X_{0.01}$ and $X_{0.1}$ quantiles distribute are built. On these distributions the 0.05 quantiles being the estimations of A- and B-values (x_A and x_B) are determined.
5. The tolerance limit factors are calculated as follows:
$$_A = (\bar{X}_0 - x_A) / \sqrt{S^2_{ek} + S^2_{bkc}}$$
$$_B = (\bar{X}_0 - x_B) / \sqrt{S^2_{ek} + S^2_{bkc}}$$
6. The A- and B-values are calculated as in the above mentioned case.

3.4 Estimation of critical per ply thickness.

As the certification criterion the requirement is suggested that A- and B-values most of the properties of elementary items produced in accordance with fixed process is not less, then the design values. If this requirement has not been implemented, then the limits of per ply thickness range may be introduced.

The critical per ply thickness at which the acceptance criterion is provided with 95% confidence level is estimated in the following manner. The upper bound of the 95% confidence interval is calculated for hypothetical batch with (i) extent that is equal to the number of process control specimens in one batch, (ii) the estimation of the batch mean value that is equal to the acceptance criterion and (iii) the standard deviation that is equal to the average for within-batch standard deviation of the process control specimen strength. The distribution of strength is considered as the normal distribution and the calculation of confidence bound is provided by the classic statistical methods [3]. The critical per ply thickness is estimated on the basis of the relationship "strength - per ply thickness".

4. Example.

The calculation of the B-value has been performed on the basis of data [1]. The full data represent the samples containing 5...9 batches for which the over influence of some factor has not been found. The between-batch standard deviations are estimated at treatment of all data. Then, one batch with the least batch mean has been chosen from each sample.. This batch has been used for the estimation of the B-value. Each sample has also been treated by the method [1]. The comparison of the results obtained is given in the table 1.

Table 1.

No	Estimation of B-values	
	full data	Least batch
1	55.99	58.31
2	54.72	53.68
3	64.45	64.57
4	27.37	28.08
5	27.68	28.62
6	61.22	62.10

The estimation of the difference does not exceed 5%. It is necessary to note that the batch number in each sample is not great. A more high accuracy can be expected with use of the test results of a larger number of batches.

Conclusion

An efficient procedure for certification of composite structures is developed in accordance with which for calculating basic values of mechanical and fatigue properties it is enough to obtain test results for the objects certified from one batch only. The procedure is based on the probabilistic model, formed as summary of extensive experimental investigations of strength and fatigue properties for composite materials, prefoems and elements made of them. Estimation error for basic values accor-ding to the proposed procedure does not exceed 5% when scatter values of strength and fatigue properties are typical for composite materials.

References

1. Military Handbook "Polymer Matrix Composites", MIL-HDBK-17-1C, 1992.

2. Trunin,Y.P. "Certification of Preforms and Structure Elements out of Composite Materials", Lecture Series TCP 04, AGARD-NATO, 1995

3. Brownlee,K.A. "Statistical Theory and Methodology in Scince and Engineering", John Wyley and Sons, INC., New York - London -Sidney, 1965

4.Smirnov N.W.,Dudin-Barkovsky I.W. "Course of probability theory and statistics for technical application", Moscow, Science, 1965.

ENSURING COMPOSITE STRUCTURE STRENGTH

by

V.I. BIRYUK
TsAGI, ZHUKOVSKY 140160
MOSCOW REGION, RUSSIA

CORRECTION FOR IN-SERVICE ENVIRONMENTAL AGGRESSIONS DURING COMPOSITE STRUCTURE STRENGTH EVALUATION

The present paper considers variation of properties of composite materials subjected to environmental aggressions. Airframes, while in long-term service and/or storage, experience adverse temperature/humidity combinations which usually change the mechanical properties governing the materials limits. The moisture absorbed decreases strengths and stiffnesses, thus increasing in-service deformation. Elevated temperatures intensify moisture absorption. The extent of variation in characteristics depends on the filler, and stability of material performance worsens in going from CFRP to organoplastic and, further, to GFRP. Fibers are less sensitive to moisture than polymer matrices, therefore the moisture content may severely influence the properties defined by the matrix strength, i.e., the compressive and shear stress limits.

Within a certain temperature range, the moisture effects are reversible: a composite recovers its properties with decrease in the moisture content.

Long exposure to environmental aggressions changes the properties of polymer matrix composites (PMCs). The characteristic of the most widely used PMCs are related to the following changes mecanisms caused by long exposure:

- the increase in strength of the material due to post-cure of the polymeric resin,

-gradual development of damage both in constituents of the material system and over fiber/matrix interface.

Post-cure is formation of additional chemical links between radicals in the resin. The phenomenon holds at usual temperatures due to activation from moisture absorbed, this influence becoming stronger at elevated temperatures.

Mechanisms of degradation are numerous and depend on the resin formula, fiber type, interface condition, processing conditions, etc. External pliesof a composite structure destructs more notably than internal layers.

The two simultaneous but opposite processes result in a situation typical of the PMCs: initially, the ultimate stresses increase, thereafter, due to long aging, the strengths decrease.

The impact of the in-service environment on static, fatigue, and residual strengths (and stiffnesses) must be experimentaly evaluated. The test data already available may only be used after showing their direct applicability to a specific material in a specific structural system. There is a need for "environmental design" criteria to reveal the most critical in-service situations.

The environmental effects on the strength of the composite structures are to be evaluated by testing the full-size structural elements by a program which incorporates the following extreme situations:

- the maximum temperature likely to occur in service (variation of strengths and stiffnesses at elevated temperatures);

- the minimum temperature defined by the basic conditions and/or long flights at high altitudes (variation of mechanical properties due to low operational temperatures);

- extreme accumulation of moisture (strength degradation because of the presence of water);

- dwelling of the structure in severe environment during the service life (degradation of strength).

Investigations should estimate the influence of various combinations of the critical conditions listed above, as well as the effects of temperature/humidity cycles.

The maximum temperature of a subsonic passenger-carrying airplane depends on the basic conditions including ambient temperature and solar radiation.

If there are no limitations imposed on routes and in the airport, the typical day/night cycle in environmental conditions (to be used to define the structural temperature) is that corresponding to torrid arid climate.

An equilibrium temperature T_e is determined from the balance of heat fluxes on an airplane surface at an in airport at the hottest hour:

$$h(T_{amax}-T_e) - eS_o(T_e/100)^4 + AV_{smax}\cos\Upsilon = 0.$$

Here, h = surface heat release factor,
T_{amax} = maximum air temperature,
e = surface emissivity,
A = surface radiation absorptivity,
V_{smax} =maximum solar radiation intensity,
Υ = angle between solar beams and the normal to the surface,
S_0 = 5.77ú10__, the Stephan--Boltzmann constant.

Paper presented at the AGARD SMP Lecture Series on "Advanced Polymeric & Metallic Composite Materials for Space and Aerospace Vehicle Structures. . .", held in Stuttgart, Germany from 11-12 December 1995; Châtillon, France from 14-15 December 1995 and Ohio, USA from 18-19 December 1995 and published in LS-204.

One should assume T_{emax} =326 K and V_{smax} =1150 W/sq.m; the surface heat release factor, h, may be taken to be equal to 11,6 W/sq.múK (for a 4 m/s wind); usually, e=A=0.9; solar beams should be assumed to be normal to the surface (Y=0). Now, solving the equation, we obtain the equilibrium temperature

T_e =354 K (=81°C).

This means that the strength of structures out of PMCs should be estimated at 80°C. The need for such tests is confirmed by foreign practices: temperature of a horizontal stabilizer out of a CFRP on Boeing 737 during certification tests was 82°C, and a CFRP vertical stabilizer of A-300/310 was tested for static strength at 70°C.

The extremely low temperatures are characteristic of aircrafts operated in adverse cold regions and also of the subsonic passenger airplanes flying at altitudes of up to 30 km.

The minimum day-averaged ground temperature adopted for the adverse cold climate is -60°C; the minimum month-averaged temperature is -40°C.

When studying the effects of moisture on the strength of a composite structure, one should assume that the structure is operated in a torrid humid climate for a long time . The moisture accumulation rate and the extent of degradation notably depend on structure temperature which is a function of both ambient temperature and solar radiation intensity. One can employ the equation above to calculate temperatures over a day/night period for humid torrid climate.

To estimate strengths of PMC structures the tests should be conducted under maximum moisture accumulation conditions expected to occur in service. The maximum moisture accumulation level is specified from calculations and operating experience; otherwise, it can be determined by testing the specimens and structural components after long-term exposure to conditions corresponding to a standardized daily cycle for torrid humid climate.

Tests may be simplified by averaging the daily variations of the parameters defining the moisture accumulation. The tests have to be conducted at constant parameters: structural temperature T=35°C, Relative Humidity j=85%. The structure will be exposed until saturation is attained (when the weight of a test article does not increase anylonger).

The possible saturation level (i.e., the weight increment W, %) for exposure to torrid humid climate is estimated to be 1% for CFRP and 2% for organoplast .

Saturating full-scale structures in environmental test chambers makes the tests very long. The process could be accelerated by increasing both temperature and relative humidity. However, it should be reminded that there exist limiting temperatures that depend on the type of the material. Long exposure to high RH coupled with temperature in excess of the limit can result in matrix destruction.

For PMCs on epoxy resins, the limit temperature, T_{ult}, is established to be 65°C.

To saturate a full-size unit, the unit is inserted into an environmental test chamber (or into a temporary stand) and exposed until the prescribed moisture content level is reached; the process is monitored by weighing the test unit.

If a structural unit is difficult (or impossible) to weigh, use is made of "accompanying" specimens typical of a specific unit. These are placed into a chamber along with the test unit. The moisture content of the unit is estimated on the basis of weights of the specimens. In order for a specimen not to absorb moisture through the surfaces that, in the actual structure, are not in contact with the environment (the specimen edges included), such zones are sealed hermetically.

The limit moisture-content and the duration of the process could be determined by extrapolating the weight increment function

$$W(t)=A(1-e^{-B\,t})$$

which is drawn from results obtained at the initiatory stage (Fig. 7 overview).

To obtain similar weight gains for the main structure and the "accompanying" specimens in respect of moisture contents, all these articles should be dried preliminarily at 60°C (as for PMCs with epoxy matrices).

The influence of long exposure to heating/cooling and high humidity is currently a poorly studied factor, therefore experimental estimation of residual strength as of the last stage in the airframe service is a mandatory action. A structure may be brought to a state corresponding to the last stage by subjecting the structure to real-time exposure under typical operating conditions. The standardized schedule of daily variations of structural temperature and atmospheric humidity characterizes the maximum values, so adopting it for estimates will be too severe an assumption. In usual service, airplanes are not subjected to this extreme schedule every day, a notable portion of time is spent flying at altitude where temperature is negative and relative humidity is nearly zero . Therefore, long aging and strength degradation processes are recommended to be studied within a programme in which environmental conditions are kept constant: temperature, 38°C, and RH =0.7.

Real-time exposure is almost impossible to implement in the testing of airframes of passenger-carrying airplanes, because these are planned to be operated for 15 - 20 years. Therefore tests should be accelerated.

Aging may be accelerated (thus making the test duration shorter) by increasing both the relative humidity and temperature to limits characteristic of a

specific material (for example, 65°C for epoxy matrices).

Special experiments are carried out to obtain the relation between the strength-degradation rate and environmental exposure duration and parameters. This relation can be employed to determine duration of the accelerated tests depending on specific parameters.

We would like to illustrate this statement by the relation characteristic of epoxy-based PMCs.

The rate of the process affecting the strength under specified environmental conditions may be defined by the following equation:

$$V=A\ exp(-C/T\varphi).$$

Since the time is inverse to the rate, the exposure duration may be calculated as

$$\frac{\tau_2}{\tau_1} = \frac{\exp(-C/T_1\varphi_1}{\exp(-C/T_2\varphi_2)}$$

Here, C is a coefficient to be determined by experiment, T is structural temperature (°C), j is the RH of the surrounding air, the subscripts 1 and 2 are for the actual parameters and the accelerated test parameters, respectively.

In particular, the limited test data available show that C = 46.1 for epoxy-based composites. Figure 1 demonstrates the possibility to shorten the tests by both providing a higher RH and heating structure.

A programme of testing units (PMC) incorporates a set of experiments that allows researchers to estimate the stresses and stiffnesses at normal conditions and under extreme RH and temperature.

A typical cycle of static tests includes

- determining the stresses and strains in an as-delivered unit subjected to normal, minimum, and maximum temperatures and moisture contents;
- showing the structural strength for the ultimate load;
- evaluating the load-bearing capability assuming extreme conditions (temperature and moisture content at upper levels).

The design conditions in respect to moisture content and temperature are ensured by exposing the structure to the moist air with a specified temperature. This requires chambers of adequate dimensions (for installing both the structure and the load application devices) and with wide ranges of test conditions : R.H. =0.7 - 95%, T=308K (35°C).

Environmental tests may also be performed in temporary installations. A test structure is mounted on a stand surrounded by a flexible-wall chamber (made of polymers). The structure is subjected to heating by humid air flow. Should the structural displacements be large, the chamber is attached to the test structure and moved together with it. If displacements are small, the chamber shell may be fixed separately from the structure, but one should envisage an adequate volume in the chamber to deform the structure. Figure 2 represents a stand for testing an aileron under climatic effects. The moistened heated air is circulated through the chamber, heating a structural unit and supplying moisture to it. The load application system is set apart during the moisture supply stage. Loads from a hydraulic force-generator are applied to the structure by using an additional device that presses the structure through the flexible polymeric wall. For maintenance's sake, both the load system and the flexible walls are removed.

This facility may also be used in fatigue strength evaluation tests, in studies on residual strength and damage evolution, when improving the repair procedures. Such a wide range of application for such facilities is a sufficient reason for them. The above approach to investigation into environmental effects on composite structure was practiced when preparing the TU-204 airliner. Figure 3 represents the programme of combined static and fatigue strength tests. The latter have been subdivided into three phases:

1. The as-delivered structure is impregnated with moisture to a significant level, then loaded using flight cycle loads to reach or a given design service life; residual strength is determined.

2. Standardized damage is introduced to simulate the in-service damage which can be revealed by nondestructive inspection techniques; flight cycle loads are applied to reach an accurate design service life; residual strength is determined.

3. At the outset of the phase 3 standardized damage is introduced which can be revealed visually; residual strength is determined; the aileron is repaired in accordance with a typical process; flight cycle loads are applied to reach an accurate design service life; finally, the load is increased to failure in order to evaluate the load-bearing capacity and safe strength limits.

In general, environmental aggressions can reduce the strength by 10 - 15%, which should be taken into account at the design stage. However, each combination of materials, operating conditions, and load levels must be evaluated by experiments to be performed at least on specimens.

REFERENCES

1. Birjuk V.I., Kut'inov V.F. Certification of civil aircraft units manufacturing from polymer composite materials. Report of TsAGI. 1992.

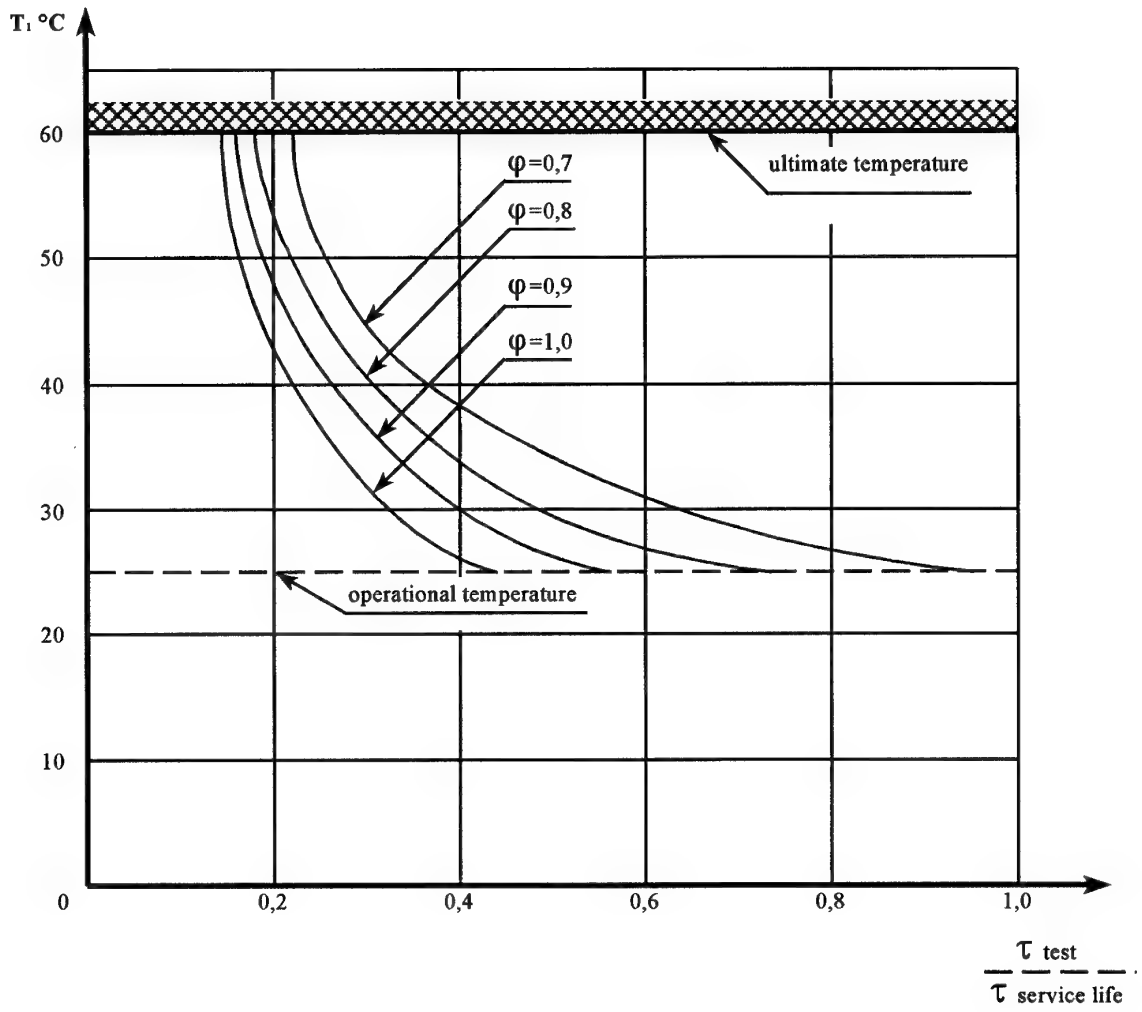
T₁ °C
60
50
40
30
20
10
0
0,2
0,4
0,6
0,8
1,0
φ=0,7
φ=0,8
φ=0,9
φ=1,0
ultimate temperature
operational temperature
τ test
τ service life

Fig. 1

AILERON TEST STAND

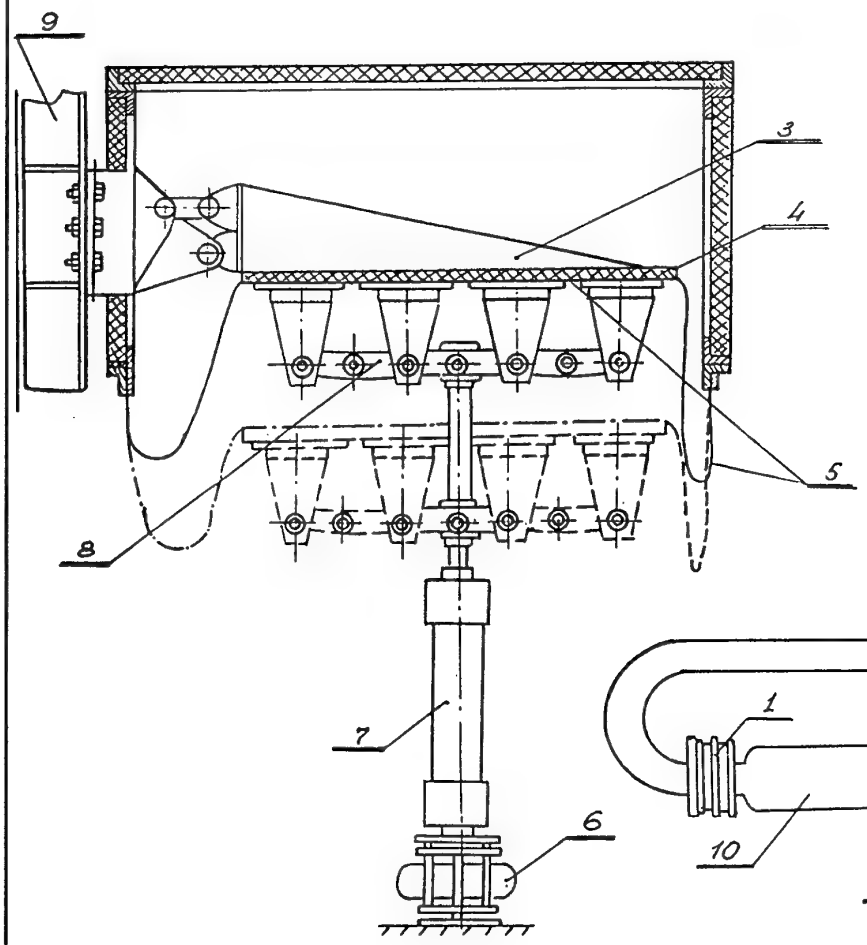

Membrane during loading

Memrane during moisture accumulation and inspection.

1. Fan.
2. Return duct.
3. Aileron.
4. Rubber washer.
5. Elastic membrane.
6. Load cell.
7. Hydraulic force exciter.
8. Levers.
9. Support.
10. Steam generator.

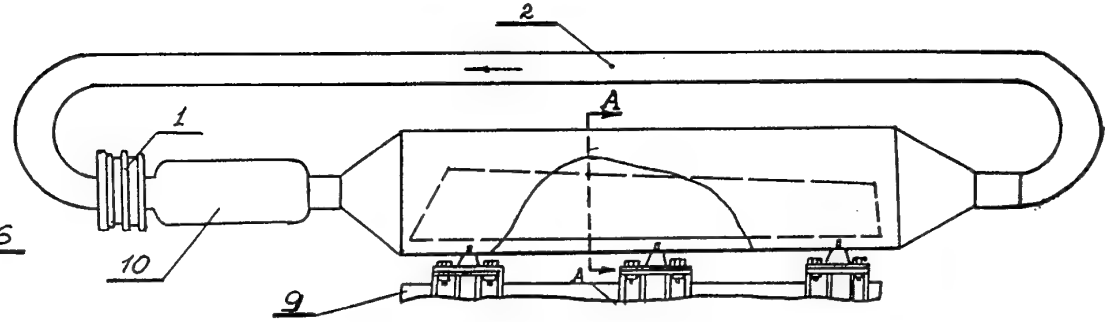

Fig. 2

ENDURANCE TESTING PROGRAM

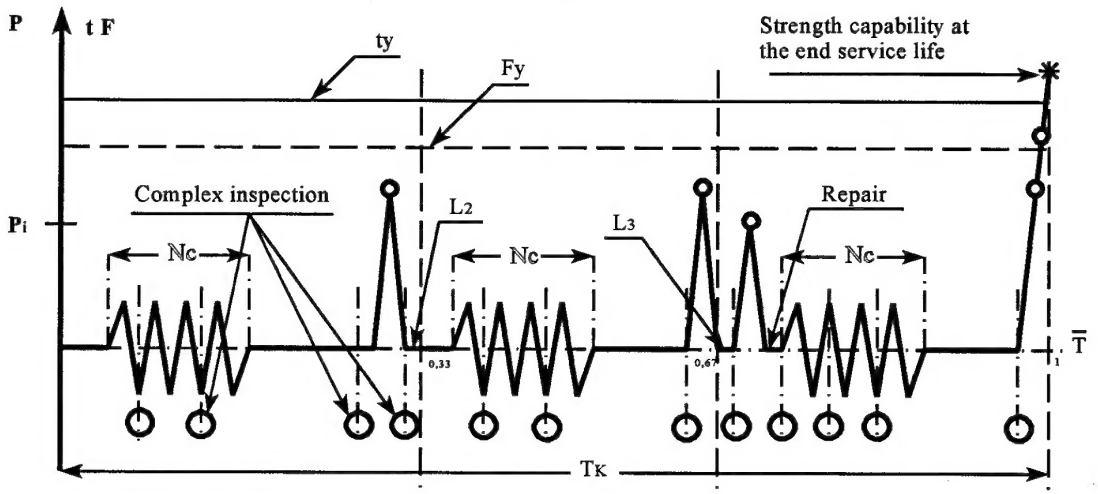

STAGE	1	2	3
DURATION	O,33 Tk	O,33 Tk	O,33 Tk
DAMAGE	L1	L2	1)L3 ,2)REPAIR
CYCLE NUMBER	Nc	Nc	Nc
STATIC LOAD	1.2 Pl	1.2 Pl	1)Pl,2)1.2Pl,3)1.5Pl
TEMPERATURE	ty	ty	ty
HUMIDITY	Fy	Fy	Fy

Tk - service life
Pl - limite load
Nc - cycling loading for one service life

L1 - undetectable.
L2 - detectable by instruments.
L3 - detectable visually

Fig. 3

REPORT DOCUMENTATION PAGE

1. Recipient's Reference	2. Originator's Reference	3. Further Reference	4. Security Classification of Document
	AGARD-LS-204	ISBN 92-836-1027-X	UNCLASSIFIED/ UNLIMITED

5. Originator Advisory Group for Aerospace Research and Development
North Atlantic Treaty Organization
7 rue Ancelle, 92200 Neuilly-sur-Seine, France

6. Title

Advanced Polymeric & Metallic Composite Materials for Space and Aerospace Vehicle Structures & Strength Optimization of Composite Structures and their Certification

7. Presented at/sponsored by

The AGARD SMP Lecture Series held from 11-12 December in Stuttgart, Germany, 14-15 December in Châtillon, France, and 18-19 December in Ohio, USA.

8. Author(s)/Editor(s)	9. Date
Multiple	December 1995
10. Author's/Editor's Address	**11. Pages**
Multiple	160

12. Distribution Statement There are no restrictions on the distribution of this document. Information about the availability of this and other AGARD unclassified publications is given on the back cover.

13. Keywords/Descriptors

Composite materials
Composite structures
Polymers
Airframes
Panels
Aircraft
Spacecraft
Shells (structural forms)
Designs
Fatigue (materials)
Static tests
Mechanical properties
Metal matrix composites

14. Abstract

This Lecture Series will present and discuss the scientific problem of advanced polymer and metallic composite materials for aerospace structures, strength optimization of composite structures and their certification. Some challenges of using composite structures, including airframe concept definition are studied. Also fibre orientation optimization principles for composite panels and shells are outlined. Procedures for certification of assemblies made out of composites are dealt with.

Certification requirements, including requirements to estimate static and fatigue strengths are formulated.

Design conditions for composite structures are analyzed, including development.

This Lecture Series, endorsed by the Structures and Materials Panel of AGARD has been implemented by the Technical Cooperation programme.

AGARD

NATO OTAN

7 RUE ANCELLE • 92200 NEUILLY-SUR-SEINE

FRANCE

Télécopie (1)47.38.57.99 • Télex 610 176

DIFFUSION DES PUBLICATIONS

AGARD NON CLASSIFIEES

Aucun stock de publications n'a existé à AGARD. A partir de 1993, AGARD détiendra un stock limité des publications associées aux cycles de conférences et cours spéciaux ainsi que les AGARDographies et les rapports des groupes de travail, organisés et publiés à partir de 1993 inclus. Les demandes de renseignements doivent être adressées à AGARD par lettre ou par fax à l'adresse indiquée ci-dessus. *Veuillez ne pas téléphoner.* La diffusion initiale de toutes les publications de l'AGARD est effectuée auprès des pays membres de l'OTAN par l'intermédiaire des centres de distribution nationaux indiqués ci-dessous. Des exemplaires supplémentaires peuvent parfois être obtenus auprès de ces centres (à l'exception des Etats-Unis). Si vous souhaitez recevoir toutes les publications de l'AGARD, ou simplement celles qui concernent certains Panels, vous pouvez demander à être inclu sur la liste d'envoi de l'un de ces centres. Les publications de l'AGARD sont en vente auprès des agences indiquées ci-dessous, sous forme de photocopie ou de microfiche.

CENTRES DE DIFFUSION NATIONAUX

ALLEMAGNE
Fachinformationszentrum Karlsruhe
D-76344 Eggenstein-Leopoldshafen 2

BELGIQUE
Coordonnateur AGARD-VSL
Etat-major de la Force aérienne
Quartier Reine Elisabeth
Rue d'Evere, 1140 Bruxelles

CANADA
Directeur, Services d'information scientifique
Ministère de la Défense nationale
Ottawa, Ontario K1A 0K2

DANEMARK
Danish Defence Research Establishment
Ryvangs Allé 1
P.O. Box 2715
DK-2100 Copenhagen Ø

ESPAGNE
INTA (AGARD Publications)
Pintor Rosales 34
28008 Madrid

ETATS-UNIS
NASA Headquarters
Code JOB-1
Washington, D.C. 20546

FRANCE
O.N.E.R.A. (Direction)
29, Avenue de la Division Leclerc
92322 Châtillon Cedex

GRECE
Hellenic Air Force
Air War College
Scientific and Technical Library
Dekelia Air Force Base
Dekelia, Athens TGA 1010

ISLANDE
Director of Aviation
c/o Flugrad
Reykjavik

ITALIE
Aeronautica Militare
Ufficio del Delegato Nazionale all'AGARD
Aeroporto Pratica di Mare
00040 Pomezia (Roma)

LUXEMBOURG
Voir Belgique

NORVEGE
Norwegian Defence Research Establishment
Attn: Biblioteket
P.O. Box 25
N-2007 Kjeller

PAYS-BAS
Netherlands Delegation to AGARD
National Aerospace Laboratory NLR
P.O. Box 90502
1006 BM Amsterdam

PORTUGAL
Força Aérea Portuguesa
Centro de Documentação e Informação
Alfragide
2700 Amadora

ROYAUME-UNI
Defence Research Information Centre
Kentigern House
65 Brown Street
Glasgow G2 8EX

TURQUIE
Millî Savunma Başkanliği (MSB)
ARGE Dairesi Başkanliği (MSB)
06650 Bakanliklar-Ankara

Le centre de distribution national des Etats-Unis ne détient PAS de stocks des publications de l'AGARD.
D'éventuelles demandes de photocopies doivent être formulées directement auprès du NASA Center for AeroSpace Information (CASI) à l'adresse ci-dessous. Toute notification de changement d'adresse doit être fait également auprès de CASI.

AGENCES DE VENTE

NASA Center for
AeroSpace Information (CASI)
800 Elkridge Landing Road
Linthicum Heights, MD 21090-2934
Etats-Unis

ESA/Information Retrieval Service
European Space Agency
10, rue Mario Nikis
75015 Paris
France

The British Library
Document Supply Division
Boston Spa, Wetherby
West Yorkshire LS23 7BQ
Royaume-Uni

Les demandes de microfiches ou de photocopies de documents AGARD (y compris les demandes faites auprès du CASI) doivent comporter la dénomination AGARD, ainsi que le numéro de série d'AGARD (par exemple AGARD-AG-315). Des informations analogues, telles que le titre et la date de publication sont souhaitables. Veuiller noter qu'il y a lieu de spécifier AGARD-R-nnn et AGARD-AR-nnn lors de la commande des rapports AGARD et des rapports consultatifs AGARD respectivement. Des références bibliographiques complètes ainsi que des résumés des publications AGARD figurent dans les journaux suivants:

Scientific and Technical Aerospace Reports (STAR)
publié par la NASA Scientific and Technical
Information Division
NASA Headquarters (JTT)
Washington D.C. 20546
Etats-Unis

Government Reports Announcements and Index (GRA&I)
publié par le National Technical Information Service
Springfield
Virginia 22161
Etats-Unis
(accessible également en mode interactif dans la base de données bibliographiques en ligne du NTIS, et sur CD-ROM)

Imprimé par le Groupe Communication Canada
45, boul. Sacré-Cœur, Hull (Québec), Canada K1A 0S7

AGARD

NATO OTAN

7 RUE ANCELLE • 92200 NEUILLY-SUR-SEINE

FRANCE

Telefax (1)47.38.57.99 • Telex 610 176

DISTRIBUTION OF UNCLASSIFIED

AGARD PUBLICATIONS

AGARD holds limited quantities of the publications that accompanied Lecture Series and Special Courses held in 1993 or later, and of AGARDographs and Working Group reports published from 1993 onward. For details, write or send a telefax to the address given above. *Please do not telephone.*

AGARD does not hold stocks of publications that accompanied earlier Lecture Series or Courses or of any other publications. Initial distribution of all AGARD publications is made to NATO nations through the National Distribution Centres listed below. Further copies are sometimes available from these centres (except in the United States). If you have a need to receive all AGARD publications, or just those relating to one or more specific AGARD Panels, they may be willing to include you (or your organisation) on their distribution list. AGARD publications may be purchased from the Sales Agencies listed below, in photocopy or microfiche form.

NATIONAL DISTRIBUTION CENTRES

BELGIUM
Coordonnateur AGARD — VSL
Etat-major de la Force aérienne
Quartier Reine Elisabeth
Rue d'Evere, 1140 Bruxelles

CANADA
Director Scientific Information Services
Dept of National Defence
Ottawa, Ontario K1A 0K2

DENMARK
Danish Defence Research Establishment
Ryvangs Allé 1
P.O. Box 2715
DK-2100 Copenhagen Ø

FRANCE
O.N.E.R.A. (Direction)
29 Avenue de la Division Leclerc
92322 Châtillon Cedex

GERMANY
Fachinformationszentrum Karlsruhe
D-76344 Eggenstein-Leopoldshafen 2

GREECE
Hellenic Air Force
Air War College
Scientific and Technical Library
Dekelia Air Force Base
Dekelia, Athens TGA 1010

ICELAND
Director of Aviation
c/o Flugrad
Reykjavik

ITALY
Aeronautica Militare
Ufficio del Delegato Nazionale all'AGARD
Aeroporto Pratica di Mare
00040 Pomezia (Roma)

LUXEMBOURG
See Belgium

NETHERLANDS
Netherlands Delegation to AGARD
National Aerospace Laboratory, NLR
P.O. Box 90502
1006 BM Amsterdam

NORWAY
Norwegian Defence Research Establishment
Attn: Biblioteket
P.O. Box 25
N-2007 Kjeller

PORTUGAL
Força Aérea Portuguesa
Centro de Documentação e Informação
Alfragide
2700 Amadora

SPAIN
INTA (AGARD Publications)
Pintor Rosales 34
28008 Madrid

TURKEY
Millî Savunma Başkanliği (MSB)
ARGE Dairesi Başkanliği (MSB)
06650 Bakanliklar-Ankara

UNITED KINGDOM
Defence Research Information Centre
Kentigern House
65 Brown Street
Glasgow G2 8EX

UNITED STATES
NASA Headquarters
Code JOB-1
Washington, D.C. 20546

The United States National Distribution Centre does NOT hold stocks of AGARD publications.
Applications for copies should be made direct to the NASA Center for AeroSpace Information (CASI) at the address below.
Change of address requests should also go to CASI.

SALES AGENCIES

NASA Center for
AeroSpace Information (CASI)
800 Elkridge Landing Road
Linthicum Heights, MD 21090-2934
United States

ESA/Information Retrieval Service
European Space Agency
10, rue Mario Nikis
75015 Paris
France

The British Library
Document Supply Centre
Boston Spa, Wetherby
West Yorkshire LS23 7BQ
United Kingdom

Requests for microfiches or photocopies of AGARD documents (including requests to CASI) should include the word 'AGARD' and the AGARD serial number (for example AGARD-AG-315). Collateral information such as title and publication date is desirable. Note that AGARD Reports and Advisory Reports should be specified as AGARD-R-nnn and AGARD-AR-nnn, respectively. Full bibliographical references and abstracts of AGARD publications are given in the following journals:

Scientific and Technical Aerospace Reports (STAR)
published by NASA Scientific and Technical
Information Division
NASA Headquarters (JTT)
Washington D.C. 20546
United States

Government Reports Announcements and Index (GRA&I)
published by the National Technical Information Service
Springfield
Virginia 22161
United States
(also available online in the NTIS Bibliographic
Database or on CD-ROM)

Printed by Canada Communication Group
45 Sacré-Cœur Blvd., Hull (Québec), Canada K1A 0S7

ISBN 92-836-1027-X